A STUDY ON REPAIR STRATEGY OF SEVERELY DAMAGED RC STRUCTURES BY USING SACRIFICIAL ANODE CATHODIC PROTECTION

ピンタ, アストゥティ

A STUDY ON REPAIR STRATEGY OF SEVERELY DAMAGED RC STRUCTURES BY USING SACRIFICIAL ANODE CATHODIC PROTECTION

深刻な損傷を受けたRC構造物の犠牲陽極方式電気防食による補修工法に関する研究

PINTA ASTUTI

Acknowledgments

After an intensive period of my doctoral study, today is the day, writing this note of acknowledgments is the finishing touch on my doctoral thesis. It has been a period of intense learning for me, not only in the scientific arena but also on a personal level. Writing this dissertation has had a significant impact on me. I would like to reflect on the people who have supported me so much throughout this period.

I would like to express my special appreciation and sincere gratitude to my supervisor Prof. Hidenori HAMADA, for his patience, motivation, enthusiasm, endless encouragement, immense knowledge and guidance throughout my three years of doctoral study and my new life in Japan. He has always been available to advise me even he is busy with his daily routine work, make him a very great supervisor. He inspired me about the art of research in repair techniques of seriously damaged structures. Thank you for your kindness and for accepting me three years ago to experience your extensive knowledge in Concrete Engineering.

My thousands of appreciation also goes to the advisory committee, Prof. Koji TAKEWAKA, Assoc. Prof. Shigenobu KAINUMA, Assoc. Prof. Yasutaka SAGAWA, and Assoc. Prof. Tomoyuki KOYAMA for their precious suggestions and insightful comments concerning improve this research work. Thank you also for letting my defense be a memorable moment in my life.

My thanks also go to Dr. Daisuke YAMAMOTO for his tremendous help, precious friendship during my study and his non-stop support throughout my experimental work. Thanks also to Assist. Prof. Takayuki FUKUNAGA for his assistance during this last half-year in laboratory.

My special gratitude also is dedicated to the Japan International Cooperation Agency (JICA) project for AUN/SEED-Net for providing financial study assistance during my doctoral program in Japan. My grateful acknowledgment also to PS. Mitsubishi Construction Co. Ltd. and DENKA Co. Ltd. for their support by providing material in this research.

My grateful appreciation is also addressed to Dr. Eng. Rahmita Sari Rafdinal and Dr. Eng. Maki KODA for patient and kindness in guiding and helping me during collaborative research with their company.

My appreciation and thank also extends to present and past members of Concrete Engineering Laboratory for helping me through thick and thin time. Thank you for working together during specimen preparations. Thank you for the memorable technical site visit, laboratory party, excellent work environment, and fun chat. My thanks also go to Khalilah binti Khamarulzaman, Loke Yen Theng, Volana Andriamisa, Zhang Yi Chen, Xie Caiyun, Sabrina Harahap, and Dr. Eng. Dahlia Patah who actively supported this research.

Thank you very much also addresses to the colleagues of the Department of Civil Engineering, Faculty of Engineering, Universitas Muhammadiyah Yogyakarta, Indonesia for supporting me during my study at Kyushu University, Japan. Thank you also to Bapak Jazaul Ikhsan, Ph.D. and Bapak Puji Harsanto, Ph.D. who motivated me to finish my study on time and always appreciated my achievement during my study.

I would also like to take this opportunity to express the profound gratitude of my sincere heart to my beloved parents and Dr. Eng. Adhitya Yoga Purnama for their love, wise counsel, a sympathetic ear, patience, and unstopable support during my study in Japan. I love you all!

Finally, there are my friends. We were not only able to support each other by deliberating over our research problems but also happily by talking about everything other than just our academics.

Thank you very much!

Pinta

Fukuoka, 2020.

Abstract

Chloride induced corrosion is one of the major causes of RC structures deterioration in the marine environment that leads to performance degradation and premature failure before the expected service life. From the literature, cathodic protection (CP) is one of the reliable repairing methods that proven to control chloride-induced corrosion. Therefore, sacrificial anodes, which is one of CP types with less instrument and maintenance requirement, have been used to limit the extent of concrete replacement due to chloride contamination and extend the service life of damaged RC structures. However, the specification of the repair method by sacrificial anodes in RC members is still unclear. The objective of this study is to find a suitable repair strategy on naturally damaged RC beam structures by sacrificial anodes cathodic protection. This dissertation consists mainly of seven chapters.

Chapter 1 explains the background of the study, research objectives and limitations, research contribution and standing point, and dissertation arrangement.

Chapter 2 describes the literature review from the previous study related to the durability issues in the RC structures due to chloride-induced corrosion; corrosion inspection, assessment, and monitoring method; and repair method of chloride-induced corrosion in RC structures.

Chapter 3 presents the fundamental research on the utilization of sacrificial anodes in laboratory cases. From the viewpoint of arresting macro-cell corrosion due to different chloride contamination after five years of observation, the point sacrificial anodes in the repair part is still generating protection to the segmented steel bars indicated by the depolarization test value. The longer the span of repair part, the higher depolarization value. In the preparation of sacrificial anodes application, rust removal process on steel surface in repair concrete is the most desirable initial condition of steel bars when the sacrificial anode is applied to it. Regarding the temperature in the exposure condition, it can be reported that the application of sacrificial anodes in low temperature around -17°C performs a good result until three years but four years of utilization sacrificial anodes in high temperature (40°C) presents not effective protection due to crack formed around the steel bar protected by anodes. The experiment to reduce the high anode consumption in the early connection was

succeeded in the last part of this chapter by the implementation of half of the initial sacrificial anodes current flow by using the impressed-current method.

Chapter 4 demonstrates repair methods by sacrificial anodes cathodic protection in more than 40-years severely damaged RC beams. RC-1 and RC-2 present the application of sacrificial anodes in patch repair to protect patch area only due to the electrochemical incompatibility of polymer mortar and existing concrete and after one year, the additional sacrificial anodes were applied in the non-patch repair. Both RC-1 and RC-2 show good protection identified by depolarization and improved steel bar conditions in all cross-sectional of the beams. RC-3 and RC-4 present the application of sacrificial anodes in non-patch repair only while the corrosion inhibitor was painted in the steel bar surface in the patch repair area. The corrosion inhibitor membrane reduces the required electric current for attaining the steel bar potential change in the patch repair. So, the application of corrosion inhibitor is recommended in RC structures repaired by sacrificial anodes. From RC-1~RC-4, it can be seen that small current flow generated by sacrificial anodes affects not only on polarization but also modifies the steel bar condition. Depolarization values of more than 100 mV cannot have a significant effect on the improvement of steel bar conditions. The application of sacrificial anodes in the patch and non-patch repair is also presented in RC-5. The obtained result indicates that the repair method by combining a different kind of sacrificial anodes in the patch and non-patch repair presented no significant polarization of rebar nor current flow. Therefore, the combined sacrificial anodes in the patch and non-patch repair method at the same time with closed distance could not be suitable repairing system.

Chapter 5 illustrates the utilization of titanium wire sensors as a new embeddable corrosion monitoring sensor in four RC members repaired by sacrificial anodes cathodic protection. Titanium wires sensor (TWS) is working as a corrosion monitoring sensor in concrete with stable potential reading in around the areas wherein it is embedded until 18 months of exposure. It is indicated by the stable potential development of sensors vs. time and current density of sacrificial anodes.

Chapter 6 formulates the proper sacrificial anode cathodic protection application method in the deteriorated RC beams. The installation of sacrificial anodes in patch repair deliver limited protection in patch repair only. If the sacrificial anodes were installed in existing concrete, it could cover protection not only in existing concrete but also in some part of patch repair. The application of sacrificial anodes both in the patch and in non-patch repair can protect a bigger area, but the time-lapse application is important. The design

parameters of SACP application including environmental conditions, structural deterioration degree, and repairing technology are performed by the different protective current density and depolarization set values.

Chapter 7 conveys a summary, conclusion, and recommendation for future research.

Table of Contents

List of Tables

List of figures

CHAPTER I

General Introduction

1.1 Background of study

Reinforced concrete (RC) has been one of the most utilized materials in the construction sector, especially in the construction of bridges, ports, buildings, tunnels, and skyscrapers (Shi *et al.*, 2012; Aguirre-Guerrero and Guiérrez, 2018). Nowadays, RC is an ideal construction material due to the characteristic of composite material with the amalgamation of the high compressive strength of Portland cement concrete and the high tensile strength of steel bar (Bertolini *et al.*, 2004). The environment variety that RC structures are exposed to make it necessary to consider the durability of the concrete as an additional property to the mechanical strength because the service life of the structure depends on its durability (Neville, 2001).

The main problem of RC's durability is the corrosion of the steel bar, which diminishes the mechanical and structural properties (Bertolini *et al.*, 2004). The aggressive exposure environments mainly cause the corrosion of the steel bar, mostly the existence of chloride ions and/or carbonation (Ahmad, 2003). Non-carbonated concrete is defined as high alkalinity material with a pH between 12.6 and 13.6 (Alonso and Andrade, 1987). Under these pH conditions, the steel bar spontaneously forms a passive protective layer. The aggressive agents such as chloride ions and/or carbon dioxide can destroy this layer, which results in de-passivation (Bertolini *et al.*, 2004; Fajardo *et al.*, 2009). Chloride attack is one of the most aggressive causes that leads to corrosion of the steel bar. In this case, the chloride ions are spread through the concrete until they reach the steel surface, where they accumulate and reach a critical concentration. This chloride accumulation destroys the passive layer of the steel bar and begins the corrosive process (Angst *et al.*, 2009). Carbonation is a process in which carbon dioxide from the environment enters concrete. It decreases the alkalinity of concrete by reducing the pH to approximately 9. Therefore, the passive layer is destablished, which causes corrosion in the steel bar (Baccay *et al.*, 2006; Han *et al.*, 2013).

RC structures in the marine environment are particularly subjected to chloride-induced corrosion. Problems develop when the chloride-ion penetrates into concrete and reaches the steel bar surface. Steel bar, which is normally in a passive state due to the high alkalinity of

concrete, loses passivity and begins to corrode when a threshold level of chloride-ion concentration is exceeded (West and Hime, 1985). The corrosion products can occupy several times the original volume of steel bar, causing tensile forces to develop in concrete. These stresses lead to cracking of the concrete cover, delamination, spalling, and further corrosion damage to the structure (Steven, 2003).

Some of the countermeasures developed to stop chloride induced-corrosion focus on the reinforcement itself and other techniques to control corrosion by reducing the porosity of the concrete cover. The further corrosion damage also can be controlled by isolating the structure from the environment through surface protection treatments or by altering the kinetics of the reactions or electrochemical potential of the affected metals (Navarro, 2018). Several ways of the corrosion mitigation procedure on RC structures in marine environment are existed such as cathodic protection, coating, corrosion inhibitor, desalination, electrochemical realkalization (ER), and electrochemical chloride extraction (ECE) (Bertolini *et al.*, 2004; Cardenas *et al.*, 2010; Karthick *et al.*, 2016; Kupwade-Patil *et al.*, 2012; Pan *et al.*, 2008). Among these methods, cathodic protection (CP) is the oldest, and it has been widely used in steel structures submerged in water. The application of CP in concrete began around 1955 for submerged and buried structures. Since the mid-1970s, cathodic protection has been used in RC structures such as buildings, bridged, tunnel, etc. Therefore, CP is the standardized electrochemical technique in some countries (Martínez *et al.*, 2009). The general principle of CP is a corrosion mitigation method that imposes an external voltage on the steel bar surface, which forces the steel bar to become cathodic, thereby mitigating corrosion. Both impressed current (active systems) and galvanic or sacrificial anode (passive systems) are used. CP is still considered one of the only technologies that have proven to stop corrosion of steel bar, regardless of the chloride-ion contamination in concrete (Daily, 2003).

During the application of CP especially sacrificial anodes, patch repairs are sometimes necessary to remove of all cracked and delaminated concrete, cleaning of all corroded steel bar, application of the protective coating on the embedded steel bars, and repairing with new mortar material or micro concrete (Ali *et al.*, 2018). Patch repair has limited success against chloride-induced corrosion because of the surrounding chloride-contaminated concrete; as a result, the steel bar continues to remain susceptible to corrosion (Morgan, 1996; Miyagawa, 1991). The patched area of new repair material often causes the formation of incipient anodes or macro-cell corrosion adjacent to the repairs (Ali *et al.*, 2018).

There are a few crucial factors, which should be considered in selecting a suitable durable repair strategy, such as the level of deterioration, specific condition of structures, and the environmental condition (Morgan, 1996; ACI 546R, 2014; ACI 562M, 2016).

1.2 Research objective and limitation

The objective of this study is to find a suitable repair strategy on naturally damaged RC beam structures by sacrificial anodes cathodic protection. Several considerations of utilization sacrificial anodes in repair structures were demonstrated in laboratory cases such as temperature effects, steel surface condition, the ability of sacrificial anodes to mitigate macro-cell corrosion, and an attempt to decrease the high consumption of sacrificial anodes in the early stage of repair. Further, the application of several repair methods on 44-years naturally damaged RC beams structures using sacrificial anodes, patch repair, and corrosion inhibitor were presented as a field case. In addition, a new corrosion monitoring device made of titanium probe iridium-enriched mixed with metal oxide was used as a new sensor in repair strategy. The repair and maintenance procedures based on laboratory and field applications were presented in the last part of this study. The limitation of this study is that the deterioration of RC structures results from chloride-induced corrosion. The observation of corrosion monitoring sensor is limited only in the repaired RC members.

1.3 Research contribution and standing point

This study completes an evaluation of the repair methods of serious corrosion damaged RC beam structures, specifically using sacrificial anodes cathodic protection on 44-years naturally damage RC beam structures. This result is necessary for the maintenance procedure of actually damaged structures in the marine or aggressive environment during the service life.

1.4 Dissertation arrangement

Figure 1.1 illustrated the dissertation arrangement which is composed of seven chapters as follows.

Chapter 1 describes the background of this study, research objectives, limitations, research contribution, and standing point.

Chapter 2 discusses the literature review related to corrosion and corrosion protection method by cathodic protection in RC structures at the current situation and the issues to be addressed in this research.

Chapter 3 demonstrates the fundamental study and discussion of the effectiveness of sacrificial anodes cathodic protection on RC structures in laboratory cases. Some considerations during the application of sacrificial anodes cathodic protection such as the effect of the rust removal process on steel bar surface before repair, the influence of high and low temperature, and the occurrence of macro-cell corrosion in repair RC member are presented. The method of reducing the high current consumption of sacrificial anodes in the early stage is also reviewed.

Chapter 4 presents the field case demonstration on repair strategy of 44-years naturally damaged RC beams using sacrificial anodes cathodic protection.

Chapter 5 contains the utilization of a new embeddable corrosion monitoring sensor in repaired RC member.

Chapter 6 formulates the design and maintenance procedure of repair method by sacrificial anodes cathodic protection applied to RC structures based on Chapter 4 and Chapter 5.

Chapter 7 summarizes the results obtained from Chapter 3 to Chapter 6. Some future research works were recommended based on the results.

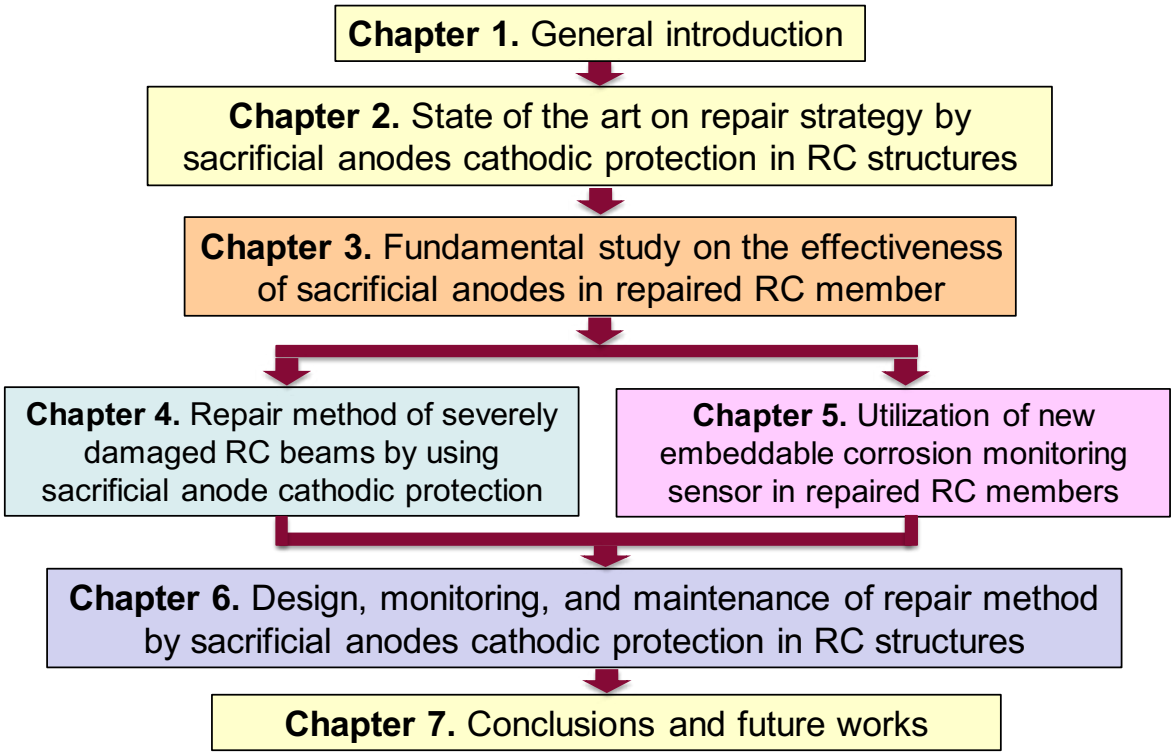

Figure 1.1 Flowchart of dissertation arrangement

1.5 References

ACI 546R-14, 2014. "Guide to Concrete Repair", *in American Concrete Institute (ACI) Committee 546.* Farmington Hills, MI.

ACI 562M-16, 2016. "Code requirements for assessment, repair and rehabilitation of existing concrete structures and commentary", *American Concrete Institute (ACI) Commitee 562.* Farmington Hills, MI.

Ahmad, S., 2003. "Reinforcement corrosion in concrete structures, its monitoring and service life prediction – a review". *Cem. Concr. Compos.* Vol. 25 (4–5), 459–471.

Aguirre-Guerrero, A. M, Guiérrez, R. M., 2018, "Eco-efficient Repair and Rehabilitation of Concrete Infrastructures: Part 13 – Assessment of corrosion protection methods for reinforced", *Woodhead Publishing Series in Civil and Structural Engineering,* pp. 315-353.

Ali, M. S., Leyne, E., Saifuzzaman, M., Mirza, M. S., 2018. "An experimental study of electrochemical incompatibility between repaired patch concrete and existing concrete". *Construction and Building Materials*, Vol. 174, pp. 159-172.

Alonso, C., Andrade, C., 1987. "Corrosion behavior of steel during accelerated carbonation of solutions which simulate the pore concrete solution". *Materiales de construccio´n.* 37 (206), 5–16.

Angst, U., Elsener, B., Larsen, C.K., Vennesland, Ø., 2009. "Critical chloride content in reinforced concrete—a review", *Cem. Concr. Res.* Vol. 39, No. 12, pp. 1122–1138.

Baccay, M.A., Otsuki, N., Nishida, T., Maruyama, S., 2006. "Influence of cement type and temperature on the rate of corrosion of steel in concrete exposed to carbonation", *Corrosion,* Vol. 62, No. 9, pp. 811–821.

Bertolini, L., Elsener, B., Pedeferri, P., Polder, P., 2004. "Corrosion of Steel in Concrete: Prevention, Diagnosis, Repair", *Wiley-VCH Verlag GmbH & Co. KGaA,* Weinheim.

Cardenas, H., Kupwade-Patil, K., Eklund, S., 2010. "Corrosion mitigation in mature reinforced concrete using nanoscale pozzolan deposition", *J. Mater. Civil En,* Vol. 23, No. 6, 752–760.

Daily, S. F., 2003. "Galvanic cathodic protection of reinforced and prestressed concrete using thermally sprayed aluminium coating", *Concrete Repair Bulletin,* July/August 2003.

Karthick, S.P., Madhavamayandi, A., Muralidharan, S., Saraswathy, V., 2016. "Electrochemical process to improve the durability of concrete structures", *J. Build. Eng.* Vol. 7, pp. 273–280.

Kupwade-Patil, K., Cardenas, H.E., Gordon, K., Lee, L.S., 2012. "Corrosion mitigation in reinforced concrete beams via nanoparticle treatment", *ACI Mater. J.* Vol. 109, No. 6.

Fajardo, G., Valdez, P., Pacheco, J., 2009. "Corrosion of steel rebar embedded in natural pozzolan based mortars exposed to chlorides", *Constr. Build. Mater.* Vol. 23, No. 2, pp. 768–774.

Han, S.-H., Park, W.-S., Yang, E.-I., 2013. "Evaluation of concrete durability due to carbonation in harbor concrete structures", *Constr. Build. Mater.* Vol. 48, pp. 1045–1049.

Martínez, I., Andrade, C., Castellote, M., de Viedma, G.P., 2009. "Advancements in nondestructive control of efficiency of electrochemical repair techniques", *Corros. Eng., Sci. Technol.* Vol. 44, No. 2, pp. 108–118.

Morgan, D. R., 1996. “Compatibility of concrete repair materials and systems”, *Construction and Building Materials,* Vol. 10, No. 1, pp. 57-67.

T. Miyagawa, 1991. “Durability design and repair of concrete structures: chloride corrosion of reinforcing steel and alkali-aggregate reaction”, *Mag. Concr. Res.* Vol. 43, No. 156, pp. 155–170.

Navarro, I. J., Yepes, V., and Marti, J. V., 2018, “Life cycle cost assessment of preventive strategies applied to prestressed concrete bridges exposed to chlorides”, *Sustainability*, 10, 845.

Neville, A., 2001. “Consideration of durability of concrete structures: past, present, and future”, *Mater. Struct.* Vol. 34, No. 2, pp. 114–118.

Pan, T., Nguyen, T., Shi, X., 2008. “Assessment of electrical injection of corrosion inhibitor for corrosion protection of reinforced concrete”, *Transp. Res. Rec. J. Transp. Res. Board.* Vol. 2044, pp. 51–60.

Shi, X., Xie, N., Fortune, K., Gong, J., 2012. “Durability of steel reinforced concrete in chloride environments: an overview”, *Constr. Build. Mater.* Vol. 30, 125-138.

Steven, F. D., 2003, “Galvanic cathodic protection of reinforced and prestressed concrete using a thermally sprayed aluminum coating”, *Concrete Repair Bulletin*, July/August 2003.

West, R. E and Hime, W. G., 1985, “Chloride profiles in salty concrete”, *Materials Performance,* vol. 24, pp. 29-36.

CHAPTER II

State of the art on repair strategy by sacrificial anodes cathodic protection in RC structures

2.1 Introduction

In this chapter, several kinds of literature regarding deterioration and repair strategy of corrosion damaged RC structures are reviewed. The detailed information of the cathodic protection system from the previous researcher is presented as well. The application of cathodic protection in concrete from some experienced countries was shown. In addition, the present issues that address in this study are discussed in the last part of this chapter. The organization of content in this chapter is summarized as follows.

2.2 Durability of RC structures

Durability of RC structures in the marine environment depends on the deterioration of concrete and the steel bar corrosion (Okada, 1976). Further, the corrosion affected by two phenomena either cracked on concrete surface or chloride penetration. Both crack and chloride could exist even from the beginning or even during service life. These two problems are related to each other. When the reinforcing steel rusts, the corrosion products generally occupy considerably more volume than that of the original steel (CEB, 1989). It promotes

the internal pressure inside the concrete and initiates the concrete cover cracked and spalled. As a result, the rate of corrosion is accelerated.

One of the most common causal factors of reinforcement corrosion is the ingress of chloride ions through the concrete pore network when the concrete is located in marine environments. Chloride ions cause localized corrosion of the reinforcement and, therefore, produce premature and unexpected structural failure. Chloride penetration may occur either by diffusion from water-saturated concrete or due to absorption/desorption phenomena throughout the wet/dry cycle in tidal or splash zone exposure. These cycles produce faster chloride ion ingress mechanisms because, besides diffusion, capillary absorption or saline mist phenomena also induce higher moisture diffusivity. Chloride penetrating through concrete cover to steel bar breaks the passivation of reinforcement to initiate corrosion.

The deterioration progress of RC structures from chloride attack involves the initiation, propagation, acceleration, and deterioration stages (JSCE, 2007), as shown in **Figure 2.1**. In each stage, the deterioration has different influences on the RC member. The degree of deterioration progress with performance degradation also varies according to the performance attribute under investigation.

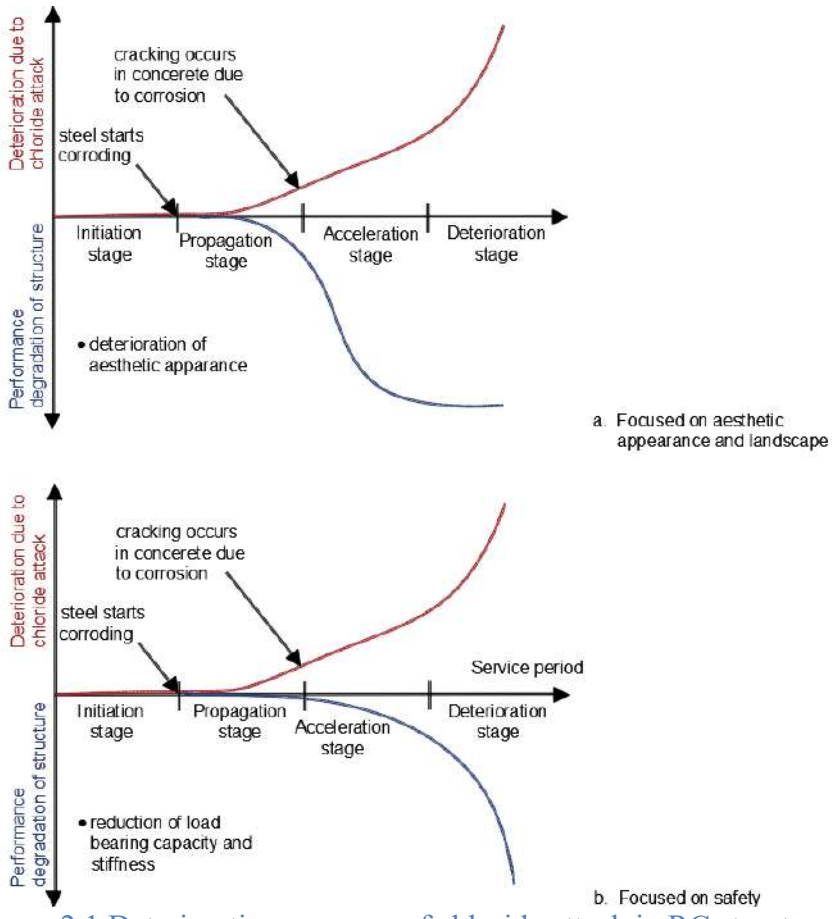

Figure 2.1 Deterioration progress of chloride attack in RC structures

Table 2.1 and **Table 2.2** present the definition and criteria for the diagnosis of deterioration degree (JSCE, 2007).

Table 2.1 Definition of deterioration stages due to chloride attack (JSCE, 2007)

Stage of deterioration	Definition	Stage determined by
Initiation	Until the chloride ion concentration on the surface of the steel reaches the marginal concentration for the occurrence of corrosion (standard value is 1.2 kg/m^3).	Diffusion of chloride ions Initially contained chloride ion concentration.
Propagation	From the initiation of steel corrosion until cracking due to corrosion.	Rate of steel corrosion.
Acceleration	Stage in which steel corrodes at a high rate due to cracking due to corrosion.	Rate of corrosion of steel with cracks.
Deterioration	Stage in which load-bearing capacity is reduced considerably due to the increase of corrosion amount.	

Table 2.2 Criteria for diagnosis of deterioration degree (JSCE, 2007)

Evaluation Items	Deterioration Degree					
	0	1	2	3	4	5
Corrosion of steel bar	None	Rust spots found on the concrete surface	Partial rust stains found on the concrete surface	Significant rust staining	Significant floating rust	A dramatic increase in the amount of floating rust
Cracking	None	Partial cracks found on the concrete surface	Some cracks	Many cracks, including some of several mm or more in width	Many cracks of several mm in width	-
Spalling covering concrete	None	None	Partial floating concrete found	Partial spalling found	Significant spalling	Drastic spalling

2.2.1 Corrosion mechanism

A highly alkaline pore solution in concrete with pH between 12.6 and 13.6, principally of sodium and potassium hydroxides, is formed during the hydration process of cement in concrete (Bertolini *et al.*, 2004). The thermodynamically stable compounds of iron are iron oxides and oxyhydroxides in this environment. A thin protective oxide film (the passive film) is formed spontaneously on ordinary steel bars embedded in alkaline concrete (Stratfull, 1957; Stratfull, 1974; Pedeferry, 1965). The passive film is only consisted of a few nanometers thick and is composed of more or less hydrated ion oxides with varying degree of Fe^{2+} and Fe^{3+} (Page, 1997). The passive film protects and immune to mechanical

damage of the steel surface, and it can be destroyed by carbonation of concrete or by the existence of chloride ions, then the steel bar is depassivated (Bertolini et al., 1998).

The stability of iron metal as a function of potential and pH called the Pourbaix diagram is presented in **Figure 2.2.** The region of immunity shown in the Pourbaix diagram for Fe–H_2O reveals that the corrosion cannot occur in this region. For instance, at a point *X* in the diagram as the activity of Fe^{2+} would be very low (~10^{-10}). As iron is transformed into soluble species in the corrosion region, it is expected that iron would corrode. An oxide species in contact with an aqueous solution along a boundary will not allow corrosion to proceed if it is impervious and highly adherent. The thin layer of oxide on the metal surface, such as Fe_3O_2 or Fe_3O_4, is highly protected under the above condition. Metals like steel are known to resist corrosion because of the development of oxide films in the air (Ahmad, 2006).

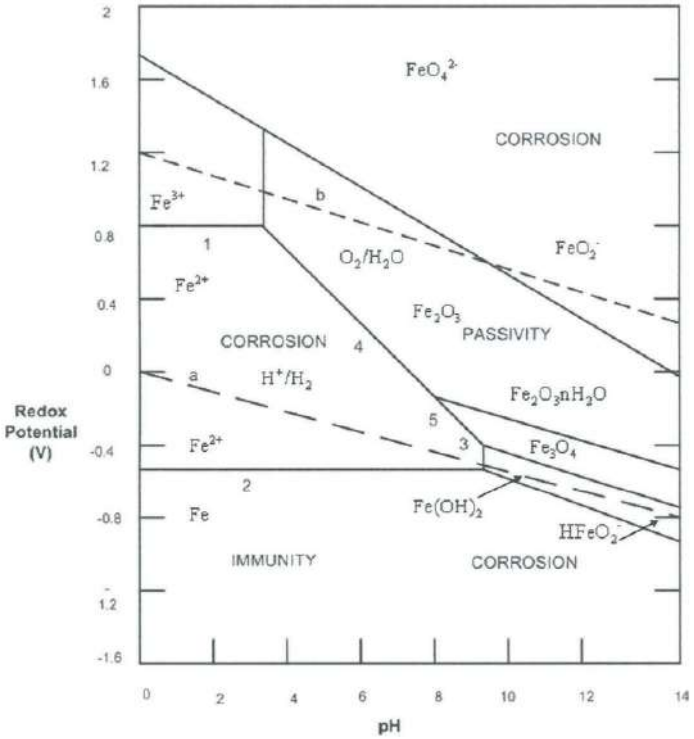

Figure 2.2 Potential-pH diagram for iron (Ahmad, 2006)

Corrosion in concrete is the process in which iron at the anode and oxygen is reduced at the cathode, with the electrons flowing in the steel surface between anode and cathode. The electrolyte is the alkaline pore solution while the steel bar serves as the metallic path between the anode and cathode in RC members. The anodes and cathodes are formed on the steel surface are depicted in **Figure 2.3.** The anodic reaction leads to the iron cations formation

is shown in **Equation 2.1**, and **Equation 2.2** presents the cathodic reaction, which balances the anodic reaction by oxygen reduction with hydroxyl anions production.

Anodic reaction: $Fe \rightarrow Fe^{2+} + 2e^-$ **(2.1)**

Cathodic reaction : $\frac{1}{2}O_2 + H_2O + 2e^- \rightarrow 2OH^-$ **(2.2)**

In the RC structures case, the stability of the passive film on the steel bar was built from the combination of the products of the anodic and the cathodic reaction. Oxygen availability and the pH value in the interface of steel bar/concrete are the main factors of the stability of this passive film (Rincón *et al.*, 2008). Steel bar embedded in concrete is naturally protected against corrosion by the high alkalinity of the cement pore solution (pH > 12.5) and by the barrier effect of the concrete cover, which limits the oxygen and moisture required for active corrosion. The high pH suppresses steel corrosion by permitting the formation of a very thin (1-10 nm thick) passivating ferric oxide film (γ-Fe_2O_3) on the steel surface (Richardson, 2002). Either a reduction in alkalinity (typically in carbonated concrete) or by chloride ingress in the marine environment can be disrupted or de-passivated the passive layer on the steel. Depassivation renders the steel thermodynamically liable to corrode; whether it does so depend primarily on the availability of moisture and oxygen at the cathode.

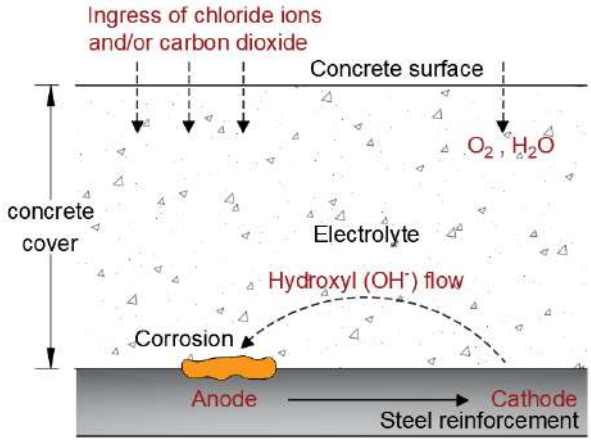

Figure 2.3 A schematic illustration of the corrosion process in concrete

In the presence of chloride ions, oxygen, and water in concrete, they may act as a catalyst by introducing additional anodic reactions are represented in **Equation 2.3.**

$$Fe + 3Cl^- \rightarrow FeCl_3^- + 2e^-$$

Followed by $FeCl_3^- + 2OH^- \rightarrow Fe(OH)_2 + 3Cl^-$

or

$$Fe + 4Cl^- \rightarrow FeCl_4^{2-} + 2e^-$$

Followed by $FeCl_4^- + 2OH^- \rightarrow Fe(OH)_2 + 4Cl^-$

or

$$Fe + 6Cl^- \rightarrow FeCl_3{}^{3-} + 3e^-$$

followed by $$FeCl_3{}^{3-} + 2OH^- \rightarrow Fe(OH)_2 + 6Cl^- \quad \textbf{(2.3)}$$

These reactions remove ferrous of ferric ions from the steel by forming complex ions with the chlorides then deposited near the anode where they join with hydroxyl ions to form various corrosion products. The chloride ions are released to repeat the process. Secondary reactions may occur due to the expansive products of corrosion. Although the Fe^{2+} and OH^- ions both diffuse into the concrete (from anode to cathode, respectively), the corrosion products formed near the anode because of the OH^- ions are smaller and more diffuse through the concrete more readily (Bertolini, 2013). If the supply of oxygen is restricted, ferrous oxides and hydroxides form (**Equation 2.4** and **Figure 2.3)** as follows.

$$Fe^{2+} + 2(OH)^- \rightarrow Fe(OH)_2$$

or

$$Fe^{2+} + 2(OH)^- \rightarrow FeO + H_2O \quad \textbf{(2.4)}$$

If the oxygen is available, ferric oxides and hydroxides form (**Equation 2.5**) (Christodoulou, 2008; Bertolini, 2013).

$$2Fe(OH)_2 + \tfrac{1}{2}O_2 \rightarrow Fe_2.H_2O + H_2O \quad \text{(red rust)}$$

or $$2Fe(OH)_2 + \tfrac{1}{2}O_2 + H_2O \rightarrow 2Fe(OH)_3 \quad \text{(red rust)}$$

or $$3Fe(OH)_2 + \tfrac{1}{2}O_2 \rightarrow Fe_3O_4 + 3H_2O \quad \text{(black rust)}$$

or $$2FeO + \tfrac{1}{2}O_2 + H_2O \rightarrow Fe_2O_3.H_2O \quad \text{(red rust)}$$

or $$2FeO + \tfrac{1}{2}O_2 + 3H_2O \rightarrow 2Fe(OH)_3 \quad \text{(red rust)}$$

or $$3FeO + \tfrac{1}{2}O_2 \rightarrow Fe_2O_4 \quad \text{(black rust)} \quad \textbf{(2.5)}$$

The preceding chemical reactions show the transformation of steel from ferrous hydroxides ($Fe(OH)_2$), which will react with oxygen and water to produce ferric hydroxides ($Fe(OH)_3$), and the last component, which is the hydrated ferric oxide (rust); its chemical term is $Fe_2O_3.H_2O$. Ferric hydroxide has more effect on concrete deterioration and spalling of concrete cover as its volume will increase the volume of the original steel bars by about two times or more. When iron goes to hydrated ferric oxides in the presence of water, its

volume will increase more to reach about six times its original volume and will become soft. In this stage, cracks on concrete start until the concrete cover falls; rust, with its brown color, can be seen on the steel bar. Iron (Fe) that has been converted to Fe^{2+} can produce the corrosion products of hydroxides, oxides, and oxide-hydroxides, depending on conditions of temperature, atmospheric pressure, potential, and pH. These corrosion products occupy larger volumes than the original iron, as shown in **Figure 2.4**. The expansion volume of these corrosion products causes cracking and spalling in the concrete cover.

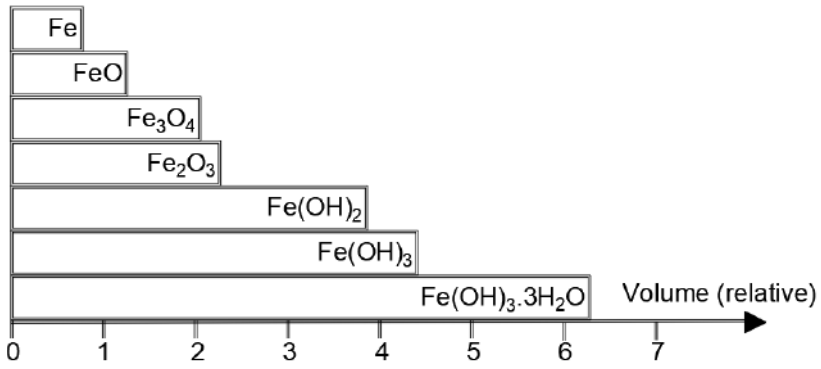

Figure 2.4 Relative volume of iron corrosion product (Liu, 1996)

2.2.2 Chloride-induced corrosion

Chloride-induced corrosion is a frequent cause of steel bar corrosion (Arup, 1983). The recent standard design codes for reinforced concrete structures impose restrictions on the amount of chloride that may be introduced from raw materials containing significant amounts of chlorides. According to European standard EN 206, the maximum allowable chloride contents are 0.2%-0.4% chloride ions by mass of binder (Bertolini, 2004). These restrictions are aimed to reduce the corrosion risk due to chloride in the fresh concrete mix. In some RC structures in the past, chlorides have been unknowingly added to the concrete mix, through contaminated mixing water, aggregates (sea gravel or sands without washing them with chloride-free water) or admixtures (calcium chlorides, which is now prohibited, in the past was the most common accelerating admixture). The other chloride source in concrete is penetration from the environment in the marine environment in a road structure in the regions where chloride-bearing de-icing salts are used in wintertime (Bertolini, 2004).

Corrosion of steel bar in non-carbonated concrete can only take place once the chloride contamination in concrete in contact with the steel surface has reached a threshold value. This threshold value depends on several parameters; however, the electrochemical potential of the steel bar, which is related to the amount of oxygen that can reach the steel surface, has a major influence. Relatively low levels of chlorides are sufficient to initiate corrosion in

structures exposed to the atmosphere, where oxygen can easily reach the steel bar. Much higher levels of chlorides are necessary for structures immersed in seawater or in zones where the concrete is water-saturated so that oxygen supply is hindered, and thus the potential of the steel bar is rather low (Arup, 1983; Pedeferri, 1996; Alonso *et al.*, 2000; Bertolini *et al.*, 2004).

2.2.3 Forms of corrosion

Corrosion may result from many different sets of circumstances (Akid, 2004). Corrosion in concrete is electrochemical and therefore requires electron transfer between anodic and cathodic sites. In the case where the anodic and cathodic processes are distributed homogeneously over the metal surface, as demonstrated in **Figure 2.5** Schematic illustration of (a) uniform and (b) localized or macrocell corrosion (Akid, 2004)**(a),** uniform corrosion has occurred. Where oxidation and reduction reactions occur at fixed, spatially separated sites, localized corrosion, or macro-cell corrosion results, as shown in **Figure 2.5 (b)**.

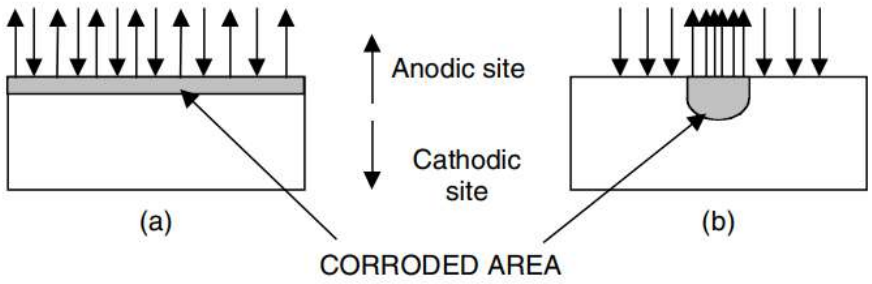

Figure 2.5 Schematic illustration of (a) uniform and (b) localized or macrocell corrosion (Akid, 2004)

Chlorides lead to a local breakdown of the protective oxide film on the steel bar in alkaline concrete so that a subsequent localized corrosion attack takes place. Areas no longer protected by the passive layer act as anodes (active zones) concerning the surrounding still passive areas where the cathodic reaction of oxygen reduction takes place. The detailed illustration of macro-cell corrosion is shown in **Figure 2.6**.

If very high levels of chlorides reach the steel surface, the attack may involve larger areas, so that the morphology of pitting will be less evident. Once corrosion has initiated, a very aggressive environment will be produced inside pits. The current flowing from anodic areas to surrounding cathodic areas both increases the chloride content (chlorides, being negatively charged ions, migrate to the anodic region) and lowers the alkalinity (acidity is produced by hydrolysis of corrosion products inside pits). On the contrary, the current strengthens the protective film on the passive surface since it tends to eliminate the chlorides,

while the cathodic reaction produces alkalinity. Consequently, both the anodic behavior of active zones and the cathodic behavior of passive zones are stabilized. Corrosion is then accelerated (autocatalytic mechanism of pitting) and can reach very high rates of penetration (up to 1 mm/y) that can quickly lead to a remarkable reduction in the cross-section of the rebars.

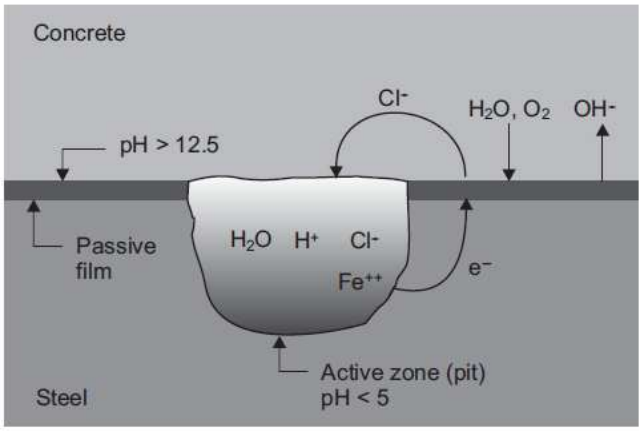

Figure 2.6 Detailed schematic illustration of macro-cell corrosion of steel bar in concrete

Macro-cell corrosion may occur on both the microscopic and macroscopic scale and is the most destructive type of corrosion. In the case of macro-cell corrosion, the rate of metal loss is often very unpredictable. It applies particularly to pitting in which the location, distribution, and size of pits depend upon the precise microstructure and environmental condition prevailing. Several factors control the rate of macro-cell corrosion as follows (Akid, 2004).

- **Anode/cathode area ratio**. The rate of reaction is governed by the relative surface areas of the anode and cathode and will be limited by the smallest surface area. The local attack will, therefore, be more pronounced when the cathodic area is larger than the anodic area. This occurs because the anodic process is confined to a relatively small area, and therefore a large anodic current can be sustained through the availability of a large cathode area.
- **Differential aeration cells**. Differential aeration cells can arise when a metal is in contact with a solution in which the concentration of oxygen within the solution differs from one site to another. This may be the result of limited transport of oxygen due to inadequate solution agitation. The concentration of oxygen determines the corrosion rate and the site at which the cathodic reaction takes place. As oxygen is easily replaced where the electrolyte is exposed to the atmosphere, this area is favored for the cathodic

reduction of O_2 to OH^-. The site of lower oxygen concentration, that is, below the waterline, favors the formation of anodic sites.

- **Changes in solution pH**. The pH value of a solution is dependent upon the concentration of H^+ (in the form of H_3O^+) or correspondingly of OH^- ions. Where the dissolved oxygen of H+ are involved in the corrosion reactions, the rate of the anodic and cathodic reactions will, therefore, depend upon the pH of the solution. For the near-neutral solutions, the cathodic reaction (reduction of oxygen/water to hydroxide) involves a decrease in acidity, that is, an increase in pH, while the anodic reaction, via hydrolysis, leads to a decrease in pH, that is, an increase in H^+ concentration.
- **Corrosion products and deposits**. Corrosion products such as surface films, for example, oxide films/layer, often have the effect of reducing the overall rate of corrosion, for example, stainless steels depend for their corrosion resistance on a thin chromium oxide film. However, if these surface films are disrupted, for example, by cracking under stress, then localized corrosion may result. Where deposits lie on the surface of a metal, cathodic sites are often formed at the outer edge of the deposit. As the degree of aeration decreases away from this location, that is, toward the center of the deposit, corrosion activity (dissolution) is favored beneath the deposit.
- **Active–passive cells.** Passivity is a property exhibited by a material when an insoluble film forms on the corroding surface preventing metal – electrolyte contact, hence greatly reducing the corrosion rate. Where a surface has lost its passive film, that is, is depasivated, the local corrosion rate increases markedly. The electrode potential of the passive and active surfaces differ, and an electrochemical cell is formed. The magnitude of corrosion enhancement depends upon the ratio of active and passive surface areas and the nature of the electrolyte. Usually, the passive (cathodic) surface is far more significant than the active (anodic) surface and rapid localized corrosion results.

2.2.4 Electrochemical aspects of corrosion in concrete

The corrosion process of the steel bar can be expressed with the following reaction.

Iron + oxygen + water → corrosion product **(2.6)**

The electrochemical reaction is composed of four partial processes (Pourbaix, 1973; Pedeferri, 1980; Shreir *et al.*, 1994; Revie, 2000), as follows.

- The oxidation of iron (anodic process) that liberates electrons in the metallic phase and gives rise to the formation of iron ions ($Fe \rightarrow Fe^{2+} + 2e^{-}$) whose hydrolysis produces acidity ($Fe^{2+} + 2H_2O \rightarrow Fe(OH)_2 + 2H^{+}$).
- The reduction of oxygen (cathodic process) that consumes these electrons and produces alkalinity ($O_2 + 2H_2O + 4e^{-} \rightarrow 4OH^{-}$).
- The transport of electrons within the metal from the anodic regions where they become available, to the cathodic regions where they are consumed (since the electrons carry a negative charge, this gives rise to a nominal electrical current flowing in the opposite direction).
- Finally, for the circuit to be complete, the flow of current inside the concrete from the anodic regions to the cathodic ones, transported by ions in the pore solution.

All of the processes are complementary, which is to say that they occur at the same rate. The anodic current I_a (i. e. the number of electrons liberated by the anodic reaction in a unit of time), the cathodic current I_c (i. e. the number of electrons that are consumed in the cathodic reaction), the current that flows inside the reinforcement from the cathodic region to the anodic (I_m) and finally the current that circulates inside the concrete from the anodic region to the cathodic (I_{con}), must all be equal, as demonstrated in **Figure 2.7**.

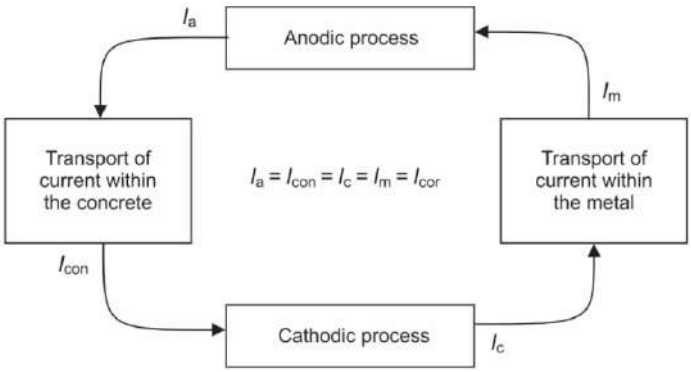

Figure 2.7 Electrochemical mechanism of corrosion of steel bar in concrete (Pedeferri and Bertolini, 2000)

The standard value of all these currents (I_{corr}) is, in electrochemical units, the rate of the overall process of corrosion. The corrosion rate will thus be determined by the slowest of the four partial processes. In reality, the electrical resistance of the steel bar is always negligible concerning that of the concrete. Therefore, the transport of current within the reinforcement is never a slow process and thus never contributes to reducing the rate of corrosion. Instead, under particular conditions inside the concrete, each of the other three

processes can take place at the negligible rate and thus become the kinetically controlling one. The corrosion rate is negligible when one of the following conditions exists.

- The anodic process is slow because the reinforcement is passive, as when the concrete is nor carbonated and does not contain chlorides.
- The cathodic process is slow because the rate at which oxygen reaches the surface of the reinforcement is low, as in the case of water-saturated concrete.
- The electrical resistance of the concrete is high, as in the case of structures exposed to environments, which are dry or low in relative humidity.

The first case is referred to as passive control, the second as control of oxygen transport, and the third as ohmic control. On the other hand, the corrosion rate is high in those cases where the three following conditions are present simultaneously:

- the reinforcement is no longer in the condition of passivity
- oxygen can reach the surface of the steel
- the resistance of the concrete is low (i. e. below 1000 Ωm).

The moisture content in concrete is the main factor controlling the corrosion rate. When concrete is in equilibrium with the atmosphere, the absorbed water can be correlated to the relative humidity of the environment. Actually, in real structures, this condition occurs typically only at the concrete surface. Often concrete is periodically wetted and, since it tends to absorb water more quickly than it releases it, the moisture content at a depth of the reinforcement tends to be higher than that of equilibrium with the humidity in the environment.

In concrete of low porosity, the maximum values of corrosion rate can be found for moisture content equivalent to the equilibrium with relative atmospheric humidity (R. H.) of about 95 %. For less dense concrete, it corresponds to equilibrium with atmospheres with a slightly higher R. H. Moving away from these values of humidity in either direction, the corrosion rate decreases (**Figure 2.8**) (Tuutti, 1982). Concrete with high water content (that is, near saturation) is characterized by low resistivity, but the oxygen diffusion is slow. The controlling process is then the cathodic process, and the corrosion rate will decrease as the water content increases until it nearly becomes zero in conditions of saturation. Conversely, in the concrete of lower water content, although oxygen diffusion can take place unhindered, the resistivity is high, and it increases as the moisture content decreases. The corrosion rate

then depends on the resistivity of the concrete; the lower the moisture content, the lower the corrosion rate.

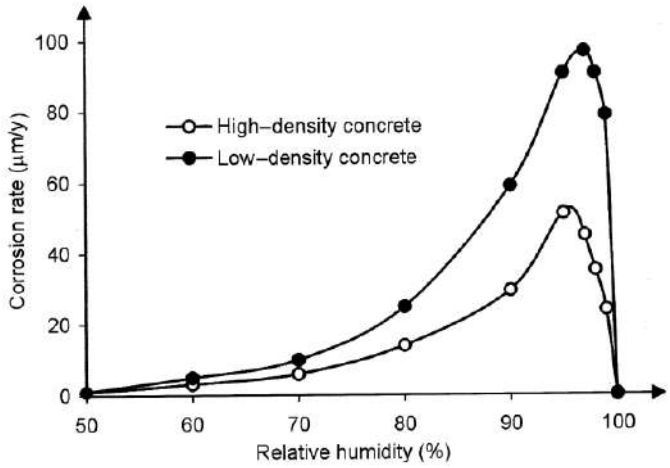

Figure 2.8 Corrosion rate as a function of external relative humidity in case of initiation due to chloride for concrete with low and high density (Tuutti, 1982)

The rate at which the anodic or the cathodic process takes place depends on the potential (E). The corrosion behavior of the reinforcement can be described employing polarization curves that relate the potential and the anodic or cathodic current density. Unfortunately, the determination of polarization curves is much more complicated for steel bars in concrete than in aqueous solutions, and often curves can only be determined indirectly, using solutions that simulate the solution in the pores of cement paste. This is only partly due to the difficulty encountered in inserting reference electrodes into the concrete and positioning them in such a way as to minimize errors of measurement. The main problem is that diffusion phenomena in the cement paste are slow. So when determining polarization curves, pH and ionic composition of the electrolyte near the surface of the reinforcement may be altered.

2.2.4.1 Concrete without chloride

Several electrochemistry parameters on steel bar corrosion in concrete without chloride are explained as follows.

2.2.4.1.1 Anodic polarization curve

In non-carbonated concrete without chlorides, the steel bar is passive, and a typical anodic polarization curve is shown in **Figure 2.9**. The potential is measured versus the saturated calomel reference electrode (SCE), whose potential is +244 mV versus the standard hydrogen electrode (SHE). Other reference electrodes used to measure the potential of steel bar in concrete are Ag/AgCl, $Cu/CuSO_4$, MnO_2, and activated titanium types. From this point

on in the text, unless explicitly stated otherwise, potentials are given versus the SCE electrode.

Iron tends oxidation at potentials more positive than the equilibrium potential of the reaction $Fe \rightarrow Fe^{2+} + 2e^{-}$, which is about −1 V SCE. Therefore, below −1 V steel is in a condition of immunity.

In the range of potentials between −800 mV and −600 mV, the anodic current is very low (0.1 μA/m^2) because the steel is covered by a very thin film of iron oxide that protects it completely (passive film). Thus in this interval of potentials, the dissolution rate of iron is negligible (~ 0.1 μm/y). (A dissolution rate of 0.1 mA/ m^2 corresponds to a penetration rate of about 0.1 μm/y. Such a low corrosion rate can only be measured electrochemically.) These are known as conditions of passivity, and they exist in the interval of potentials known as the *passivity range*.

In the interval of potentials between equilibrium and about −800 mV, the protective film does not form spontaneously. In this condition, called activity, steel can theoretically corrode. Nevertheless, given the proximity to equilibrium conditions, the rate of the anodic process is still negligible. To emphasize the fact that these conditions of activity are characterized by low corrosion rates because of this proximity to equilibrium, they are also called *quasi-immunity conditions*.

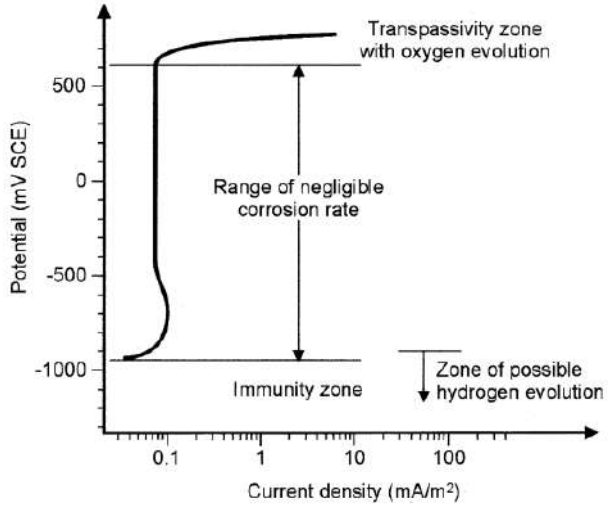

Figure 2.9 Schematic anodic polarization curve of steel in non-carbonated concrete without chlorides (Bertolini, 2004)

Above the passivity range, that is for potentials above about −600 mV, the steel is brought to conditions known as transpassivity: oxygen may be produced on its surface according to the anodic reaction of oxygen evolution: $2H_2O \rightarrow O_2 + 4H^+ + 4e–$, which

produces acidity. Steel reaches these conditions only in the presence of an external polarization (for example, in the presence of stray currents). Since the anodic reaction is oxygen evolution, the dissolution of iron and consequent corrosion of the steel does not take place (i. e. the passive film is not destroyed). Nevertheless, if these conditions persist until the quantity of acidity produced is sufficient to neutralize the alkalinity in the concrete in contact with the steel, the passive film will be destroyed, and corrosion will initiate.

2.2.4.1.2 Cathodic polarization curve

The kinetics of oxygen reduction is illustrated by the cathodic polarization curves a and b shown in **Figure 2.10**. Even if the equilibrium potential for oxygen reduction within the concrete (pH about 13) has a value of approximately –200 mV SCE, the reaction takes place at significant rates only at potentials below 0 mV SCE. The rate of the cathodic process for potentials lower than 0 mV SCE depends on the oxygen availability at the surface of the steel. For a given potential it decreases as the moisture content in concrete increases and is reduced by 2–3 orders of magnitude in passing from concrete in equilibrium with atmospheres of relative humidity (R.H.) of about 70 % ("semi-dry") to saturated concrete (in which the current density reaches values as low as about 0.2–2 mA/m^2, concerning the thickness of the concrete cover and the quality of the concrete). For potential values more negative than –900 mV SCE, along with the process of oxygen reduction, there is also that of hydrogen evolution ($H_2O + e^- \rightarrow H_{ad} + OH^-$), so that the cathodic current density begins to grow once again. If the concrete is completely saturated with water, and thus there is no oxygen, the only cathodic process possible is hydrogen evolution, and the cathodic polarization curve is curve *c*.

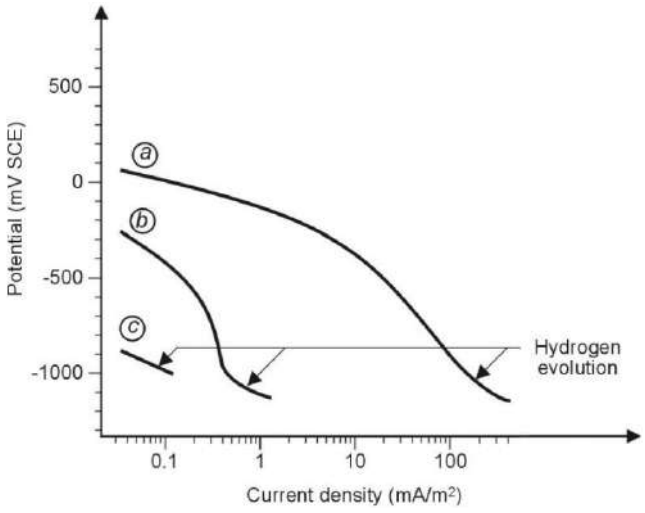

Figure 2.10 Schematic cathodic polarization curves in alkaline concrete: (a) aerated and semi-dry; (b) wet, (c) completely saturated with water (Bertolini, 2004)

2.2.4.2 Concrete containing chlorides

2.2.4.2.1 Corrosion initiation and pitting potential

The existence of chloride ions in concrete leads to variations in the anodic behavior of steel, modifying the anodic polarization curve, as shown in **Figure 2.11**. The passivity range is reduced because its upper limit, E_{pit}, known as the breakdown potential or pitting potential decreases as the chloride content increases (Page and Treadaway, 1982) it passes from values of about −600 mV SCE in uncontaminated concrete to values below −500 mV in concrete with a high content of chloride.

The presence of chloride ions produces, at more positive potentials than E_{pit}, localized breakdown of the passive film and thus allows the attack on the underlying metal. For potentials below E_{pit}, the action of chloride is, to a first approximation, negligible. The chloride content being equal, E_{pit} decreases as the pH of the pore solution in concrete decreases and as temperature and porosity increase. E_{pit} is difficult to measure with laboratory measurements since, during the measurement, significant variations of pH and chloride level in the concrete near the surface of the steel can be introduced, altering the result.

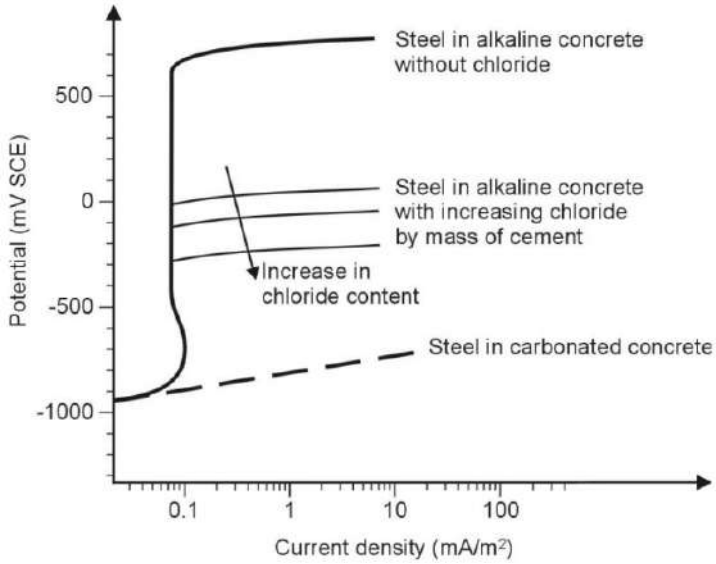

Figure 2.11 Schematic representation of the anodic polarization curve of steel in concrete with different chloride contents (Bertolini, 2004)

For a given potential of the steel, the highest content of chlorides compatible with conditions of passivity is the critical chloride content (or chloride threshold) at that potential. Structures exposed to the atmosphere (whose reinforcement operates at a potential around 0 mV vs. SCE) the critical level is usually considered to be in the range of 0.4 % to 1 % of the cement content. For structures immersed in water (whose reinforcement operates instead at

a much lower potential, around −400 to −500 mV vs. SCE) or for reinforcement that is cathodically polarized for any reason, the chloride threshold is much higher.

2.2.4.2.2 Propagation

Once the attack has initiated, acidity is produced progressively in the anodic zone, and the chloride level increases until stable conditions are reached. As shown in **Figure 2.6**, current that circulates from the anodic zones (which corrode) to the cathodic zones (passive) induces the transport of chlorides in the opposite direction (since they are negatively charged ions). Chlorides are thus concentrated in the area where the attack occurs. In addition, because of the hydrolysis of anodic products, acidity is created in the same zone (pH to levels, even below three can be reached in some cases). Consequently, the local environment becomes more and more aggressive. In time, a condition of "stable propagation" is reached, in correspondence with which there is equilibrium between chlorides carried by the current and those that move away by diffusion, and between hydrogen ions produced in the anodic zone and those that move away and/or hydroxyl ions (which move in the same direction of chloride ions).

In practice, the potential in structures exposed to the atmosphere is about −500 to −600 mV SCE in the anodic zones and about −100 to −200 mV SCE in the cathodic zones. Corrosion penetration may even exceed 1 mm/y in the most critical situations, which occur with high levels of chlorides and moisture content near saturation. For lower moisture contents, the ohmic resistance increases, and the corrosion rate slows down until it becomes negligible when humidity is less than that of equilibrium with an atmosphere of 40–50 % R. H.

2.2.4.2.3 Repassivation

Once pitting has initiated, circulation of current in the anodic region provokes and maintains an increase in acidity and chloride content, so that propagation may take place even if the potential of the steel is reduced, e. g. owing to an external cathodic polarization. This behavior is clarified in **Figure 2.12.** It shows the progress of current exchanged anodically during cyclical polarization in which the potential of the steel (by external polarization) is first raised above E_{pit} to initiate the localized attack and then lowered until conditions of passivity are established again.

It can be seen how to stop the attack, and it is necessary to reach a potential value, called the protection potential (E_{pro}) more negative than E_{pit}. Thus the interval of potential included

between E_{pit} and E_{pro} is characterized by the fact that it does not initiate the attack, but if the attack has already begun, it permits propagation of the attack. E_{pro} varies, as does E_{pit}, with chloride level, pH, and temperature, and the difference between them is of the order of 300 mV (**Figure 2.13**). Depending on the potential of steel and chloride content in the concrete, it is possible to define different domains where pitting corrosion can or cannot initiate and propagate, and other effects may take place.

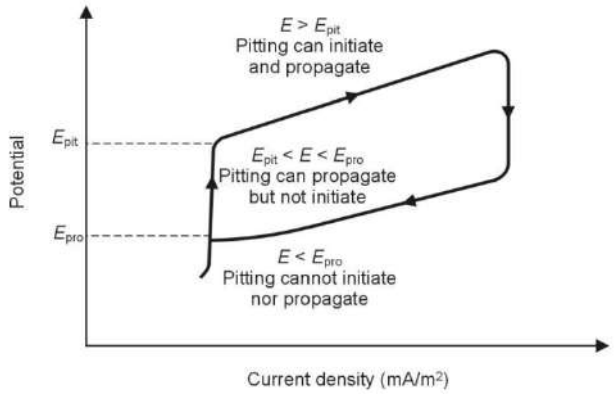

Figure 2.12 Schematic representation of a cyclic anodic polarization curve of an active-passive material in a chloride-containing environment: pitting potential (E_{pit}) and protection potential (E_{pro}) are identified (Pourbaix, 1973)

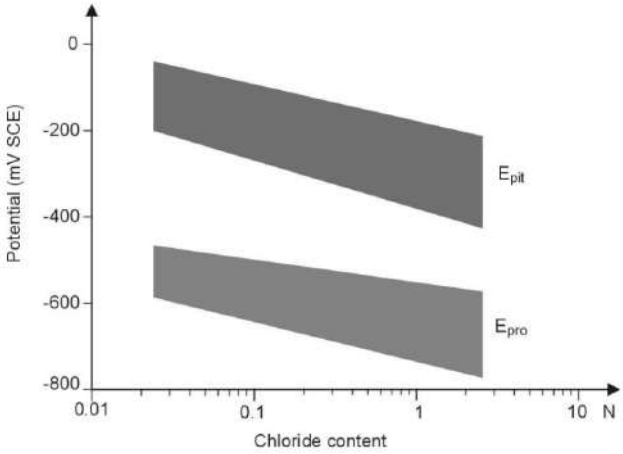

Figure 2.13 Values of the pitting (E_{pit}) and protection (E_{pro}) potentials determined with tests on steel immersed in saturated solutions of calcium hydroxide (pH=12.6) at various levels of chlorides (Cigna and Fumei, 1981)

2.2.4.2.4 Structures cathodically or anodically polarized

In the case of steel that exchanges a current I with the concrete from an external source, either anodic or cathodic, the relation $I_c = I_a$, which expresses equality between the electrons produced and consumed at the surface of the steel in the absence of exchanged current, should be modified. Electrons extracted or provided by the external current also have to be taken into consideration. If the current is exchanged anodically, the following condition occurs:

$I_a = I_c + |I|$ **(2.7)**

while for a current exchanged cathodically:

$I_c = I_a + |I|$ **(2.8)**

Consequently, the rates I_a of both oxidation (corrosion) and I_c of reduction, which takes place on the surface of the steel, are modified according to **Figure 2.14**. If the current exchanged passes from the concrete to the steel or vice versa, the above equations are verified for a potential, respectively, more negative or more positive than the corrosion potential, so that the steel is polarized either cathodically or anodically.

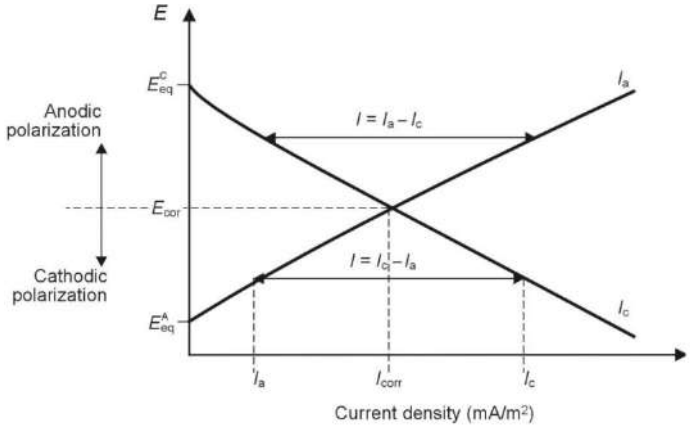

Figure 2.14 Schematic representation of the influence of external anodic or cathodic polarization (Bertolini, 2004)

Variations of the rate of anodic and cathodic processes, as well as variations of potential, due to the external current, depending on the direction and magnitude of the current and the anodic and cathodic polarization curves.

2.3 Corrosion inspection, assessment, and monitoring

The principles and application of electrochemical inspection techniques for RC structures are presented. **Figure 2.15** shows that different measurement techniques will give different information types.

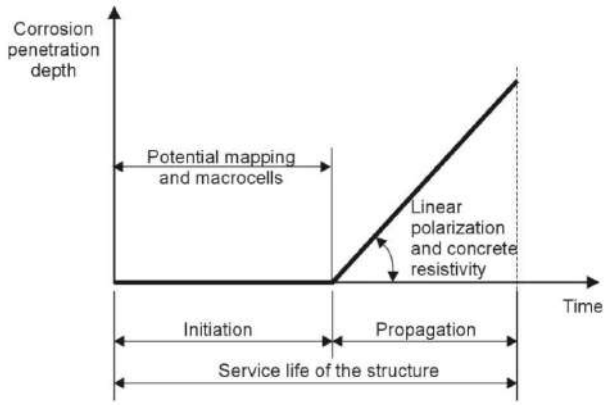

Figure 2.15 Types of information obtainable from different electrochemical techniques (Bertolini, 2004)

2.3.1 Half-cell potential mapping

Potential mapping is a widely recognized and standardized nondestructive method for assessing the corrosion probability of steel bars in concrete structures. In addition to the American standard ASTM C876-91 (ASTM, 2015), a RILEM recommendation has been published recently (Elsener and Andrade, 2003), where the extensive recent experience with potential mapping has been included. Several national guidelines (e. g. the Swiss SIA 2006 (SIA, 2006)) describe the use and interpretation of half-cell potential measurements.

Half-cell potential mapping has provided a very useful, non-destructive means to locate areas of corrosion for monitoring and condition assessment as well as in determining the effectiveness of repair work (Schiegg, 1995). As an early-warning system, corrosion is detected long before it becomes visible at the concrete surface. Based on the potential mapping, other destructive and laboratory analyses (e. g. cores to determine chloride content) and corrosion-rate measurements can be performed more rationally (SIA, 2006). In addition, the amount of concrete removal in repair works can be minimized because the corrosion sites can be located precisely.

- **Principle.** Corroding and passive rebars in concrete show a difference in electrical potential of up to 0.5 V; thus, a macrocell generates and current flows between these areas. The electric field coupled with the corrosion current between corroding and passive areas of the rebars (**Figure 2.16**) can be measured experimentally with a suitable reference electrode (half-cell) placed on the concrete surface, resulting in equipotential lines (potential field) that allow the location of corroding rebars at the most negative values (Stratfull, 1967; Elsener and Böhni, 1987 & 1990; Hunkeler, 1991).

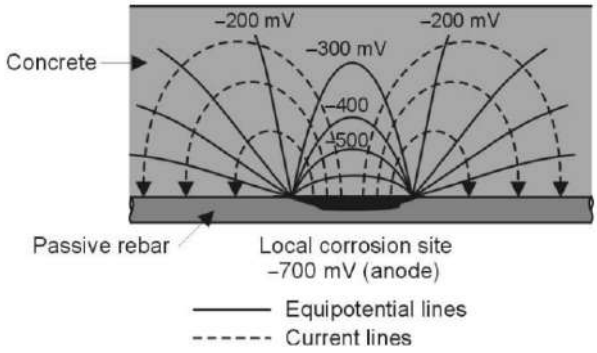

Figure 2.16 Schematic view of the electric field and current flow in an active/passive macrocell

- **Procedure.** The procedure for measuring half-cell potentials is straightforward (**Figure 2.17**): a sound electrical connection is made to the reinforcement, an external reference electrode is placed in a wet sponge on the concrete surface, and potential readings are

taken with a high impedance voltmeter (10 MV) on a regular grid on the free concrete surface. Good electrolytic contact is essential to get stable readings; the point of measurement should be clean and wetted with a watersoaked sponge on the surface. The use of tap water with the addition of a small amount of detergent is recommended. A few types of reference electrodes are used for potential mapping, mainly silver/ silver chloride (Ag/AgCl) or copper/copper sulfate (CSE). They differ in their standard potential, which is the potential difference to the standard hydrogen electrode (SHE). Standard potentials of these reference electrodes are given in **Table 2.3**, together with some other types used as embedded probes in concrete.

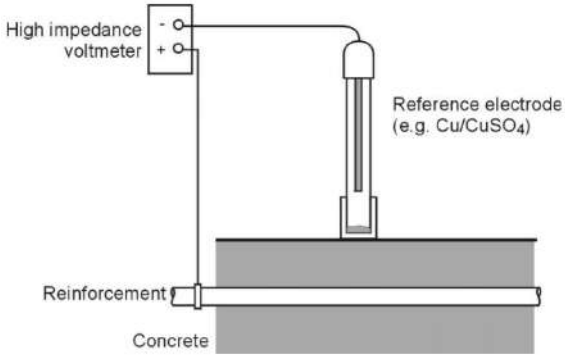

Figure 2.17 Schematic representation of the measurement of potential of steel reinforcement

Table 2.3 Potentials vs. NHE for reference electrodes (Myrdal, 1997; Vennesland, 2007)

Electrode	Potential (mV vs. NHE)
Saturated Calomel (SCE)	+244
Silver/silver chloride (SSE)*	+199
Copper/copper sulfate (CSE)	+316
Manganese dioxide	+365
Graphite	+150/–20
Activated titanium	+150/–20
Stainless steel	+150/–20
Lead	–150

* value depends on internal KCl electrolyte concentration

- **Interpretation.** Half-cell potential measurements allow the location to be determined of corroding rebars area being the most negative zones in a potential field. However, the interpretation of the readings is not straightforward because the concrete cover and its resistivity, in addition to the actual corrosion potential of the steel, influence the readings at the concrete surface. In atmospherically exposed reinforced concrete, the potential of passive steel is between –50 and –200 mV CSE (**Figure 2.18**). If corrosion is ongoing, the potential becomes more negative: chloride-induced pitting corrosion results in values

from –400 to –700 mV CSE, corrosion due to carbonation usually results in values from –200 to –500 mV CSE, strongly depending on the presence of moisture (**Figure 2.18**).

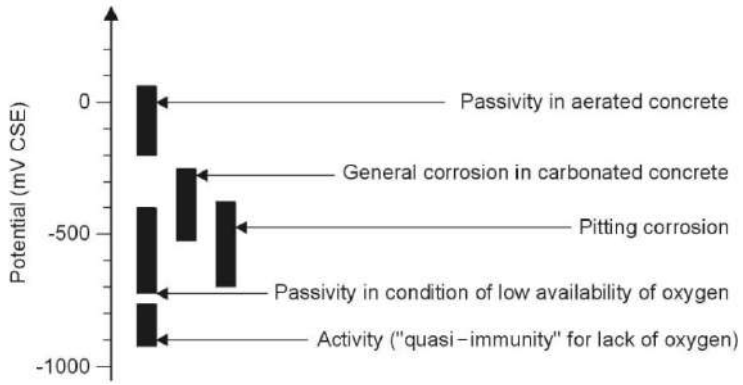

Figure 2.18 Correlation between potential and state of corrosion of carbon-steel reinforcement (Bertolini, 2004)

Problems in the interpretation of "negative" potentials may occur when dealing with structures that are completely immersed in the ground or seawater, or are water-saturated (or in any other condition of lack of oxygen); such conditions are characterized by very negative potentials (lower than –700 mV CSE). It is important to point out that despite these negative potential values, the steel in such water-saturated concrete normally does not exhibit a significant corrosion rate (Arup, 1983).

For reinforced concrete structures exposed to the atmosphere (e. g. bridge decks), the American Standard ASTM C876 provides criteria for interpretation, summarised in **Table 2.4**. This way of interpretation was derived empirically from chloride-induced corrosion of cast-in-place bridge decks in the USA; thus, the values reflect a specific condition, concrete type, and cover and are not universally applicable. Indeed, as theoretical considerations and practical experience on a large number of structures (Elsener and Böhni, 1987; Elsener *et al.*, 1996) have shown, there are no absolute potential values to indicate the probability of corrosion in a structure, in contrast to the interpretation given in the ASTM C876-91 that relies on a fixed potential value of –350 V CSE. Depending on moisture content, chloride content, temperature, carbonation of the concrete and cover thickness, different potential ranges indicate corrosion of the rebars in different structures. In order to locate areas of corroding rebars, the gradient between corroding and passive zones is more important than the absolute value of the potential. This information and its consequences for the interpretation of half-cell potential readings have been incorporated into a RILEM recommendation (Elsener *et al.*, 2003).

Table 2.4 Interpretation of potential measurements according to the American Standard ASTM C876

Measured potential E (mV vs. CSE)	Probability of corrosion
$E > -200$	< 10 %
$-200 < E < -350$	Unknown
< -350	> 90 %

2.3.2 Resistivity of concrete

The electrical resistivity of concrete may be useful for monitoring and inspection of reinforced-concrete structures concerning reinforcement corrosion (COST 509, 1997; Polder *et al.*, 2000). The resistivity of concrete in a given structural element exposed to chloride load gives information about the risk of early corrosion damage because generally a low concrete resistivity is correlated to more rapid chloride penetration (Nilsson *et al.*, 1996; Tuutii, 1982). In addition, resistivity mapping may show the most porous spots, where chloride penetration is likely to be fastest, and future corrosion rates will be highest; preventative measures may be taken accordingly. The resistivity can be measured nondestructively using electrodes placed on the concrete surface. Together with information from half-cell potential mapping or chemical analysis, the corrosion risk can be determined. The resistivity of cement paste, mortar and concrete depends on the pore volume and pore-size distribution of the cement paste, the pore-water composition (alkali content, chloride content) and the moisture content of the concrete (Tuutti, 1982; Bürchler *et al.*, 1996). Depending on environmental conditions and concrete quality, resistivity may vary by several orders of magnitude, from 100 to 100 000 Ω m. High resistivities are found for dry concrete, concrete with low w/c ratio or with blended cement. Because the electrical current is transported only by the ions in the pore liquid in the cement paste, concrete is not a homogeneous conductor. Aggregate particles are essentially isolating bodies. Coarse aggregates may have a similar size as the concrete cover, and the spacing of the measuring electrodes has to be adjusted accordingly.

According to the electrochemical nature of the corrosion process and the macrocell-corrosion model, a relationship may be expected between the concrete resistivity and the corrosion rate of the reinforcement after depassivation. Using a simplified approach, the corrosion rate of steel in concrete should be inversely proportional to the resistivity. This was confirmed in a general sense (Gonzalez *et al.*, 1993; Bürchler *et al.*, 1996), although the relationship is not universal; rather it depends on the concrete composition (Bertolini, 2004).

❖ **Measurements at the concrete surface.** All methods for on-site measurement of concrete resistivity involve at least two electrodes (of which one may be a reinforcing bar). A voltage is superimposed between the electrodes, and the resulting current is measured; the ratio gives a resistance (measured in Ω). The resistivity is obtained by multiplying the measured resistance by a geometrical conversion factor, the cell constant. This approach is valid only for a homogeneous material.

Resistivity can be measured using a four-point probe placed directly on the concrete surface. The probe consists of four equally spaced point electrodes that are pressed on the surface (**Figure 2.19**). Usually, a small amount of conducting liquid is applied locally to improve the contact between electrode tips and the concrete surface. The two outer point electrodes induce the measuring current (usually with an AC current at a frequency of between about 100 and 1000 Hz (avoiding the exact values 100, 150 Hz, etc., which may induce power line interference) and the two inner electrodes measure the resulting potential drop of the electric field. The measured resistance R is given by $\Delta E/\Delta I$ and the resistivity of the concrete, ρ, is calculated as:

$$\rho = 2\pi aR \qquad (2.8)$$

where a is the spacing between the electrodes. The applicability of this formula to concrete has been shown in references (Millard *et al.*, 1989; Elsener, 1988). A good correlation was found between calibrated data measured with a cast in electrodes and 4-point resistivity obtained on the surface (Polder *et al.*, 1992; Weydert and Gehlen, 1998).

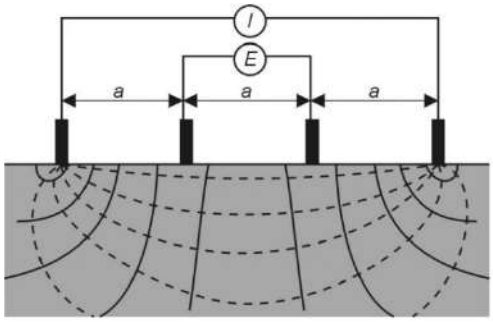

Figure 2.19 Scheme of the Wenner technique to determine the electrical resistivity of concrete from the surface. Spacing of the electrodes shall be larger than the maximum aggregate diameter (Bertolini, 2004)

Other types of resistance measurements, especially also involving the rebar network, have been applied. Commercially available instruments combine half-cell potential mapping with resistance measurements between the electrode and the rebars. This results in resistance maps; however, conversion to true resistivity is much more difficult because

the cell constant is also influenced by the cover depth to the steel bars and the size of the external electrode.

- **Procedure.** The detailed procedure for the measurement of resistivity of concrete is described in a RILEM recommendation (Polder *et al.*, 2000). The measuring system should be calibrated on concrete with known resistivity. As with half-cell potential measurements, concrete shall be clean, and good electrolytic contact between the electrodes and the concrete surface is important, but complete wetting of the surface should be avoided. When using the 4-point method, measurements should be taken as far from the rebars as possible (e. g. diagonally inside the rebar mesh, **Figure 2.20**).

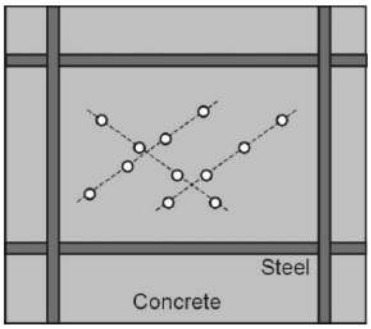

Figure 2.20 Positioning of Wenner probe electrodes on the concrete surface in order to stay as far as possible from the rebars after locating the reinforcement mesh

- **Interpretation.** The results of concrete resistivity measurements can be used for a quantitative or qualitative interpretation. Resistivity data measured on a structure and corrected for the temperature effect can be compared to reference data of similar concrete types. If, for example, a wet structure made with OPC has a mean resistivity value of 50 Ω m, it means that the water-to-cement ratio and the porosity must be quite high. Consequently, the corrosion rate after depassivation will be high. If the concrete composition is relatively homogeneous, mapping the resistance may show wet (low-resistance) and dry (high-resistance) areas. The average resistivities in the wet or dry areas can be interpreted quantitatively, as explained above. In addition a rough relationship between resistivity and corrosion rate can be obtained as suggested for OPC concrete (**Table 2.5**).

Table 2.5 Interpretative criteria for measurement of electrical resistivity of concrete structures exposed to the atmosphere for OPC concrete (COST 509, 1997)

Concrete resistivity (Ω m)	Corrosion rate
>1000	Negligible
>500	Low
200–500	Modest
100–200	High
<100	Very high (no ohmic control)

2.3.3 Corrosion rate

There are two meanings of corrosion rates, average corrosion rate, and instantaneous corrosion rate. The average corrosion rate is the average value over a long period by measuring weight loss or loss of cross-section of the steel bar. If the depassivation or time to start corrosion is not known, the calculated average corrosion rates will include an unknown error. In the real structures exposed to changing environmental conditions, the average value consists of periods with high and low corrosion rates (Andrade et al, 1996; Zimmermann et al., 1997; Sciegg et al., 2001). On the other hand, the instantaneous corrosion rate (i_{corr}) can be determined using electrochemical methods, in particular, polarization resistance (R_p) measurements (Gonzales et al., 1980). The calculation of the corrosion rate from R_p measurements is straightforward and correct only for general corrosion attacks. It is obvious that corrosion rate value measured at different times during the life of a structure or on different structures have to be corrected for the influence of moisture, temperature, etc., in order to allow a reasonable comparison.

- Determination of polarization resistance. The linear polarization resistance (LPR) is the polarization resistance measurement method based on the observation that the polarization curve close to the corrosion potential is linear, as shown in **Figure 2.21**. The slope $\Delta E/\Delta I$ (ΔE = step in potential, ΔI = resulting current) being defined as polarization resistance, R_p.

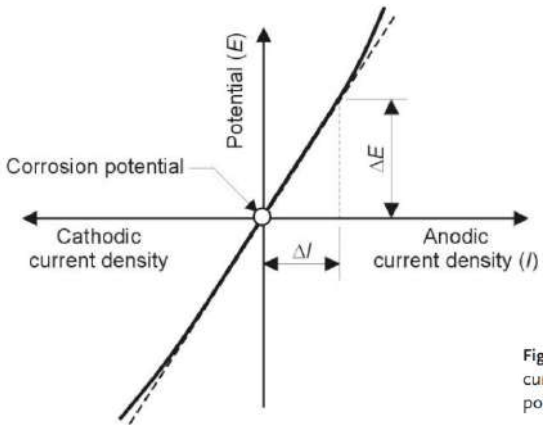

Figure 2.21 Polarization curve close to the corrosion potential (Bertolini, 2004)

The R_p value is related to the corrosion current I_{corr} as formulated as follows.

$$I_{corr} = B/R_p \qquad (2.8)$$

where: B is a constant containing the anodic and cathodic Tafel slopes. The principal relationships in linear polarization is summarized in **Table 2.6**.

For actively corroding steel bars in concrete, usually B 26 mV is used, for passive steel bar B = 52 mV (Andrade and Gonzales, 1978). R_p and thus I_{corr} is related to the area of the sample under test, resulting in the specific polarization resistance R_p*(Ωm^2) and the corrosion current density i_{corr} (mA/m^2), the instantaneous corrosion rate. Several precautions have to be taken in order to get reliable values, namely, compensation of the high electrical (ohmic) resistance of the concrete cover, achievement of a quasi-steady-state and linearity of the $\Delta E/\Delta I$ slope as discussed in more detail in references (COST 509, 1997; Andrade *et al.*, 1986; Elsener, 1998).

Table 2.6 Principal relationships in linear polarization (Bertolini, 2004)

$R_p = (dE/i)$	R_p = polarization resistance (Ωm^2) dE = polarization with respect to corrosion potential (mV) i = applied current density (mA/m^2)
$i = I/A$	I = applied current (A) A = polarized surface (m^2)
$i_{corr} = B/R_p$	i_{corr} = corrosion rate (expressed as corrosion current density, mA/m^2)
$V_{corr} = K \cdot i_{corr}$	v_{corr} = corrosion rate (μm/y) K = 1.17 (μm/y)/(mA/m^2) for iron

❖ **Procedure of measurement**. The measurement device of polarization resistance on-site is illustrated in **Figure 2.22**. It consists of a counter electrode disk and a reference electrode placed on the surface of the structures.

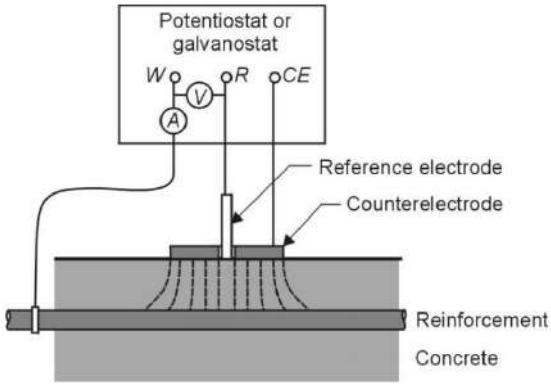

Figure 2.22 Illustration of linear polarization resistance measurements (Bertolini, 2004)

A potentiostat as the supply unit is connected to the steel bar as a working electrode to the counter electrode and reference electrode. After having selected the measuring position (preferably based on half-cell potential mapping), proper connections to the rebar and between the counter electrode and concrete surface are made (wetting). The corrosion potential is measured, and then a predetermined variation of potential (dE), in general, equal to 10 mV, is applied and the current di that the system requires to achieve this variation is recorded. The measurement lasts about one minute. From the

polarization resistance, R_p = dE/di (Ωm^2), the corrosion current density i_{corr} (mA/m^2) is calculated using **Equation (2.8).** Finally, the corrosion rate expressed as penetration rate (mm/y) is obtained, keeping in mind that for iron, an anodic current density of 1 mA/m^2 corresponds to a corrosion rate of 1.17 mm/y.

- **Corrosion rate measurements on-site.** The main difference in measuring the polarization resistance R_p on-site and not in the laboratory is the geometrical arrangement of the electrodes. In the laboratory, uniform geometry and thus uniform current distribution can be achieved usually with small specimens, whereas on-site a there is a non-uniform current distribution between the small counter-electrode (CE) on the concrete surface and the large rebar network (WE). The current fed by the external counter electrode (**Figure 2.23**) not only polarize the surface of the reinforcement below the CE itself but also spreads laterally or may reach deeper layers of the reinforcement. Due to the current spread out, the measured polarization resistance is related to an unknown rebar surface and cannot be converted directly to a corrosion rate with the Stern–Geary equation (Elsener, 1995; Feliù *et al.*, 1988). The current spread-out, given by the critical length Lcrit where 90 % of the current vanishes, depends both on the concrete resistivity and on the specific polarization resistance R_{p*} of the rebar (thus on the corrosion state).

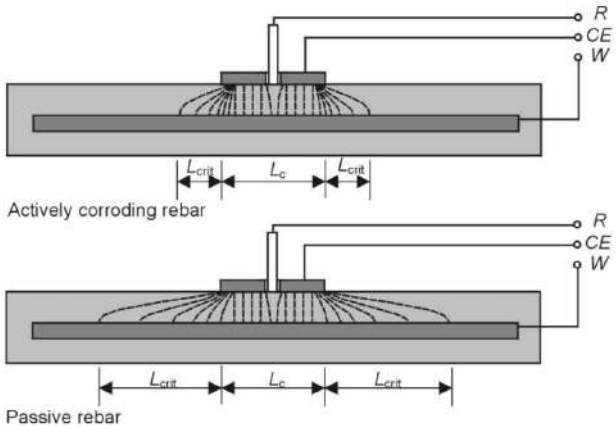

Figure 2.23 On-site measurements of corrosion rate (Bertolini, 2014)

Briefly summarizing the available literature (Elsener, 1998; Feliù *et al.*, 1988), it can be stated that in the case of homogeneous, actively corroding rebars (small specific polarization resistance Rp*) the applied current is concentrated nearly completely beneath the counter-electrode (**Figure 2.23**). Conversely, if the steel is passive (high specific polarization resistance), a large current spread out has to be expected, and the measured

apparent polarization resistance $R_{p,eff}$ is related to an area of rebars that may be up to 100 times larger than the CE surface. The concept of a sensorised guard ring (Broomfield, 1993) is usually implemented in commercial instruments and avoids the current spread-out on passive rebars. The calculation of a local corrosion rate (penetration rate) is intrinsically difficult because the area of the localized attack is not known (Elsener, 1998).

- **Interpretation of the results.** The interpretation has to be done by corrosion specialists with experience in reinforced concrete structures in the context of other information from condition assessment. The results can be used to pinpoint sites with high corrosion activity (in addition to half-cell potential measurements), to predict future deterioration of the structure or to assess residual service life. Daily and seasonal variations in the corrosion current due to changes in temperature and relative humidity will induce variations in Icorr values by more than a factor 2. To predict future deterioration, several measurements in time are usually needed. When only one single value is available, it is recommended to assume a variation in Icorr between 50 % and 200 % of the measured value. The interpretation of single values can be improved by taking cores, measuring their resistivity "as received", wetting them, and measuring again. If the resistivity at the time of measurement was high (compared to the wet value), the corrosion rate is on the low side of the temporal (seasonal) variation. If the resistivity "as received" is low and comparable to the wet value, the corrosion rate measured then is more representative for wet and high corrosion rate parts of the seasonal cycle. This approach was proposed by Andrade (COST 521, 2003). Several examples of applications are given in the literature (Polder, 2002), e. g. for predicting the residual service life of a corroding bridge and testing the efficiency of protection with a corrosion inhibitor (Broomfield, 1993).

2.3.4 Chloride determination

Information on chloride level at the steel bar surface is not only to predict the probability of corrosion but also to determines the future development of corrosion (Bertolini, 2004). If the value is more than a critical chloride content, pitting corrosion of the steel bar will start. During the determination of location for chloride profile analysis based on a half-cell potential map, e. g. cores should be taken at corroding areas, passive areas, and in the transition region to collate half-cell potential and chloride content.

Chloride contents can be measured by different methods, described in several recommendations or standards. Field methods are rapid but usually of poor accuracy,

whereas laboratory methods are more accurate, but more time consuming and costly. All methods (except the "dry" method of X-ray fluorescence) require three working steps: 1) sampling, 2) crushing to powder, and 3) dissolution, before the actual chloride analysis, can be performed. As concrete is an inhomogeneous material and chlorides are present only in the cement paste, a minimum diameter of 50 mm for cores or three to five points for 20 mm diameter dust drilling is recommended in order to get representative chloride depth profiles. Relatively simple methods based on spraying the surface of split cores with silver nitrate have been proposed; a color change indicates the chloride penetration front (Collepardi, 1995). The result may depend on the original color of the concrete and its particular chemistry. More complex tests are based on cutting slices from cores and pressing out the pore solution for determination of the free chloride concentration; this technique was developed for hardened cement paste (Page and Vennesland, 1983) but is also used for concrete (Polder *et al.*, 1995).

- **Chloride profile based on cores or powder drilling**. The location of the cores to be taken should be based on a problem-oriented approach, e. g. on a half-cell potential map. For cores, dry drilling is preferable; in any case, excess of water should be avoided due to the risk of washing out chlorides. The cores shall be identified and stored in plastic bags until analysis in the laboratory. Cores are cut in slices of a maximum of 10 mm thickness that are then crushed and milled. The resulting powder should have a controlled fineness (usually obtained with a constant time of crushing and milling). The equipment has to be carefully cleaned after every slice, in order to avoid cross-contamination of powders from different depths or samples. The location of powder drilling should be determined as for cores. Three to five 20 mm diameter holes should be drilled to the required depth (e. g. in steps of 10 mm), and the powder sampled. It is essential to mix the powder of the individual depths and to store it dry. After every depth sample is drilled, the equipment has to be cleaned carefully in order to avoid cross-contamination between different depth samples.
- **Dissolution of the powder**. After homogenizing the powder, obtained either directly by drilling or by crushing core slices, a part is weighed precisely and dissolved in a constant amount of liquid, most frequently in concentrated nitric acid solution with ISA (ionic strength adjuster). In this way, the total or acid-soluble chloride content is determined. The dissolution process is the most important step in determining the reproducibility of the chloride analysis. Alternatively, the Soxhlet extraction technique (reflux of boiling

water on the concrete powder for 24 h) is used to dissolve chloride ions. Both methods result in similar total chloride content. Considerable work has been done to differentiate between bound and free chlorides, using cold-water dissolution, alcohol dissolution, etc. The results of such chloride-extraction processes strongly depend on the level of powder fineness, time of dissolution, etc., and no sufficient reproducibility has been obtained. For routine analysis, only acid soluble (Andrade and Castellote, 2002a) or Soxhlet procedures are recommended. Recently, a method was proposed for determining water-soluble chloride (Andrade and Castellote, 2002b).

- **Chemical analysis**. Chloride ions in the extraction solution described above can be determined by different analytical techniques such as color-based titration, potentiometric titration, chloride-ion selective electrodes, etc. All of the analytical techniques have been shown to give comparable results with good accuracy, provided that frequent calibration with standard solutions is carried out. For very small amounts of liquid (as obtained by pore-water expression), the ICP technique (inductively coupled plasma spectroscopy) has been used successfully. However, this instrumentation is available only in specialized analytical laboratories.
- **Interpretation**. The presence of an above-critical amount of chloride ions at the rebars leads to depassivation and in the presence of oxygen and water to corrosion attack. In combination with results from potential mapping, the critical chloride content for the specific structure can be obtained. On chloride-contaminated structures, an empirical correlation between chloride content and half-cell potential could be established; thus the chloride distribution can be roughly obtained from the potential map.

2.3.5 Corrosion monitoring

Monitoring of reinforced-concrete structures exposed to aggressive environmental loads with regard to the time evolution of their durability can optimize the management of structures and secure their reliability and safety. However, the monitoring strategy has to be clearly defined, otherwise heavily instrumented structures produce large amounts of data with little or no practical value.

- **Objective of monitoring**. A monitoring system, eventually with computerized data acquisition, should meet specifically defined objectives, such as a) to monitor the durability of the structure and its condition in order to make timely decisions for preventive and/or repair actions, b) to monitor the effect of preventative or repair actions, c) to monitor the condition of structures based on new materials and/or new technology

(including service-life prediction models), d) to follow the time development in areas where access is difficult.

- **Monitoring design**. To meet one or several of the objectives, the number and location of permanently installed sensors should be defined based on the geometry of the structure, structural and environmental loads, previous experience with similar types of structures, and the planned level of maintenance of the structure. The representativity of the individual sensor location should be evaluated. Early-warning probes should be located in critical areas for the initiation of corrosion. Procedures and responsibilities regarding operation and service of the monitoring system and quality assurance and control of the recorded data have to be established. Data collected should be presented clearly, understandable for the end-user.
- **Choice of sensors and probes**. The choice of the sensors should take into account their stability as a function of time so that the necessary calibrations and maintenance can be planned. Initial sensor calibration has to be documented. For remote or inaccessible locations, only very robust and durable sensors should be installed.

2.4 Repair method of chloride-induced corrosion damaged RC structures by cathodic protection

Cathodic protection (CP) is an electrochemical repair technique that has increasingly been used for the repair of reinforced concrete structures worldwide. CP is rapidly being accepted as a repair option for steel-reinforced concrete structures deteriorated by chloride-induced corrosion (Hobbs, 2001). This technique requires the permanent application of a small direct current to protect the steel (Pedeferri, 1996).

The objective of the cathodic protection application is to polarize the reinforcement to an instant-off potential more negative than -850 mV (CSE) [-770 mV (SCE)]. This potential should decay (become less negative) by at least 100 mV from the instant-off potential within 24 hours after the system is disconnected (so-called depolarization). With CP, chloride ions slowly migrate away from the reinforcing steel toward the anode. Furthermore, the production of hydroxide ions at the steel surface causes the concrete to revert to an alkaline state. These factors quickly arrest the corrosion process when current is applied, and allow the passivating film to reform on the surface of reinforcing steel.

Cathodic protection reduces the corrosion rate by cathodic polarization of the reinforcing steel in concrete. The rationale behind cathodic protection is to prevent the reinforcing steel from giving up electrons so that corrosion does not occur. This retention of

steel electrons is achieved by supplying the electrons from another source. Considering the corrosion half-cell reactions, if there is an excess of electrons, the rate of the anodic reaction decreases. On the other hand, an excess of electrons will increase the rate of cathodic reaction. There are two main methods of supplying the electrons: by applying an impressed current or by introducing a sacrificial anode.

A simplified graphic of corrosion cell for reinforcing steel in concrete is shown in **Figure 2.24.** The electrochemical characteristics of each reaction can be studied by examining the confined half-cell reactions. The resulting polarization, also known as activation polarization, in the absence of other effects, is governed by the following relationship:

$$\eta = a + b(\log I) \qquad (2.9)$$

where

η	= activation of polarization
a	= potential intercept
b	= Tafel constant
I	= current

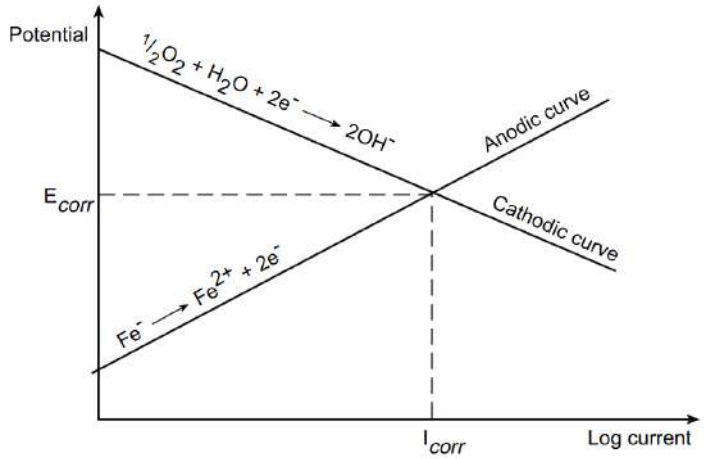

Figure 2.24 Simplified representation of a corrosion cell of steel in concrete (Etcheverry et al., 1998)

The anodic and cathodic half-cells polarize to a common corrosion potential E_{corr}. This potential is also called mixed potential because the resulting potential is the combination of the half-cell potentials for the anodic and cathodic reactions. The corrosion current, I_{corr}, is directly proportional to the corrosion rate. I_{corr} and E_{corr} are represented in **Figure 2.25** by the intersection of the anodic and cathodic curves.

Two other types of polarization affect the corrosion of steel in concrete. Cathodic diffusion is associated with the concentration of polarization by which the rate of oxygen diffusion through concrete influences the corrosion rate. As shown in **Figure 2.26**, the higher

the oxygen diffusion (as shown in Curve 2), the higher the corrosion rate. The other type of polarization is ohmic polarization. Because concrete is not a very conductive medium, the resistance of concrete influences the corrosion rate. As shown in **Figure 2.27**, the higher the resistance, the lower the corrosion rate.

On a practical level, reinstating corrosion protection in concrete using sacrificial anode cathodic protection does not require perfect repairs; only physical damages need to be repaired, without the need to remove a lot of chloride-contaminated concrete and perfect cleaning of steel (Pedeferri, 1996).

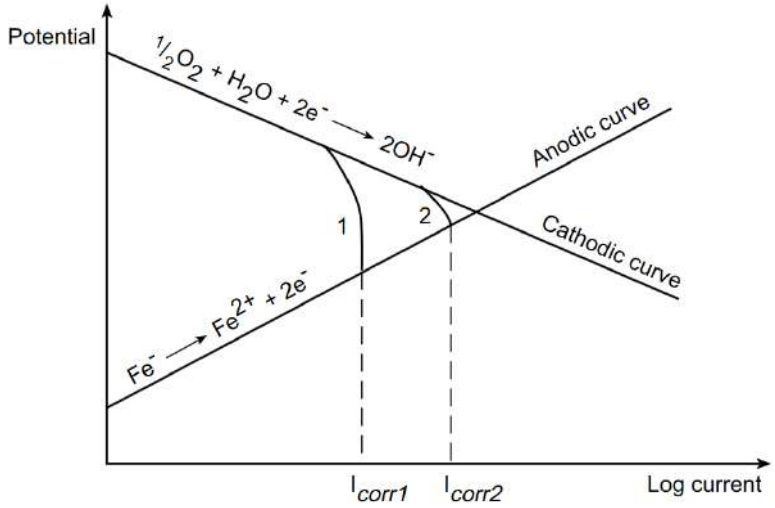

Figure 2.25 Effect of cathodic diffusion on polarization (Etcheverry et al., 1998)

The two principal types of cathodic protection systems commonly used are the impressed current cathodic protection (ICCP) and the sacrificial anode cathodic protection (SACP). The direct current (DC) for the CP system can be supplied either via mains power in an impressed current CP (ICCP) system or by sacrificial anode CP (SACP) system. In a SACP device, single or multiple anodes distribute the cathodic current to the protected structure (Garcia *et al.*, 2012). The decision on which of the two cathodic protection (CP) systems to use is usually also influenced by several factors including but not limited to the condition of the structure, the client's budget and the anticipated life expectancy of the structure following the repairs. Cathodic protection can work in three stages as shown in **Figure 2.27**.

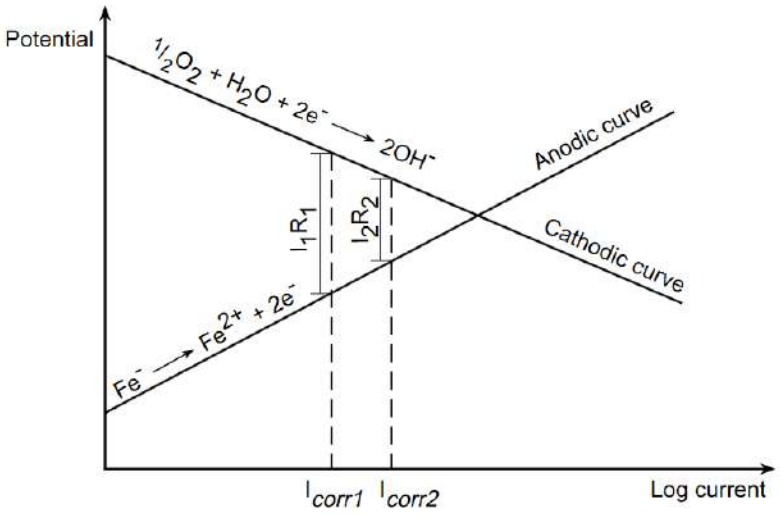

Figure 2.26 Effect of concrete resistance on polarization (Etcheverry *et al.*, 1998)

Natural corrosion will produce electrons that make a cathodic area, as shown in (a). An external supply of electrons can also produce a cathodic reaction for the available amount of oxygen. If the supply of electrons is insufficient, corrosion may also produce electrons, as shown in (b). Full cathodic protection (c) is only achieved where the supply of electrons from an external source is able to react with all the oxygen.

CP`s current circulation between an anode and a cathode causes steel polarizes to a negative potential, increases the alkalinity of concrete, and reduction of chloride content at the cathodic area by electrochemical reactions inside the electrolyte.

The negative potential shift can reduce the driving force for the anodic process (thermodynamic effect) and increase or maintain the resistance of the anodic process (kinetic effect) (Takewaka, 1993). The cathodic reactions reduce oxygen content and generate alkalinity on the steel surface, which preventing corrosion because they widen the passive region and depolarize the cathodic process. In the case of passive steel, they hinder local acidification and also interfere with pitting initiation (Takewaka, 1993). Besides, CP current also reduces the chloride concentration on the steel surface by electrophoresis.

The use of CP current in reinforced concrete gives not only benefical effects but also negative effects such as concrete degradation, bond loss, and hydrogen embrittlement. These caused by ion migration of sodium (Na^+) and potassium (K^+) towards the concrete-steel interface (Bennett, 1993; RILEM, 1994). The application of a greater CP current can promote hydrogen activity at the concrete-steel interface and the consumption of electron from the corrosion process (Watanabe *et al., 2001*). Also, hydrogen evolution can occur only at potentials more negative than about -950 mV vs. SCE in the case of alkaline environments

(pH > 12) (Takewaka, 1993). For these reasons, it is necessary to determine suitable CP criteria for reinforced concrete structures.

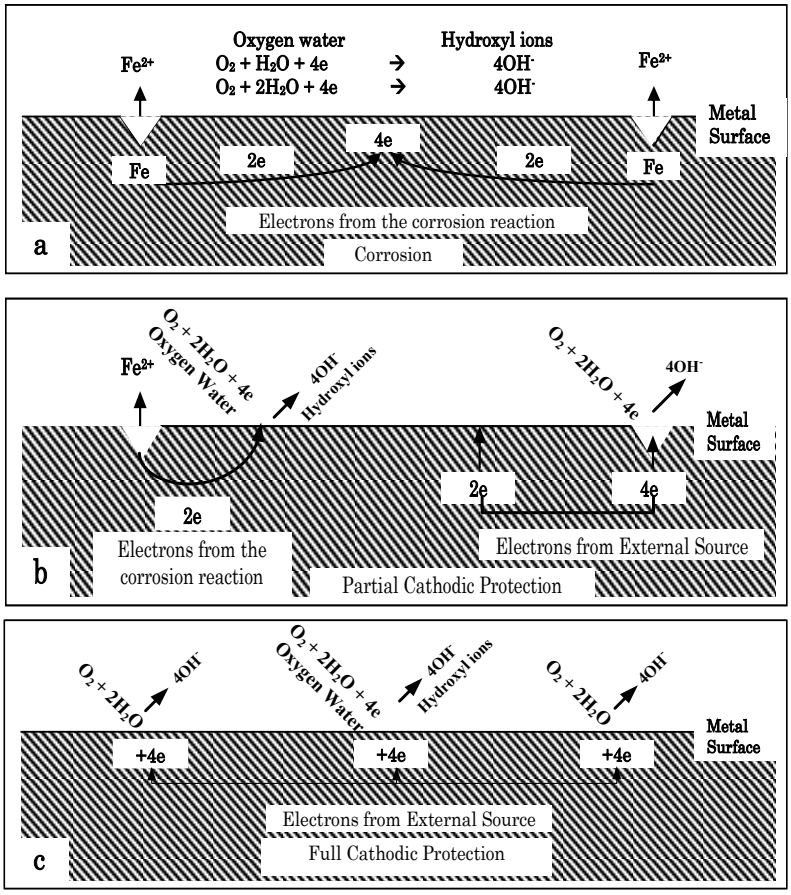

Figure 2.27 Stage of the cathodic protection system (Garcia *et al.*, 2012)

2.4.1 Impressed current cathodic protection (ICCP)

In the ICCP, the large electrochemical is formed between an anode and the structure to be protected by a power supply that is controlled by reading a reference electrode close to the structure, as shown in **Figure 2.28**. ICCP is reached by applying a small amount of direct current through the concrete. An anode is usually laid on the concrete surface connected to the positive terminal, and the steel acts as the cathode is connected to the negative terminal of the DC power supply. Concrete contains enough pore water to serve as the electrolyte so that when DC is applied, current can flow from the anode to the cathode.

In ICCP systems, a small direct current is passed from a permanent anode to the reinforcing steel. An external power supply needs to be connected between the anode and the steel with appropriate polarity and voltage to prevent the reinforcing steel from giving up electrons. **Figure 2.29** shows an impressed current system schematically and the reactions involved (Etcheverry *et al.*, 1998).

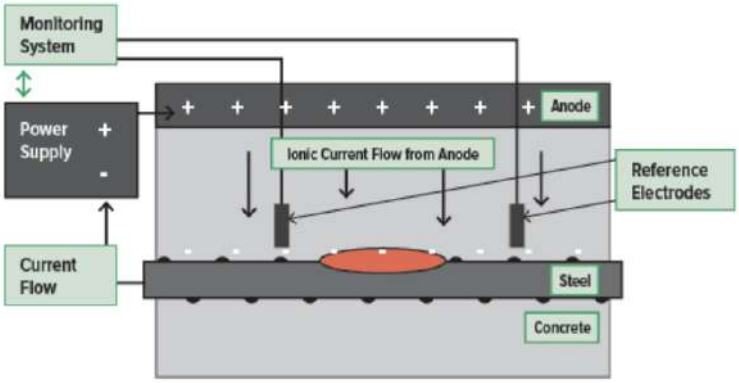

Figure 2.28 Cathodic protection system in ICCP (Chess and Broomfield, 2014)

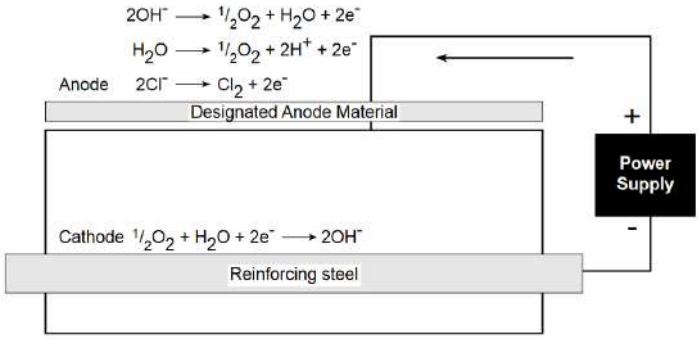

Figure 2.29 Reactions involved in the impressed current system (Etcheverry *et al.*, 1998)

If the current applied is enough to stop the anodic reaction from occurring, the only reaction at cathode should be:

$$2e^- + \frac{1}{2}O_2 + H_2O \rightarrow 2(OH)^- \qquad \textbf{(2.10)}$$

If the potential goes too negative, which means the current applied is excessive, the hydrogen evolution reaction can occur.

$$e^- + H_2O \rightarrow H + OH^- \qquad \textbf{(2.11)}$$

The monatomic hydrogen migrates into the steel metal lattice, reducing the strength and resulting in failure under load. This phenomenon is known as *hydrogen embrittlement*. Hydrogen embrittlement is not a problem for conventional reinforcing steel but may be a problem for certain high-strength steels. Caution is justified for cathodic protection installations on structures contain prestressed or post-tensioned steel. Both possible reactions at the cathode described above, lead to the production of hydroxyl ions, which restore the passivating film broken down by chloride attack. Chloride ions are driven away from the reinforcing steel. Because the chloride ions are negatively charged, it is repelled from the now-cathodic reinforcing steel and moves towards the installed anode.

$$Cl^- \rightarrow Cl^2 + 2e^- \quad \textbf{(2.12)}$$

Another reaction that occurs at the cathode is the consumption of the hydroxyl ions formed at the cathode to produce oxygen. Water is then oxidized to give rise to hydrogen ions leading to acid etching of the concrete. If the potential gets too negative, the acidification around the anode increases.

$$2OH^- \rightarrow H_2O + \frac{1}{2}O_2 + 2e^- \quad \textbf{(2.13)}$$

$$H_2O \rightarrow \frac{1}{2}O_2 + 2H^+ + 2e^- \quad \textbf{(2.14)}$$

The electrochemical principle of impressed current cathodic protection can be explained by polarization curves of the reactions involved. **Figure 2.30** shows the polarization of the two reactions involved. When an electric current is supplied, I_{app}, the potential shifts in the direction from E_{corr} to E owing to the excess of metal electrons supplied at the metal surface (Cortes, 1993). The rate of the anodic reaction, corrosion rate, is reduced to I_{corrA}.

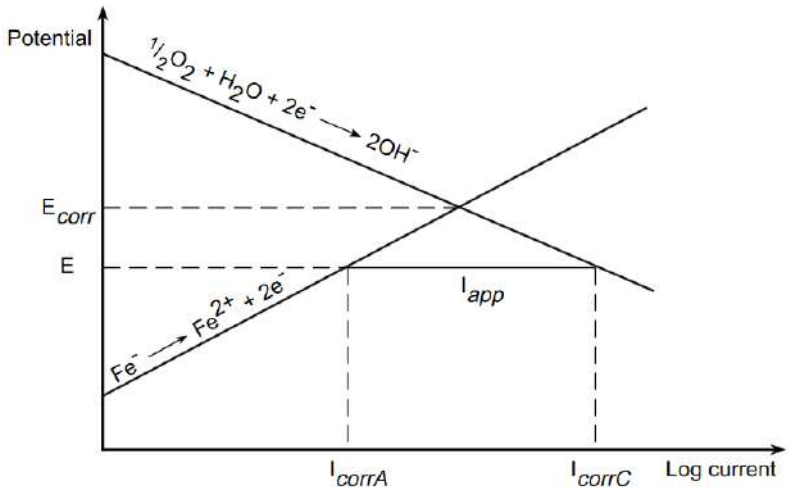

Figure 2.30 Electrochemical principle of the impressed current system (Etcheverry et al., 1998)

The main advantage of the ICCP system is its flexibility and durability (Wilson *et al.*, 2013). The current output of the power supply can be adjusted to optimize the protection delivered. Also, the ICCP system can be controlled to accommodate variations in exposure conditions and future chloride contamination. The performance of the ICCP system is widely determined by the material composition, shape, type and orientation of the anode (Cortes, 1993). There are a number of different types of the anode that are used in the ICCP system for a reinforced concrete structure. These include conductive coating, titanium-based mesh in the cementitious overlay, conductive overlay incorporating carbon fibers, flame-sprayed

zinc, and various discrete anode systems. The selection of the anode system must consider environmental conditions, anode zoning, accessibility, maintenance requirements, performance requirements and operating characteristics, life expectancy, weight restriction, track record, and costs (Chess and Broomfield, 2014).

2.4.2 Sacrificial anodes cathodic protection (SACP)

In contrast to impressed current anodes, the possibility of sacrificial anodes application is limited by the electrochemical properties. The rest potential of the anode material should be sufficiently more negative than the protection potential of the object to be protected so that an adequate driving voltage can be maintained. The anode metals from numerous less easily soluble compounds from which, under normal circumstances, hydroxides, hydrated oxides and oxides, carbonates, phosphates, and several basic salts can arise. With the use of sacrificial anodes for internal protection, still further compounds that are less easily soluble can be formed. In general, the insoluble compounds do not precipitate on the working anode because the pH is lowered thereby hydrolysis. If the anode is not heavily loaded or the concentration of the film-forming ions is too high, the less easily soluble compounds can cover the anode surface. Many surface films are soft, porous, and permeable and do not interfere with the functioning of the anode. However, some films can become as hard as enamel, completely blocking the anode, but on drying out alter their structure and become brittle and porous.

Sacrificial anodes should exhibit as low polarizability as possible. The extent of their polarization is important in practice for their current output. A further anode property is the factor Q for the equivalence between charge and mass, according Faraday`s Law, as in **Equation 2.15.**

$$\Delta m = \frac{MQ}{zF} \qquad (2.15)$$

Where Δm is the mass of dissolved metal, M is the atomic weight, Q is the transferred electric charge, z is the valence of the metal ions, and F is Faraday`s constant. The factor Q is termed current content. It is larger than smaller the atomic weight, and the higher the valence of the anode metal.

The anodes are generally not of pure metals but alloys. Certain alloying elements serve to give a fine-grained structure, leading to a relatively uniform metal loss from the surface. Others serve to reduce self-corrosion and raise the current field. Finally, alloying

elements can prevent or reduce the tendency to surface film formation or passivation. Such activating additions are necessary with aluminum.

At the time when the Sacrificial Anode Cathodic Protection (SACP) system is selected, the service life is expected to be shorter than an ICCP system because the anode must consume (sacrificed) to produce the protective current. Hence, if a concrete structure has a relatively long life remaining, the SACP may need replacement during the remaining service life of the structure. In general, the life expectancy of a sacrificial anode maybe 5-20 years (or longer) and is dependent on the type of material used and the environmental condition (Chess and Broomfield, 2014). Aluminum (Al), zinc (Zn) and magnesium (Mg) are the types of metals that are commonly used for SACP. These metals are also covered with a highly alkaline mortar to improve long-term performance and dissolution characteristics.

2.4.2.1 Principles of sacrificial anodes

Sacrificial cathodic protection, or galvanic protection as it is often referred to, is based on the principle of dissimilar metal corrosion. When two dissimilar metals are connected, one will tend to act as an anode and will corrode, while the other will form the cathode. The main sacrificial metals used to protect steel in concrete, are aluminum alloys and zinc. These metals are sacrificed in the generation of the protection current. No external power supply is required. Because each element of anode surface acts as its power supply, the anode system does not need to be installed in zones, and it is relatively easy to target the system to an area of need. A typical material used is zinc. Such an anode has about 0.5 to 1.0 V available to drive the current to the steel. **Figure 2.31** illustrated about the SACP system for embedded steel in concrete.

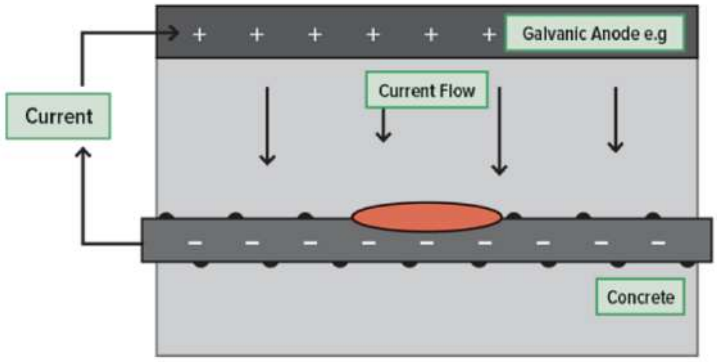

Figure 2.31 Cathodic protection system in SACP (Chess and Broomfield, 2014)

The sacrificial anode corrodes preferentially producing electrons. Sacrificial anodes need to be more active than iron to protect the reinforcing steel. Typical anodes are zinc,

aluminum, magnesium, and their alloys. **Figure 2.32** shows a sacrificial system schematically and the reactions involved.

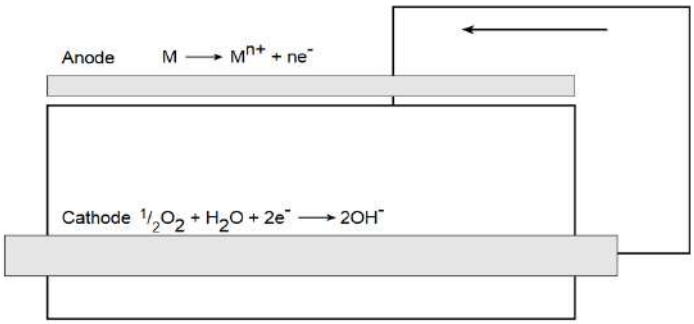

Figure 2.32 Reactions involved in the sacrificial anode system (Etcheverry *et al.*, 1998)

The reaction at the anode is the consumption of the anode to procedure the electrons that the steel would be otherwise giving up.

$$M \rightarrow M^{n+} + ne^- \qquad (2.16)$$

The resistance of the concrete electrolyte is the crucial element to determine whether the use of sacrificial anodes is viable. In cases where the electrolyte resistance is too high, the effective potential difference between the steel and the anode may not be sufficient to adequately protect the structure. Thus, sacrificial anodes are very common for structures exposed to seawater and to other electrolytes that decrease the concrete resistivity.

The electrochemical principle of sacrificial anode protection can be explained by the polarization curves of the reactions involved. **Figure 2.21** shows the polarization of the two reactions involved. When a sacrificial anode is used, the reinforcing steel and the sacrificial anode are polarized to the same potential E. The corrosion rate for the reinforcing steel is reduced to I_{corrA}. The rate of consumption of the sacrificial anode is given by I_{corr}.

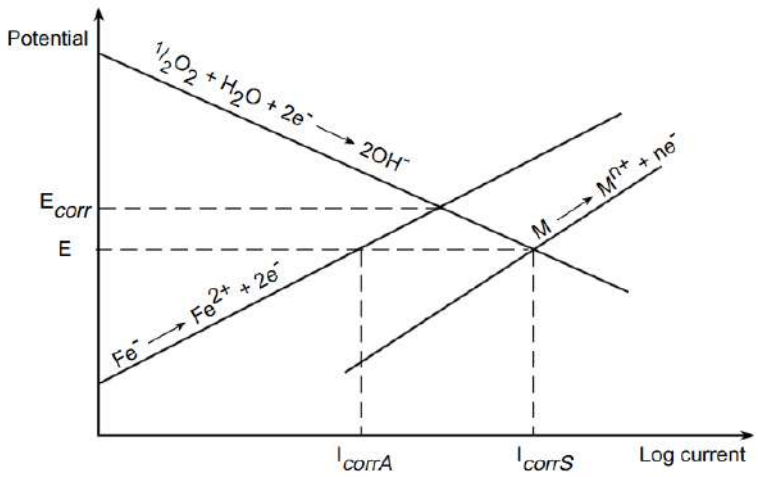

Figure 2.33 Electrochemical principle of the sacrificial system (Etcheverry *et al.*, 1998)

2.4.2.2 Type of sacrificial anodes

The application of sacrificial anode CP systems to concrete is relatively new compared to their use in protecting steel in soils and seawater. Issues affecting the sacrificial anode system for concrete structures include maintaining the activity of the sacrificial metal, expansive products of metal dissolution and attachment to the reinforced concrete structure. The natural alkalinity and density of concrete may cause some sacrificial metals to passivate or prevent the dissipation of the corrosion product, and concrete may cause some sacrificial metals to passivate or prevent the dissipation of the corrosion products in the same way that seawater and soils do.

A number of systems have been developed that address these issues and an increasing range of sacrificial anodes is being offered by suppliers. The known sacrificial anode products may be divided into the following types:

1. Metal coatings applied directly to the concrete surface.
2. Sheet anodes attached to the concrete surface.
3. Distributed anodes embedded in a cementitious overlay.
4. Discrete anodes embedded in cavities in the concrete.

Experience of sacrificial anode system on the reinforced concrete structure is more limited than impressed current systems. Zinc, thermally applied as a coating to concrete is probably the most widely used galvanic system in the world. These systems are not proprietary products and are not promoted by any particular company. In 1990s various surface applied proprietary systems were developed, and from 1999 discrete anode system embedded in cavities in the concrete were introduced to the market. The most widely used systems in the UK are discrete sacrificial anodes that are embedded in holes formed for this purpose and in repair areas in the concrete.

Sacrificial anode products currently known to be available in the UK include thermally sprayed zinc and aluminum, jacketed zinc mesh with a cementitious overlay, adhesive line zinc sheeting and discrete anodes for embedment in areas of concrete patch repair, discrete anodes for use in cavities formed for the purpose of installing anodes and sacrificial anodes that can be used as both impressed current and sacrificial anodes. Most of these anode systems are proprietary products. Non-proprietary products include thermally sprayed zinc and zinc or aluminum mesh in a porous overly that may be achieving using an air-entrained cementitious material that usually contains some chloride as an activating agent. **Figure 2.24** shows typical commercially available of the sacrificial anode.

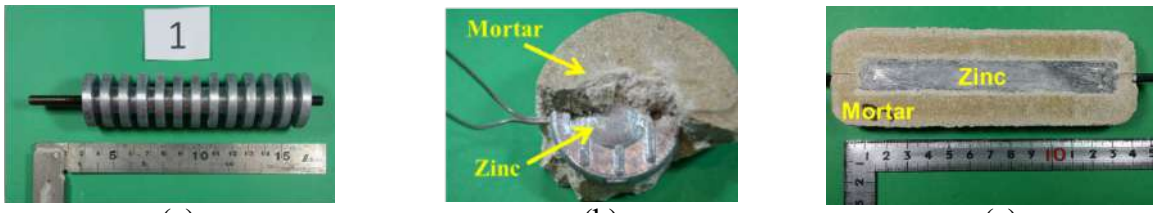

(a) (b) (c)

Figure 2.34 Commercial type of sacrificial anodes (a) ribbed cylindrical anode, (b) galvashield XP and (c) galvashield F

The protection delivered by a sacrificial anode system is largely determined by the current output of the anode system and its distribution to the protected steel. The anode current density is approximately 50 times the steel protection current density. In both cases, the anodes deliver sufficient current to act in a preventative role (1 to 2 mA/m^2 protection current to the steel on average. The anodes appear to be effective in delivering cathodic prevention current densities).

Long term current output data on the sacrificial anode system is limited. The cyclic behavior is evident and is usually attributed to the responsive behavior of the anode to changing environmental conditions. The principal environment factor affecting the performance in terms of the protection current delivered to the steel by a sacrificial anode is resistivity, which is a function of moisture content, chloride content, and temperature. The protection delivered is also a function of current distribution. This effects discrete sacrificial anode assembly's more than distributed surface applied anode assemblies and is discussed in greater detail below.

Anode life service primarily determined by anode`s current output, anode charge capacity, anode utilization, and anode efficiency and may be calculated using Faraday's law. In simple terms, anode life is given by the useful mA-hours (charge capacity) of the sacrificial metal divided by average output in mA. A current of 1 mA delivered for 50 years is equivalent to a charge of 440 Amp hrs (1 Amp-hr = 3.6 kC) the useful charge capacity of an anode system is determined by the anode efficiency and utilization. Longer life may generally be achieved by using more anodes or anodes with high charge capacities that deliver low current densities.

These parameters may be requested from the anode suppliers or obtained from independent tests. Various factors may affect the utilization of an anode system. These include the loss of sacrificial anode activities and loss of adhesion of the anode system to the concrete. The loss of adhesion is mainly associated with anode system applied to concrete surfaces and is discussed further below. The level of anode activity is particularly important

in small surface area embeddable discrete anodes that are required to deliver a high anode current density.

For reinforced concrete application, zinc anode has become the most common SACP used presently because of several advantages (Rajendran and Murugesan, 2013), as follows.

a. Zinc has high corrosion efficiency, i.e. high percentages of the electrons that are discharged when the zinc corrodes are available to protect the steel.
b. As the zinc corrodes, it has a relatively low rate of expansion compared to other metals including steel. This makes zinc anodes particularly suitable for application where the anodes are embedded into the concrete structure.
c. Zinc anodes are suitable for use with prestressed and/or post-tensioned concrete because their native potential is not sufficient to generate atoms or cause hydrogen embrittlement in a concrete environment.

The main benefit of SACP is its simplicity and the fact that minimal or no maintenance is required. In the SACP system, an external power source is not required to maintain the protective current because directly electrically connected to the steel. This significantly reduces the start-up costs as no provision has to be made to connect to a power supply. Also, SACP usually operates below the threshold for hydrogen embrittlement (~ -900 mV vs. CSE) (Bennett, 1993).

Meanwhile, the major disadvantages of the SACP system are the uncertain lifespan of the anodes, and it is dependent on the average current output of the anodes. The amount of current that is generated by SACP is significantly influenced by environmental factors, such as temperature, oxygen content, humidity and also chloride content. In addition, the resistivity of the concrete must be taken into account as the lower driving voltage of the anodes means they may not be effective in the high resistivity of concrete.

There are a number of factors affecting the performance of a sacrificial anode system. These are summarized in **Table 2.7**. The main advantage of sacrificial systems owing to current systems is that they do not require a power supply. Impressed current systems require more monitoring than sacrificial anode systems. Sacrificial anode systems are, however, limited in the current and voltage that they can produce. For concrete with high resistivity, as found in atmospheric concrete, the energy output is generally not sufficient to achieve protection. In other environments, such as contact with seawater or seawater splash, protection may be achieved with the use of sacrificial anodes. Impressed current systems

provide greater flexibility because current or output can be easily adjusted. While sacrificial anodes corrode, requiring periodic replacement, the service life of the anodes used for the impressed current system is usually much longer.

Table 2.7 Summary of factor affecting performance of anode systems applied to reinforced concrete structures (Christodoulou *et al.*, 2008)

Factor	Effect
Charge capacity/ current output	The maximum theoretical life cannot exceed a period determined by the anode charge capacity ad anode current output.
Anode activity/ surface area	Determines protection current output and discrete anodes, in particular, need a method of anode activation. For alkali-activated systems, anode activation is dependent on the quantity of alkali in assembly.
Anode delamination/ adhesion to concrete	Sacrificial anode systems applied to the concrete surface, in particular, are at risk of suffering from delamination and loss of contact with concrete.
Current distribution	Discrete anodes distribute current poorly compared to surface applied anodes, but protection can be targeted to the area of need.
Continuing corrosion	Products design for use in a preventative role may fail when trying to arrest an active corrosion process.
Concrete Resistivity	An increase in concrete resistivity reduces the protection current output of a sacrificial anode, which limits the protection delivered.

2.4.3 Performance Criteria of Cathodic Protection in Concrete

The method of CP has introduced to be an effective method to mitigate the corrosion of steel in reinforced concrete structures. But, there is still a different opinion about the appropriate criteria for the CP system. A variety of CP criteria have been proposed, including using electrode operating potential, potential shift, potential decay, current-potential relationship (E-log*I*), macrocell probes, chloride concentration and statistical treatment of static potentials (Bennett and Broomfield, 1997). Many of these criteria are complex and difficult to apply, and few experimental studies have been conducted to determine the actual effectiveness of the various criteria.

2.4.3.1 Decay Shift Criteria

After reinforcing steel was installed with the CP system inside the concrete, they were evaluated for when to replace the new anode and measured how long CP could protect steel from corrosion risk. Decay shift can be calculated from off potential deducted by instant-off

potential. CP can maintain reinforcing steel from corrosion. The decay shift is more than 100 mV from half-cell potential measurement versus copper/copper sulfate.

The 100 mV depolarization criterion is the most popular criterion currently used for the CP system and has been adopted by several codes. This criterion was investigated empirically by Bennett and Mitchell in 1989 (Bennett and Mitchell, 1989). In their investigation, the procedure for measuring the instant-off potential (current interruption) and the duration of the test are proposed. Also, the effect of temperature, static potential, and steel density was investigated by the test. They recommended that if the chloride concentration is not known, the 100 mV depolarization criterion is reasonable. Although 150 mV should be required if conditions are known to be very corrosive.

NACE SP0290 calls for a minimum of 100 mV polarization from native potentials, or 100 mV depolarization from an "Instant Off" reading (NACE, 2007). The duration of the test can have a clear impact on the values recorded. Per SP0290 the "Instant Off" reading is typically read between 0.1 and 1.0 seconds after the rectifier is interrupted. Readings at times less than 0.1 seconds often include reactive components that have nothing to do with CP. If one waits more than one second, the observed change will be understated. **Figure 2.35** provides a stylized diagram. Starting on the left with the base potential before CP is applied the polarization is shown, whereby the steel potential is polarized in a negative, cathodic direction. About midway, the rectifier is turned off and the potential shifts in a positive direction. The area between 'CP Off' and 'Instant Off' includes IR error and reactive transients resulting from interrupting the CP current. At a point between 0.1 and 1 second is the start of the depolarization.

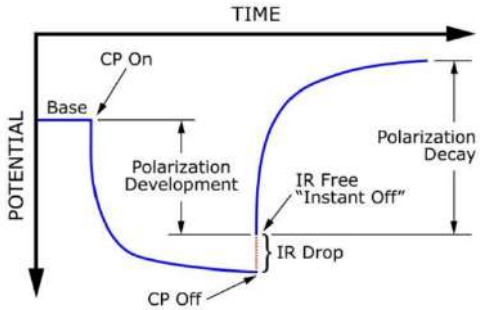

Figure 2.35 Polarization and depolarization scheme (Tinnea and Tinnea, 2014)

Various researchers have been investigated to determine the effectiveness of this criterion on the corrosion rate of steel in concrete. Funahashi and Young (1992) observed the total depolarization needed for complete protection for macrocell and microcell currents under various environments. They discovered that the 100 mV depolarization criterion does

not adequate to eliminate both macrocell and microcell corrosion. Takewaka (1993) studied the relationship between corrosion weight loss and depolarization value on the 18 concrete blocks with 0.5% chloride by weight of concrete under a dry and wet cycle. The current density level from 0 to nearly 500 mV was used to polarize the steel for eight months. The research results concluded that 100 mV criterion may not be sufficient and that 150-200 mV is necessary to protect the steel under these conditions. Another study was reported by Bennett *et al.* (1993); the amount of polarization needed to control corrosion to an acceptable level was found to be a complex function of many variables. 100 mV of polarization was adequate if chloride concentration was less than 0.26% by weight of concrete. However, at higher chloride concentrations, polarizations up to 150 mV were needed.

The 100 mV decay shift criteria also described as briefly in **Table 2.8**. If the potential of the CP system is more negative than 850 mV, it means steel is polarized to be in the cathodic state, and no corrosion will occur. However, in the case of reinforcing steel in concrete with a passive state and availability of dissolved oxygen, the application of such criteria has been found to result in very high unneeded current requirements (Dugarte and Sagues, 2014). This might because of premature deterioration of the anode, hydrogen evolution, and the loss bond between concrete and steel. So decay shift criteria are used to determine the performance of the sacrificial anode cathodic protection system in RC structure.

Table 2.8 Acceptance criteria for cathodic protection (EN 12696, 2000; DNV, 2010)

Test Method	Criteria
ON potential	Negative more than 850 mV potential of steel with CP applied (on potential)
Instant-off potential	Negative more than 850 mV potential of steel with CP applied (instant-off potential)
OFF potential	Negative more than 100 mV potential of steel

In real situations, concrete construction attached to many environments such as the humidity of air moisture, chloride attached from rain, carbon dioxide gas and other factors affecting to reinforcing steel inside concrete. Reinforcing steel embedded in concrete exposed in the different environments must have different current density requirements too. The efficiency of CP in concrete was described by current density criteria in **Table 2.9**. It is important to determine the amount of protective current or potential difference that required

for the CP system to apply to reinforced concrete structures and to make sure that the anode can provide that current uniformly across the structure.

Several observations have been carried out to understand the effectiveness of the E-log I criterion (RILEM, 1994). Although these investigations depict the experimental procedure in detail and the effects of variables such as concrete cover, temperature, and moisture content, there is no documentation of the actual effectiveness of this criterion. Bennett and Mitchell (1993) observed the current density established by the E-log I criterion. They discovered that the current density requires higher than that required to achieve 100 mV of polarization. It might be that the current density determined by E-log I criterion is sufficient to controlling corrosion even data not available to support this conclusion. An empirical test method (E-log I) has been developed to determine the steel potential versus applied current relationships in particular cases. As varying levels of current are applied to the steel, the potential E_m can be measured and recorded.

Table 2.9 Practical CP current density requirements for varying steel conditions (Tinnea and Tinnea, 2014)

Environmental surrounding steel reinforcement	**Current density (mA/m^2)**
Alkaline, no corrosion occurring, a little oxygen resupply	0.1
Alkaline, no corrosion occurring, exposed structure	1 - 3
Alkaline, chloride present, dry, good quality concrete, high cover, light corrosion observed on the steel	3 - 7
Chloride present, wet, poor quality concrete, medium-low cover, widespread pitting and general corrosion on steel	8 - 20
High chloride levels, wet fluctuating environment, high oxygen level, hot, severe corrosion on steel and low cover	30 - 50

From this data, an E-log I curve can be developed. Over section of the curve close to its natural potential, there should be an almost linear portion from where the relationship between applied current and resulting potential shift can be determined. There should be a change in gradient as the steel moves from anodic to cathodic conditions.

The limitations of this technique are that it is limited to first polarization only, and it requires orders of magnitude of applied current. It is, therefore, quite difficult to determine if the start and endpoints of the test. It is also difficult to arrange the testing equipment on sites, and there remains the possibility of overprotection that can damage the concrete. It is not generally considered to be a practical-on site test. The protection current required is taken

to be the current at the start of the linear portion of the E-log I curve. Which is sometimes difficult to achieve or detect in real cases.

2.5 Summary of problem to be solved

The repairing method by cathodic protection using sacrificial anodes is one strategy to extend the service life of RC structures as its easy and less maintenance effort during operation. The sacrificial anodes are normally embedded in patch repair material without chloride contamination. It will prevent the macro-cell corrosion due to the potential difference between existing and new material in the surrounding of patch repair boundary. However, the specifier of intervention methods using patch repair and sacrificial anodes cathodic protection (SACP) is often unclear what systems should be used under which circumstances. In this study, a laboratory and field investigation in severely damaged RC beam structures were carried out to examine the effectiveness of repairing method and the results obtained are used to design the reliable repair method and management using sacrificial anodes for RC structures.

The laboratory works related to some consideration during utilization of sacrificial anode in RC structures were reported in **Chapter 3**. The experiments focus on the effect of extreme temperature, rust removal process, and macro-cell corrosion in repair concrete to the application of sacrificial anodes as a repair method in RC structures. The strategy to reduce the initial high current consumption by sacrificial anodes is also reviewed.

In order to understand the actual response, repairing methods using sacrificial anodes applied for more than 40-years of severely damaged RC structures was presented in **Chapter 4**. A new monitoring system using a titanium wire sensor in the repaired RC members was also demonstrated in **Chapter 5.** Therefore, the appropriate parameter for repairing design and maintenance management of damaged RC beam structures based on laboratory and field observations were formulated in **Chapter 6.**

2.6 References

ASTM C876-15, 2015. "Standard test method for half-cell potential of reinforcing steel in concrete", *American Society for Testing and Materials*.

Ahmad, Z., 2006. "Chapter 2 – Basic consepts in corrosion", *Principles of corrosion engineering and corrosion control.* pp. 9-56.

Alonso, C., Castellote, M., Andrade, C., 2000. "Dependence of chloride threshold with the electrical potential of reinforcements", *Proceeding of 2nd International RILEM Workshop Testing and Modelling the Chloride Ingress into Concrete,* Andrade, C., Kropp, J (Eds.), Pro 19, RILEM Publications, pp. 415-425.

Akid, R., 2004. “Chapter 11– Corrosion of Engineering Materials”, Handbook of Advanced Materials, Wessel, J. K. (Eds), *John Wiley & Sons, Inc.*

Andrade, C., Castelo, V., Alonso, C., Gonzales, J. A., 1986. “The determination of the corrosion rate of steel embedded in concrete by the polarization and AC impedance methods”, in: Corrosion Effect of Stray Currents and the Techniques for Evaluating Corrosion of Rebars in Concrete, *ASTM STP 906*, V. Chaker (Ed.), Philadelphia, pp. 43–63.

Andrade, C., Sarria, J., Alonso, C., 1996. “Statistical study on simultaneous monitoring of rebar corrosion rate and internal RH in concrete structures exposed to the atmosphere”, in: *Corrosion of Reinforcement in Concrete Construction*, Page, C. L., Bamforth, P., Figg, J. W., SCI, pp. 233–242.

Andrade, C., Castellote, M., 2002a. “Analysis of total chloride content in concrete”, Rilem TC 178-TMC Recommendation, *Materials and Structures*, Vol. 35, pp. 583–585.

Andrade, C., Castellote, M., 2002b. “Analysis of water soluble chloride content in concrete”, Rilem TC 178-TMC Recommendation, *Materials and Structures*, Vol. 35, pp. 586–588.

Arup, H., 1983. “The mechanisms of the protection of steel by concrete”, *Corrosion of reinforcement in concrete construction,* Crane, A. P. (Ed.), Ellis Horwood, Chichester, pp. 151-157.

Bennett, J. E. and Mitchell, T. A., 1989. “Depolarization of Cathodically Protected Reinforcing Steel in Concrete”, NACE CORROSION/89, Paper No. 373.

Bennett, J. E., 1993. “Cathodic Protection Criteria Related Studies Under SHRP Contract”, Paper No. 323, NACE CORROSION/93.

Bennett, J. and Broomfield, J. P., 1997. “An Analysis of Studies Conducted on Criteria for the Cathodic Protection of Steel in Concrete”, NACE CORROSION/97, Paper No. 251.

Bertolini, L., Bolzoni, F., Lazzari, L., Pastore, T., Pedeferri, P., 1998. “Cathodic Protection and Cathodic Prevention in Concrete. Principles and Applications”, *Journal of Applied Electrochemistry,* Vol. 28, pp. 1321–1331.

Bertolini, L., Elsener, B., Pedeferri, P., Polder, P., 2004. “Corrosion of Steel in Concrete: Prevention, Diagnosis, Repair”, *Wiley-VCH Verlag GmbH & Co. KGaA,* Weinheim.

Bertolini, L., Elsener, B., Pedeferri,P., Redaelli, E., Polder, R., 2013. “Corrosion of Steel in Concrete”, *Wiley-VCH Verlag GmBH & Co KGaA*.

Bürchler, D., Elsener, B., Böhni, H., “Electrical resistivity and dielectric properties of hardened cement paste and mortar”, in: *Electrically based Microstructural Characterization*, Gerhardt, R. A., Taylor, S. R., Garborczi, E. J. (Eds.), *Mater. Res. Soc. Symp. Proc.*, Vol. 411, 407, 1996.

Broomfield, J. P., Rodriguez, J., Ortega, L. M., Garcia, A. M., 1993. “Corrosion rate measurements in reinforced-concrete structures by a linear polarization device”, *Int. Symp. on Condition Assessment, Protection Repair and Rehabilitation of Concrete Bridges Exposed to Aggressive Environments*, ACI Fall Convention, Minneapolis.

CEB, Comité Euro International du Béton, 1989. “Durable Concrete Structures - CEB Design Guide”, *Bulletin D'Information*, No. 182, Lausanne, p. 310.

Chess, P, M., and Broomfield, J, P., 2014. “*Cathodic Protection of Steel in Concrete and Masonry; Second Edition*”, Taylor & Francis Group, LCC, CRC Press, Boca Raton.

Christodoulou, C., Glass, G. K., Webb., J., Ngala, V., Beamish, S., Gilbert, P., 2008. “Evaluation of Galvanic Technologies Available for Bridge Structures”, *12th*

International Conference on Structural Faults and Repair, Edinburgh, UK, pp.11.

Collepardi, M., 1995. "Quick method to determine free and bound chlorides in concrete", *Proc. Int. Rilem Workshop Chloride Penetration into Concrete*, Saint Rémy lès Chevreuse, 15–18 October 1995.

Cortes, E. V, 1993. "Electrochemical Procedures to Rehabilitate Corroded Concrete Structures", *Master's Thesis*, The University of Texas, Austin.

COST 509, 1997. "Corrosion and Protection of Metals in Contact with Concrete", Cox, R. N., Cigna, R., Vennesland, O., Valente, T. (Eds.), Final Report, *European Commission*, Brussels.

COST 521, 2003. "Corrosion of Steel in Reinforced Concrete Structures", Final report, ed. Cigna, R., Andrade, C., Nürnberger, U., Polder, R., Weydert, R., Seitz, E., *European Communities EUR 20599*, Luxembourg, pp. 183–195.

de Rincón, O. T., Hernández-López, Y., de Valle-Moreno, A., Torres-Acosta, A. A., Barrios, F., Montero, P., Oidor-Salinas, P., Montero, J. R., 2008. "Environmental influence on point anodes performance in reinforced concrete", *Construction and Building Materials*, Vol. 22, No. 4, pp.494-503.

Det Norske Veritas (DNV), 2010. "Cathodic Protection Design", Recommended Practice DNV-RP-401, pp. 37.

Dugarte, M. J. and Sagues, A. A., 2014. "Sacrificial Point Anode for Cathodic Prevention of Reinforcing Steel in Concrete Repairs: Part 1 – Polarization Behavior," *Corrosion*, NACE International, Houston, 70(3), pp. 303-317.

Elsener, B., Böhni, H., 1987. "Location of corroding rebars in RC structures" (in German), *Schweiz. Ingenieur und Architekt*, Vol. 105, pp. 528.

Elsener, B., 1988. "Electrochemical methods for monitoring of structures" (in German), *SIA Documentation D020, Non-destructive Testing of Reinforced Structures, Schweiz Ingenieur- und Architekten-Verein*, Zürich, pp. 27–37.

Elsener, B., Böhni, H., 1990. "Potential mapping and corrosion of steel in concrete", in: Corrosion Rates of Steel in Concrete, ASTM STP 1065, Berke, N. S., Chaker, V., Whiting, D. (Eds.), *American Society for Testing and Materials*, Philadelphia, pp. 143–156.

Elsener, B., 1995. "Condition evaluation of reinforced concrete bridges – The benefits of potential mapping", in: *Proc. Int. Conf. Structural Faults & Repair*, London, Vol. 1, No. 47.

Elsener, B., Flückiger, D., Wojtas, H., Böhni H., 1996. "Methoden zur Erfassung der Korrosion von Stahl in Beton", *VSS Forschungsbericht Nr. 520*, Verein Schweiz, Strassenfachleute Zürich.

Elsener, B., 1998. "Corrosion rate of steel in concrete – From laboratory to reinforced-concrete structures", EFC Publication No. 25: Corrosion of Reinforcement in Concrete, *The Institute of Materials*, London, pp. 92–103.

Elsener, B., Andrade, C., Gulikers, J., Polder, R., Raupach, M., 2003. "Recommendation on half-cell potential measurements", *Materials and Structures*, Vol. 36, pp. 461–471.

EN 12696, "Cathodic Protection of Steel in Concrete," European Standard, 2000.

Etcheverry, L., Fowler, D. W., Wheat H, G., and Whitney D. P., 1998. "Evaluation of Cathodic Protection Systems for Marine Bridge Substructures", Research Report 2945-1, *Center for Transportation Research Bureau of Engineering Research The University of Texas*, Austin.

Feliù, S., Gonzales, J. A., Andrade, C., Feliù, V., 1988. “On site determination of the polarization resistance in a reinforced concrete beam”, Corrosion/ 88, *NACE*, Paper No. 44.

Feliù, S., Gonzales, J. A., Andrade, C., 1996. “Electrochemical methods for onsite determinations of corrosion rates of rebars”, in: Techniques to Assess the Corrosion Activity of Steel Reinforced Concrete Structures, *ASTM STP 1276*, Berke, N. S., Escalante, E., Nmai, C. K., Whiting, D. (Eds.), American Society for Testing and Materials, Vol. 107.

Funahashi, M. and Young, W. T., 1992. “Investigation of 100 mV Shift Criterion for Reinforcing Steel in Concrete”, NACE CORROSION/92, Paper No. 193.

Garcia, J., Almeraya, F., Barrios, C., Gaona, C., Nunez, R., Lopez, I., Rodriguez, M., Martinez-Villafane, A., and Bastidas, J. M, 2012. “Effect of Cathodic Protection on Steel-Concrete Bond Strength Using Ion Migration Measurements”, *Cement and Concrete Composites*, Vol. 34, No. 2, pp. 242-247.

Gonzales, J. A., Algaba, S., Andrade, C., Feliu, V., 1980. “Corrosion of reinforcing bars in carbonated concrete”, *British Corrosion Journal*, Vol. 15, No. 135.

Gonzalez, J. A., Lopez, W., Rodriguez, P., 1993. “Effects of moisture availability on corrosion kinetics of steel embedded in concrete”, *Corrosion*, Vol. 49, pp. 1004–1010.

Hobbs, D. 2001. “Concrete Deterioration: Causes, Diagnosis, and Minimizing Risk”. In: *International Materials Reviews 46.3*, pp. 117–144.

Hunkeler, F., 1991. “Bauwerksinspektion mittels Potentialmessung”, *Schweizer Ingenieur und Architekt,* Vol. 109, pp. 272.

JSCE, 2007. “Standard Specification for Concrete Structures (Part: Maintenance)”, *Japan Society of Civil Engineers*, Japan.

Liu, Y., 1996. “Modeling the time-to corrosion cracking of the cover concrete in chloride-contaminated reinforced concrete structures”, *Diss. Virginia Tech*.

Millard, S. G., Harrison, J. A., Edwards, A. J., 1989. “Measurements of the electrical resistivity of reinforced-concrete structures for the assessment of corrosion risk”, *Journal of Non-destructive Testing*, Vol. 31, No. 11.

Myrdal, R., 1997. “Evaluation of electrochemical techniques for assessing corrosion of steel in concrete”, *dissertation for the degree of Doctor Scientarium*, University of Oslo.

NACE SP0290-07, 2007. “Impressed Current Cathodic Protection of Reinforcing Steel in Atmospherically Exposed Concrete Structures”, NACE International, Houston, TX, p. 15.

Nilsson, L. O., Poulsen, E., Sandberg, P., Sorensen, H. E., Klinghoffer, O., 1996. “Hetek, Chloride penetration into concrete”, *State of the art report No. 53, The Road Directorate*, Copenhagen.

Okada, K., 1976. “Reinforcement corrosion in concrete structures”, *Report of the Corrosion and Corrosion Inhibition Committee JSMS 1976,* Vol. 14, No. 74.

Pedeferri, P., 1996. “Cathodic Protection and Cathodic Prevention”, *Construction and Building Materials*, Vol. 10, No. 5, pp. 391-402.

Polder, R. B., Valente, M., Cigna, R., Valente, T., “Laboratory investigation of concrete resistivity and corrosion rate of reinforcement in atmospheric conditions”, *Proc. Rilem/ CSIRO Int. Conf. on Rehabilitation of Concrete Structures*, Melbourne, Ho, D. W. S., Collins, F. (Eds.), pp. 475–486.

Polder, R. B., Bamforth, P. B., Basheer, M., Chapman-Andrews, J., Cigna, R., Jafar, M. I., Mazzoni, A., Nolan, E., Wojtas, H., 1994. "Reinforcement corrosion and concrete resistivity – State of the art, laboratory and field results", *Proc. Int. Conf. on Corrosion and Corrosion Protection of Steel in Concrete*, Swamy, R. N. (Ed.), Sheffield Academic Press, 24–29 July 1994, pp. 571–580.

Polder, R., Andrade, C., Elsener, B., Vennesland, O., Gulikers, J., Weydert, R., Raupach, M., 2000. "Test methods for on site measurement of resistivity of concrete", *Materials and Structures*, Vol. 33, pp. 603–611.

Polder, R. B., Peelen, W. H. A., Bertolini, L., Guerrieri, M., 2002. "Corrosion rate of rebars from linear polarization resistance and destructive analysis in blended cement concrete after chloride loading", *ICC 15th International Corrosion Congress*, Granada, 22–27 September 2002.

Pourbaix, M., 1973. "Lectures on corrosion", *Plenum Press,* New York.

Rajendran, V and Murugesan, R., 2013. "Study on Performance of Self Regulating Sacrificial Galvanic Anodes with and without Preconditioning Against Control Specimen and Using Accelerated Corrosion", *Asian Journal of Civil Engineering (BHRC)*, Vol. 14, pp. 181-199.

Richardson, M. G., 2002. "Fundamentals of durable reinforced concrete", *CRC Press.*

Revie, R., V., 2000. "Uhlig's corrosion handbook", 2nd Edn., *J. Wiley and Sons.*

Shciegg, Y., 1995. "Potentialfeldmessungen nach der Instandsetzung", *SIA Dokumentation D0126*, Schweiz. Ingenieur und Architektenverein Zürich.

SIA 2006, 2006. "Richtlinie zur Potentialfeldmessung", *Schweiz Ingenieur und Architektenverein*, Zürich.

Shreir, L. L., Jarman, R. A., Burnstein, G. T., (Eds.), 1984. "Corrosion", 3rd Edn, *Buttherworth Heinemann.*

Stratfull, R., F., 1957. "The corrosion of steel in a reinforced concrete bridge", *Corrosion,* Vol. 13, 173.

Stratfull, R., F., 1974. "Cathodic protection of a bridge deck", Materials Performance, Vol. 13, No. 4, 24.

Page, C. L., Treadaway, K. W. J., 1982. "Aspects of the electrochemistry of steel in concrete", *Nature,* Vol. 297, No. 13, pp. 109-114.

Page, C. L., Vennesland, Ø., 1983. "Pore solution composition and chloride binding capacity of silica fume cement pastes", *Materials and Structures*, Vol. 16, No. 91.

Page, C. L., 1997. "Cathodic protection of reinforced concrete – Principles and applications", *Proc. Int. Conf. on "Repair of Concrete Structures"*, Svolvaer, Norway, 28–30 May 1997, pp. 123–132.

Pedeferri, P., 1980. "Corrosion and protection of metallic materials", *Clup,* Milan.

Pedeferri, P., 1996. "Cathodic protection and cathodic prevention", *Construction and Building Materials,* Vol. 10, pp. 391–402.

Pedeferri, P., Bertolini, L., 2000. "Durability of reinforced concrete, *McGrawHill,* Italia.

Polder, R. B., Walker, R., Page, C. L., 1995. "Electrochemical desalination of cores from a reinforced concrete coastal structure", Magazine of Concrete Research, Vol. 47, pp. 321–327.

RILEM Technical Committee 124-SRC, P. Schiessel (ed), 1994. "Draft Recommedation for Repair Strategies for Concrete Structures Damaged by Reinforcement Corrosion", *Materials and Structures*, Vol. 27, pp. 415 – 436.

Schiegg, Y., Audergon, L., Elsener, B., Böhni, H., 2001. “On-line monitoring of the corrosion in reinforced-concrete structures”, *Eurocorr 2001*, Associazione Italiana di Metallurgia, Milano.

Takewaka, K., 1993. “Cathodic Protection for Reinforced Concrete and Prestressed Concrete Structures”, *Corrosion Science*, Vol. 35, pp. 1617-1626.

Tinnea, J. S., and Tinnea, R. J., 2014. “Cathodic Protection Evaluation”, Final Report, ODOT Contract PSK28885, *Oregon Department of Transportation*, Bridge Preservation Unit, pp. 82.

Tuutti, K., 1982. “Corrosion of steel in concrete”, *Sweedich Foundation for Concrete Research,* Stockholm.

Vennesland, Ø., 2007 “Electrochemical techniques for measuring corrosion in concrete – measurements with embedded probes”, *Rilem TC-EMC*, *Materials and Structures*, Vol. 40, pp. 745-758.

Watanabe, H., Hamada, H., Yokota, H., and Yamaji, T., 2001. “Long Term Performance of Reinforced Concrete under Marine Environment (20 Year of Exposure Test)”, *3rd International Conference on Concrete under Severe Condition*, Vancouver, Canada, pp. 530 – 537.

Weydert, R., Gehlen, C., 1998. “Electrolytic resistivity of cover concrete: relevance, measurement and interpretation”, *8th Conf. on Durability of Materials and Components.*

Wilson, K., Jawed, M., and Ngala, V., 2013. “The Selection and Use of Cathodic Protection Systems for the Repair of Reinforced Concrete Structures”, *Construction and Building Material*s, Vol. 39, pp. 19-25.

Zimmermann, L., Schiegg, Y., Elsener, B., Böhni, H., 1997. “Electrochemical techniques for monitoring the conditions of concrete bridge structures”, *Repair of Concrete Structures*, Svolvaer, Norway, A. Blankvoll (Ed.), Norwegian Road Research Laboratory, pp. 213–222.

CHAPTER III

Fundamental study on the effectiveness of sacrificial anodes in RC members

3.1 Overview

The purpose of the repair will be to ensure that significant deterioration does not occur in the future. Sometimes this is simply the removal of the cause and replacement of the deteriorated concrete. Where the corrosion of the steel bar is involved, the planning process requires significantly more consideration (The Concrete Society, 2009). Focusing on the optimal life-cycle scenarios for concrete structures in service, it is important to make sure the quality of structures during their service life. The rational evaluation of deterioration and damage in concrete as early as possible is important for performing the preventive maintenance and subsequently constructing rational life cycle scenarios (Shitani *et al.*, 2017). Once the problem is clearly defined and the extent of the current and future deterioration is known, the repair option, the potential costs, and timescales can be assessed. The Concrete Society (2009) defined six option for effective concrete repair is commonly used, singly or more often in a combination of:

- do nothing, but monitor
- reanalyze the structural capacity of the weakened element
- prevent or reduce further deterioration
- strengthen or refurbish all or part of the structure
- replace all or part of the structure
- demolish, completely or partially.

In this chapter, several fundamental experimental studies related to the consideration of the repair process using sacrificial anodes in the viewpoint of non-homogeneous chloride contamination, rust removal process, temperature effect, were explained in **Chapter 3.2**, **3.3**, and **3.4**.

3.2 Effect of non-homogeneous chloride contamination

3.2.1 Introduction

Nowadays, sacrificial anode as one of the cathodic protection system is considered as one of the most effective and widely used electrochemical methods in controlling chloride-induced rebar corrosion. On a practical level, reinstating corrosion protection in concrete using sacrificial anode does not need perfect repairs; only physical damages need to be repaired, without the need to remove a lot of chlorides contaminated concrete and without perfect cleaning of steel. However, as commonly knows, many patch repair or partially-repaired concrete and their surrounding areas have exhibited new corrosion damage after a few months to a year (Elsener, 2002).

Moreover, in some cases, the partial repair causes to generate more local macro-cells corrosion and make the structure deteriorate more rapidly. Macro-cell corrosion with the local anode and large cathode mainly occur in chloride-induced corrosion of rebar embedded in concrete and cause very local corrosion damage (Mohammed *et al.*, 2003). One of the approaches to studying the macro-cell corrosion introduced by Miyazato is the segmented steel bar (Hobbs, 2001). Regardless of the method of partial repair concrete, this situation may eventually create an environment characterized by a non-homogeneous distribution of chloride ions (Bertolini *et al.*, 2013). Regarding the definition of macro-cell corrosion, anodic and cathodic reactions are spatially separated along with the reinforcing steel. In the case of segmented-reinforcing steel embedded in concrete, when the corrosion progresses, electronic current travels from element to element through the wire connection. It is supposed that each element only represents either anode or cathode. Since the length of the steel element is different, the possibility of anodic and cathodic reactions occurring in the same element is affected. The longer the length of the element is, the possibility becomes larger (RILEM, 1994). From the viewpoint of the repair method, the effectiveness of anode utilization on partially-repaired concrete is very important to investigate.

To contribute to a better knowledge concerning these issues, this study attempts to identify the effectiveness of sacrificial anode concerning the effective length of embedded steel in partially-repaired concrete that can be protected by the sacrificial anode. The results are discussed with respect to consequences for corrosion monitoring by macro-cell protective and corrosion current density, depolarization and polarization curve of embedded steel and sacrificial anode. The aim of the works in this subchapter is to identify the long-term performance of embedded steel elements on partially-repaired concrete protected by sacrificial anode against macro-cell corrosion under a non-homogeneous chloride environment until four years.

3.2.2 Experimental program

3.2.2.1 Materials

A sacrificial anode with 60 mm in diameter and 30 mm in thickness was used as shown in **Figure 3.1**.

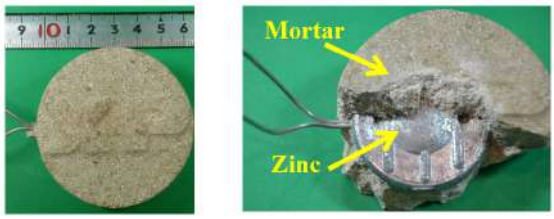

Figure 3.1 Sacrificial anodes

Ordinary Portland Cement (OPC) was used in the concrete specimen. Tap water (temperature 20±2°C) was used as mixing water. Sea sand passing 5 mm sieve with a density of 2.58 g/cm^3 and water absorption of 1.72 % which was less than 3.5% as stated in JIS standard, was used as fine aggregate. Meanwhile, crushed stone with a 20 mm maximum size was used as a coarse aggregate. All aggregates were prepared under surface saturated dry conditions. The ratio of fine aggregate to total aggregate volume (s/a) was 0.47. The properties of aggregates and admixtures are shown in **Table 3.1**.

Table 3.1. Properties of materials

Component	**Physical properties**	
Ordinary Portland Cement	Density, g/cm^3	3.16
Fine Aggregate	Density, g/cm^3 (SSD Condition)	2.58
	Water absoption (%)	1.72
	Fineness modulus	2.77
Coarse aggregate	Density, g/cm^3	2.91
AEWR agent	Polycarboxylate ether-based	
AE agent	Alkylcarboxylic	

3.2.2.2 Mix proportion

The composition of concrete mixture proportions for four specimens is described in **Table 3.2**.

Table 3.2 Mix proportion

Material	**Existing Concrete**		**Repair Concrete**	
	Series A	**Series B**	**Series A**	**Series B**
Water-cement ratio (w/c), %	45	45	45	45
Sand-aggregate ratio (s/a), %	47	47	47	47
Water, kg/m^3	190	190	190	190
Cement (C), kg/m^3	422	422	422	422
Sand, kg/m^3	766	766	766	766
Gravel, kg/m^3	970	970	970	970
Chloride, kg/m^3	4	10	-	-
Additive:				
- AE, mL	C*0.45%			
- AE-WR, gr	2.5mL/kg-C			

3.2.2.3 Specimen design, casting process, and curring method

The specimens in this subchapter were prepared and observed for early age by Rafdinal, 2016. Four beams specimens with 150x100x795 mm in dimension were prepared in this study to identify the long-term performance of the segmented steel reinforcement element, which is embedded under a non-homogeneous chloride environment, namely A1, A2, B1, and B2. Each concrete specimen contained a segmented steel bar connected with a sacrificial anode (SCP), a segmented steel reinforcement without connection sacrificial anode (SNCP) and a steel bar without segmented and without sacrificial anode (S) positioned in parallel with an in-between distance of 35 mm. The detail of the concrete specimen is depicted in **Figure 3.2**.

Three bars have a clear cover thickness of 30 mm from the bottom surface of the specimen. It was also ensured that the segmented steel reinforcement showed no sagging in order to maintain a constant cover thickness along the total exposure length. Series A1 and B1 consist of one segmented rebar 75 mm length in repair concrete. Meanwhile, A2 and B2 consist of two segmented 75 mm length in repair concrete, which means 150 mm in total. The length of the element gradually increases from 75 mm to 100 mm.

The casting of concrete specimens with non-uniform chloride ion concentrations was carried out in two steps. Firstly, the casting of existing concrete with chloride contaminated in the molds and demolded after 24 hours. After demolding, all specimens were subject to 14 days of sealed curing with wet towels. Secondly, before placing repair concrete in the molds, the sacrificial anode was installed on the steel bar as figures in **Figure 3.3**. Furthermore, followed by casting the repair concrete, demolded after 24 hours and were kept to 28 days of sealed curing again with wet towels.

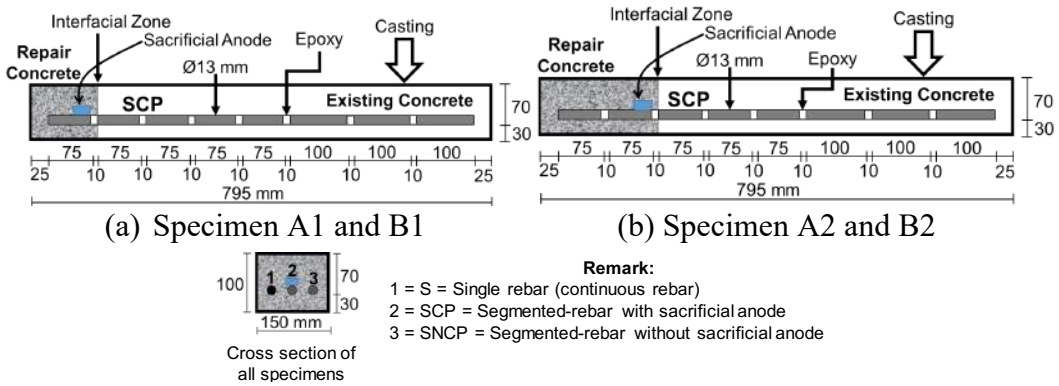

Figure 3.2 Specimen design

After 28 days of sealed curing, sacrificial anode connected to lead wires on the segmented steel in repair concrete, so current flows to existing concrete were started.

Adjacent steel elements were connected through wires to allow the flow of current. However, these connectors were temporarily disconnected to measure macro-cell and protective currents.

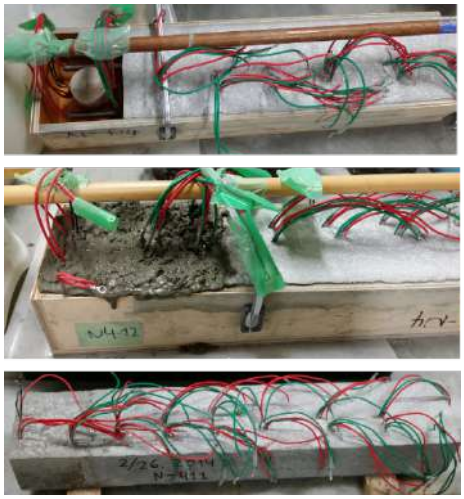

Figure 3.3 Casting process by Rafdinal, 2016

3.2.2.4 Exposure condition

After existing and repair concrete casting were finished, all specimens were subject to exposure conditions in the form of wet-and-dry cycling. Wet cycle means immersion in 3% NaCl solution through two days followed by five days of dry condition; hence, one cycle corresponded to seven days. At the end of the dry cycle, measurements were taken weekly. Continuous cyclic exposure condition was maintained throughout until two years and continued by the dry condition.

3.2.2.5 Measurement methods

In order to observe the performance of segmented steel with sacrificial anode embedded in partially repaired concrete, several electrochemical investigations were conducted. However, this paper focuses on presenting macro-cell corrosion and protective current density, depolarization test, and anodic polarization curve testing. Macro-cell corrosion and protective current measurement were carried out periodically once a week at the end of the dry cycle by using a data logger. In macro-cell corrosion, a divided steel bar is used to measure the actual macro-cell currents passing through one steel element to the adjacent element, as represented in **Figure 3.4**. Depolarization test was regularly carried out by disconnecting the steel bars from sacrificial anodes for 24 hours. Also, it was continued by anodic-cathodic polarization curve which was conducted to determine the conditions of the passivity film of steel bars.

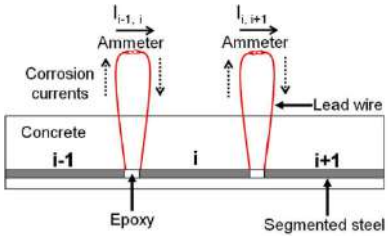

Figure 3.4 Measurement method of macro-cell corrosion current

Macro-cell corrosion current density of specimens with non-uniform chloride concentrations was measured periodically by using zero resistance ammeter, as shown in **Figure 3.4**. The following equation was used to calculate the macro-cell current density over a steel element:

$$I_{mac} = \frac{I_o - I_i}{A} \qquad (3.1)$$

where I_{mac} = macro-cell current density of a steel element (μA/cm^2); I_o = outflow current in μA from the steel element; I_i = inflow current in μA to the steel element; and A = surface area of the steel element (cm^2). If the value of I_{mac} is positive, the steel element is defined as an anode, and if negative as a cathode.

3.2.3 Result and discussion

3.2.3.1 Protective current density of sacrificial anodes

The periodic macro-cell protective current density on anode with one-steel bar element in repair concrete against the distance from the edge of repair concrete is shown in **Figure 3.5** and **Figure 3.6**. It was also observed that protective current still flows up to 60-months from steel bar in patch repair concrete to segmented steel bar in existing concrete. The current flow is ~8 μA/cm^2 for A1 and ~0.2 μA/cm^2 for B1 at 24-months of polarization time. At 60-months, the current flow of A1 and B1 is gradually decreased until almost zero.

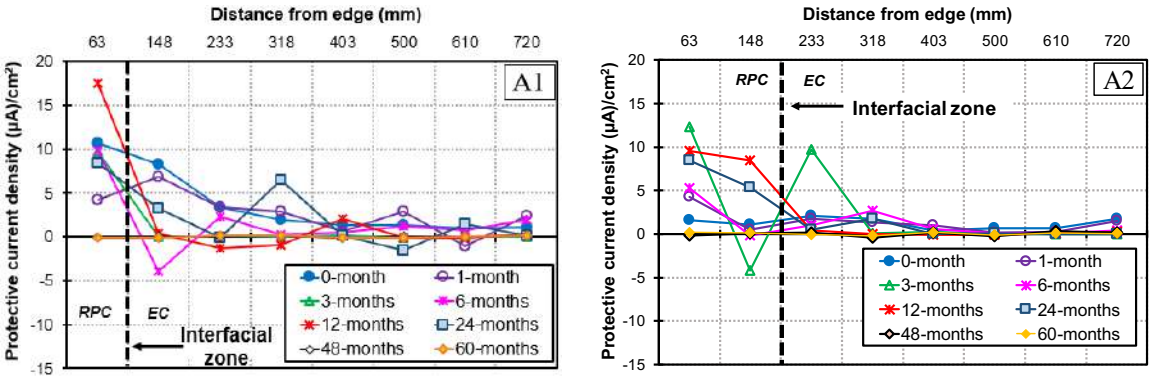

Figure 3.5 Protective current density of A1 and A2

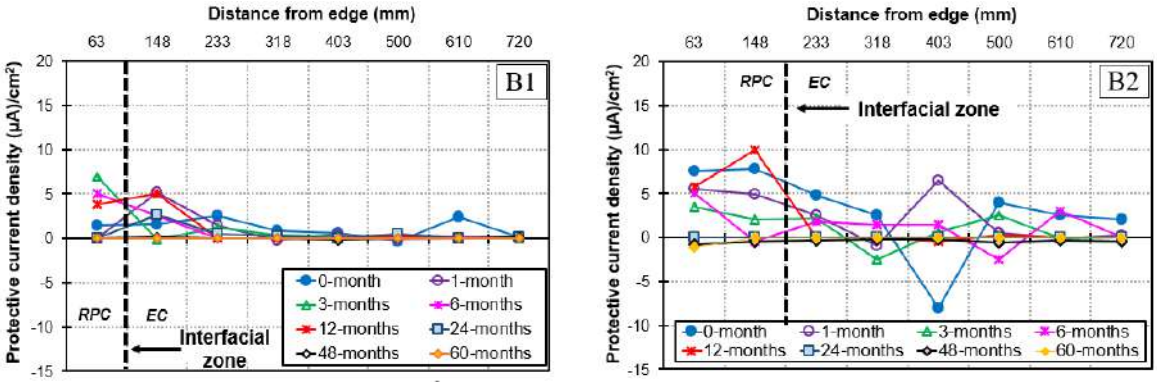

Figure 3.6 Protective current density of B1 and B2

The current flow is ~8 μA/cm^2 for A2 and ~0.39 μA/cm^2 for B2 at 24-months of polarization time. It means the throwing current of anode fulfills the cathodic protection current design. After the specimens moved to dry conditions, the current flow generated by anodes was significantly decreased until almost to be zero until 60-months of exposure.

3.2.3.2 Macro-cell corrosion current density of steel bars

The macro-cell corrosion current density on anode at A1 and B1 with one-steel bar element in repair concrete against the distance from the edge of repair concrete are present in **Figure 3.7** and **Figure 3.8**.

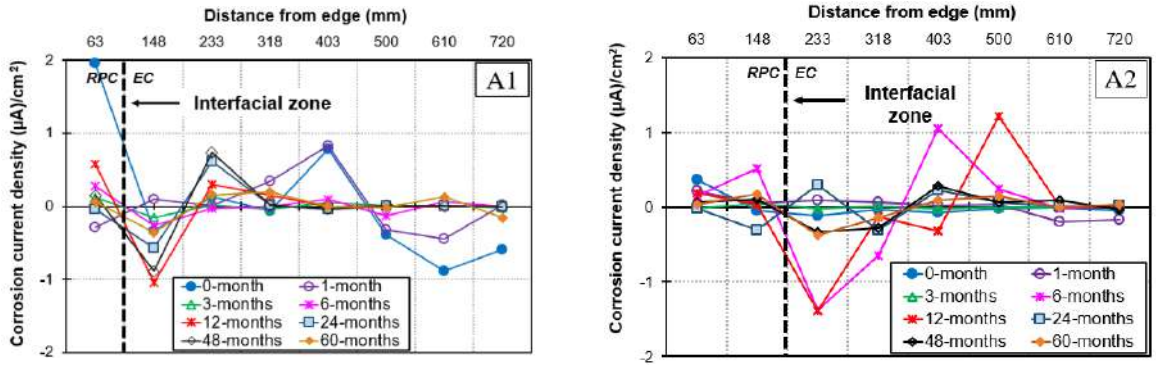

Figure 3.7 Macro-cell corrosion of steel bar protected by anode in A1 and A2

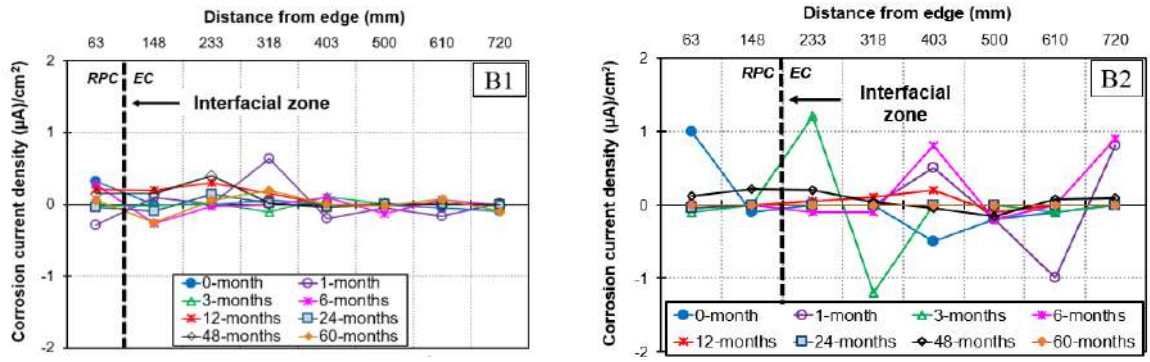

Figure 3.8 Macro-cell corrosion of steel bar protected by anode in B1 and B2

Macro-cell corrosion current density is found at a relatively early age and is disappeared at a relative later age. This time-dependent behavior is observed for all of the specimens. The figures also show that macro-cell corrosion was formed coupling between the steel element located at chloride contaminated existing concrete as an anode and other steel elements as a cathode. It was also observed that macro-cell corrosion was formed coupling in the boundary between chloride-free concrete as an anode and its surrounding chloride contaminated as a cathode, in the early age of exposure period. The measurement at 48-months and 60-months shows a relatively small macro-cell corrosion.

In the case of A2, even at 182 days of exposure, macro-cell corrosion was formed coupling in the boundary, and also in the existing concrete. In B2 specimen, at the early age of exposure, macro-cell current occurred. In general, both A2 and B2 specimens show the same tendency with A1 and B1, wherein the macro-cell corrosion current density tends to change over the exposure time at the interfacial zone of non-homogenous chloride environment. After the specimens moved to dry conditions, the macro-cell corrosion decrease to be a very small value at 48-months and 60-months.

3.2.3.3 Potential development of steel bars

On the potential of steel bar protected by the sacrificial anode (SCP) in all specimens are depicted in **Figure 3.9**, and **Figure 3.10**. **Figure 3.11** and **Figure 3.12** illustrate the evolution of the instant-off potential of steel bars embedded in the specimens.

The data shows that anode polarize steel bar in patch repair concrete of A1 more negative -1000 mV at 24-months of exposure time and it shifts to around -400 mV ~ -300 mV at 48-months and 60-months both repair and existing concrete. Meanwhile, the potential of steel bar increased to noble value at a steel bar position around 230 mm from the edge. Furthermore, the anode in B1 also polarizes the steel bar in patch repair concrete in protection condition up to 24-months of exposure time and the polarization decrease over time until 60-months. However, this potential value increased in a positive direction in the existing concrete.

The data also was shown that anode polarize steel bar in repair concrete of A2 more negative -900 mV at 24-months of polarization time and around -400 mV~-300 mV at 48-months and 60-months. Meanwhile, the potential of steel bar increased to noble value at a steel bar position around 310 mm from the edge. Nevertheless, the anode in B2 also polarizes the steel bar in patch repair concrete by -700 mV up to 24-months of exposure time and

around -400 mV~-300 mV at 48-months and 60-months. However, this potential value increased to a positive direction in the existing concrete as same as SCP-A1 and SCP-B1.

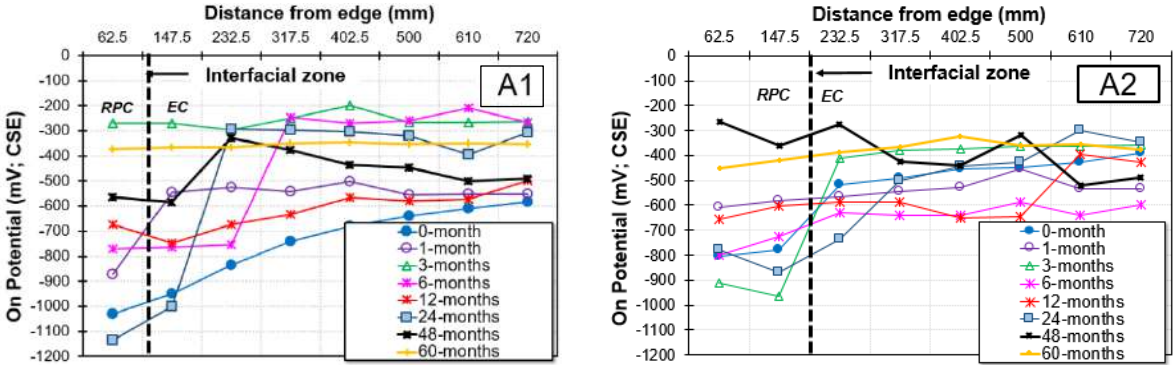

Figure 3.9 On potential of steel bar protected by sacrificial anode in A1 and A2

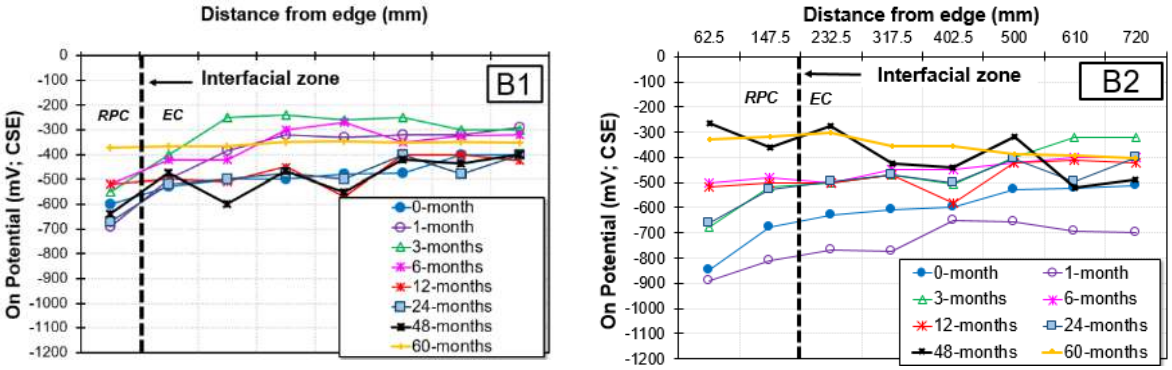

Figure 3.10 On potential of steel bar protected by sacrificial anode in B1 and B2

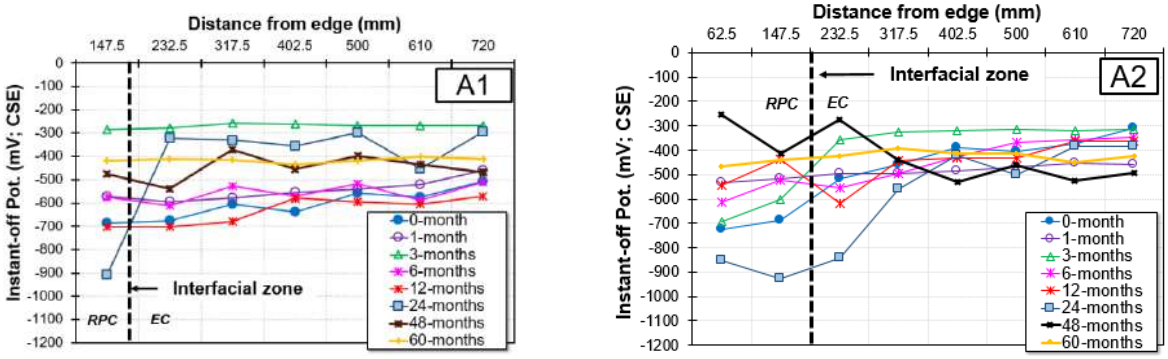

Figure 3.11 Instant-off potential of steel bar protected by sacrificial anode in A1 and A2

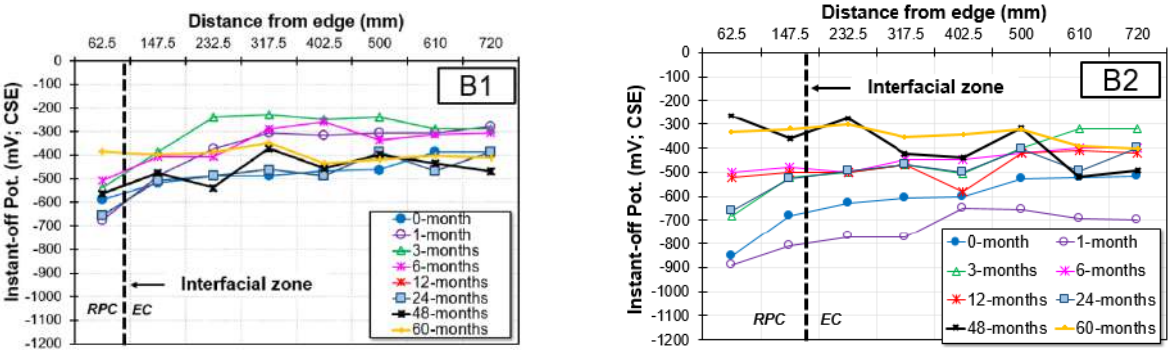

Figure 3.12 Instant-off potential of steel bar protected by sacrificial anode in B1 and B2

The rest potential of the segmented steel bar protected by sacrificial anode in all specimens was depicted in **Figure 3.13** and **Figure 3.14**.

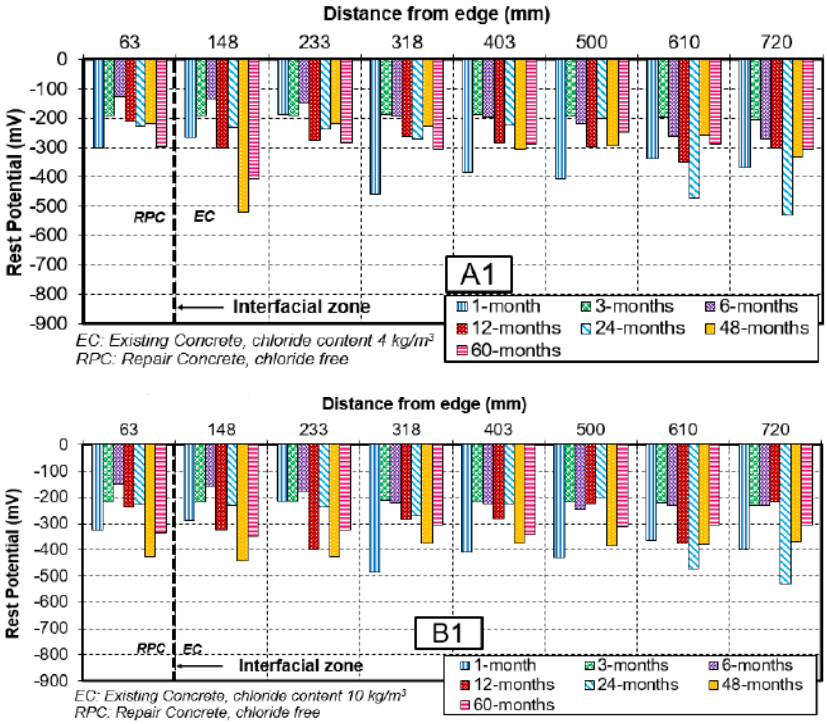

Figure 3.13 Rest potential of steel bar protected by sacrificial anode in A1 and B1

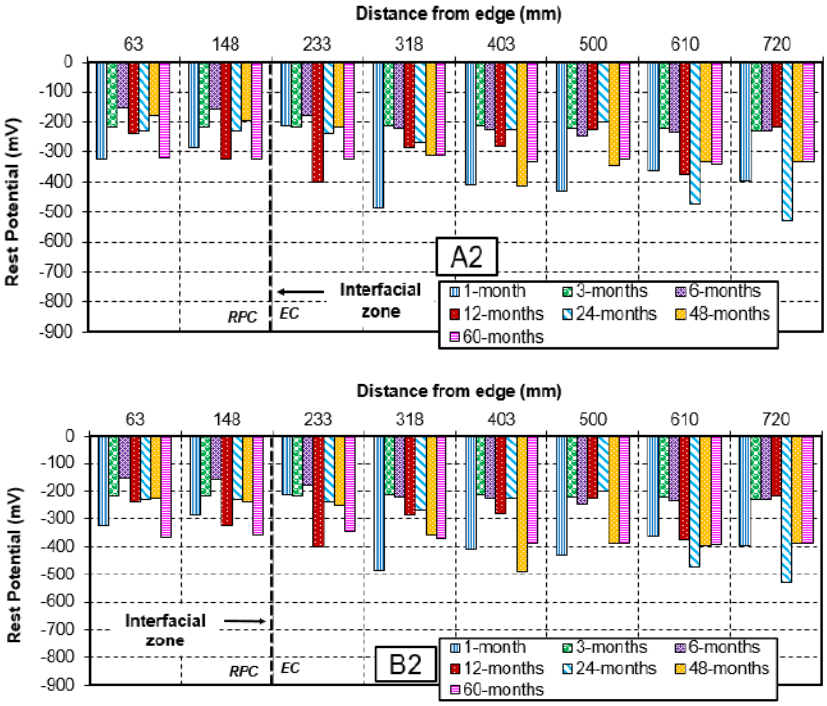

Figure 3.14 Rest potential of steel bar protected by sacrificial anode in A2 and B2

The rest potential of the steel bar in A1 presents more potential shifts than in B1. It may due to the existing concrete of A1 has lower than chloride contamination in B1. Furthermore, the length of the repair part also affects the polarization of steel bar presented by the rest

potential of steel bars in A1 and B1 is more positive than A2 and B2. It indicates that the smaller patch repair part more positive the rest potential after the application of sacrificial anodes.

Figure 3.15 and **Figure 3.16** present the rest potential of half-cell potential of steel bar without sacrificial anode protection. It clearly can be seen that the steel bar protected by sacrificial anodes presents more positives rest potential value at all specimens.

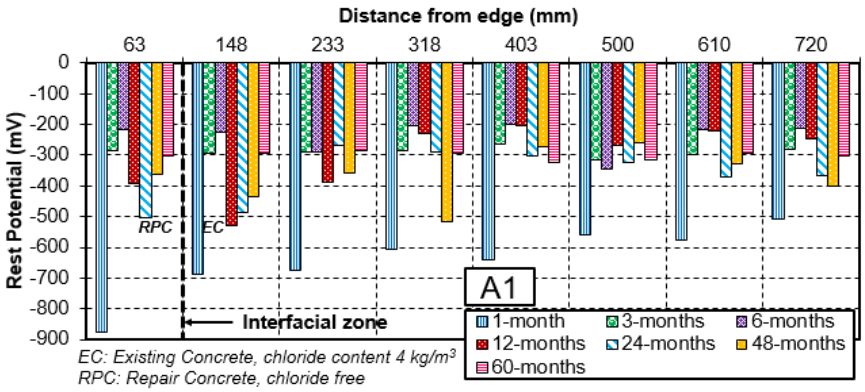

Figure 3.15 Rest potential of steel bar without sacrificial anode in A1

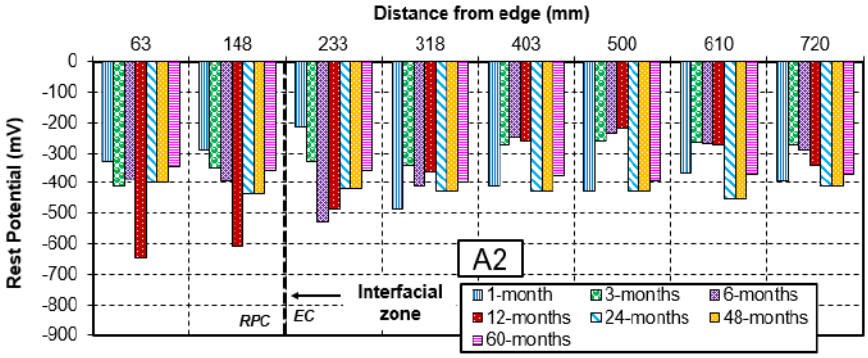

Figure 3.16 Rest potential of steel bar without sacrificial anode in A2

3.2.3.4 Potential development of anodes

The potential development of sacrificial anodes, including on potential, instant-off potential, and rest potential, were presented in **Figure 3.17** and **Figure 3.18**. It shows that the potential of anodes is more than -900 mV in the early connection and it gradually increases over time.

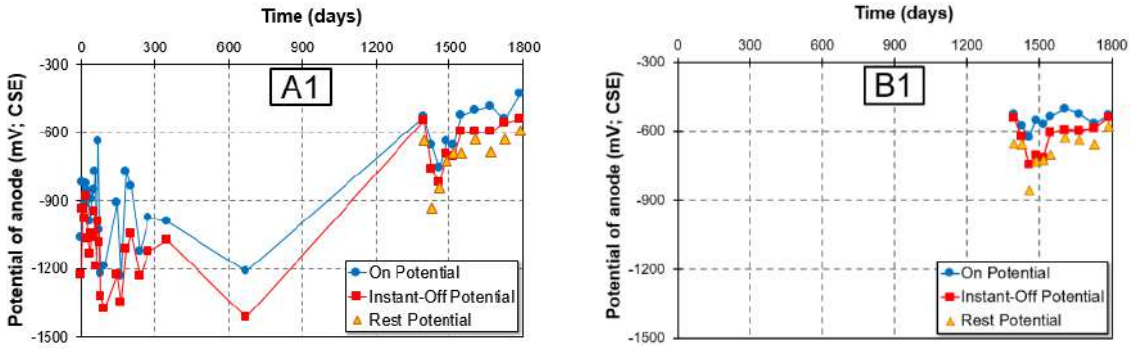

Figure 3.17 Potential development of sacrificial anodes in A1 and B1

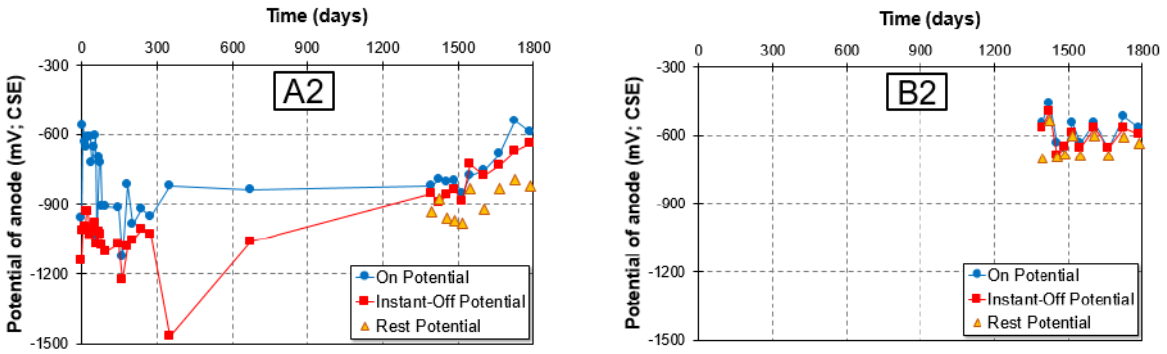

Figure 3.18 Potential development of sacrificial anodes in A2 and B2

3.2.3.5 Depolarization test

Depolarization tests as performance criteria of cathodic protection were regularly carried out by disconnecting the steel bars from the sacrificial anode for 24 hours. Instant off potentials was measured immediately after the disconnection of the sacrificial anodes (E_{off}) and the potential values were measured after 24 hours ($E_{off,24h}$). The commonly used criterion for sufficient protection is 100 mV potential decay (the difference between $E_{off,24h}$ and E_{off}).

Figure 3.19 illustrates the depolarization test of A1 and B1 on SCP against the distance from the edge of repair concrete and **Figure 3.20** illustrates the depolarization test on SCP at A2 and B2 specimens. From these figures, it was observed that the potential decay decreases as the exposure time increases. The data shows that potential decay exceeds 100 mV for SCP-A1 and SCP-B1 around 403 mm and 318 mm respectively from the edge of the specimen at 12-months. Or around 340 mm and 216 mm from the anode position in patch repair concrete for SCP-A1 and SCP-B1 successively. This distance decreased significantly at 24-months of polarization time, reaching 170 mm from the interfacial zone for SCP-A1 and SCP-B1. The effective length of A1 decreases to be almost zero at 48-months but A2 shows that the effective length increases to be 250 mm at the same time.

Meanwhile, the data from **Figure 3.20** indicates that potential decay exceeds 100 mV for SCP-A2 and SCP-B2 around 500 mm and 318 mm respectively from the edge of the specimen at 12-months of exposure, it means around 440 mm and 260 mm from the anode position in patch repair concrete for SCP-A2 and SCP-B2 successively. This distance decreases significantly at 24-months of polarization time for SCP-A2 by reaching 260 mm from the interfacial zone for SCP-A2. However, the effective length for SCP-B2 kept constant by 260 mm with polarization time. The effective length of B1 and B2 presents the same value (200 mm) at 48-months. It relatively no change at B2 and it decreases into zero at B1 after 60-months.

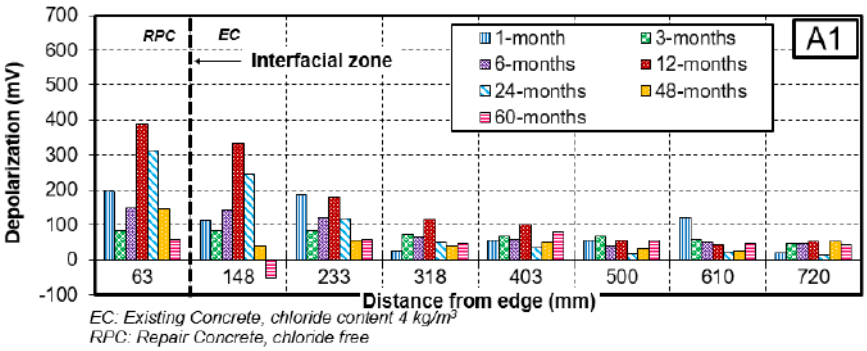

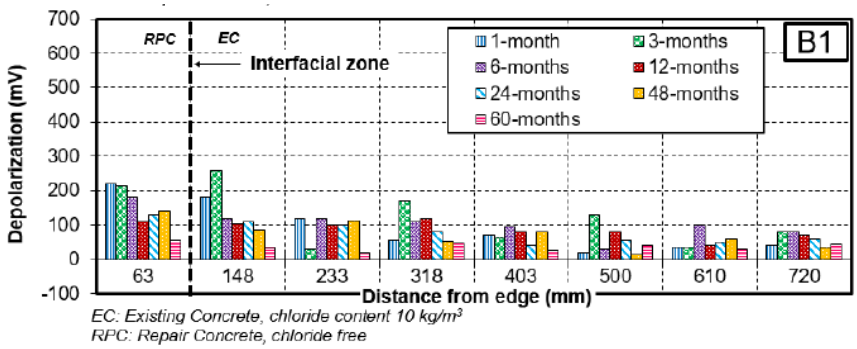

Figure 3.19 Depolarization test value of A1 and B1

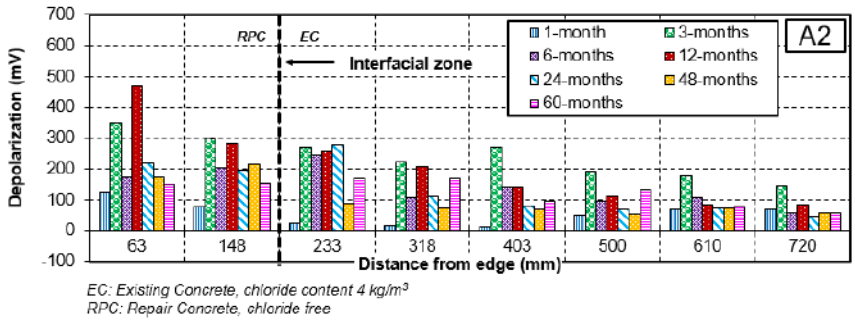

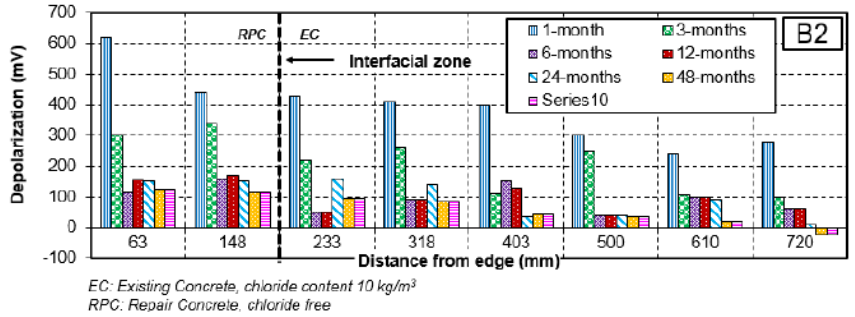

Figure 3.20 Depolarization test value of A2 and B2

Based on 100 mV CP criterion, it was observed that the effective length of embedded steel with sacrificial anode protection and 4 kg/m^3 of chloride content in existing concrete are 340 mm for one-steel bar and 440 mm for the two-steel bar from the anode position in patch repair concrete at 12-months of polarization time. Meanwhile, for 10 kg/m^3 chloride content in existing concrete, the effective length from the anode location is 260 mm and 170 mm for one-steel bar and two-steel bar element in repair concrete, respectively. It means, up

to one-year of exposure time, the higher chloride content in existing concrete, the shorter effective length could be achieved.

Meantime after 24-months of polarization time, the effective length was stand up to 170 mm from the anode position in patch repair concrete for A1 and B1, also to around 260 mm for A2 and B2. It means anodic site increases time-dependently in parent concrete mainly for A1, A2, and B1. It was noticed that after a two-year exposure time, the effective length of embedded steel element on partially-repaired concrete protected by sacrificial anode against macro-cell corrosion under a non-homogeneous chloride environment is 170 mm. **Figure 3.21** shows the summarized effective length of sacrificial anodes after more than five years of exposure in all specimens.

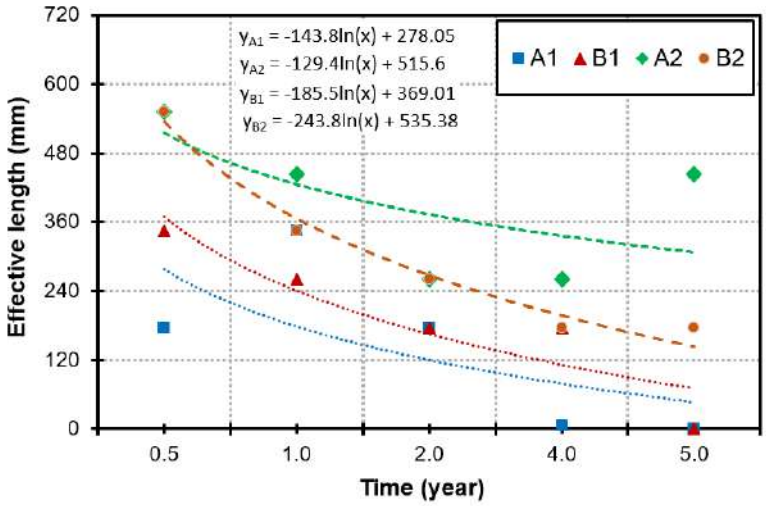

Figure 3.21 Effective length of sacrificial anode after five years of exposure

3.2.4 Conclusion

From the five-years of observation, several findings are derived.

1. From the macro-cell corrosion and protective current density test results, it was observed that macro-cell corrosion was formed coupling in the boundary between chloride-free concrete as anode and its surrounding chloride contaminated as cathode for all specimens since initial exposure condition indicated by the different potential. The protective current density and macro-cell corrosion are significantly decreased after five-years of exposure due to the exposure condition were changed to dry condition.
2. The depolarization test result shows positive value until five-years of exposure in the relatively small protective current density of anodes. It means the sacrificial anodes still work until five-years.

3. In the repairing case, the lower chloride contamination of existing concrete the higher the effectivity of sacrificial anodes application indicated by higher depolarization value and more positive rest potential value of steel bar. The smaller repairing part length the higher depolarization test value.

3.3 **Effect of the rust removal process of steel bar**

3.3.1 Introduction

The corrosion experiencing section maybe patch-repaired by removing the chloride-contaminated concrete and replacing it with chloride-free concrete. As a result, the previous active steel in the patch becomes passive, and corrosion stops. However, that transition to the passive condition also elevates the potential of the steel in the patch from its former highly negative value to one that can be several hundred mV more positive, removing the natural cathodic prevention effect initially in place (Pedeferri, 1996; Presuel-Moreno *et al.*, 2005).

The lower value of chloride threshold in the surrounding zone then maybe less than the existing local chloride concentration and active corrosion could promptly start (Alonso *et al.*, 2002). The detrimental consequence is called macro-cell corrosion around the repaired patch (Christodoulou et al., 2008). In this case, prevention may be restored by applying a sacrificial anode in the repair section. The anode takes up the function of the previous corroded rebar and prevents re-deterioration due to corrosion starting both in the repaired patch area and the boundary.

The sacrificial anode is commercially available for casting in patch repairs, for intended purposes of forestalling the macro-cell corrosion effect (Sergi, 2011). On a practical, reinstating corrosion protection in concrete using sacrificial anode cathodic protection in the repaired patch does not require perfect repairs; only physical damages need to be repaired, without the need to remove a lot of chloride-contaminated concrete and without the need to perfect rust cleaning of steel. The variability appears when evaluation of anode in such cases stems from the current demand by the rebar assembly, which may be sustained at high levels for long periods, or drop rapidly in the early life of the test depending on the initial condition of the steel surface, small variations in the pore water composition, or concrete moisture (EN 12696, 2000; ASTM, 1999). In the application of sacrificial anode cathodic protection in repaired patch concrete, accumulation of corrosion products in reinforcing bar surface may impede the passage of ionic current or even promote passivation

of the anode surface causing fail to deliver protection (Dugarte and Sagüés, 2014; Rafdinal, 2016).

Regarding the cleaning of steel bar before application of sacrificial anodes, the effect of rust removal on deteriorated reinforced concrete structures before anodes application in the repair section has not been clearly reported. In this paper, the influence of rust removal of steel bar surface on the performance of the sacrificial anode in repaired RC members during a three-year observation is presented.

3.3.2 Experimental program

3.3.2.1 Materials

Ordinary Portland Cement (OPC) was used as a binder, and tap water (temperature 20±2°C) was used as mixing water. Washed sea sand passing a 5 mm sieve with a density of 2.58 g/cm3 and water absorption of 1.72 %, which was less than 3.5% as stated in JIS standard, was used as fine aggregate. Meanwhile, crushed stone with a maximum size of 10 mm was used as a coarse aggregate. All aggregates were prepared under surface-saturated dry conditions. The ratio of fine aggregate to total aggregate volume (s/a) was 0.47. The properties of aggregates and admixtures are shown in **Table 3.3**.

Moreover, a galvanic anode made of zinc as the main material was used as the sacrificial anode. The dimension is 140 mm in length, 45 mm in depth, and 13 mm in width, as shown in **Figure 3.22**.

Table 3.3 Properties of materials (Rafdinal, 2016; Rafdinal *et al.,* 2016; Astuti *et al., 2018)*

Component	Physical properties	
Ordinary Portland Cement	Density, g/cm3	3.16
Fine Aggregate	Density, g/cm3 (SSD Condition)	2.58
	Water absoption (%)	1.72
	Fineness modulus	2.77
Coarse aggregate	Density, g/cm3	2.91
AEWR agent	Polycarboxylate ether-based	
AE agent	Alkylcarboxylic type	

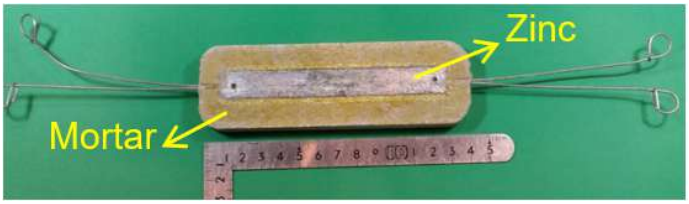

Figure 3.22 Sacrificial anode installed on the rebar (Rafdinal, 2016; Rafdinal *et al.,* 2016)

In this research, 20-year-old deteriorated reinforcing bars with a diameter of 13 mm were used, as shown in **Figure 3.23**. These steel bars were taken from the specimens exposed in a severe chloride environment with high temperatures for 20 years. For the non-rusted condition, the deteriorated rebar was immersed in a 10% (weight percentage) di-ammonium hydrogen citrate solution for 24 hours, and the rust was removed by using a steel wire brush. At both ends of each rebar, a 30 cm lead wire was screwed.

Figure 3.23 A 20-year-old deteriorated reinforcing bar

3.3.2.2 Mix proportion

A concrete mix with water to cement (w/c) ratio of 0.45 was used for specimens. Mix proportions of concrete are shown in **Table 3.4**.

Air-entraining agent and water-reducing admixture were added to the cement mass to obtain the slump and air content in all concrete mixes in the range of 10±2.5cm and 4.5±1%, respectively. There were two types of concrete mix proportions used for each specimen; existing concrete (chloride-contaminated) and patch repair concrete (chloride-free). Pure sodium chloride (NaCl) as the source of chloride ions was added around 10 kg/m^3 during mixing into the existing concrete to accelerate the corrosion process.

Table 3.4 Mix proportions of concrete specimens (Rafdinal, 2016; Rafdinal *et al.,* 2016)

Material	Existing concrete	Repair concrete
Water-cement ratio (w/c), %	45	45
Sand-aggregate ratio (s/c), %	47	47
Water, (kg/m^3)	190	190
Cement, (kg/m^3)	422	422
Sand, (kg/m^3)	766	766
Gravel, (kg/m^3)	970	970
Chloride, (kg/m^3)	10	0
Additive		
- AE, mL	19	19
- AE-WR, kg	1.34	1.34

3.3.2.3 Specimen design

Three specimens, notated as D1 and D2, with the dimensions of 580 mm in length, 150 mm in width and 100 mm in depth were fabricated. Each specimen consisted of two steel bars with a diameter of 13 mm, same surface conditions, and positioned parallel to each other with an intermediary distance of 40 mm and a cover thickness of around 30 mm from the

bottom surface of the specimen. D1 specimen illustrated rust removal before replacement material application in the repair section, and D2 specimen demonstrated the application of sacrificial anodes and material casting rust removal before. The details of the concrete specimen are depicted in **Figure 3.24**. In addition, a sacrificial anode was applied to the repair concrete section.

In order to simulate the repair process, the concrete casting process was in two steps. First, the existing concrete was placed and was demolded after 24 hours. After demolding, all specimens were subject to 14 days of sealed curing with wet towels and followed by the installation of the sacrificial anode on the steel bar, and new concrete was placed in the repair part. After 24 hours, the specimens were demolded, followed by masked curing with wet towels for 28 days.

After 28 days of sealed curing, the sacrificial anode was connected to one of the embedded steel in the patch repair concrete. Adjacent steel element and the sacrificial anode was connected through lead wires to measure the current flow generated by sacrificial anodes. At the end of the steel bar in the repair section, a 30 cm length lead wire was screwed. The connection of wire and steel bar was covered by epoxy resin to avoid the corrosion at the connection. The thickness of the epoxy layer was approximately 10 mm. However, these connectors were temporarily disconnected to measure the instant-off potential, the protective current, and depolarization. The saturated calomel electrode (SCE) is used as a reference electrode for potential measurement in this study.

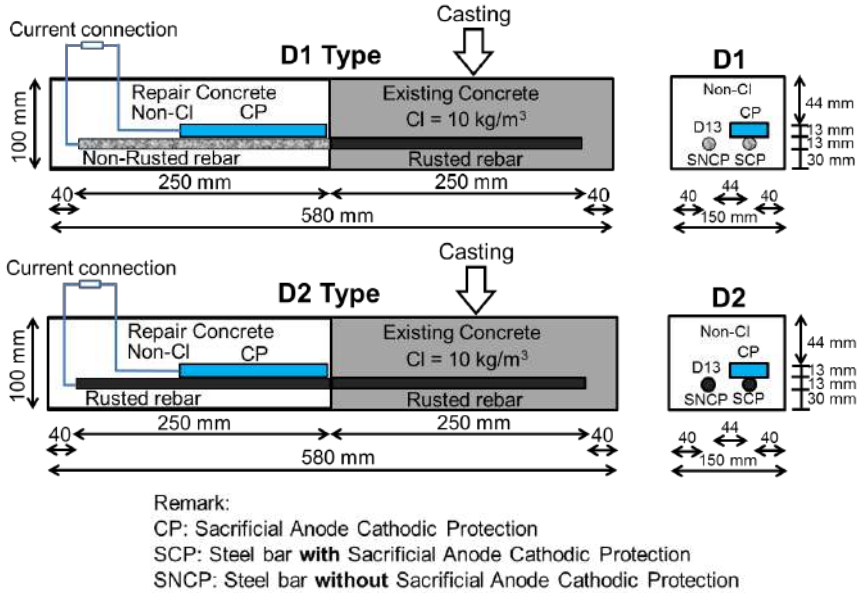

Figure 3.24 Specimen design

3.3.2.4 Exposure conditions

After the casting of both existing and repair concrete was finished, specimens were subjected to exposure conditions, in the air curing with a temperature of 20±2°C and relative humidity of 60%. This environment was kept for 105 days of exposure time. After that, the specimens were moved to the dry-wet cycle condition. Five days in dry condition was followed by two days of wet cycle involved immersion in a 3% NaCl solution up to 140-days; hence, one cycle corresponded to seven days. Measurements were taken weekly at the end of the wet cycle. Then, the specimen was stored in dry laboratory air condition up to 1000 days before moved to wet condition until 1400 days.

3.3.2.5 Measurement method

The potential of rebar in the distance of 10 mm from the boundary between the repaired patch and existing concrete was monitored during on potential, instant-off potential, and rest potential by using half-cell potential measurement. Saturated calomel electrode (SCE) was used as a reference electrode for measurement, and this potential reading was converted to copper/copper sulfate electrode (CSE) in 25°C (ASTM, 2015).

3.3.3 Results and discussion

3.3.3.1 Protective current density of sacrificial anodes

The current density generated by the anodes to the reinforcing bar as a function of exposure time until 1260-days is shown in **Figure 3.25**. The current density of all specimens shows the trend to decrease gradually as a function of time in air curing and laboratory air condition. However, the sacrificial anodes became active after the changing of exposure condition to be a wet-dry condition, due to the high moisture content of concrete (Rafdinal, 2016; Rafdinal *et al.,* 2016). In the early age of the repair process until 140-days of measurement was reported by Rafdinal (2016). In this experiment, no measurement was conducted from 140 days to 720 days. In this phase, the specimens were kept in dry laboratory conditions. The re-starting of measurement was conducted from 721-days. It shows that the increase of current flow generated by anodes was occurred due to the increase of moisture content in concrete during pre-wetting before measurement.

In this observation, only in the first 140-days (air curing and wet-dry condition) and wet condition, the protective current level was within the design limit of cathodic protection between 0.2 – 2.0 μA/cm^2 as specified in EN 12696. After the change of the environmental condition to dry laboratory air, the protective current is less than the minimum design limit

of cathodic protection. In the viewpoint of the protective current density of anodes, generally, the specimen with rust removal shows higher current density than specimen without removal time dependency.

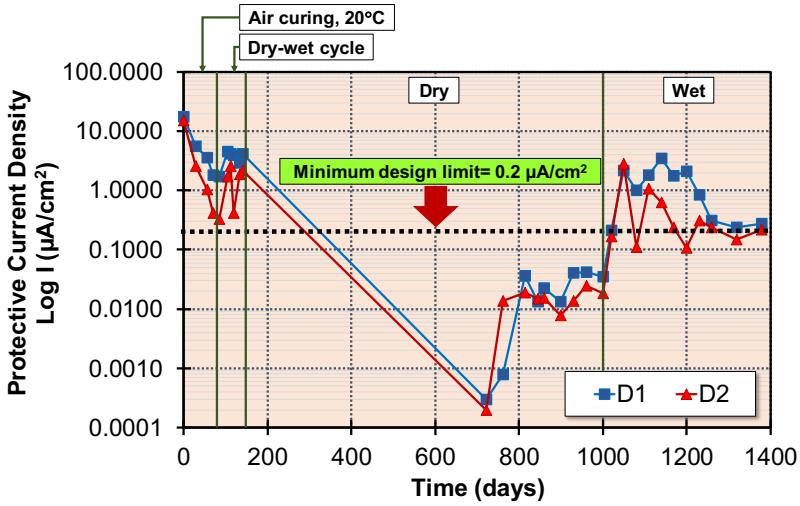

Figure 3.25 Protective current density

3.3.3.2 Potential development of rebar and anode

In the case of cathodic protection application, observation of potential development on rebar and anodes was recorded consist of on-potential, instant-off potential, and rest potential. On-potential is observed during the connection of sacrificial anode and rebars. The instant-off potential is measured between 0.1 and 1 second after switching off the protection current of anodes to remove the IR drop of measured potential. Rest potential is checked 24 hours after switching off between sacrificial anode and rebar. The position of these measurements is 50 mm from the interfacial zone to the repair and the existing concrete.

Figure 3.26, Figure 3.27, and Figure 3.28 present on-potential, instant-off potential, and rest potential of rebar, respectively. The rest potential of rebar in existing concrete with chloride-contaminated was slightly more negative than in repair part or chloride-free concrete. In specimen D1, the rebar with rust removal connected to the sacrificial anode (SCP) in repair concrete shows more negative results than rusted rebar between air curing and dry-wet condition. When the exposure condition is changed to wet-dry cycles, the potential of rebar shifted to the negative direction, and when it is changed to dry laboratory air, the potential of rebar shifted to the more positive value. This phenomenon is caused by the change in moisture and oxygen content in the concrete. The potential of rusted rebar connected to anodes is gradually decreased around -580 mV for repair concrete and approximately -600 mV for existing concrete after 1000-days of exposure in dry air condition. It is more clear when the environmental condition was changed to wet condition,

the rest potential of rebars with rust removal in the repair section was shifted to be more positive value than rebar in existing concrete. These results express that non-rusted rebar is on better protection than rusted rebar after three years of exposure.

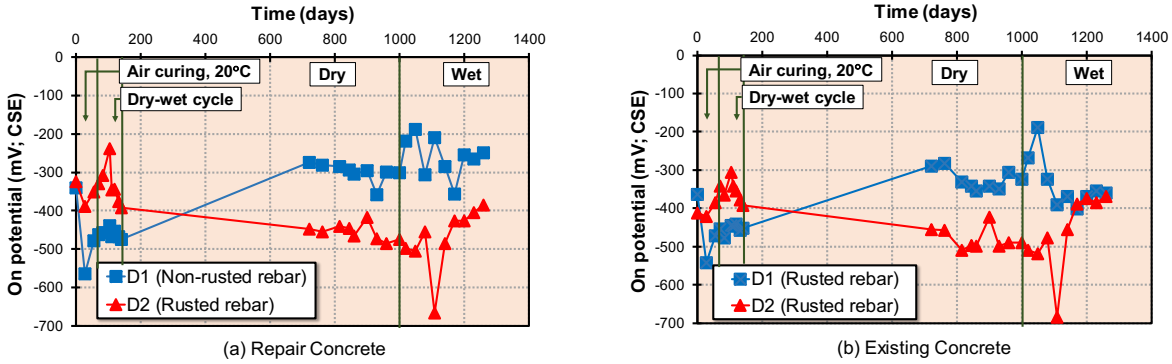

(a) Repair Concrete (b) Existing Concrete

Figure 3.26 On potential of steel bar connected by sacrificial anode

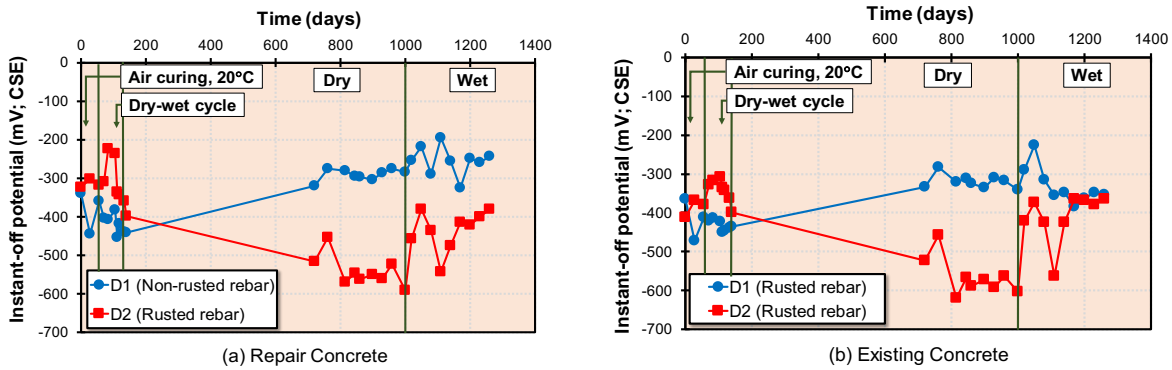

(a) Repair Concrete (b) Existing Concrete

Figure 3.27 Instant-off potential of steel bar connected by sacrificial anode

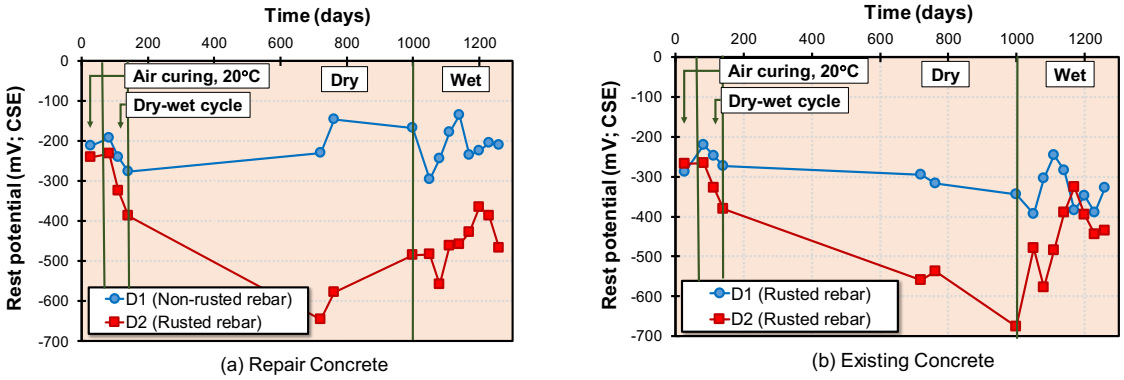

(a) Repair Concrete (b) Existing Concrete

Figure 3.28 Rest potential of steel bar connected by sacrificial anode

The half-cell potential of rebar without anodes connection (SNCP) with the instant-off potential of rebar protected by the anode (SCP) is depicted in **Figure 3.29**. After the exposure changed from wet-dry to dry condition, the potential of rebar SNCP-D1 and SNCP D2 are shifted to be more positive due to the absence of water and oxygen on the steel surface. It gradually changed to 90% corrosion condition when it moved to wet condition. Based on ASTM C876-91:2015, the rebar in "corrosion condition" during the dry-wet cycle and wet condition.

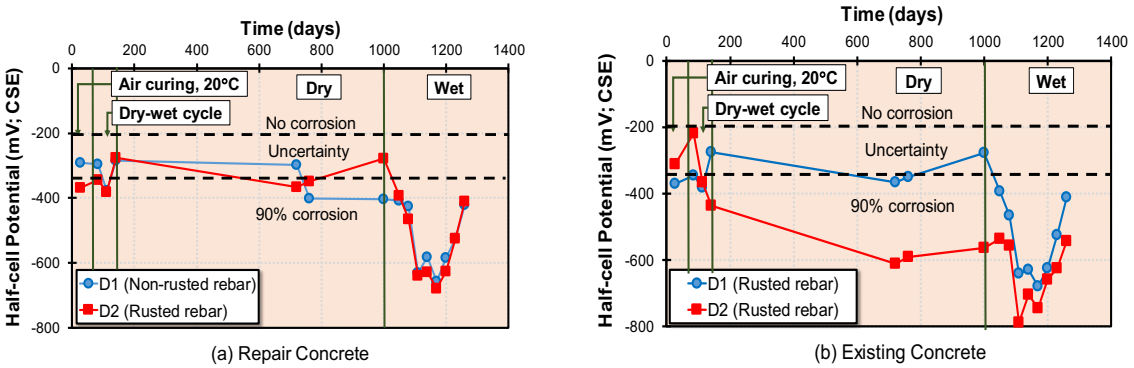

Figure 3.29 Half-cell potential of steel bar without anode connection

Figure 3.30 (a) and **(b)** show the rest potential mapping on specimens in dry conditions (1000-days) and in wet conditions (1200-days). It shows that a steel bar protected by sacrificial anode in repair and existing concrete demonstrates similar rest potential conditions in dry conditions. Meanwhile, the rest potential of the steel bar without sacrificial anode connection is greatly affected by chloride contamination. The effect of the rust removal process in repair concrete also may be one of the factors to present better conditions in the repair section. The rest potential result in dry and wet conditions indicate that higher moisture content in concrete reveals lower rest potential and increases the corrosion probability of rebar both in chloride contaminated and chloride-free concrete.

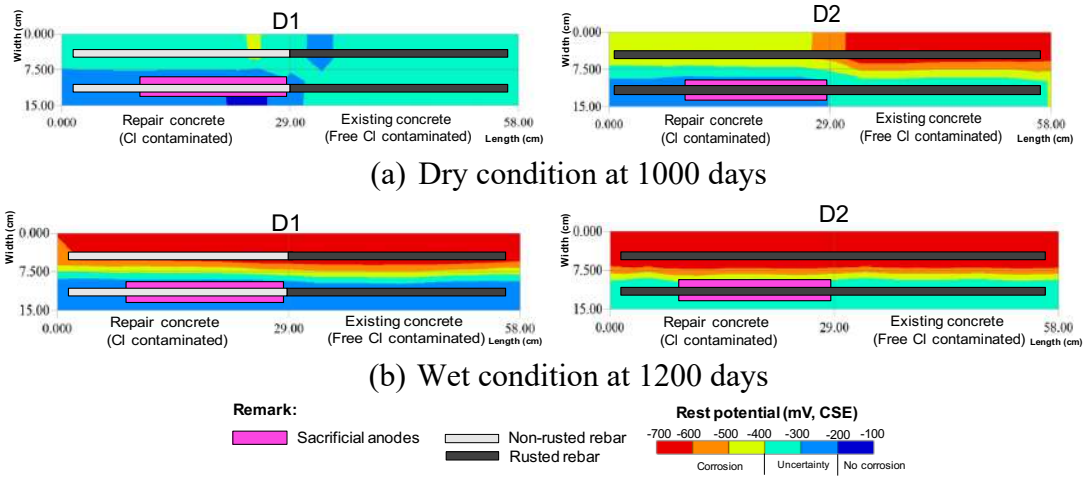

Figure 3.30 Rest potential mapping of steel bar

The potential development of anodes is shown in **Figure 3.31**. During the exposure at air curing from 0-day to 105-days, the on-potential and instant-off potential of anodes in all specimens increased gradually to be a positive value. Furthermore, when the environment changed to be a dry-wet condition, the potential of anodes in all specimens slightly shifted to be more negative again and relatively stable until the end of exposure time. The rest potential shows that in the early age of the specimen, the rest potential of anodes is around -

1100 mV ~ -900 mV. The anode in D2 specimen shows stable in dry condition but D1 specimens show increasing rest potential in -400 mV. In the last environmental condition, both D1 and D2 show a similar trend of rest potential in around -100 mV. It indicates that the moisture level of concrete affected the potential of the sacrificial anode, which is a similar trend as the potential development of rebars.

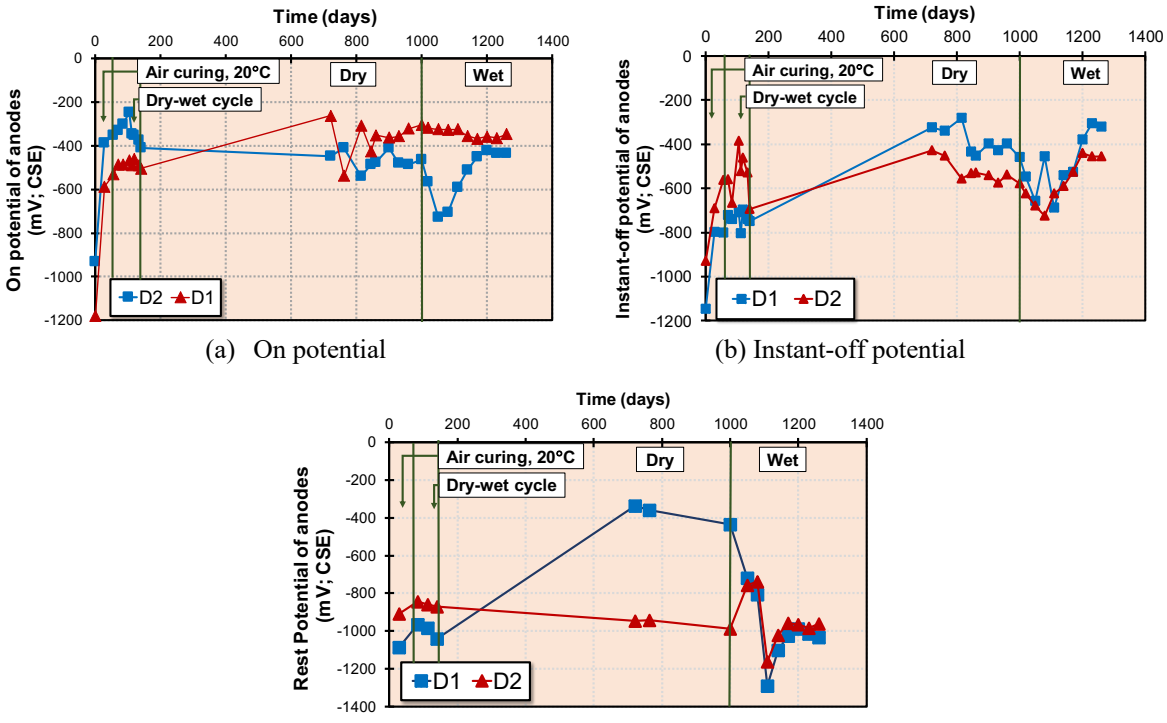

(a) On potential (b) Instant-off potential

(c) Rest potential

Figure 3.31 Potential development of anodes

3.3.3.3 Depolarization test

In this research, depolarization test was carried out by disconnecting the rebar from anodes for 24 hours and calculating the difference value between the instant-off potentials was measured immediately after disconnection of the sacrificial anodes (E_{off}), and the potential values were measured after 24 hours ($E_{off\ 24h}$). The 100 mV depolarization value is used as a criterion for evaluating the effectiveness of the cathodic protection system for reinforced concrete structures (EN 12696).

Figure 3.32 illustrates the depolarization value of rebar in repair and existing concrete during the exposure time. It can be observed that SCP-D1 (steel bar with rust removal) achieves the 100 mV potential decay criterion until 1000 days during exposure condition of air curing 20°C, wet-dry cycle, and dry laboratory air. Meanwhile, SCP-D2 (steel bar without rust removal) fails to exceed 100 mV since the beginning of exposure time. After the exposure condition is changed to wet conditions from 100-days, it was observed that the

depolarization of the steel bar in the repair part is generally in positive value. It means the sacrificial anodes effective to protect the steel bar only in the repair area.

In this research, the effect of steel bar with and without rust removal in long-term observation with several conditions until 1260 days is still not clear. It may because a new corrosion product was generated in both steel bars. From this evaluation, a non-rusted rebar condition in repair concrete (chloride-free) is the most desirable initial condition when the sacrificial anode is applied on it to protect the corroded steel bar in existing concrete (chloride contamination).

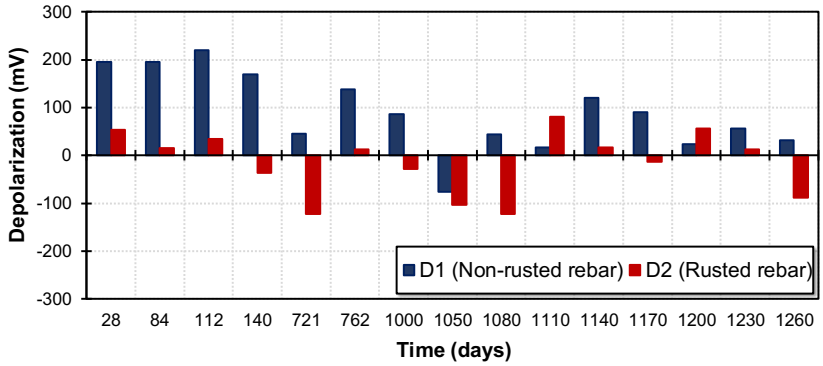

(a) Repair Concrete

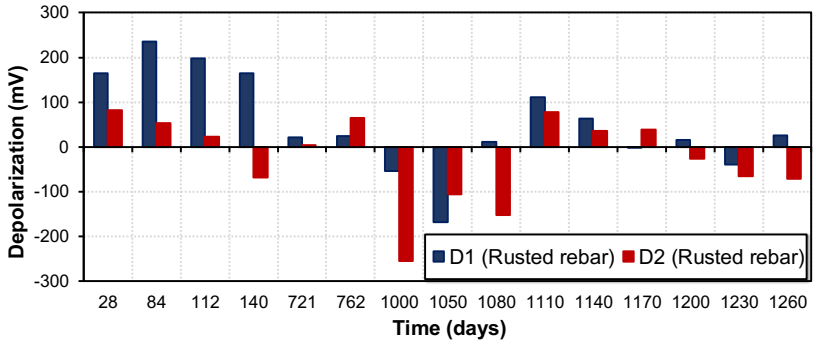

(b) Existing Concrete

Figure 3.32 Depolarization test value of steel bar connected by sacrificial anodes

3.3.4 Conclusion

From the experimental program, several findings can be explained as follows.

1. The potential development of rebar is affected by the steel surface condition and the moisture level of the concrete.
2. The protective current of the sacrificial anode became more active in the humid conditions than in dry conditions, due to the high moisture content in concrete.
3. Based on the 100 mV decay criterion, protective conditions were achieved on the steel bars connected to the sacrificial anode with rust removal as an initial condition until three-years.

4. Corrosion product on steel surface decreases the effectiveness of cathodic protection even though embedded in chloride-free concrete because the rust on the steel bar impeded the current flow from anode to the steel bar when sacrificial anode applied on it.
5. Rust removal on steel surface in repair concrete is the most desirable initial condition when the sacrificial anode is applied on it to protect the corroded steel bar in existing concrete.
6. In this research, the influence of the rust removal process in the steel bar surface is not clear during exposure time in several conditions until 1260 days. It may because the new corrosion product was generated in the steel bar.

3.4 **Effect of low and high temperature**

3.4.1 Introduction

The design of a sacrificial anode cathodic protection system should consider the type and location that it is placed to achieve sufficient and long life protection (Rafdinal, 2016). It is because the current flow generated from the sacrificial anode is related to the environment. Anodes in wet or humid conditions will produce higher levels of protective current and deliver it to the reinforcement that needs to be protected (Dugarte and Sagüés, 2009). All the processes involved in corrosion (i.e., anodic and cathodic electrochemical reactions, transport of aggressive species to the steel surface, accumulation of corrosion products on the steel surface or departure from the interface of steel/concrete, and ionic flow through concrete) are influenced by temperature (Dugarte and Sagüés, 2014).

Sacrificial anode cathodic protection should have sufficient performance to protect the rebar from active corrosion. The tropical countries are prone to corrosion risk especially on the RC structures exposed to the marine environment. Regarding the low-temperature environmental condition, sacrificial anodes which designed for several types of structures in freeze conditions, such as RC structure in the northern area, natural gas station, and CO_2 storage. The performance of the sacrificial anode application in the high and low-temperature condition is not reported in the previous study. Thus, this paper reviews the performance of sacrificial anode exposed under low and high temperatures around -17°C, 4-5% of relative humidity and 40°C, 98% of relative humidity. The relative humidity is fixed and cannot be changed during exposure due to the limitation of apparatuses. So, it simulated the extreme condition over time.

3.4.2 Experimental program

3.4.2.1 Specimen design

The geometry of the specimens employed in the present investigation is illustrated in **Figure 3.33**. The beams featured total dimensions of 100×150×290 mm and were reinforced with two D13-steel bars. The reinforcement was positioned to obtain a clear concrete cover of 30 mm at the bottom and sides of the beam, whereas the distance between bars was kept at 40 mm. Moreover, a galvanic anode F type made of zinc as the main material was used as the sacrificial anode. The dimension is 140 mm in length, 45 mm in width and 13 mm in depth, as shown in **Figure 3.34**. The identical specimen for high and low-temperature exposure was used.

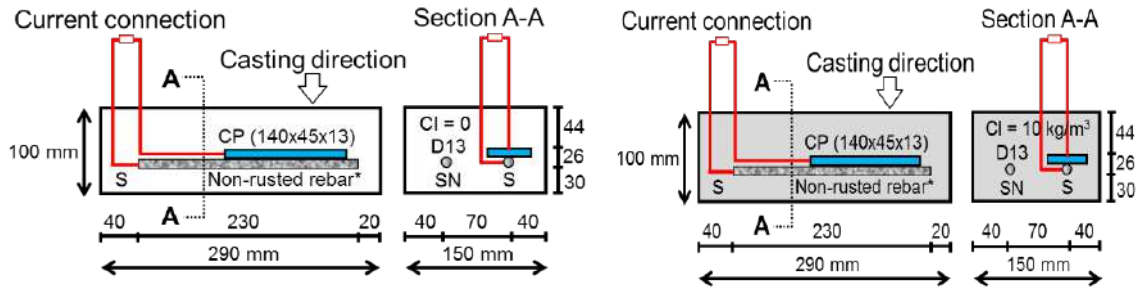

(a) CL0-H and CL0-L (b) CL10-H and CL0-L

Figure 3.33 Specimen design

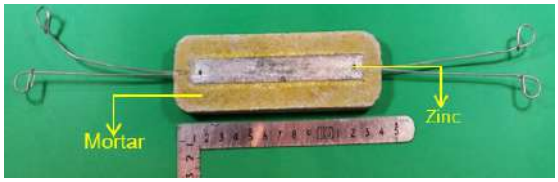

Figure 3.34 Sacrificial zinc anode F type

Ordinary Portland Cement (OPC) was used as a binder, and tap water (temperature 20±2°C) was utilized as mixing water in this study. Washed sea sand is passing 5 mm sieve with a density of 2.58 g/cm^3 and water absorption of 1.72 % which was less than 3.5% as stated in Japan Industrial Standard (JIS), which was used as the fine aggregate. Meanwhile, crushed stone with a maximum size of 10 mm was used as the coarse aggregate. All aggregates were prepared under surface-saturated dry conditions. The properties of aggregates and admixtures are shown in **Table 3.5**.

The concrete was designed with water to cement (w/c) ratio of 0.45 and the ratio of fine aggregate to total aggregate volume (s/a) of 0.47. Air-entraining agent and water-reducing admixture were added to the cement mass to obtain the slump and air content in all concrete mixes in the range of 10±2.5 cm and 4.5±1 %, respectively. Chloride ions were

deliberately added around 10 kg/m^3 during mixing into concrete to accelerate the corrosion process. Pure sodium chloride (NaCl) was used as the source of chloride ions. The mixture proportion of concrete is shown in **Table 3.6**.

In this study, a 20-year-old deteriorated (rusted) reinforcing steel bar with a diameter of 13 mm was used, as shown in **Figure 3.35**. These steel bars were taken from the specimens exposed in a severe chloride environment with high temperatures for 20 years. For non-deteriorated (non-rusted) conditions, the rusted rebar was immersed in 10% (weight percentage) diammonium hydrogen citrate solution for 24 hours in a 40°C accelerated chamber and then the rust was removed by using a steel wire brush. At both ends of each element, a 30-cm-long lead wire was screwed on.

Table 3.5 Properties of materials

Component	**Physical properties**	
Ordinary Portland Cement	Density, g/cm^3	3.16
Fine Aggregate	Density, g/cm^3 (SSD Condition)	2.58
	Water absoption (%)	1.72
	Fineness modulus	2.77
Coarse aggregate	Density, g/cm^3	2.91
AEWR agent	Polycarboxylate ether-based	
AE agent	Alkylcarboxylic type	

Table 3.6 Mixture proportion of concrete specimens

Material	
Water-cement ratio (w/c), %	45
Sand-aggregate ratio (s/a), %	47
Water, kg/cm^3	190
Cement, kg/cm^3	422
Sand, kg/cm^3	766
Gravel, kg/cm^3	970
Chloride, kg/cm^3	0 or 10
Additive: • AE, mL • AE-WR, kg	 1900 1.34

Figure 3.35 A 20-year-old deteriorated steel bar used in this study

After that, all specimens were stored (in wrapping) at constant room temperature for 28 days. After 28 days of sealed curing, the sacrificial zinc anode was connected to adjacent steel elements (S) to throw protection current. However, these connectors were temporarily disconnected to measure the instant-off potential, the protective current density, and potential decay during switch-off 24h in the depolarization test. After curing, the specimens were stored in the freezing chamber with -17°C of temperature and 4-5% of relative humidity (R.H.) until the end of the test (900-days).

3.4.2.2 Experimental methods

All potential measurements were conducted in constant room temperature around 20±2°C. The step methods are illustrated in **Figure 3.36**.

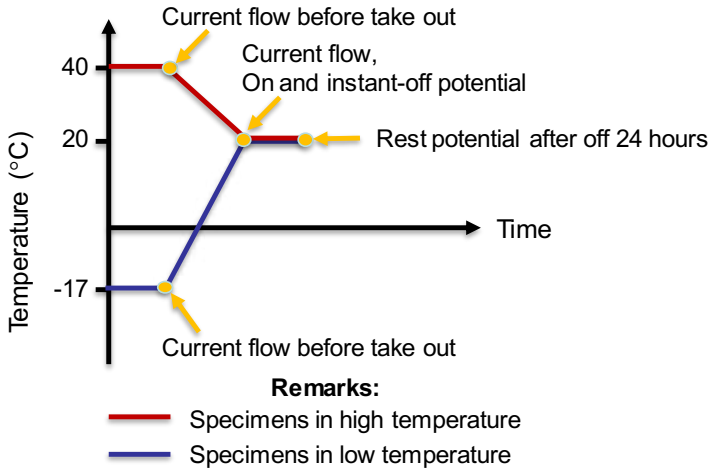

Figure 3.36 Temperature change during the measurement process

The current monitoring was conducted undertaken before and after specimens taken out from the freeze and hot, and then specimens were stored in a constant room temperature chamber for pre-wetting for 30 minutes and continued by each of the testings. After switching off the connection between sacrificial zinc anode and rebar, specimens were stored up to off 24-hours potential measurement at 20±2°C room. The potential measurement was conducted with silver/silver chloride electrode after 1 hour of pre-wetting. Then, the measured value was converted to the potential of the copper/copper sulfate electrode (CSE) at 25°C.

3.4.2.3 Measurement methods

Half-cell potentials test of rebar, according to ASTM C876-15 (2015), was conducted by silver/silver chloride reference electrode and high impedance multimeter (voltmeter

setting) after one hour of pre-wetting. The reference electrode is connected to the negative terminal and the reinforcing bar to the positive terminal of the multimeter (Elsener, 2003). On-potential (E_{on}) of rebar and anode measured under sacrificial anodes protection. Instant-off potential (E_{off}) checked immediately after disconnection, and the rest potential (E_{corr}) measured after 24 hours. The potential value is converted to the copper/copper sulfate reference electrode (CSE).

The depolarization test was measured from the potential difference value between 24 hours off potential and instant-off potential. Based on JSCE Concrete Library 107 (2011), the effectiveness of cathodic protection is defined as the depolarization test value is more than 100 mV. Polarization resistance was measured by using a Linear Polarization Resistance (LPR).

3.4.3 Results and discussion

3.4.3.1 Sacrificial anodes in low temperature around -17°C

3.4.3.1.1 Protective current density and potential development of anode

The current density generated by the anode to the rebar as a function of exposure time until 900-days is shown in **Figure 3.37**. On potential and instant-off potential of anodes are illustrated in **Figure 3.38**.

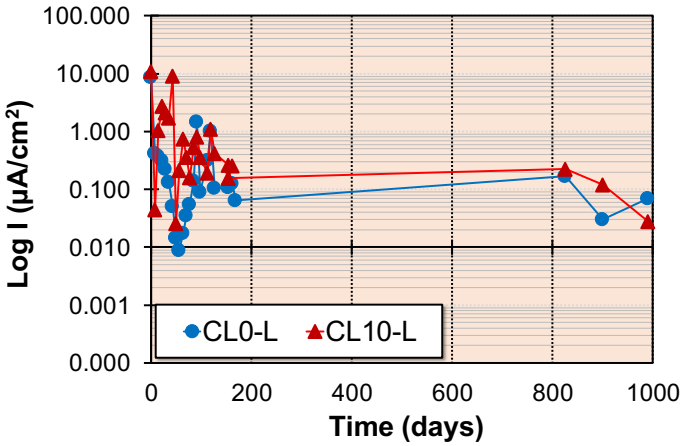

Figure 3.37 The protective current of sacrificial anodes

In the concrete without chloride contaminated (CL0-L), the current density trend was decreased gradually from 7-days to 84-days, but the current pattern of anodes in the concrete without chloride fluctuated. After this, there was a downtrend from 84-days to 168-days, reaching 0.2 µA/cm^2 and 0.9 µA/cm^2, the current density was decreased to 0.03 µA/cm^2 and 0.12 µA/cm^2 for CL0-L and CL10-L, respectively at the end of the test period (900-days). It means that anodes are very active at the beginning of the exposure, however, due to freezing

environment conditions, the current flow seems degraded under the design limit of current density on cathodic protection which is between 0.2 - 2 μA/cm^2 as specified in EN 12696. The current density required to protect steel in atmospherically exposed concrete cathodically strongly depends on the corrosion rate on steel bar surface (Glass and Buenfield, 1995).

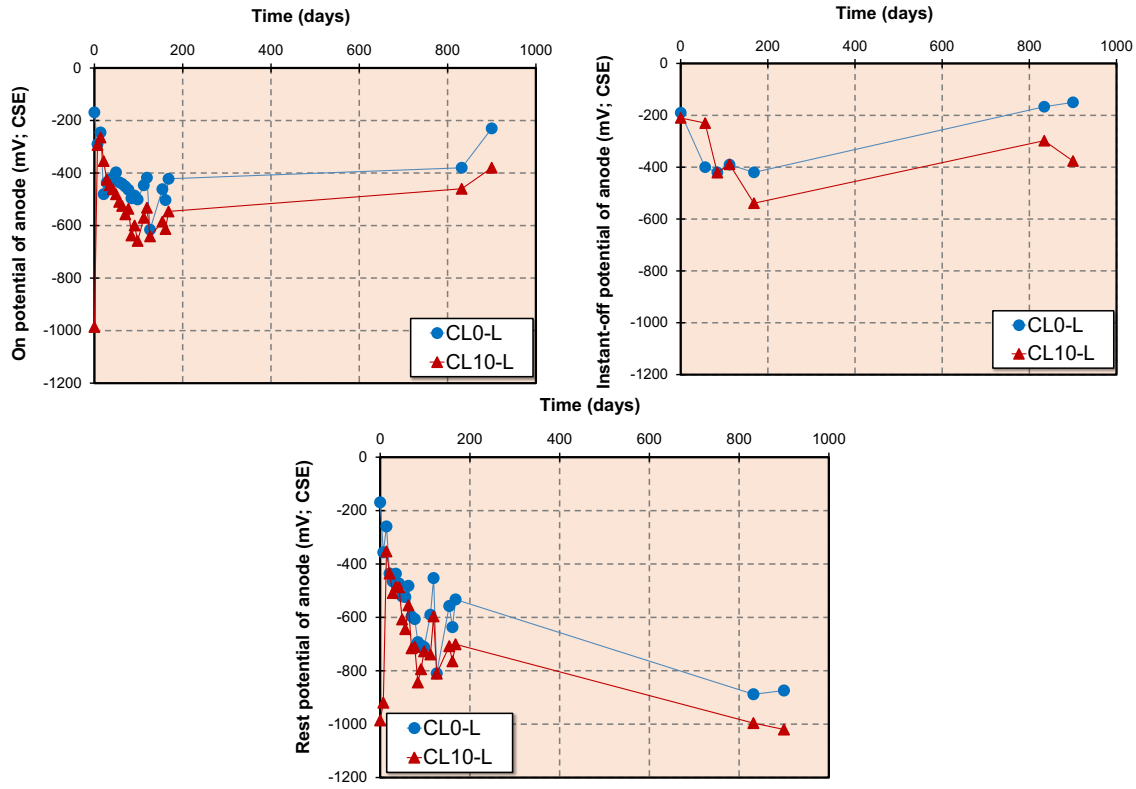

Figure 3.38 Potential development of sacrificial anodes

3.4.3.1.2 Potential development of rebar

Figure 3.39 shows on potential and instant-off potential of rebar protected by sacrificial zinc anode, while the half-cell potential of steel bar without the protection of the sacrificial zinc anode illustrated in **Figure 3.40**. From the figure below, it is indicated that during connection, sacrificial anode polarizes the rebar (connected and none-connected with the anode). In an early age, rebar embedded in chloride-free concrete (SN-CL0-L) was in the uncertainty corrosion region because the specimens were kept in moisture condition during the curing period, but it showed no corrosion at 900-days. Although rebar in chloride contaminated concrete was in the corrosion region both in early and in long-term age. Moreover, corrosion could occur on the rebar in chloride-contaminated concrete (SN-CL10-L) even though under freeze condition.The corrosion potential (E_{corr}) or rest potential of rebar is described in **Figure 3.41**.

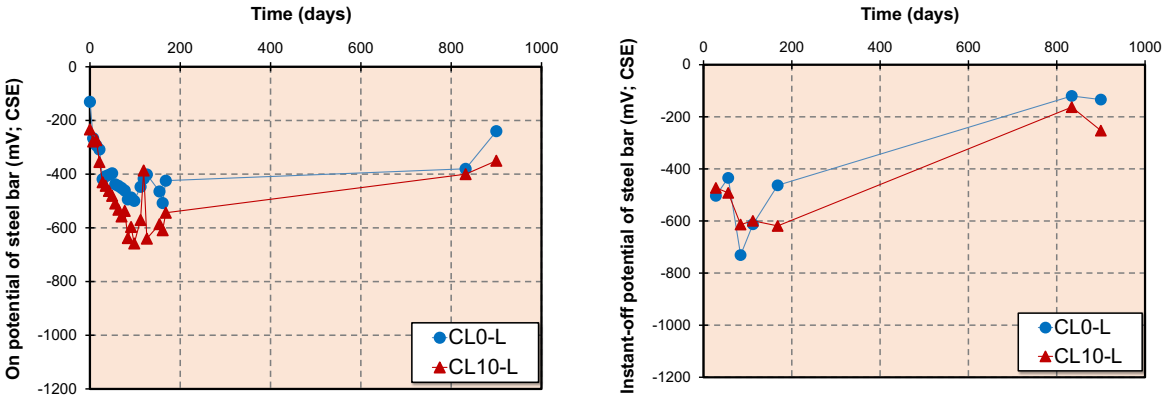

Figure 3.39 On potential and instant-off potential of a steel bar with a sacrificial anode connection

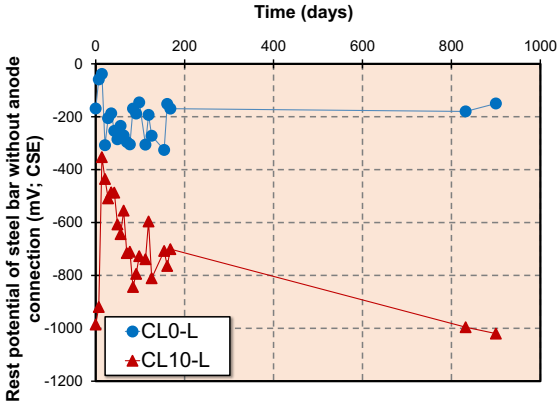

Figure 3.40 Half-cell potential of steel bar without sacrificial anode connection

Sacrificial zinc anode polarizes not only rebar with anode connection but also rebar without anode connection in chloride-free concrete. However, the anode could not polarize the rebar in chloride-contaminated concrete. It indicated that sacrificial anode couldn't be sufficient to prevent corrosion in the presence of chloride ion. This result coincides with the potential development result of rebar.

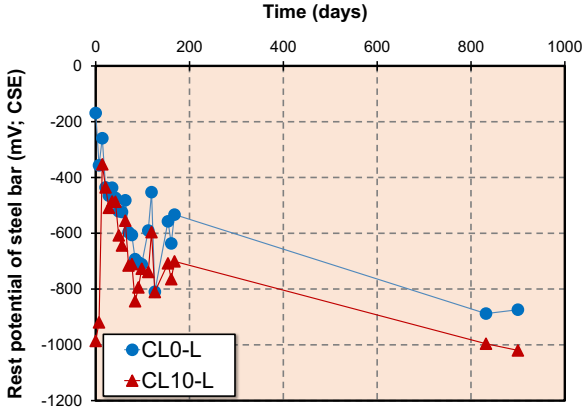

Figure 3.41 Corrosion potential of steel bar in chloride-free and chloride contaminated concrete

3.4.3.1.3 Depolarization test

Figure 3.42 illustrates the depolarization development from the specimens. It indicated that sacrificial zinc anode is sufficient to protect the rebar in chloride-free concrete exposed to the low temperature until 112-days based on 100 mV potential decay criterion.

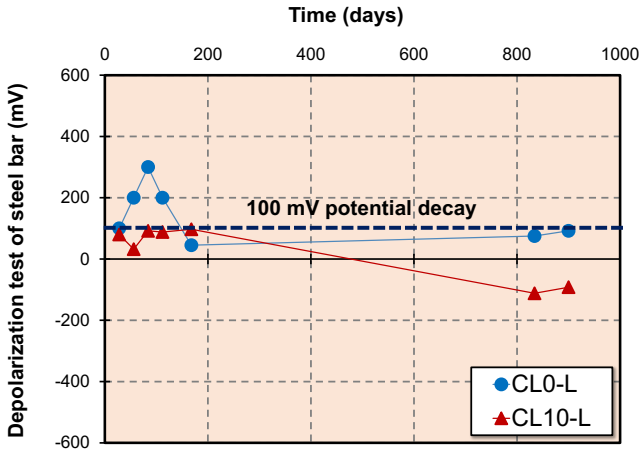

Figure 3.42 Depolarization test result

3.4.3.1.4 Polarization resistance

The rebar corrosion tendency is strongly dependent upon the corrosion potential and polarization resistance. The relationship between corrosion potential and polarization resistance is illustrated in **Figure 3.43**. Rebar embedded in free-chloride concrete and connected by the sacrificial anode is denoted as SCP-CL0-L while SCP-CL0-L is rebar in chloride contaminated concrete. SNCP-CL0-L and SNCP-CL10-L are the rebars without sacrificial anode protection embedded in chloride-free concrete and chloride contaminated concrete, respectivey. Corrosion resistance of reinforcing steel is significantly decreased on the rebar without cathodic protection connection and embedded in the chloride-contaminated concrete.

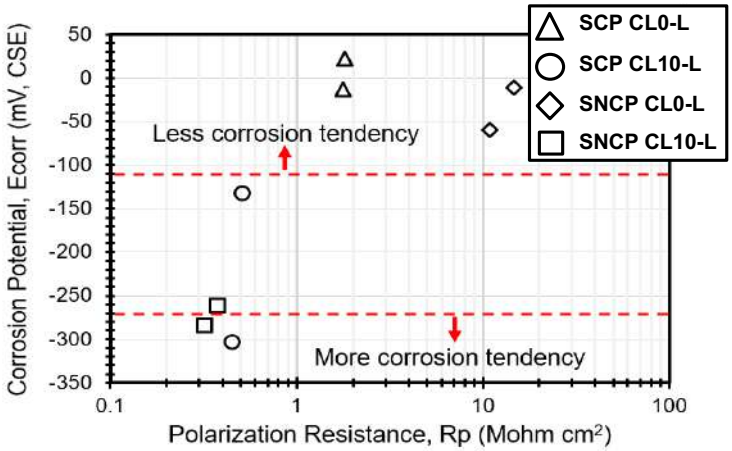

Figure 3.43 Relationship between corrosion potential and polarization resistance

3.4.3.1.5 Anodic-cathodic polarization curve

The polarization behavior of the sacrificial zinc anode in free-chloride contaminated and chloride-contaminated concrete is shown in **Figure 3.44**. It is clearly observed that concrete with chloride contaminated has a larger current density than chloride-free concrete. This phenomenon occurred due to chloride contaminated concrete causes the sacrificial zinc anode more active to provide larger current protection. The anodic and cathodic polarization curve of rebar is depicted in **Figure 3.45**. It is informed that the chloride content greatly affects the change of passivity grade of rebar and becomes worse in the chloride-contaminated specimen.

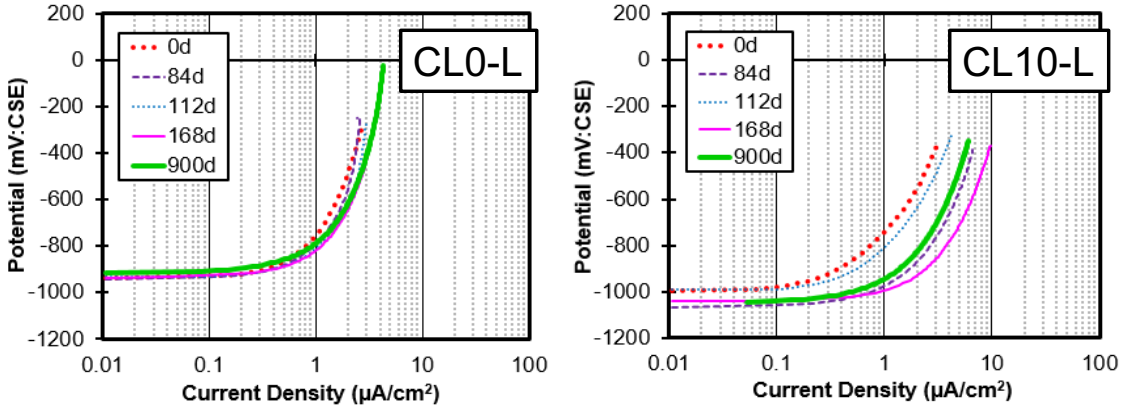

Figure 3.44 Anodic polarization curve of sacrificial zinc anode

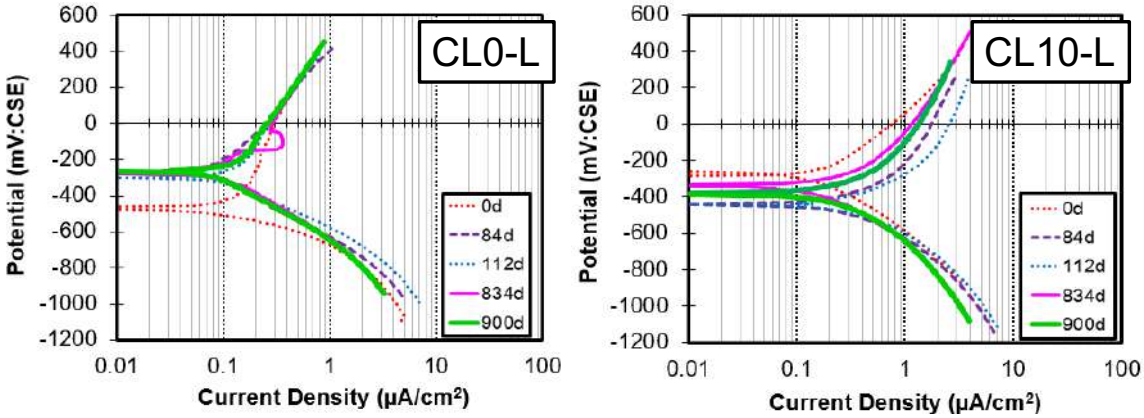

Figure 3.45 Anodic and cathodic polarization curve of rebar

3.4.3.1.6 Corroded area

Figure 3.46 presents actual corrosion conditions of rebar of the specimens after 1003 days. The corroded area was measured except one-centimeter edge from the end of rebar to avoid unexpected corrosion due to the imperfection of coating at the end of the rebar. The percentage of the corroded area is shown in **Figure 3.47**.

Figure 3.46 Appearance of rebar corroded area in CL0-L and CL10-L

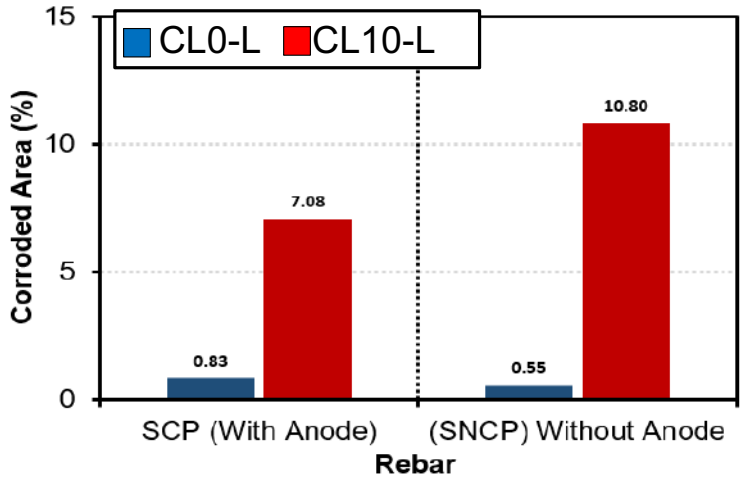

Figure 3.47 Corroded Area at 1003-days

From the visual observation, the corrosion initiation is started from the end and the middle of the rebar span. It may seem because of the imperfection of the coating of the edge span during fabrication. Meanwhile, it was observed that rebar connected to the sacrificial anodes shows a better condition than rebar without sacrificial anodes connection not only in free-contaminated but also in chloride ion contaminated concrete. It indicates that sacrificial anode could prevent the corrosion although the rebar surface is embedded in chloride ions contaminated concrete. The corroded area of rebar with anode connection both in free-chloride and in contaminated concrete is less than 1%, but the larger corroded area is found in the rebar without anode protection.

3.4.3.2 Sacrificial anodes in high temperature around 40°C

3.4.3.2.1 Protective current density and potential development of anode

The protective current density generated by sacrificial anodes in high temperature (40°C, 96-99% of RH) is presented in **Figure 3.48**. In free chloride concrete, the higher current flow is generated than in chloride contamination concrete. The current flow was significantly decreased after 1200 days of exposure and the cracks occurred in the side surface of the concrete in the position of steel bar protected by sacrificial anode.

The potential development of sacrificial anodes during exposure in the hot chamber is shown in **Figure 3.49**. On potential and instant-off potential of sacrificial anodes until more than three years were observed that after two years, the potential shifts to positive value around -200 mV. That is maybe caused by dry conditions during exposure. The rest potential of sacrificial anodes shifts to be around -200 mV in free chloride concrete and around -400 mV in 10 kg/m^3 of chloride contamination concrete after 1400 days of exposure.

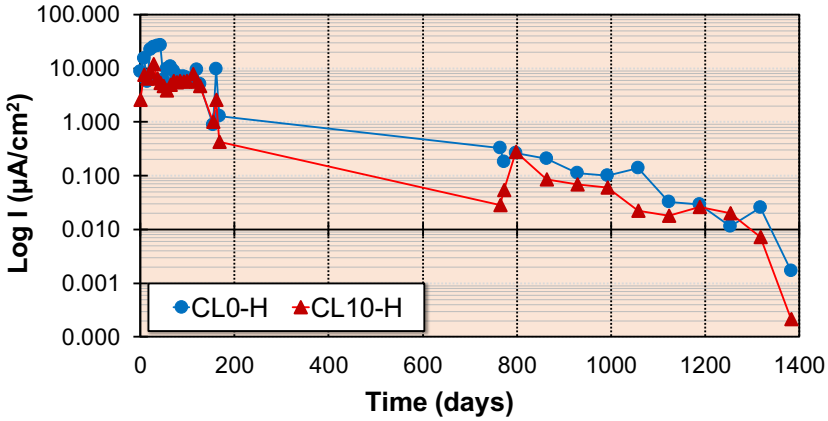

Figure 3.48 Protective current density of sacrificial anodes in high temperature

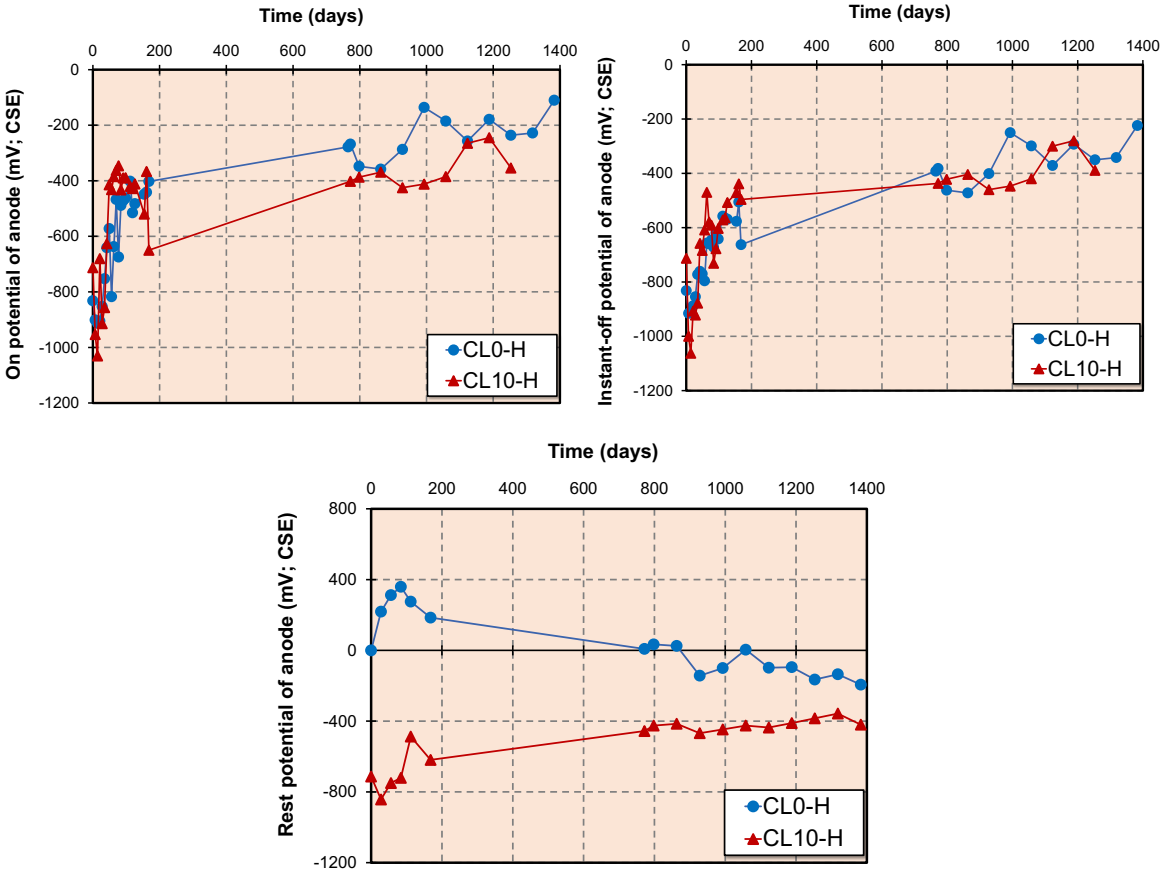

Figure 3.49 Potential development of sacrificial anode, (a) on potential, (b) instant-off potential, (c) rest potential

3.4.3.2.2 Potential development of rebar

In this study, one steel bar is also embedded without sacrificial anode connection and the half-cell potential is presented in **Figure 3.50**. It shows a steel bar in chloride-free concrete performs more positive value than in chloride contaminated.

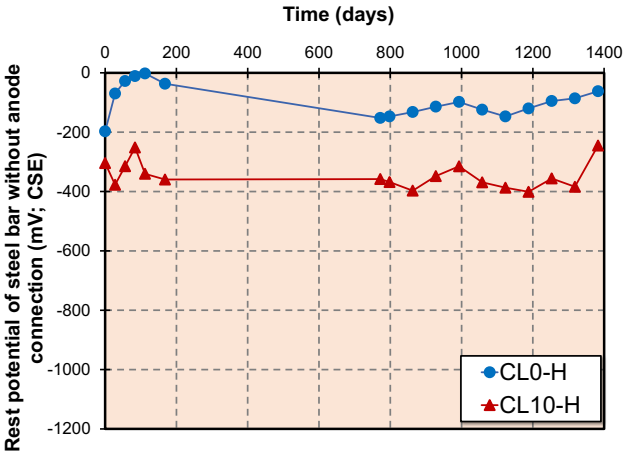

Figure 3.50 Rest potential of half-cell potential of steel bar without anode connection

The potential development including on-potential, instant-off potential, and rest potential of steel bars connected by sacrificial anodes, are presented in **Figure 3.51**.

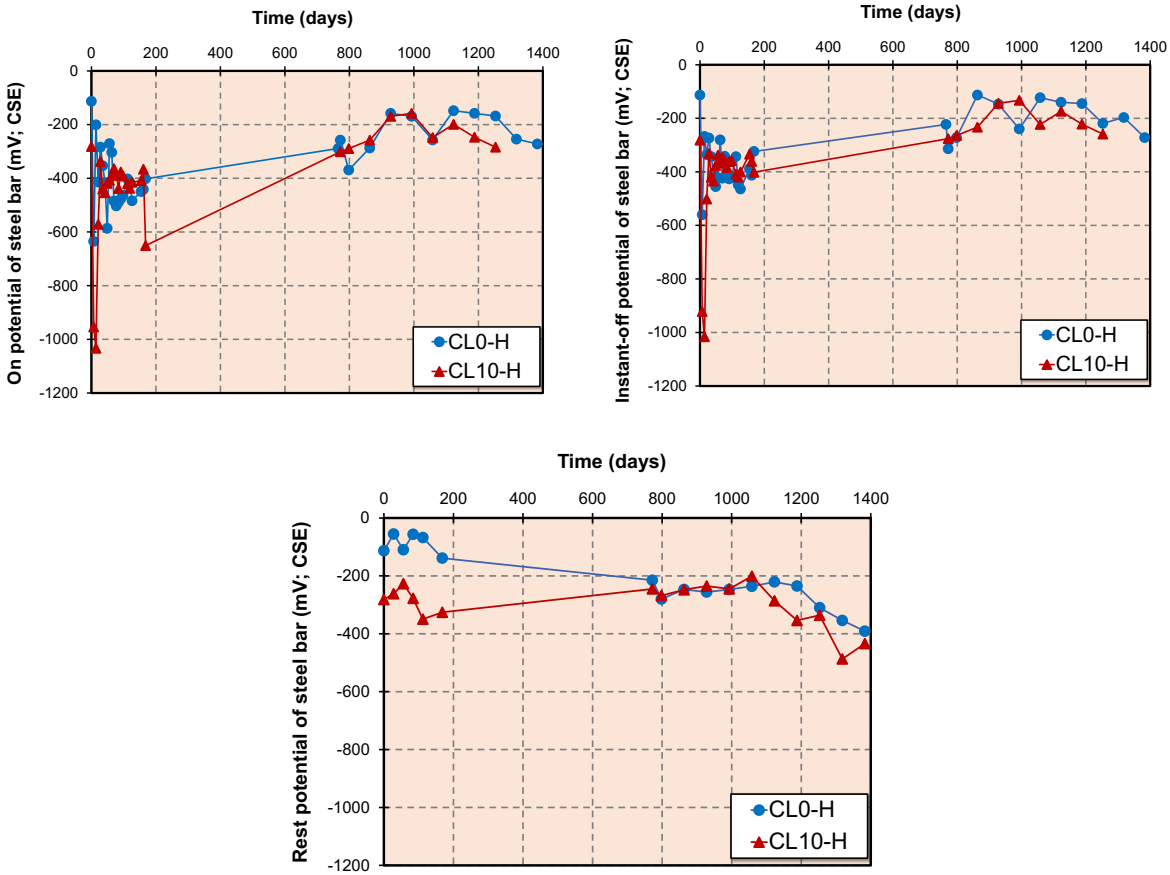

Figure 3.51 Potential development of steel bar connected by the anode, (a) on potential, (b) instant-off potential, and (c) rest potential

3.4.3.2.3 Depolarization test

The depolarization test value is an indicator of cathodic protection performance. The potential decay criterion of 100 mV is used in this study. As **Figure 3.52**, the depolarization test value of the steel bar in the high-temperature environment both in chloride and without chloride contamination concrete never reaches the potential decay criterion.

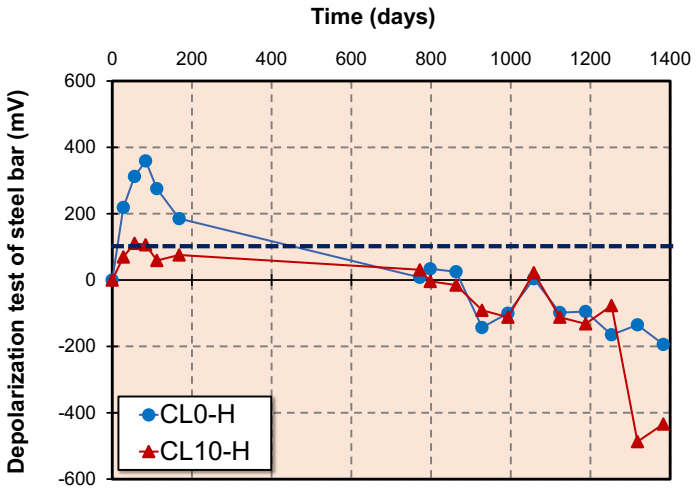

Figure 3.52 Depolarization test value

3.4.3.2.4 Defective appearance after exposure

The crack in the side part of the specimen during the exposure condition in the hot chamber is presented in Figure 3.53. A maximum crack width of 0.4 mm and 1.8 mm occur in CL0-L ad CL10-L specimens, respectively. Figure 3.54 shows the cross-sectional area of the crack pattern in CL10-L specimen. The crack is originally made from the rust of the steel bar protected by the sacrificial anode. No crack is generated in the steel bar without anode protection. The reason for this phenomenon is still unclear.

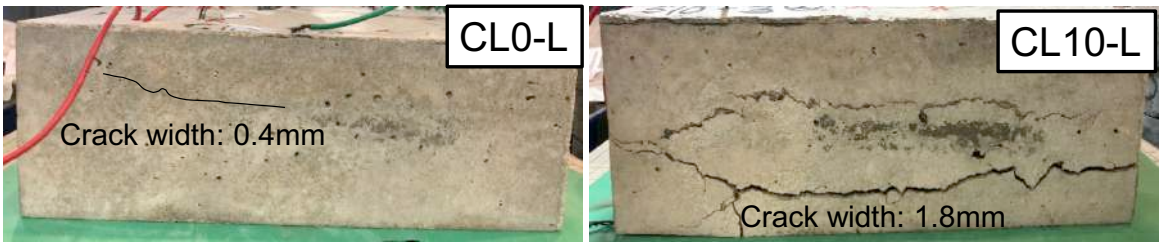

Figure 3.53 Crack appearance in the side part of specimens

From the result of specimens both in low and high temperatures, some discussion as follows. There was a downward trend in a negative direction for the potential of anode embedded in concrete with and without chloride content exposed to the freezing condition. Meanwhile, anode exposed to hot condition increases gradually to a positive direction with the function of polarization time. It means the aging of the anode is faster in high-temperature

conditions than in freeze conditions. This observation is in good agreement with the protective current condition during anodic polarization test. However, it is noted that during exposed in a high temperature chamber, anode throwing power much higher than in the freeze temperature chamber but lower during stayed in constant room temperature chamber. Vice versa for anode which exposed in freeze condition. It means that anodes produce higher levels of current in wet or humid environments compare to dry conditions.

Figure 3.54 Cross-sectional area of the specimen with 10 kg/m^3 of chloride content

Even though deliver small current, but anode exposed in frost condition could polarize steel bars to protection level during on and instant-off condition. In addition, based on the potential decay data during the depolarization test, it was observed that anode embedded in concrete without chloride contamination exposed to low and high temperature could polarize the steel bar exceed 100 mV of CP criterion. It means non-chloride contamination in concrete make anode effective to deliver the current and polarize the steel bar even though exposed to frost and hot temperature.

3.4.4 Conclusion

The results of this experiment show several findings as follows.

a. Effect of low temperature

1. Sacrificial zinc anode can work to protect steel bars against corrosion even under very low temperatures around -17°C. When the temperature plunges below zero, the anode can polarize the rebar (connected and none-connected with the anode) in the free chloride-contaminated concrete to the protection level.
2. The corrosion resistance of reinforcing steel is significantly reduced on the rebar without cathodic protection connection and embedded in the chloride-contaminated concrete.

3. Chloride content greatly affects the grade of the passivity of the rebar exposed to the low temperature around -17ºC.
4. From the visual observation of steel bar in concrete after more than 1000 days, the effectiveness of sacrificial anode on corrosion prevention was verified.

b. Effect of high temperature

1. Sacrificial zinc anode can work to protect steel bars against corrosion in high temperature (40°C) until four-years.
2. The cracks were observed in steel bar protected by sacrificial anodes. The mechanism of the phenomenon is still unclear.

3.5 Experiment on hybrid cathodic protection

3.5.1 Introduction

Steel in concrete, however, can suffer severe corrosion problems under some critical conditions. The two main elements of corrosion in the reinforced concrete structure are chloride ions and carbon dioxide. In particular, the chloride ion is plentiful in de-icing salt and seawater, and it penetrates to a concrete cover and leads to the onset of pitting corrosion with a local drop in pH. The most critical problem is an expansion in the volume of steel in concrete when the corrosion reaction is started. As reactions are processed, the volume of the steel/concrete interface is increased up to 6–7 times, which contributes to the cracking and spalling of concrete structures. To solve the corrosion problem, there has been applying various corrosion protection methods. Specifically, cathodic protection (CP) has been utilized for decades and it becomes one of the proven technologies for the protection of corrosion damages in reinforced concrete structures. CP is an electrochemical technique to stop or to mitigate corrosion of metal exposed to the conductive environment. CP system can be divided into two categories, i.e., sacrificial anode CP system and the impressed current one. In particular, the sacrificial anode CP system has inherent simplicity and low maintenance requirement. In many studies, sacrificial anode CP system good protection behavior in steel in concrete for extending service life after corrosion was initiated (Funahasi and Young, 1997; Jeong and Jin, 2014). The combined method both sacrificial anode and impressed current to enlarge the advantage of the cathodic protection system is still in limited study. The hybrid technology offers the same advantages of sacrificial anode system, in that little or no maintenance is required its design life cycle, and no permanent power supply needs to be installed as part of the works; while also packing the corrosion arrest power

traditionally associated with a full impressed-current system (Glass *et al.*, 2008; Glass *et al.*, 2012; Christodoulou *et al.*, 2013; Christodoulou and Kilgour, 2013)

Caronge (2015) reported that high current flow is generated by sacrificial anodes in the early age of connection in the three specimens with 200 × 120 × 120 mm in the dimension as presented in **Figure 3.55**. A plain steel bar with 13 mm in diameter was embedded. Sacrificial point anode was placed with 15 mm of distance above the steel bar. The chloride was added to concrete with a concentration of 0, 4, and 10 kg/m^3. The specimens were denoted as CL-0, CL-4, and CL-10.

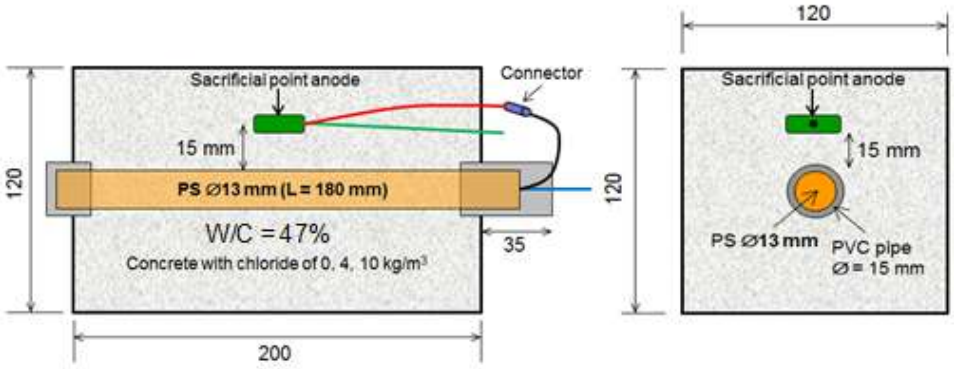

Figure 3.55 Specimen design (Caronge, 2013)

The protective current flow generated by sacrificial anodes was illustrated in **Figure 3.56**. It shows that the initial current density of anode in CL-0 specimen presents the highest among all specimens in 120 mA/m^2. After several years of exposure, the actual observation of the sacrificial anode condition was done in this study. The fluorescence microscopic of the boundary condition of the sacrificial anode and LiOH based mortar in the 50µm scale were shown in **Figure 3.57**. It was observed that the sacrificial anode with the higher initial current flow (CL-0) has seriously eroded than CL-4 and CL-10. The higher initial current flow indicates high initial anode consumption.

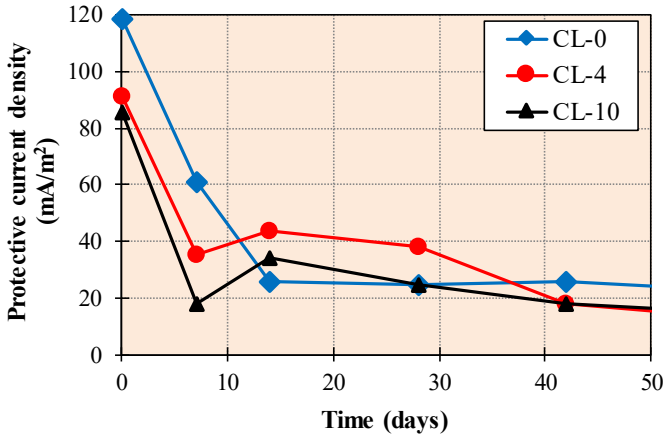

Figure 3.56 Protective current density (Caronge, 2013)

High consumption of sacrificial anodes indicated by high protective current flow in the early stage of connection will reduce the service life of sacrificial anodes. So, it is necessary to apply a method to reduce the initial of high current consumption. In this experiment, application of impressed current method in early stage of connection was conducted before switching of impressed current to sacrificial anode method.

(a) CL-0 (b) CL-4 (c) CL-10

Figure 3.57 Fluorescence microscopic of sacrificial anodes boundary in 50µm scale

3.5.2 Experimental program

3.5.2.1 Materials

Ordinary Portland Cement (OPC) was used in the concrete specimen. Tap water (temperature 20±2°C) was used as mixing water. Sea sand was used as a fine aggregate. Meanwhile, crushed stone with a 20 mm maximum size was used as a coarse aggregate. All aggregates were prepared under surface saturated dry conditions. Moreover, a galvanic anode made of zinc as the main material was used as the sacrificial anode. The dimension is 140 mm in length, 45 mm in depth and 13 mm in width, as shown in **Figure 3.58**.

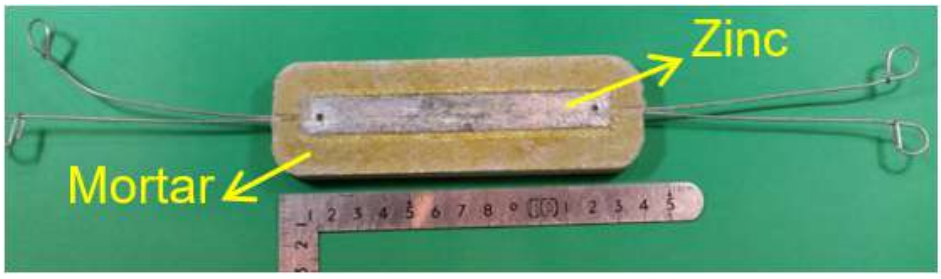

Figure 3.58 Sacrificial anode installed on the rebar (Rafdinal, 2016; Rafdinal *et al.,* 2016)

3.5.2.2 Mix proportion

The concrete mix proportion of this study is presented in **Table 3.7**.

Table 3.7 Mix proportion of concrete

W/C	Water	Cement	Sand	Gravel	Chloride content	AEWR	AE
0.55	190 kg/m^3	345 kg/m^3	841 kg/m^3	956 kg/m^3	5 kg	1.08 kg/m^3	1036 ml/m^3

3.5.2.3 Specimen design

Four specimens with 200 × 120 × 120 mm in the dimension denoted as Specimen 1-4 were fabricated. The detail of the specimens is shown in **Figure 3.59**. One plain steel bar with 19 mm in diameter was embedded in the concrete. Specimen 1 expresses the steel bar in concrete without corrosion protection. Sacrificial anode only was used in Specimen 2. In Specimen 3, the impressed current method by using titanium ribbon mesh as an anode was utilized. Combination of both sacrificial anode and impressed current was applied in Specimen 4.

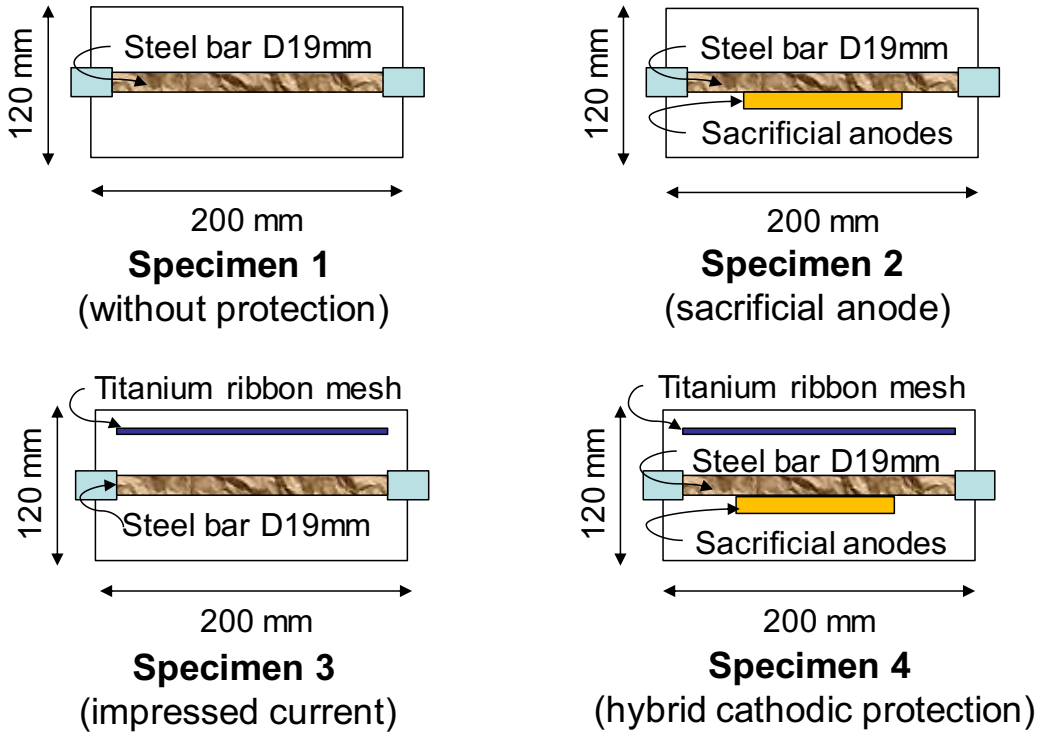

Figure 3.59 Detail of specimens

3.5.2.4 Measurement methods

The potential of rebar in concrete surface was monitored during on potential, instant-off potential, and rest potential by using the half-cell potential measurement method. Saturated calomel electrode (SCE) was used as a reference electrode for measurement, and this potential reading was converted to copper/copper sulfate electrode (CSE) in 25°C (ASTM, 2015). On-potential (E_{on}) of rebar and anode measured under sacrificial anodes protection. Instant-off potential (E_{off}) checked immediately after disconnection and the rest potential (E_{corr}) measured after 24 hours. The potential value is converted to the copper/copper sulfate reference electrode (CSE). Potentiostat and function generator were used to measure anodic and cathodic polarization curves using immersed method.

3.5.3 Result and discussion

3.5.3.1 Protective current density

The operation of the corrosion protection method in this study is explained in this part. The protective current flow of cathodic protection system in the specimens was depicted in **Figure 3.60**. Specimen 2 (sacrificial anode only) is operated to understand the initial of current flow generated by sacrificial anode. It presents that 240 mA/m^2 of current density was generated by sacrificial anode. Based on the current density generated by sacrificial anode, the current density of Specimen 3 and 4 was adjusted as 100 mA/m^2. The decreasing incremental of current flow on that specimen was as shown in **Figure 3.60**.

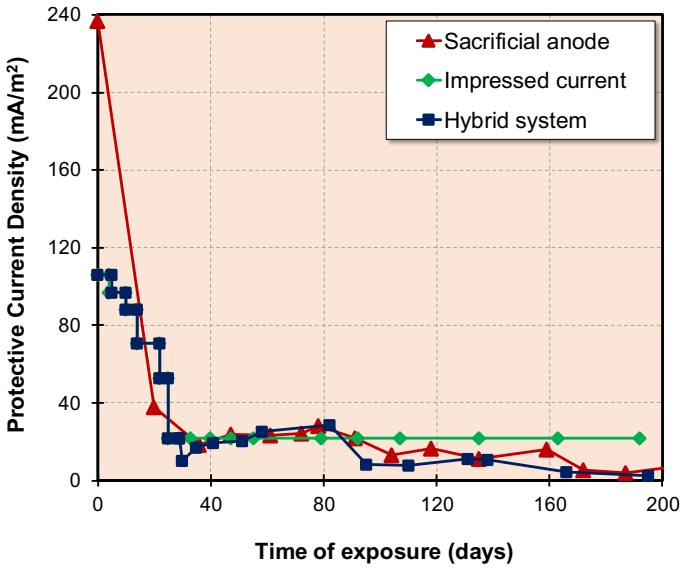

Figure 3.60 Protective current density

3.5.3.2 Potential development of steel bars

The potential development of steel bars and anodes were illustrated in **Figure 3.61**. On and instant-off potential of impressed current method shows the lowest value among them. It is due to the stable current flow adjusted by galvanostat. The potential development trend of steel bar in sacrificial anode and hybrid system is almost in the same trend.

3.5.3.3 Depolarization test

The depolarization test of steel bar is presented in **Figure 3.62**. Until 200 days of exposure, the difference value of instant-off and rest potential of steel bar exceeds 100 mV potential decay criterion. It means three types of cathodic protection systems in this study are effective. The impressed current method performs the most stable protection among them.

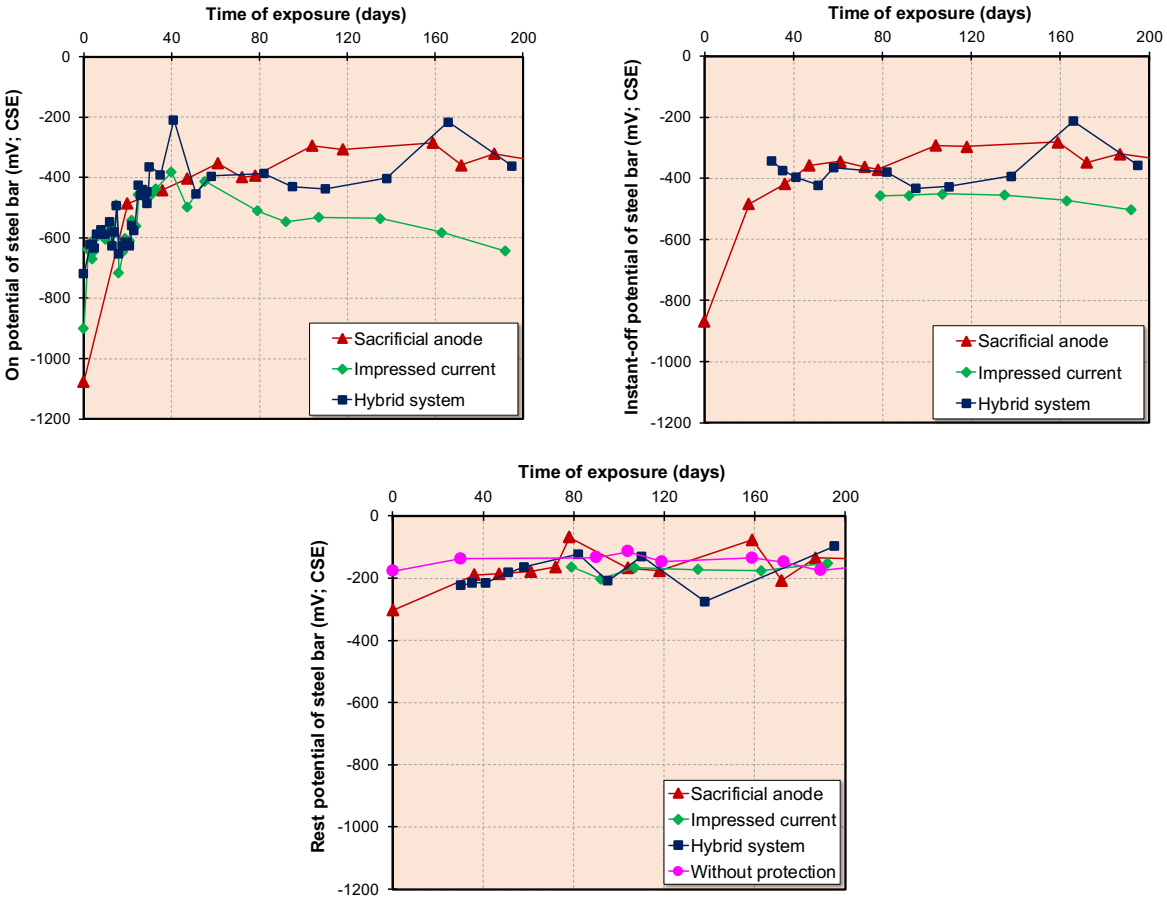

Figure 3.61 Potential development of steel bar

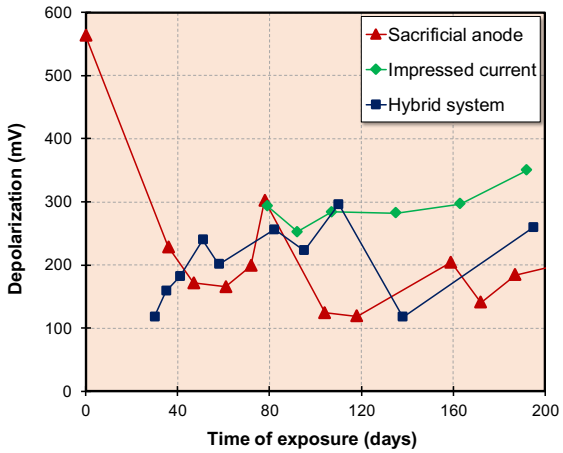

Figure 3.62 Depolarization test of steel bar

3.5.3.4 Anodic-cathodic polarization curve

Anodic and cathodic polarization curve of steel bar in all specimens were depicted in **Figure 3.63**.

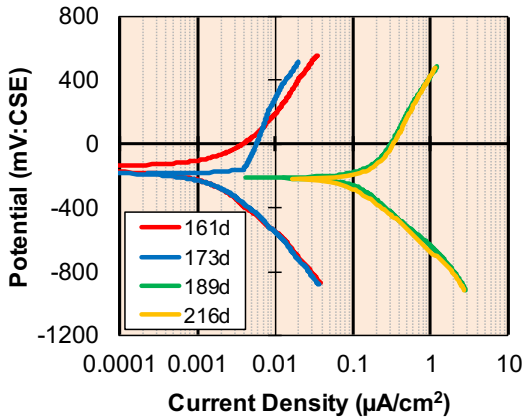

(a) Specimen 1 (without protection)

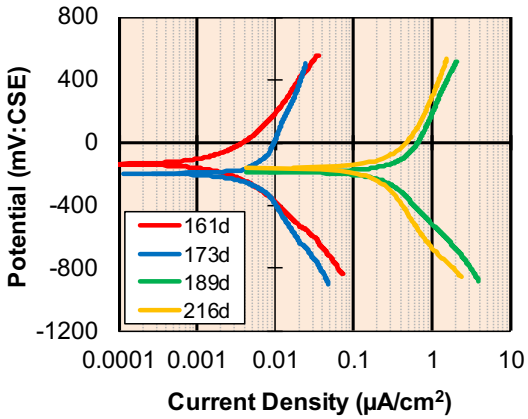

(b) Specimen 2 (sacrificial anode)

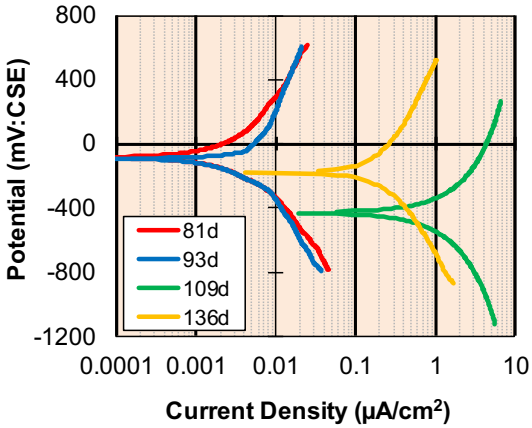

(c) Specimen 3 (impressed current)

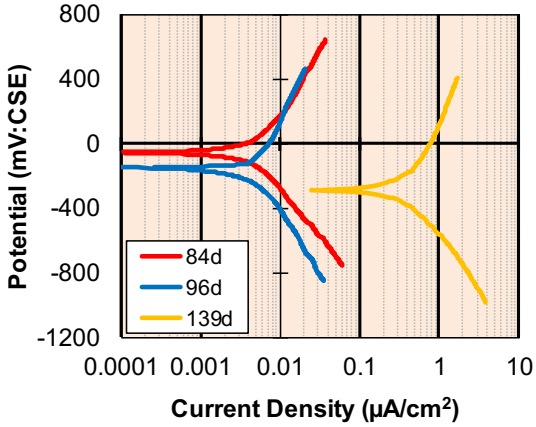

(d) Specimen 4 (hybrid system)

Figure 3.63 Anodic-cathodic polarization curve of steel bar

Anodic polarization curve of anodes is presented in **Figure 3.64**.

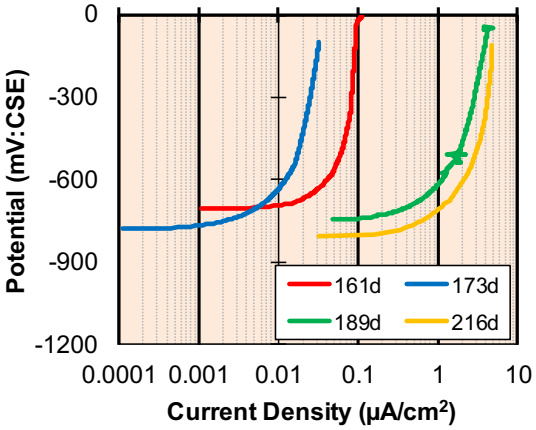

(a) Specimen 2 (sacrificial anode)

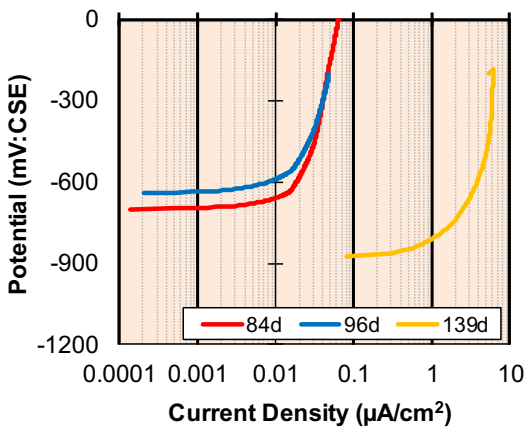

(b) Specimen 4 (hybrid system)

Figure 3.64 Anodic polarization curve of sacrificial anodes

3.5.4 Conclusion

Hybrid cathodic protection system with reduction of impressed current flow current until reaching the current flow of sacrificial anodes and switching impressed current and sacrificial anodes connection. The on-potential of rebar is relatively stable in -400 mV and

identic with on-potential of rebar due to sacrificial anode. It indicates that switching the impressed current to sacrificial anodes is a success.

3.6 **Conclusion of fundamental study**

From several experimental programs in this chapter, some findings are derived as follows.

- Effect of non-homogeneous chloride contamination in concrete

  The sacrificial anode is effective to protect steel bar in non-homogeneous chloride contamination until 5-years of exposure.

- Effect of steel surface condition

  Rust removal on steel surface in repair concrete is the most desirable initial condition when the sacrificial anode is applied on it to protect the corroded steel bar in existing concrete until 4-years of exposure.

- Effect of low and high temperature

  The application of embedded sacrificial anode at low temperatures is effective to protect steel bars from corrosion until 3-years of exposure. But, high temperature of 40°C affects the inefficiency of sacrificial anode application after 4-years of exposure.

- Experiment on the hybrid cathodic protection system

  The switching of impressed current by sacrificial anode in a hybrid cathodic protection system is a success.

3.7 **References**

Alonso, C., Castellote, M., and Andrade, C., 2002. "Chloride Threshold Dependence of Pitting Potential of Reinforcement," *Electrochemia Acta,* Vol. 47, No. 21, pp. 3447-3469

ASTM C876-15, 2015. "Standard test method for half-cell potentials of uncoated reinforcing steel in concrete," *ASTM International,* West Conshohocken, PA, 2015, www.astm.org.

Astuti, P., Rafdinal, R. S., Hamada, H., Sagawa, Y., and Yamamoto, D., 2018. "Time Dependency of Rusted and Non-rusted Rebar Protected by Sacrificial Zinc Anode in Patch Repair Section," *Proceeding of Japan Concrete Institute (JCI) Symposium on Electrochemical and Maintenance Engineering, Tokyo, Japan*.

Astuti, P., Mahasiripan, A., Rafdinal, R. S., Hamada, H., Sagawa, Y., and Yamamoto, D., 2018 "Potential Development of Sacrificial Anode Cathodic Protection Applied for Severely Damaged RC Beams Aged 44 Years," *Journal of Thailand Concrete Association,* Vol. 6, No. 2, pp. 24-31 .

Bertolini, L., Elsener, B., Pedeferri,P., Redaelli, E., and Polder, R., 2013. "Corrosion of Steel in Concrete", Wiley-VCH Verlag GmBH & Co KGaA.

Caronge, M. A., 2015. "A study on the effectiveness of cathodic protection for steel bars in concrete structures", *Doctoral Thesis,* Kyushu University, Fukuoka, Japan.

Christodoulou, C., Glass, G. K., Webb, J., Ngala, V., Beamish, S., and Gilbert, P., 2008. "Evaluation of Galvanic Technologies Available for Bridge Structures," *12th International Conference Structural Faults and Repair,* Edinburgh, UK.

Christodoulou, C. Goodier, C. Austin, S. Webb, J. Glass, G., 2013. "Hybrid corrosion protection of a prestressed concrete bridge," *European Corrosion Conference 2013 (EUROCORR 2013)*, Estoril, Portugal, 1st-5th September 2013.

Christodoulou, C. Kilgour, R., 2013. "The world's first hybrid corrosion protection systems for prestressed concrete bridges," *Corrosion & Prevention 2013*, Australasian Corrosion Association, Brisbane, Australia, 10th-13th November 2013, paper 076.

Dugarte, M., and Sagüés, A. A., 2009. "Galvanic Point Anodes for Extending The Service Life of Patched Areas upon Reinforced Concrete Bridge Members, " Contact No. BD544-09, *Final Report to Florida Department of Transportation*, 2009, pp. 1-113.

Dugarte, M. J. and Sagüés, A. A., 2014. "Sacrificial Point Anode for Cathodic Prevention of Reinforcing Steel in Concrete Repairs: Part 1 – Polarization Behavior," *Corrosion, NACE International*, Houston, Vol. 70, No. 3, pp. 303-317.

Elsener, B., 2002. "Macro-cell Corrosion of Steel in Concrete–Implication for Corrosion Monitoring", *Cement and Concrete Composites*, Vol. 24, No. 1, pp. 65-72.

Elsener, B., 2003. "Half-cell potential measurements – potential mapping on reinforced concrete structures," *RILEM TC 154-EMC: 'Electrochemical Techniques for measuring metallic corrosion', Material and Structures,* Vol. 36, pp. 461-471.

EN 12696, 2000. "Cathodic Protection of Steel in Concrete," *European Standard.*

Funahashi, M. and Young, W. T., 1997. "Three year performance of aluminum alloy galvanic cathodic protection system." NACE International, Vol. 550, pp. 1-16.

Glass, G.K. and Buenfield, N.R., 1995. "The current density required to protect steel in atmospherically exposed concrete structures," *Corrosion Science,* Vol. 37, No. 10, pp 1643-1646.

Glass, G.K., Roberts, A.C., Davison, N., 2008. "Hybrid corrosion protection of chloride-contaminated concrete. *Construction Materials*," Vol. 161, pp. 163-172.

Glass, G. Christodoulou, C. Holmes, S., 2012. "Protection of steel in concrete using galvanic and hybrid electrochemical treatments." In: Alexander, M.G. Beushausen, H.D. Dehn, F. Moyo, P. (eds). 2012. *Concrete Repair, Rehabilitation and Retrofitting III: 3rd International Conference on Concrete Repair, Rehabilitation and Retrofitting*, ICCRRR-3, 3-5 September 2012, Cape Town, South Africa. pp. 523-526. Taylor and Francis Group.

Hobbs, D. 2001. "Concrete deterioration: causes, diagnosis, and minimising risk". In: *International Materials Reviews* 46.3, pp. 117–144.

Jeong, J. A. and Jin, C. K., 2014. "Experimental studies of effectiveness of hybrid cathodic protection system on the steel in concrete," *Science of Advanched Materials,* Vol. 6, pp 2165-2170.

Mohammed, T.U., Otsuki, N., and Hamada, H., 2003. "Corrosion of Steel Bars in Cracked Concrete under Marine Environment", *Journal of Materials in Civil Engineering*, September/October 2003, pp. 460-469.

Pedeferri, P., 1996. "Cathodic Protection and Cathodic Prevention," *Construction and Building Materials,* Vol. 10, No. 5 pp. 391-402.

Presuel-Moreno, F. J., Sagues, A. A., and Kranc, S. C., 2005. "Steel Activation in Concrete Following Interruption of Long Term Cathodic Polarization," *Corrosion, The Journal of Science and Engineering* Vol. 61, No. 6, pp 428-436.

Rafdinal, R.S., 2016. “Life-extension of RC structure by cathodic protection using zinc sacrificial anode embedded in concrete,” *Doctoral Thesis*, Department of Civil and Structural Engineering, Kyushu University, Fukuoka, Japan.

Rafdinal, R. S., Hamada, H., Sagawa, Y., and Yamamoto, D., 2016 “Effectiveness of Steel Surface Conditions on Cathodic Protection by Sacrificial Anode in Concrete,” *Proceeding of Japan Concrete Institute (JCI) Annual Convention, Chiba, Japan.*

RILEM Technical Committee 124-SRC, P. Schiessel (ed), 1994. “Draft Recommedation for Repair Strategies for Concrete Structures Damaged by Reinforcement Corrosion”, *Materials and Structures*, Vol. 27, pp. 415 – 436.

Sergi, G., 2011, “Ten-years Result of Galvanic Sacrificial Anodes in Steel Reinforced Concrete,” *Materials and Corrosion* Vol. 62, No. 2, pp. 98-104.

Shiotani, T., Nishida, T., Kawaai, K., Hamasaki, H., Watanabe, T., and Imamoto, K., 2017. “Technical committee on crack repair evaluation in concrete by means of non-destructive testing,” *Committee Report- JCI-TC163A*, Japan Concrete Institute (JCI), Tokyo, Japan.

The Concrete Society, 2009. “Repair of Concrete Structures with Reference to BS EN 1504,” *Technical Report No. 69,* Report of a Joint Working Party of The Concrete Society, the Corrosion Prevention Association, and the Institute of Corrosion. Information Press Ltd., Eynsham, UK.

CHAPTER IV

Repair method of severely damaged RC beams by using sacrificial anode cathodic protection (SACP)

4.1 Introduction

Chloride-induced corrosion is one of the most common deterioration mechanisms in reinforced concrete (RC) structures exposed to the marine environment. The penetration of chloride ion concentration into concrete activates the corrosion of rebar by destructing the passivity film when the chloride ion concentration at the rebar surface reaches a critical value (Glass and Buenfeld, 1997). Whenever the threshold amount of the chloride ions reaches the surface of rebar, along with enough oxygen and moisture, steel corrosion may result in concrete cracking and spalling of the cover concrete when expansive stress exceeds the tensile strength of concrete; reduction of steel reinforcement cross-section may lead to structural failure. As a result, the corrosion of reinforcement adversely affects the safety and the serviceability of concrete structures and hence shortens the service life (Song, 2007).

In the last decades, several electrochemical repair techniques were developed for offering chloride-induced corrosion. The ordinary approach to rehabilitate the defective RC structures is the patching method. British Standard of Design Manual for Road and Bridge (1990) recommends that the section which shows the chloride ion contamination greater than 0.3% by weight of cement and half-cell potential value higher than −350 mV should be removed. On the contrary, the concrete replacement work on chloride contaminated structures can be very onerous and expensive (Christodoulou, 2008). Therefore, sacrificial anodes have been used to limit the extent of concrete replacement and extend the service life of patch repairs to corrosion damaged RC structures. They respond to the changes in the environmental conditions they are exposed to (John and Cottis, 2003; NACE, 2005; Christodoulou *et al.*, 2009). Such an effect will be more dominant in parent concrete that has a residual level of chloride contamination as opposed to non-contaminated repair concrete or mortar (Holmes *et al.,* 2011). Another practical method for control of steel corrosion in concrete is the use of corrosion inhibitors. The curative and preventive treatments can be distinguished depending on the mode of the inhibitor application. The curative treatment

consists of the application of corrosion inhibitors directly on the surface of exploited and corroding reinforced concrete structures. The preventive treatment consists in the introduction of corrosion inhibitors within mixing water to the fresh concrete. The curative corrosion inhibitor was chosen in this study as easy to use approach for application in the steel bar surface of the patch repair part (Elsener, 2001).

In this chapter, five repairing methods by sacrificial anode cathodic protection and corrosion inhibitor were demonstrated for accomplishing severely damaged RC beams aged more than 40-year-old exposed to the actual marine environment. The decision to choose the repair method to the particular structures can be in many cases based on the results of a preliminary investigation that shows some high levels of chloride contamination, corrosion possibility of rebars, and damage appearance in some parts of the structures (Cheaetami, 2000).

4.2 **Objectives**

The objective of the study in this chapter is to observe the performance of several repairing systems in severely damaged RC beams to extend the service life of structures until 70-years, and the intervention systems are explained as follows.

1. Repair method by current flow of sacrificial anodes in the patch and non-patch repair
2. Repair method using a corrosion inhibitor in patch repair and the current flow of sacrificial anode in non-patch repair.
3. Repair method by current flow using a different kind of sacrificial anode in the patch and non-patch repair.

4.3 **Detail of structures**

4.3.1 Geometry of structures

The RC beam structures used in this experiment were cast in 1974. The detail of the two types of specimens was summarized in **Table 4.1**. All the beams have an identical length of 2400 mm and the cross-sectional detail is presented in **Figure 4.1**.

Table 4.1 Summary of RC beams

Specimen ID	Cover Depth (mm)	Section/size
L-Type	50	L (200x300mm)
S-Type	30	S (150x300mm)

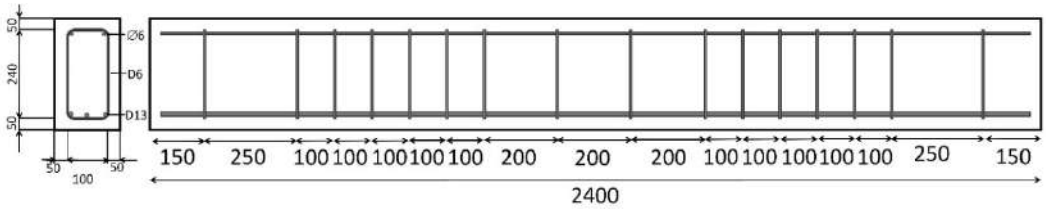

(a) L-Type

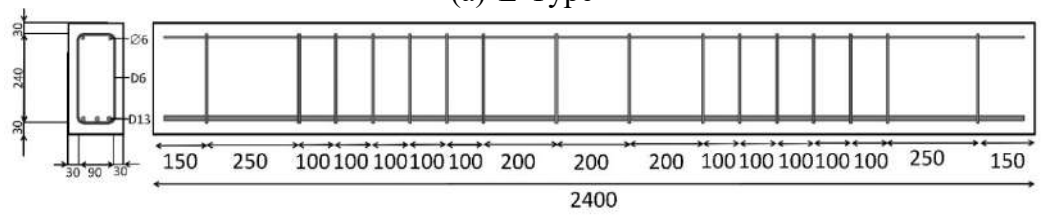

(b) S-Type

Figure 4.1 Detail of RC beams

4.3.2 Materials

Ordinary Portland Cement (OPC) was used as a binder of the concrete in these specimens. The specific gravity and fineness modulus of aggregates were summarized in **Table 4.2. Table 4.3** presents the mix proportion of the existing concrete.

Table 4.2 Material properties of aggregates same as Dasar *et al.* 2017

Aggregate	Specific gravity	Fineness modulus
Fine river sand	2.25	2.84
Coarse-crushed stone	2.75	6.63

Longitudinally deformed steel bars with a diameter of 13 mm and 363 MPa in tensile strength were embedded as tensile bars in the beam. Two round steel bars of 6 mm in diameter as compressive bars and stirrups with a spacing of 100 mm were embedded. The detailed cross-section and reinforcing bar layout were depicted in **Figure 4.1.**

Table 4.3 Mix proportion of existing concrete same as Dasar *et al.* 2017

MSA (mm)	Slump (mm)	Air (%)	w/c %	s/a %	Unit weight (kg/m^3)				
					W	C	S	G	Adm.
20	12±2	4±1	68	47	204	300	793	964	1.2

MSA:maximum size of coarse aggregate; W:water; C:cement; S:sand; G:gravel; Adm.:admixture

4.3.3 Exposure condition history

The RC beams were moisture-cured for one day and demoulded before being air-cured. The structures exposed to the natural tidal marine environment for 20 years from 1975 to 1995 at Sakata Port, northwestern part of Japan. In 1995–2010, the beams were kept and sheltered from the rain at Port and Airport Research Institute (PARI) laboratory, Yokosuka, Japan (Hamada *et al.* 1988 and Yokota *et al.* 1999) before it moved to Kyushu University site, Fukuoka, Japan. The exposure condition was presented in **Figure 4.2**.

(a) (b) (c)

Figure 4.2 Exposure condition at (a) Sakata Port (1975-1995), (b) PARI Laboratory (1995-2010), (c) Kyushu University (2010-2016)

4.4 **Investigation of structures before repair process**

4.4.1 Materials quality

The material quality of RC beam structures in this experiment was assessed by ultrasonic pulse velocity (UPV) and rebound hammer test. The measurement point of the tests is presented in **Figure 4.3**.

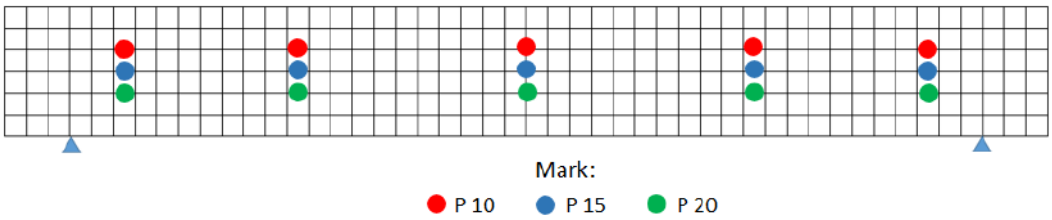

Figure 4.3 Measurement point of non-destructive test

The UPV methods have been used in inspection, operations, and monitoring of concrete structures. This test is used to measure and control a series of basic parameters to determine the concrete quality. The UPV methods can be considered as one of the most promising methods for evaluation of concrete structures, once it makes possible an examination of the material homogeneity. The result of the UPV test from specimens is shown in **Figure 4.4**. Based on ASTM C597-2002, the quality of concrete is categorized as a good quality in the range of 4000–5000 m/s with an approximate compressive strength of 25–40 MPa.

Rebound hammer test has been extremely popular inspection to estimate the concrete strength. It provides an inexpensive and quick method for non-destructive testing and evaluation of the hardness of concrete. The rebound hammer is also called Schmidt hammer that consists of a spring controlled mass that slides on a plunger within a tubular housing. The average result of the hammer test to the specimens is presented in **Figure 4.5**. The results

show that the average of the estimated compressive test in five RC beams in 44 years is 32~24 MPa.

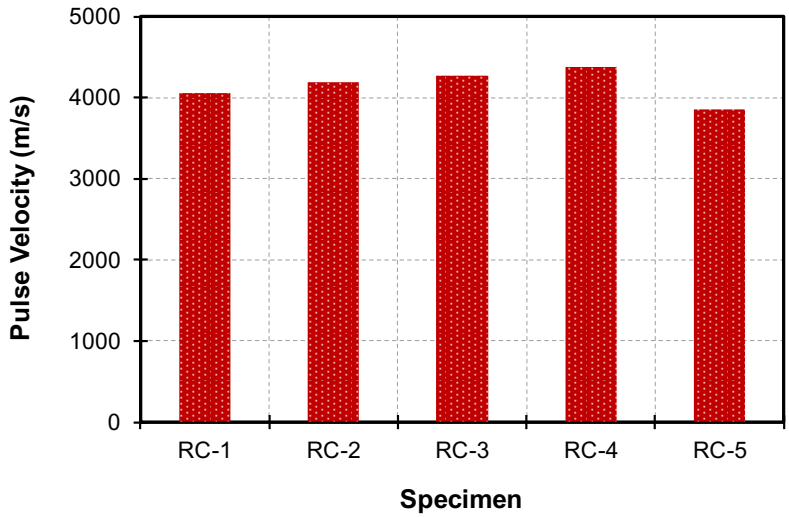

Figure 4.4 Test result Ultrasonic Pulse Velocity (UPV)

Dasar *et al.* (2017) reported that the compressive strength of structures affected by corrosion in 40 years is similar with 28-days, whereas, ~2–5 cylinder specimens of 100 mm in diameter and 200 mm in height results 30 MPa and 22 GPa of compressive strength and elastic modulus in 28-days, respectively. The yield strength of the tensile steel bar in 40 years was 363 MPa (Dasar *et al.*, 2017).

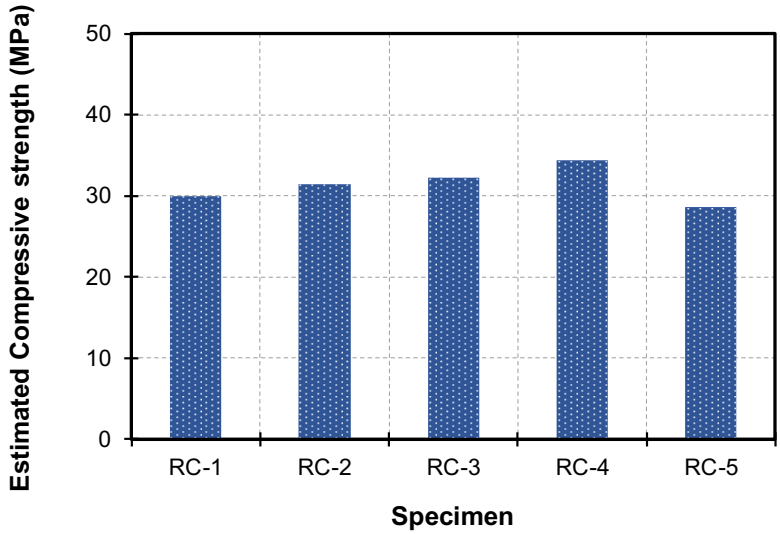

Figure 4.5 Test result of rebound hammer test

4.4.2 Defective appearance and cracking pattern

The defective appearance of the specimens were depicted in **Figure 4.6** and **Figure 4.7**. The specimens exhibit rust stain, uncovered aggregate, air bubbles, chips, and cracks. Uncovered aggregate was mostly found on the bottom side of beams due to seawater splashing, while

rust stains commonly found at the ends of beams and in the vicinity of the cracks. After exposed up to 40 years, all beam surfaces appeared rough surfaces, chips on the edges and a few spalling. Based on visual inspection results in order to check the appearance of beams, it can be concluded that there was no significant degradation for RC beams of concrete with 3cm and 5cm of cover thickness after 40 years of exposure (Rafdinal, 2016).

The cracking pattern of the specimens after more than 40-years are shown in **Figure 4.8**, **Figure 4.9**, **Figure 4.10**, **Figure 4.11**, and **Figure 4.12**. RC-1 and RC-2, RC-3 and RC-4, and RC-5 were inspected in 41-years, 43-years, and 44-years, respectively.

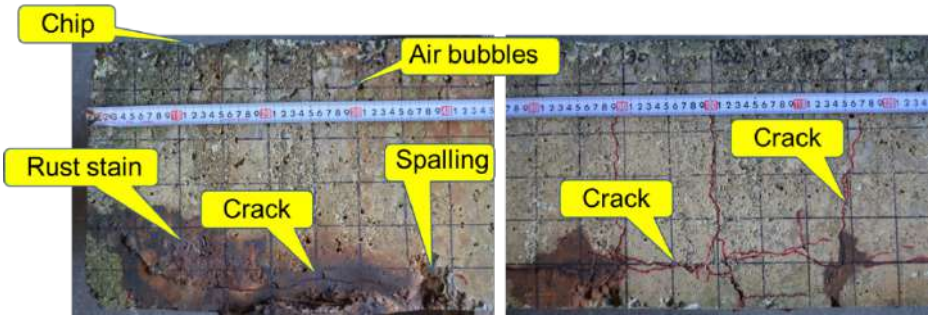

Figure 4.6 Defective appearance in RC-1 after 41-years (Rafdinal, 2016)

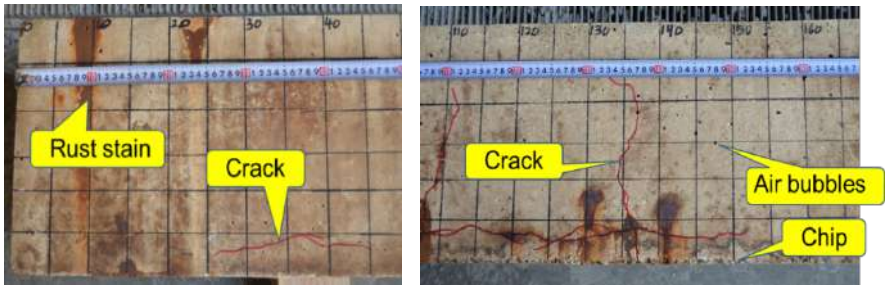

Figure 4.7 Defective appearance in RC-2 after 41-years (Rafdinal, 2016)

The crack occurred in concrete surface were observed on all sides. All beams presented cracks alongside the beam parallel to rebar and most of cracking occurred in the middle tensile area. In RC 3 and 5, many longitudinal and transversal crack both in tensile and compressive area are seen while cracks occurred only in both sides and tensile surface in other beams. RC-3 and 5 perform the most serious damage visually compare to other beams.

The longitudinal cracks are coincident with the position of tensile and compressive rebar. The transversal cracks concentrated in the middle span of the tensile area were initiated from the pre-cracking or due to stirrups corrosion (Astuti *et al.,* 2018). The maximum crack width for RC1-3 is 2.2 mm, 1.5 for RC-4, and 9.5 mm for RC-5. Air bubbles of 1~17 mm in diameter also appear on the surface of each beam.

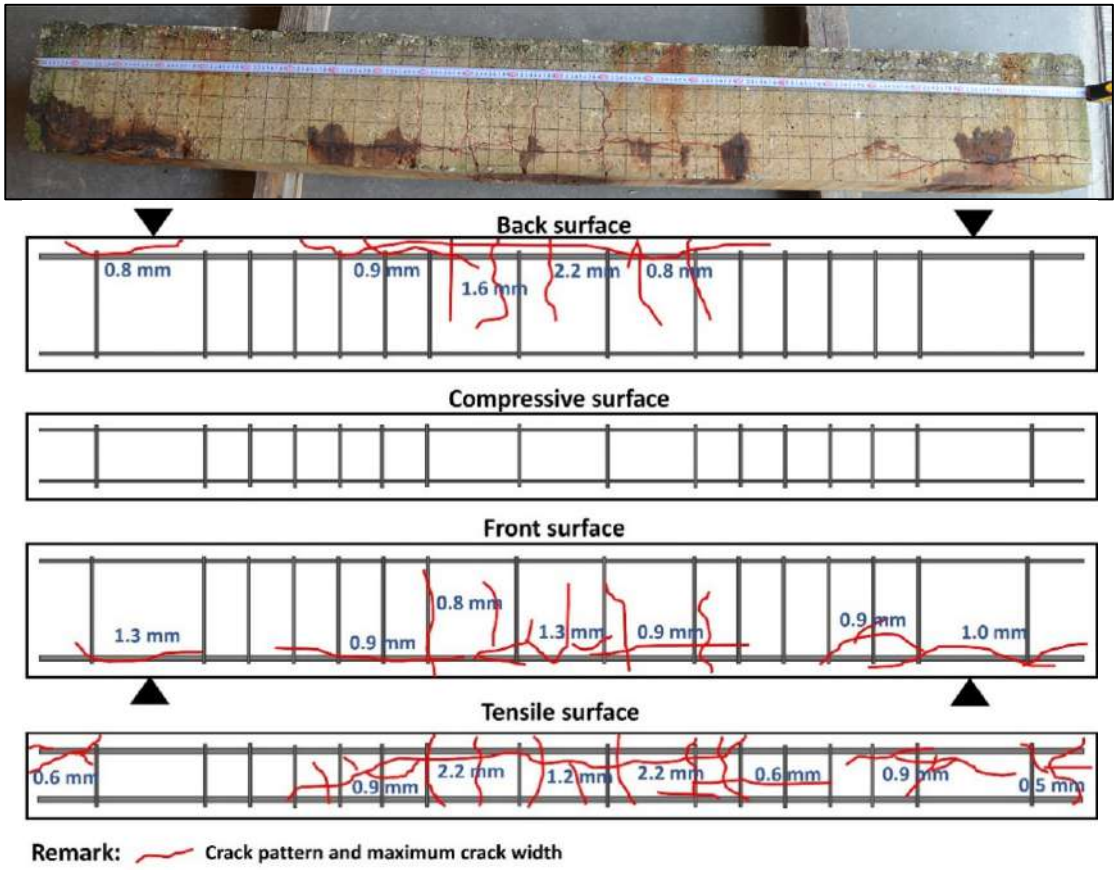

Figure 4.8 Appearance and cracking pattern of RC-1

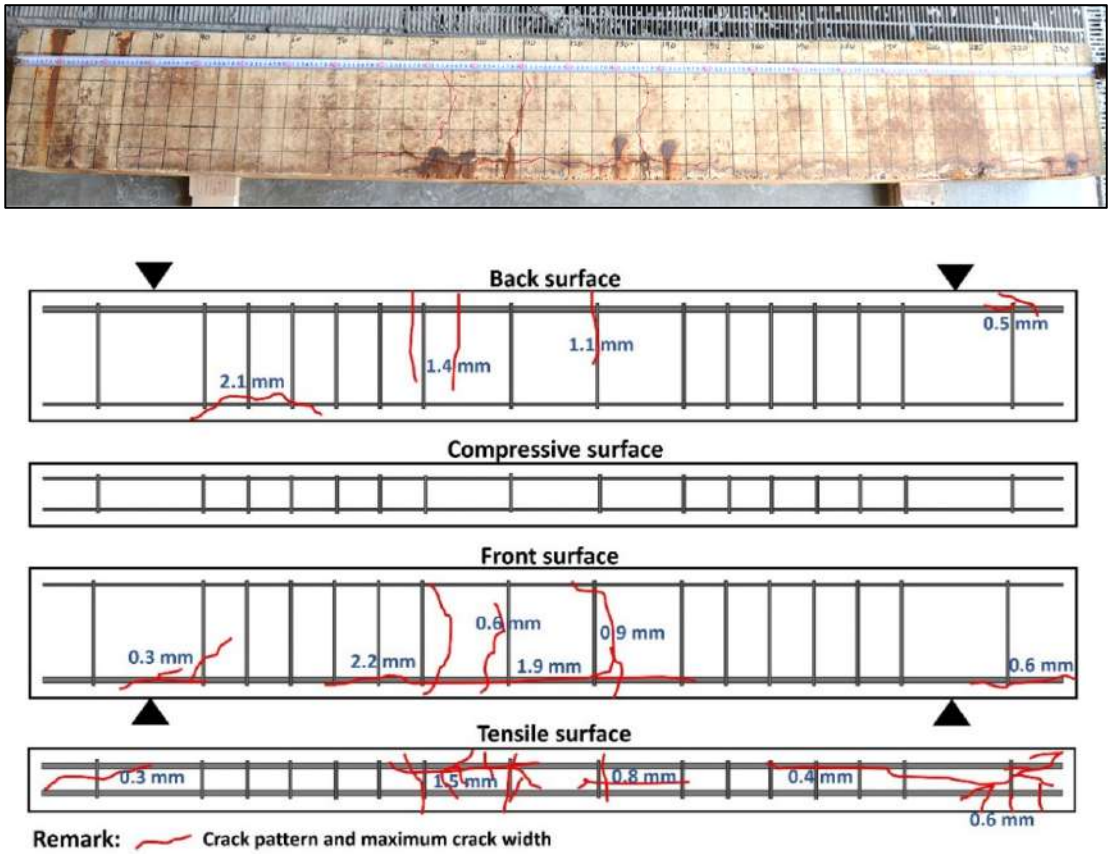

Figure 4.9 Appearance and cracking pattern of RC-2

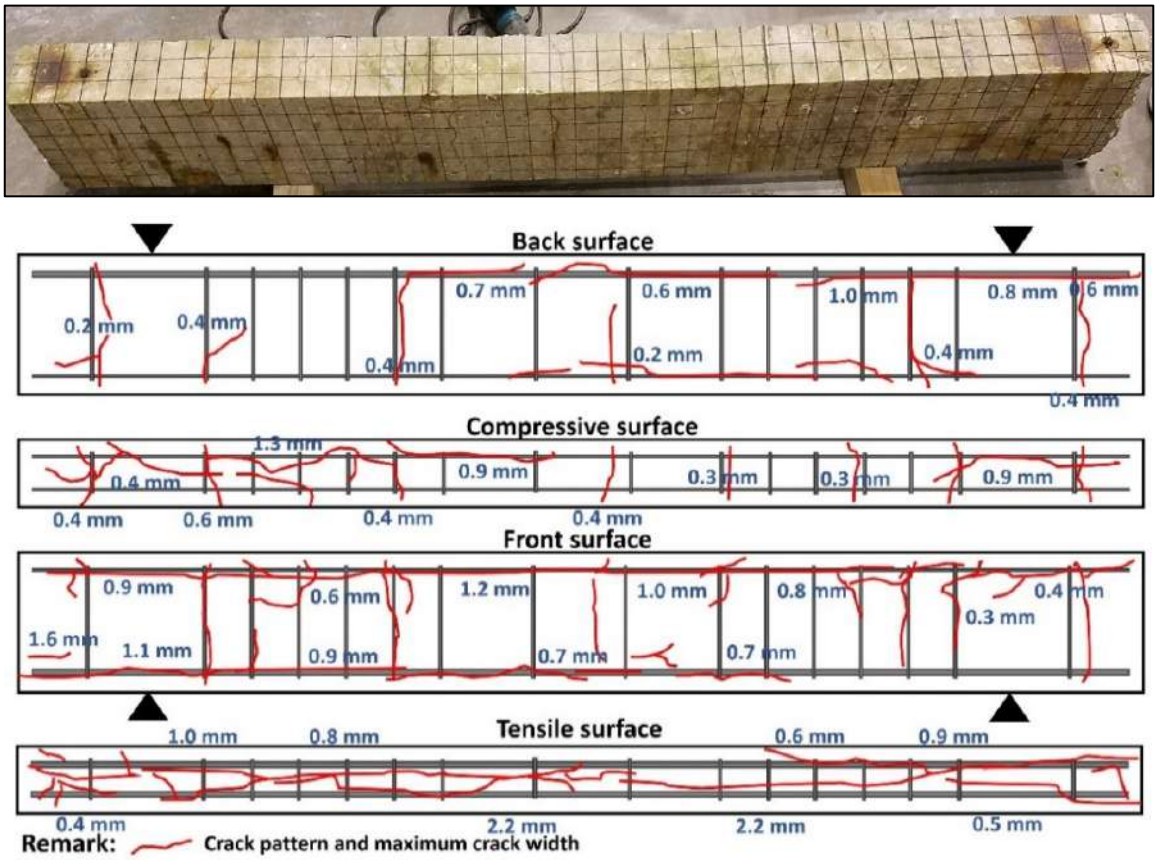

Figure 4.10 Appearance and cracking pattern of RC-3

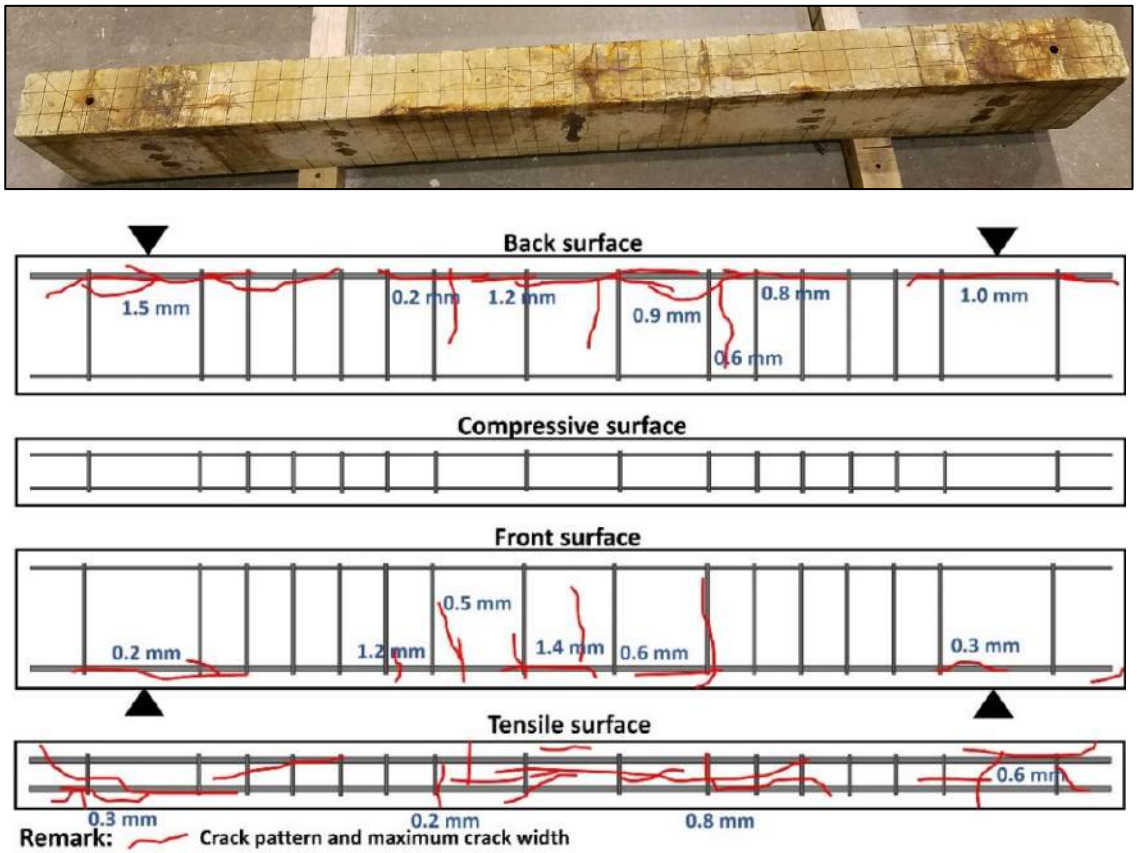

Figure 4.11 Appearance and cracking pattern of RC-4

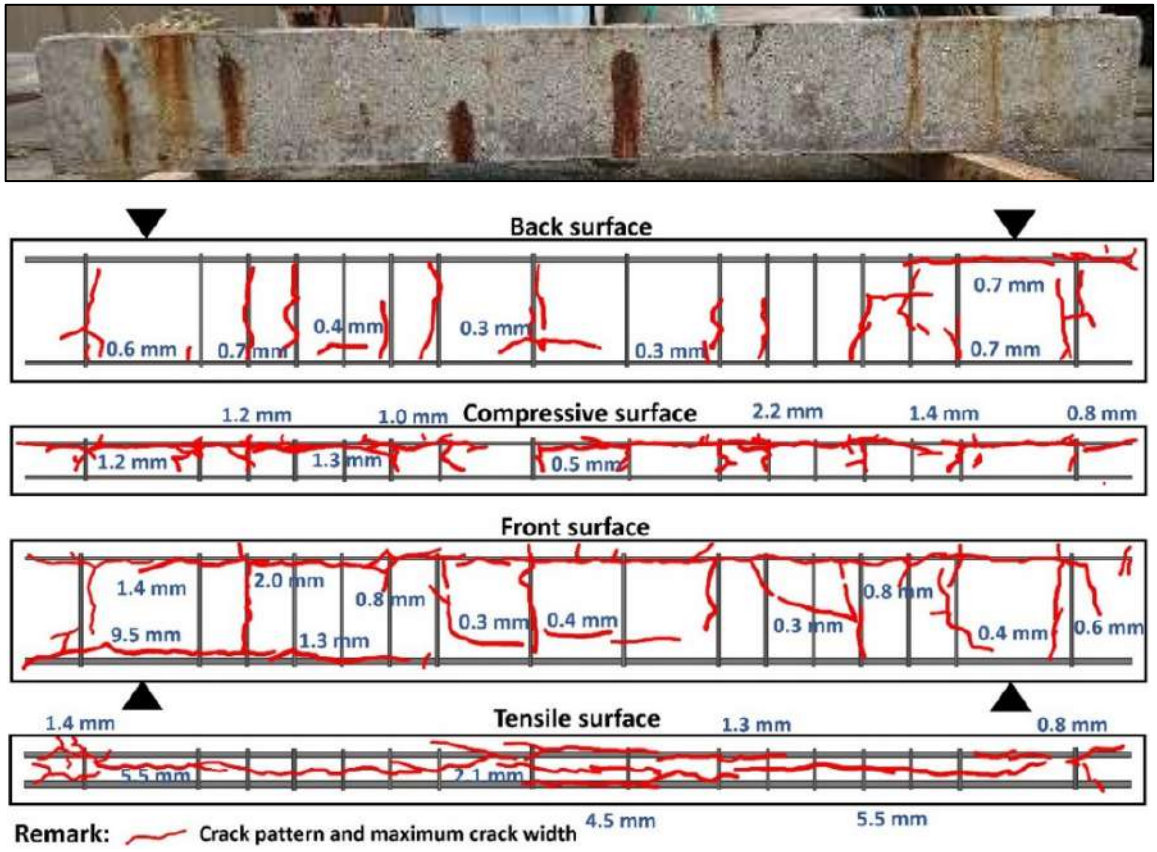

Figure 4.12 Appearance and cracking pattern of RC-5

4.4.3 Corrosion probability of rebar

Potential mapping of steel bar through half-cell potential measurements in RC beams according to ASTM C876 (2015) are presented in **Figure 4.13**, **Figure 4.14**, **Figure 4.15**, **Figure 4.16**, and **Figure 4.17**. The measurement was conducted with silver/silver chloride electrode after 1 hour of pre-wetting. Then, measurement value was converted to the potential of the copper/copper sulfate electrode (CSE) at 25°C. Measurement point divided every 5 cm from the bottom side of the beam (tensile area) to the upper side of the beam (tension area) and along the beam from 0 cm (the edge of the beam) until 240 cm length of the beam.

Figure 4.13 and **Figure 4.14** depicted the measured half-cell potential of rebars in 41 years. In RC-1, 77% area is categorized as corrosion region and 23% area is classified as uncertainty region, whereas 94% area of RC-2 is in corrosion condition and 6% is in uncertainty condition. It was observed that RC-2 performs more serious corrosion conditions than RC-1. The middle tensile part is the lowest half-cell potential value. **Figure 4.15** and **Figure 4.16** present that in RC-3, 20% area is categorized as corrosion region and 73% is classified as an uncertainty region, whereas 21% area of RC-4 is in corrosion condition and

11% is in uncertainty region. The half-cell potential of rebar in RC-5 shows the most positive value and generally in uncertainty condition.

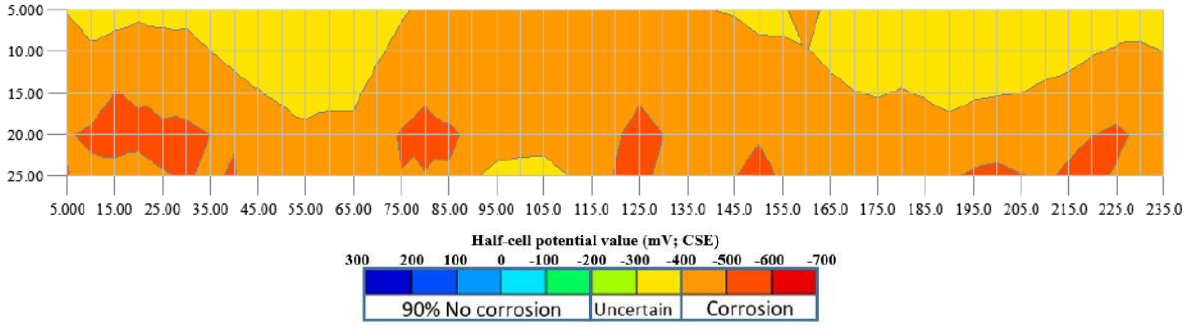

Figure 4.13 Corrosion map of RC-1

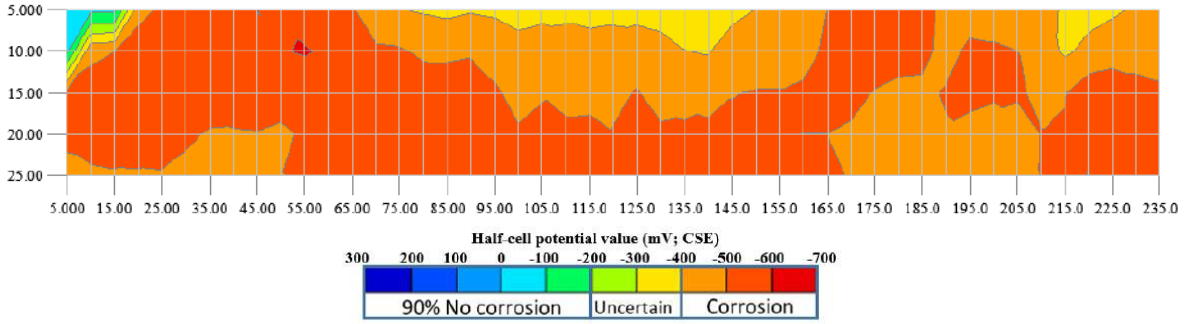

Figure 4.14 Corrosion map of RC-2

RC-1 and RC-2 were measured in wet condition so the results performs higher potential value than RC-3, RC-4, and RC-5 that measured at dry condition.

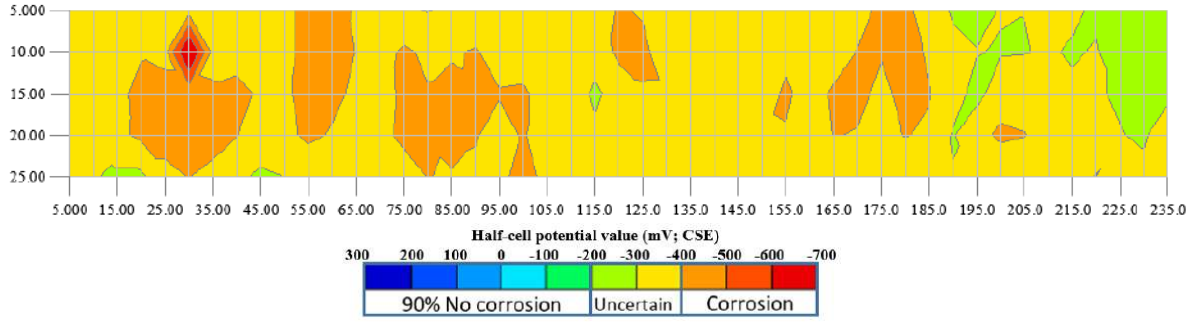

Figure 4.15 Corrosion map of RC-3

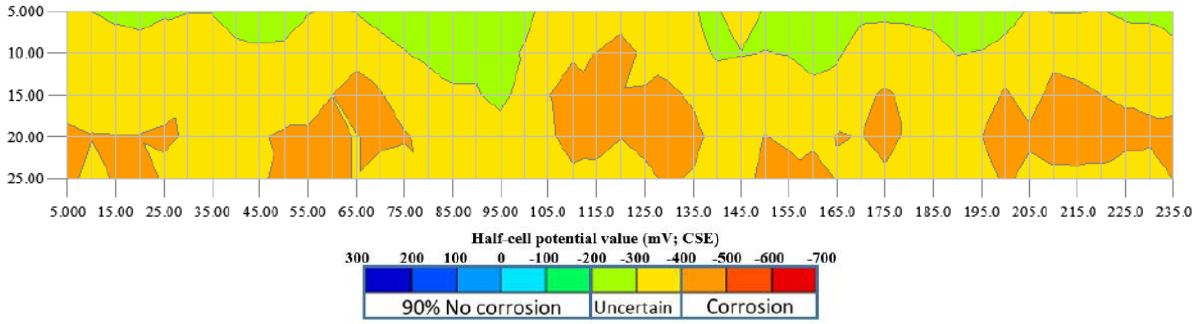

Figure 4.16 Corrosion map of RC-4

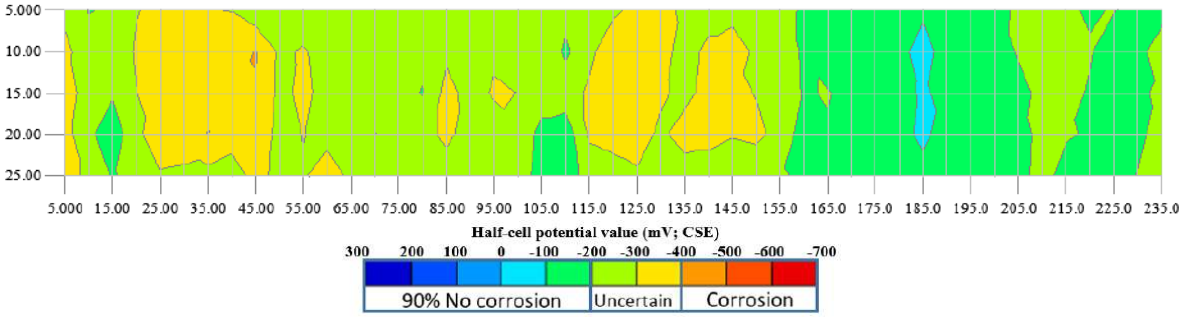

Figure 4.17 Corrosion map of RC-5

4.4.4 Chloride ion concentration

Chloride ion concentration was determined by using the titration method. Several processes such as sampling, crushing to powder, dissolution, and titration process were conducted for every centimeter in depth. In this experiment, the chloride profile was tested in four-point of each beam as shown in **Figure 4.18**. The core sample was drilled with 40 mm in diameter in A1, A2, B1, and B2 position.

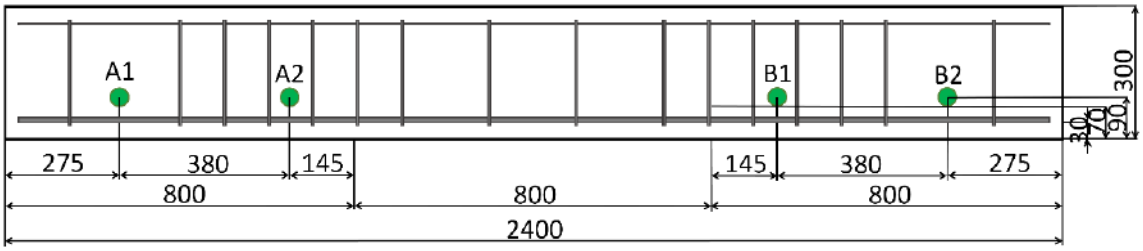

Figure 4.18 Sampling position of chloride ion profile test

The chloride ion profile from specimens was presented in **Figure 4.19**. The average of total chloride ion concentration in the surrounding of rebar is 4.65 kg/m^3, 4.75 kg/m^3, 6.05 kg/m^3, 3.08 kg/m^3, and 5.35 kg/m^3 in RC-1 until RC-5, respectively. These values are higher than the chloride ion threshold initiating corrosion of 1.2 kg/m^3 (JSCE standard specification for concrete structures – 2007 "Design").

Based on JSCE standard specifications for concrete structures – 2007 "Maintenance" Table C14.3.5.1 Grades of appearance and deterioration of structures, these specimens were categorized as Grade II-1 (former acceleration stage) where corrosion-induced cracking and rust appearance are observed. The intervention methods such as surface coating, patching, cathodic protection, and electrochemical desalination are required to extend the service life of members.

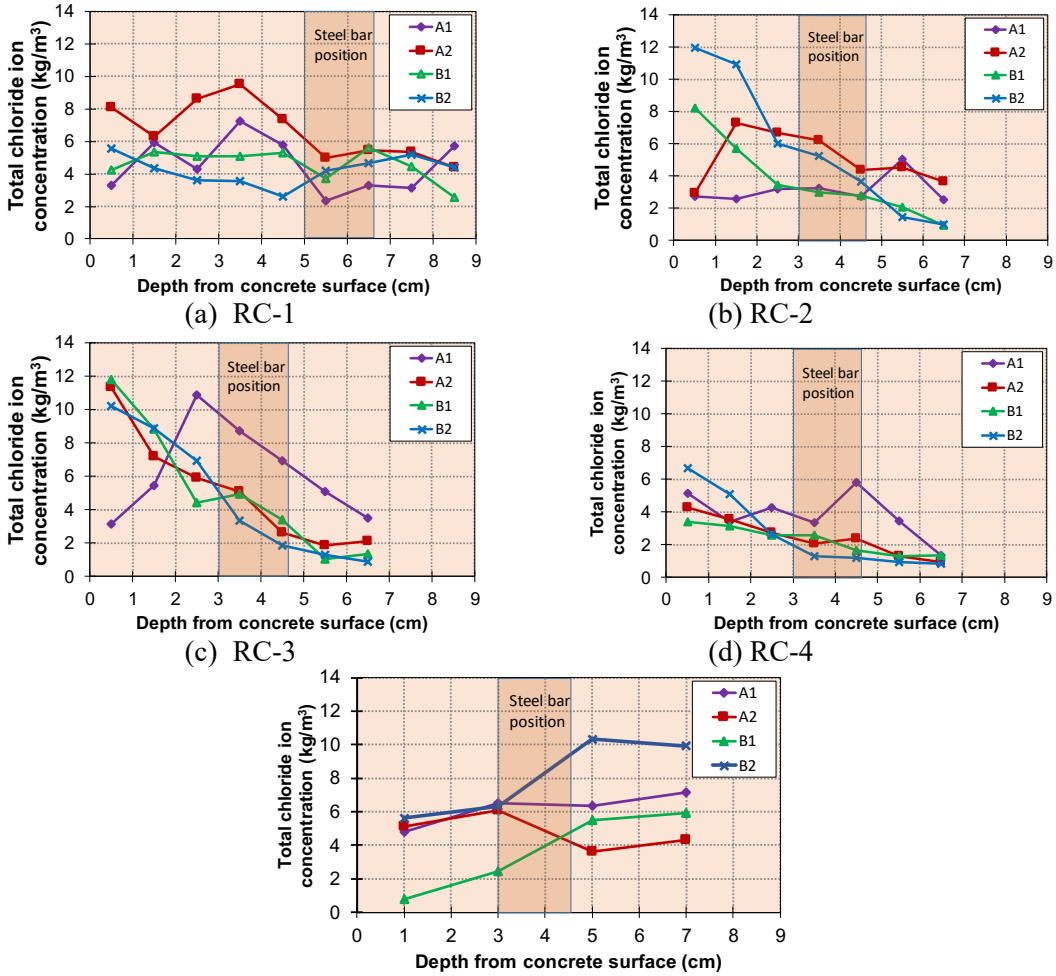

(a) RC-1 (b) RC-2

(c) RC-3 (d) RC-4

(e) RC-5

Figure 4.19 Chloride ion profile of specimens

4.5 **Repair strategy**

4.5.1 Repair design and materials

Based on the preliminary investigation, several cracks were generated in the middle tensile part. The corrosion probability of embedded steel bars was categorized as high risk with the accumulation of corrosion products (rust) on the steel bar surface. So, the patching method with sacrificial anode cathodic protection and corrosion inhibitor or its combination were applied on it to strengthen the structures and control the corrosion of the steel bar. The detailed repair designs were explained as follows.

❖ **Application of sacrificial anodes in patch and non-patch repair**

Nine and one rectangular sacrificial anodes were installed in steel bars in patch repair in RC-1 and RC-2, respectively. As the next repair stage, additional sacrificial anodes were employed by insertion into the pre-drilling hole in chloride-contaminated concrete (old concrete) to stop corrosion in existing concrete. The expected result of each stage during

three years of the repair process in RC-1 and RC-2 was summarized in **Table 4.4.** The repair design of the beams was presented in **Figure 4.20 (a) and (b**).

Table 4.4 The details of repair techniques of RC-1 and RC-2 (Astuti *et al*. 2019b)

Stage	Method	Duration	Expected Results
I	Patch repair and sacrificial anodes were applied in the middle tensile rebar part.	200 days	Protected condition on the patch repair section by replacement of chloride contaminated into chloride-free concrete and current flow generated from sacrificial anode to rebar.
II	Sacrificial anodes in patch repair were disconnected.	1 year	Protection condition was expected by the durability of new patch repair material only.
III	Additional sacrificial anodes were installed in non-patch repair concrete.	1 year	In order to protect all of the cross-sectional specimens, additional sacrificial anodes were embedded in the non-patch repair part.

The polymer-modified mortar with a compressive strength of 40.5 MPa and bending strength of 8.6 MPa at 28 days (**Figure 4.21(a)**) was used as replacement material in patch repair section after application of EVA (Vinyl Acetate/Ethylene) copolymer emulsion as an adhesive material coating agent (**Figure 4.21(b)**) between existing concrete and new patch repair material. Two types of sacrificial anodes, cylindrical ribbed and rectangular shape (**Figure 4.21 (c)**and **(d)**), were used to protect rebars in the patch and non-patch repair. The anode type selection is based on the available space where it will be embedded. Rectangular anode with thickness, width, and length of 13 mm, 45 mm, and 140 mm, respectively, was chosen to apply for the patch repair while cylindrical ribbed sacrificial anode with a diameter of 30 mm and length of 130 mm was inserted in the existing concrete. These anodes were made of zinc-coated with a porous mortar which has a lithium monohydrate solution (**Figure 4.21(e)**) to maintain zinc corrosion activation. This lithium-based solution keeps the zinc surroundings humid and the efficiency of the system is told to be constant during its lifetime (Rincon *et al.*, 2008).

- **Application of sacrificial anodes in non-patch repair and corrosion inhibitor in patch repair**

The repair detail of sacrificial anode application in non-patch repair was applied to RC-3 and RC-4 as presented in **Figure 4.20 (c) and (d).** The polymer-modified mortar (**Figure 4.21 (a)**) was applied in the middle of tension area with the dimension of 70 x 150 x 800 mm after replacing the chloride-contaminated existing concrete by crushing process and rust removal using an EVA (Vinyl Acetate / Ethylene) copolymer emulsion as an adhesive material coating agent (**Figure 4.21 (b)**) between parent concrete and patch repair mortar. Cylindrical ribbed sacrificial zinc anode (**Figure 4.21 (c)**) with a diameter of 30 mm, a length

of 139 mm and an approximate weight of 417 grams were installed in pre-drilled holes of 40 mm diameter in parent concrete and cementitious coating material with LiOH (**Figure 4.21 (e)**) was used to cover the anodes after settling position in the hole. Modified epoxy paint (**Figure 4.21 (f)**) was applied to the un-rusted tensile steel bar surface in the patch repair section of the RC-4 as a corrosion inhibitor before casting new patch repair material.

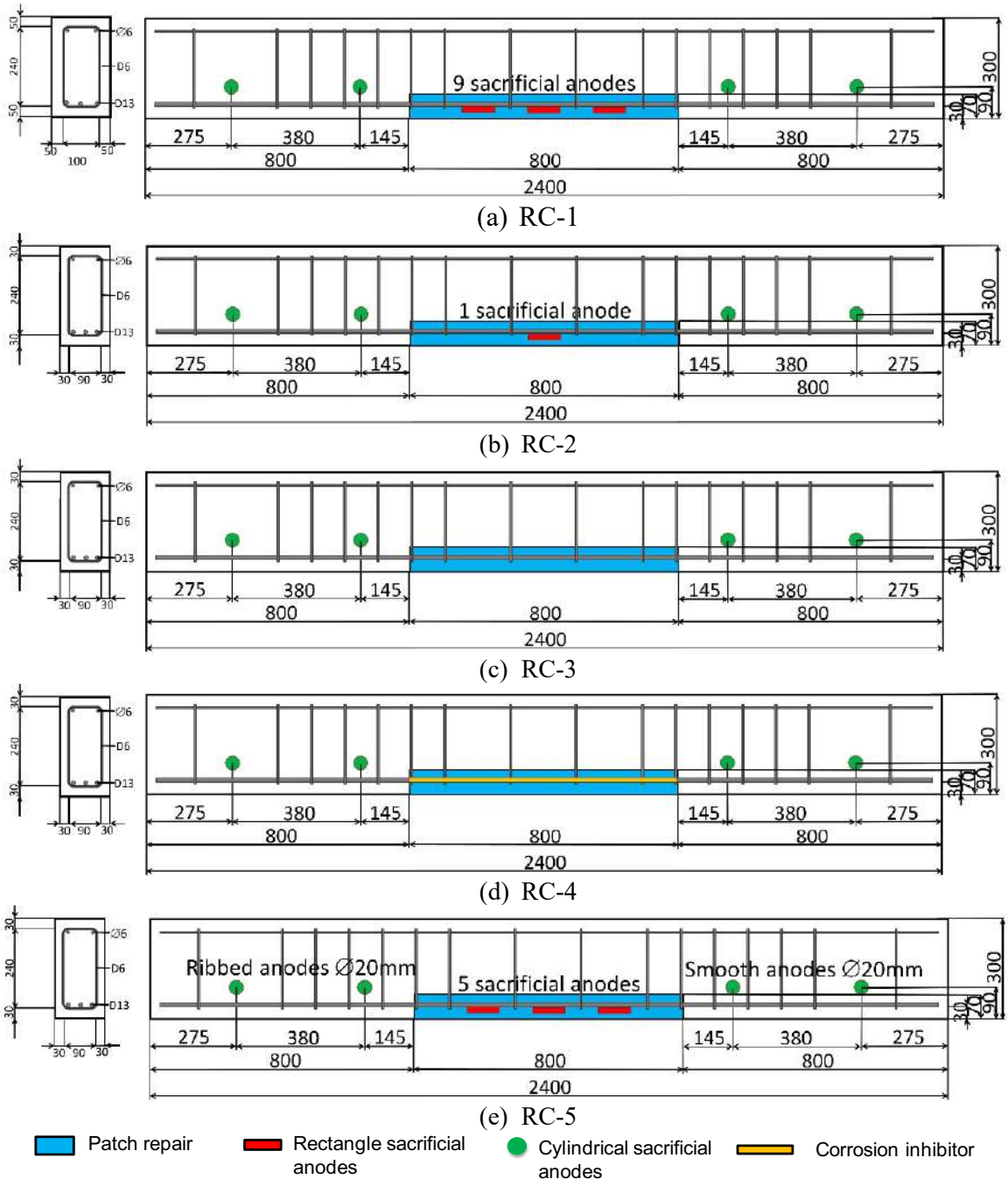

(a) RC-1

(b) RC-2

(c) RC-3

(d) RC-4

(e) RC-5

Figure 4.20 Repair design of the specimens

❖ **Application of different kind sacrificial anodes in patch and non-patch repair**

The experiment of timelapse application of different kind sacrificial anodes in the patch and non-patch repair was previously explained in RC-1 and RC-2 specimens. In this part, the application of a similar system but at the same time of operation was introduced as RC-5. The repair design of this experiment was shown in **Figure 4.20 (e).** Five rectangular sacrificial anodes were installed in the patch repair. Two cylindrical ribbed anodes were attached on the left side of the non-patch repair. Also, two smooth cylindrical anodes were installed on the right side of the non-patch repair. The diameter of sacrificial anodes in non-patch repair is 20 mm, smaller than the anodes in RC-1~RC-4. Bentonite-$LiNO_2$ mixture was used as an anode backfill material in RC-5. The new backfill material is environmentally friendly to provide a conducive environment for anode dissolution.

(a) Polymer modified mortar

(b) Coating agent

(c) Ribbed cylindrical sacrificial anode ∅30 mm

(d) Rectangle sacrificial anode

(e) LiOH cementitious anode coating

(f) Corrosion inhibitor

(g) Cylindrical anode ∅20mm

(h) Bentonite based cementitious anode coating

Figure 4.21 Material for repair process

4.5.2 Repair process

The repair process of this experiment was shown in **Figure 4.22** and **Figure 4.23**. The grid marking was done before the concrete crushing. Coating agents were applied to the old concrete in order to create new bonding with new patch material one day before sacrificial anodes setting and new patch material casting.

(a) Specimen preparation before concrete crushing

(b) After concrete crushing

(c) Application of coating agent

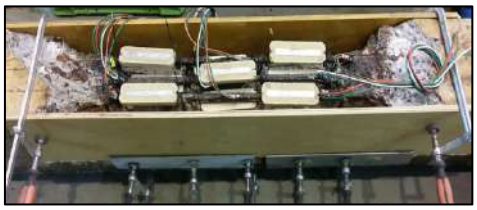

(d) SACP setting

(e) New patch material casting

Figure 4.22 Repair process in patch repair concrete (Rafdinal, 2016)

(a) Core drilling

(b) Anode setting

(c) Anode backfill material casting

Figure 4.23 Repair process in non-patch repair concrete

4.6 **Measurement method**

4.6.1 Protective current density

The current flow of sacrificial anodes was regularly monitored by high impedance ammeter. British standard EN 12696 suggested the design minimum of current flow divided by the total steel bar surface area should be more than 0.2 $\mu A/m^2$. Current density ($\mu A/m^2$) is a current flow generated by the sacrificial anode (μA) per steel bar surface area (m^2). The measurement method was expressed in **Figure 4.24.** Sacrificial anodes were connected to the negative terminal and the steel bar was tied up to the positive terminal. The current flow was recorded just after the switching off the connection.

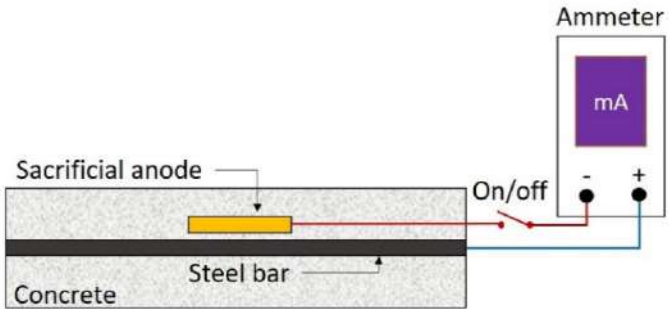

Figure 4.24 Current flow measurement method

4.6.2 Half-cell potential test (E_{corr})

According to ASTM C876-15 (2015), half-cell potential test of steel bars and sacrificial anodes was conducted by a saturated calomel electrode (SCE) and high impedance voltmeter on the grid points of 50 mm spacing after one hour of pre-wetting. The measurement is taken by connecting the high resistance voltmeter negative lead to the reference electrode and connecting the positive lead to the steel bar or anode being tested. The measurement method of sacrificial anode and steel bar potential were depicted in **Figure 4.25** and **Figure 4.26**, respectively.

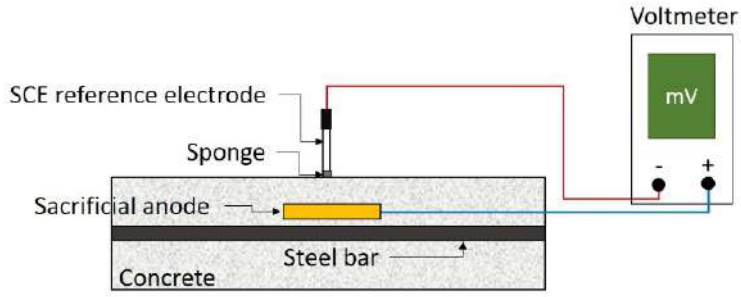

Figure 4.25 Measurement scheme of sacrificial anode potential

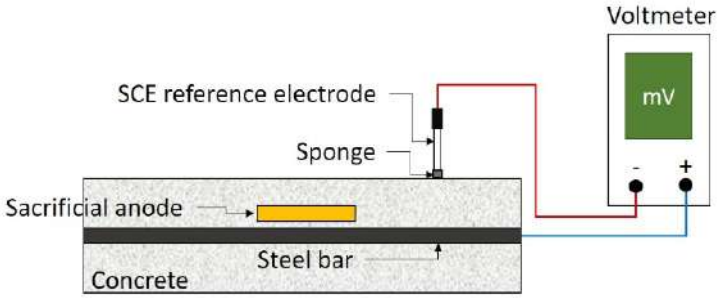

Figure 4.26 Measurement scheme of steel bar potential

4.6.3 Depolarization test

Performance assessment of cathodic protection was checked by depolarization test measurement, and 100 mV potential decay was chosen as an effectiveness criterion. On-potential (E_{on}) of rebar and the anode was measured under sacrificial anode cathodic

protection. Instant-off potential (E_{off}) was checked immediately after disconnection, and the rest potential (E_{corr}) was measured at 24 hours after the disconnection. The schematic measurement method was explained in **Figure 4.27**.

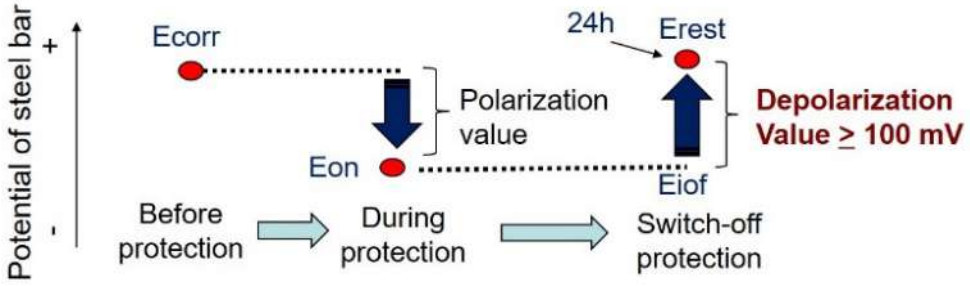

Figure 4.27 Schematic method of depolarization test

4.6.4 Polarization resistance and corrosion current density

The polarization resistance was measured by using the silver/silver chloride reference electrode (Ag/AgCl) and portable corrosion meter after one-hour pre-wetting. **Figure 4.28** shows the details of the measurement. The following equation was used to calculate the corrosion current density (I_{corr}) using the Stern-Geary Formula (Stern and Geary, 1957; Andrade and González, 1978) as presented in **Equation 4.1**.

$$I_{corr} = \frac{B}{R_p} x\ 10^6 \qquad (4.1)$$

Where I_{corr} is corrosion current density (μA/cm^2), R_p is polarization resistance (Ω.cm^2) and B is 0.026V considering steel in active condition (Pech-Canul and Castro, 2002; ASTM, 2015). The specified limits of corrosion current density (0.5-1.0 μA/cm^2) are considered to be moderate to high corroding as per CEB Standard (CEB, 1998).

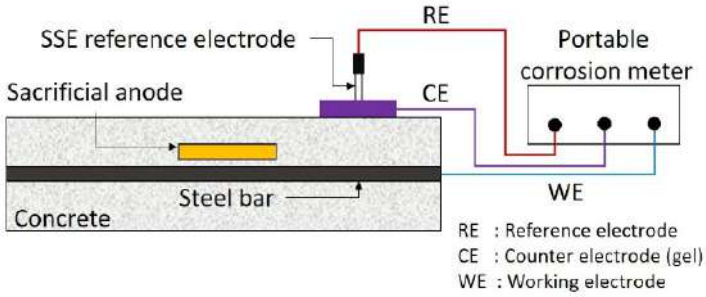

Figure 4.28 Schematic measurement of polarization resistance

4.6.5 Anodic-cathodic polarization curve

The anodic polarization curve is related to the passivity condition of the steel bar. When the current density becomes larger, the grade of passivity film of the steel bar becomes worse (Otsuki, 1985) while the cathodic polarization curve is related to the diffusion of oxygen. **Figure 4.29** shows the details of the measurement.

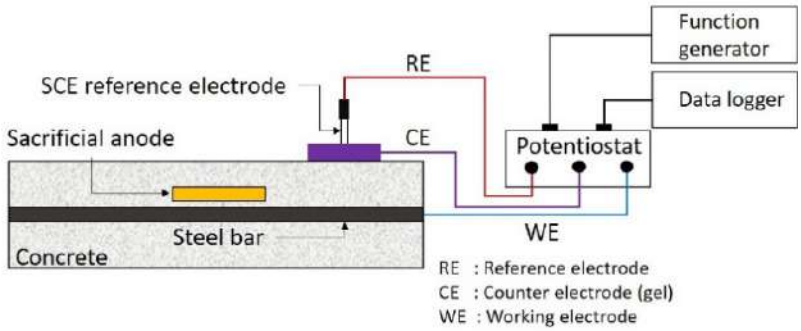

Figure 4.29 Schematic measurement setting of anodic-cathodic polarization curve test

When the current density becomes larger, the level of oxygen diffusion becomes larger. For this, similar testing equipment as for polarization behavior test was used. Saturated calomel electrode (SCE) and gel were used as the reference electrode and counter electrode, respectively. The rest potential of the steel bars gradually shifted to +700 mV for APC and -700mV for CPC with a scan speed of 50 mV/min by a potentiostat. The maximum current density obtained from the anodic polarization curve was then used to judge the passivity grade of the steel bar (Otsuki, 1985).

4.7 **Application of sacrificial anodes in patch and non-patch repair**

Corrosion due to chloride attack is one of the most common deterioration factors in reinforced concrete (RC) structures exposed to the marine environment. The penetration of chloride ion concentration into concrete activates the corrosion of rebar by destructing the passivity film when the chloride ion concentration at the rebar surface reaches a critical value (Glass and Buenfeld, 1997). Whenever the threshold amount of the chloride ions reaches the surface of rebar, along with enough oxygen and moisture, steel corrosion may result in concrete cracking and spalling of the cover concrete when expansive stress exceeds the tensile strength of concrete; reduction of steel reinforcement cross-section may lead to structural failure. As a result, the corrosion of reinforcement adversely affects the safety and the serviceability of concrete structures and hence shortens the service life (Song *et al.* 2007).

The ordinary approach to rehabilitate the defective RC structures is the patching method. British Standard of Design Manual for Road and Bridge (1990) recommends that the section which shows the chloride ion contamination greater than 0.3% by weight of cement and half-cell potential value higher than −350 mV should be removed. On the contrary, the concrete replacement work on chloride contaminated structures can be very onerous and expensive (Christodoulou, 2008). In the last decades, several electrochemical repair techniques were developed for offering chloride-induced corrosion. Sacrificial anodes

have been chosen as one of a method to limit the extent of concrete replacement and extend the service life of patch repairs to corrosion damaged RC structures (NACE, 2005).

In this study, the different times of sacrificial anode cathodic protection (SACP) application in the patch and non-patch repair concrete were evaluated for accomplishing severely damaged RC beam aged 44-year-old exposed to the actual marine environment. The decision to apply sacrificial anode cathodic protection and patch repair method to the particular structures can be in many cases based on the results of a preliminary investigation that shows some high levels of chloride contamination, corrosion possibility of steel bars, and damage appearance in some part of the structures (Cheaitami, 2000). The anode setting position in RC-1 and RC-2 was expressed in **Figure 4.30** and **Figure 4.31**.

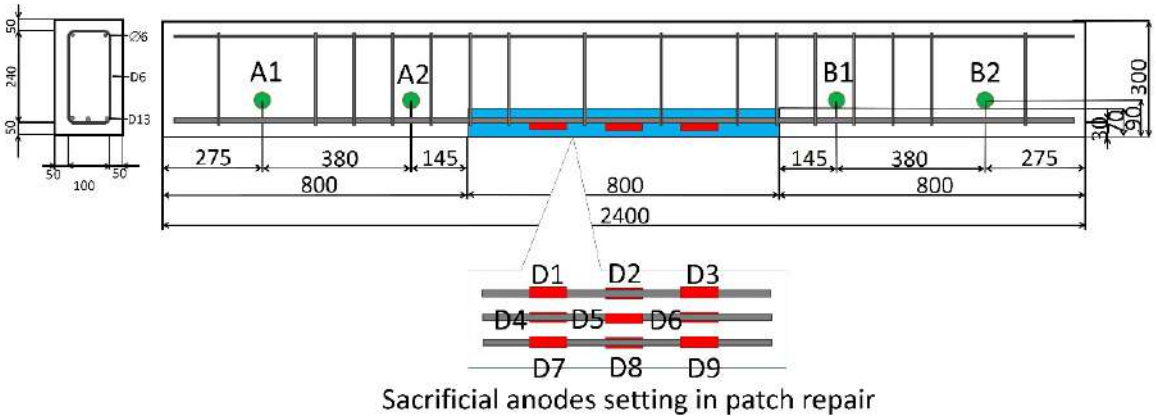

Figure 4.30 Anode setting position in RC-1

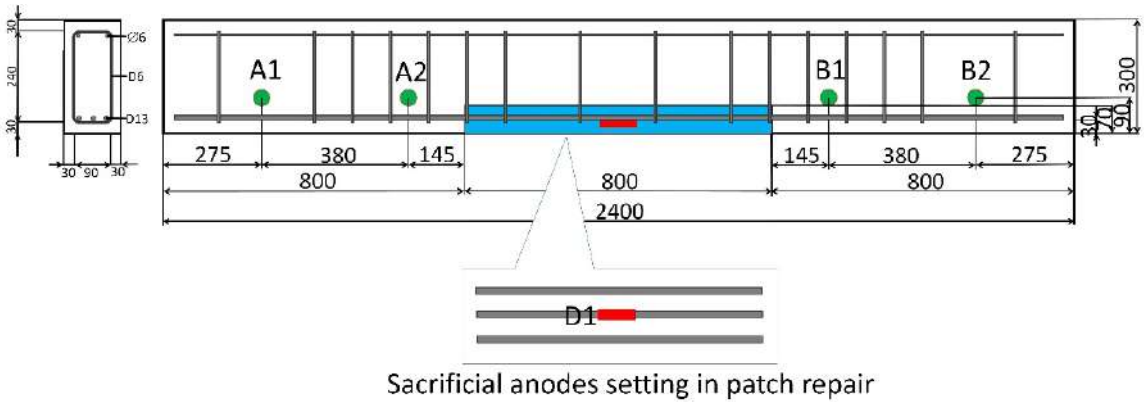

Figure 4.31 Anode setting position in RC-2

As the first repair stage, application of sacrificial anodes in patch repair, three and one anodes were installed on the compressive steel bar before polymer mortar placing as new patch material. After 200 days of connection, sacrificial anodes in patch repair were interrupted almost for one-year as the second stage of repair. The RC beams were exposed to a dry condition in the laboratory. As the last stage of repair, four additional sacrificial anodes were installed at both sides of existing concrete to protect its area. After two months

of additional anodes connection, the re-connection of sacrificial anodes in patch repair was conducted.

4.7.1 Protective current density of sacrificial anodes

The protective current density of sacrificial anodes is presented in **Figure 4.32**. The protective current density of RC-1 shows larger than RC-2 due to its larger number of anodes (nine anodes) than RC-2 (one anode). The current flow generated by sacrificial anodes is stable until 60-days of exposure. Then, the sacrificial anodes were stopped at 200-days. No current flow in Stage II. After the disconnection, the connection of sacrificial anodes in patch repair is started as Stage III.

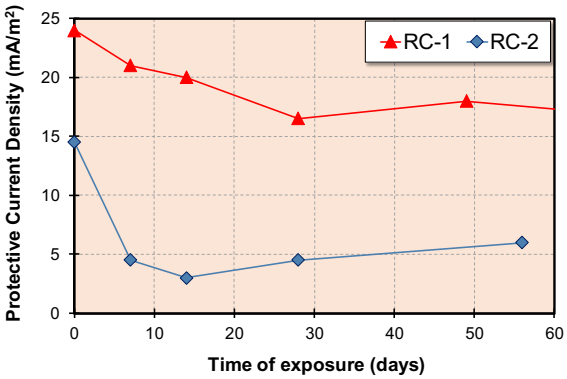

Figure 4.32 Protective current density of anodes in Stage I of repair

The current flow of sacrificial anodes in non-patch repair (A1, A2, A3, and A4) is shown in **Figure 4.33**. After two months of sacrificial anodes in non-patch repair, the sacrificial anodes in patch repair were re-connected, and the current flow is presented in **Figure 4.34**. The total current density of all anodes in Stage III is revealed in **Figure 4.35**. The protective current density suddenly jumps during the re-connection step at 60-days, especially on the RC-1 specimen.

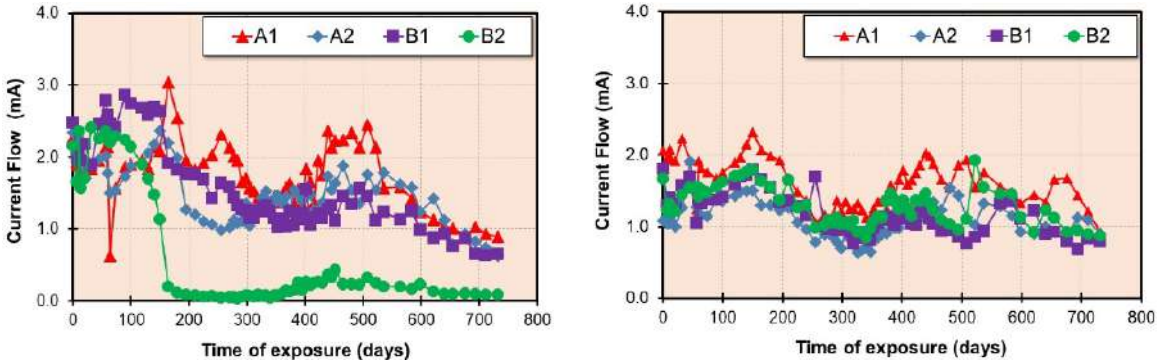

(a) RC-1 (b) RC-2

Figure 4.33 Current flow of cylindrical ribbed-sacrificial anodes in Stage III of repair

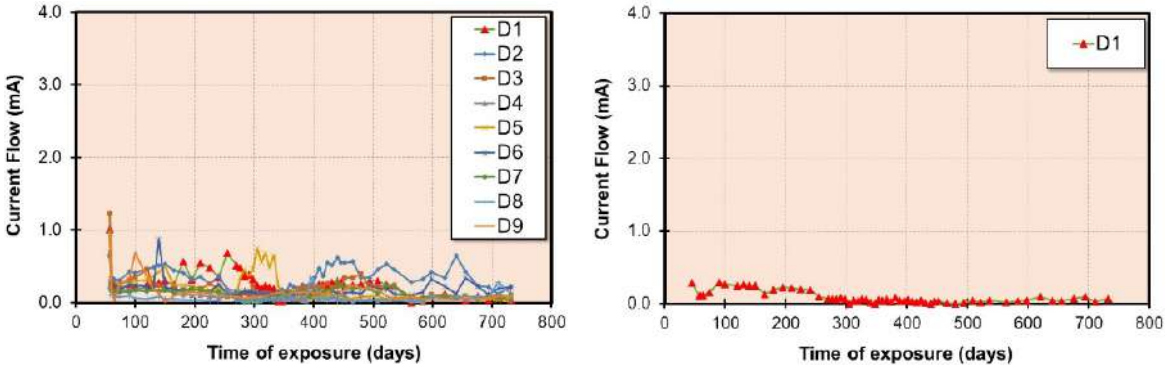

(a) RC-1 (b) RC-2

Figure 4.34 Current flow of rectangular sacrificial anodes in Stage III of repair

The current density of both specimens expresses stable value until 600-days of exposure. It shows that the protective current density tends to fall with time as the anode is consumed. As a result, sacrificial anodes cathodic protection is not generally achieved by sustaining an adequate level of steel polarization, as in the case for other electrochemical treatments (Glass and Christodoulou, 2012). Even though the protective current flow of these specimens decreased until less than the minimum design limit of cathodic protection based on BS EN ISO 12696 after 600-days of repair period, and it still polarized the steel bar more than 100 mV.

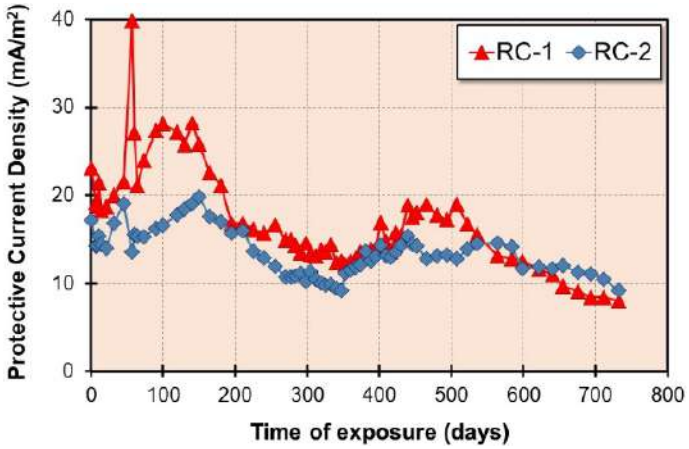

Figure 4.35 Protective current density in Stage III of repair

4.7.2 Potential development of sacrificial anodes

The instant-off potential sacrificial anodes in non-patch and patch repair in both specimens in Stage II of the repair process were expressed in **Figure 4.36** and **Figure 4.37**, respectively. It can be seen that the potential development of sacrificial anode in patch repair is more positive than in non-patch repair due to its different types of anodes.

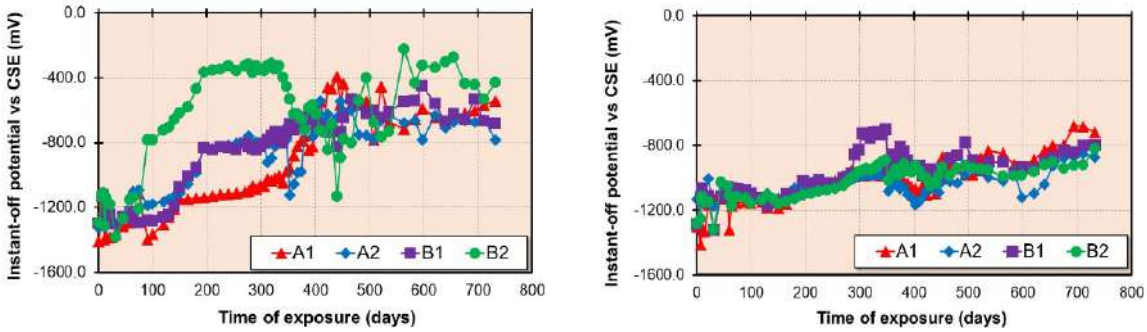

(a) RC-1 (b) RC-2

Figure 4.36 Instant off potential development of sacrificial anodes in non-patch repair

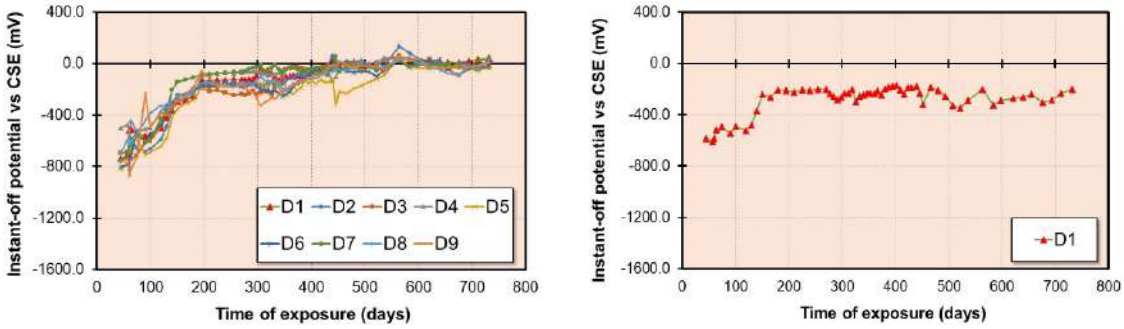

(a) RC-1 (b) RC-2

Figure 4.37 Instant off potential development of sacrificial anodes in non-patch repair

4.7.3 Anodic polarization behavior of sacrificial anodes

The anodic polarization behavior of sacrificial anodes embedded in the patch and non-patch repair parts during Stage III of repair process is illustrated in **Figure 4.38** and **Figure 4.39**.

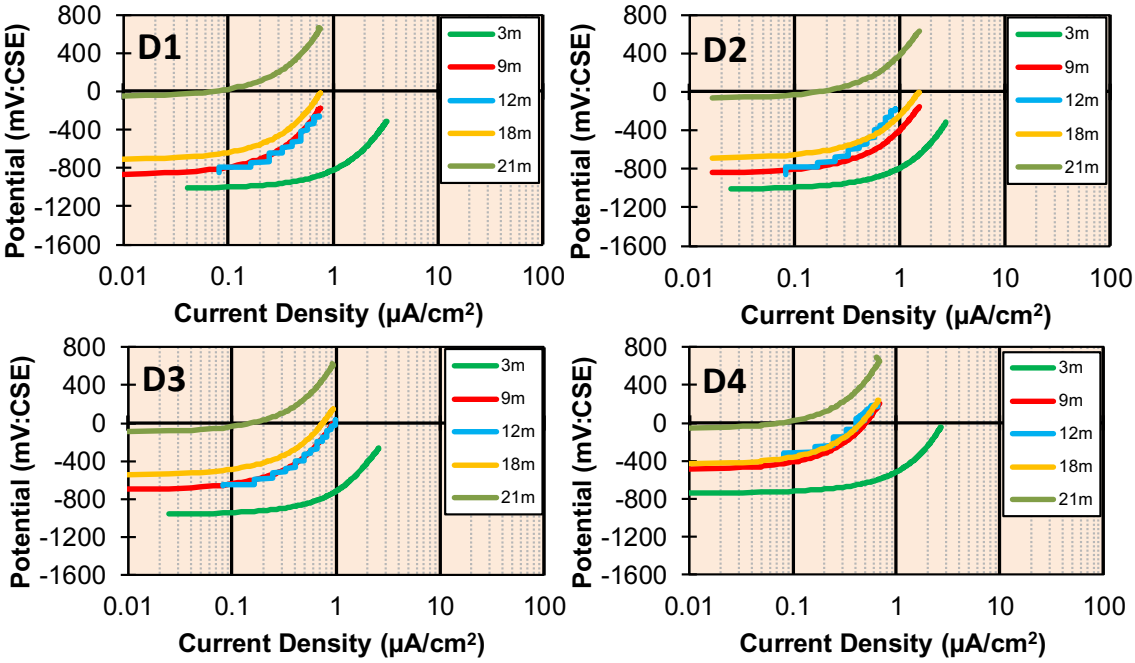

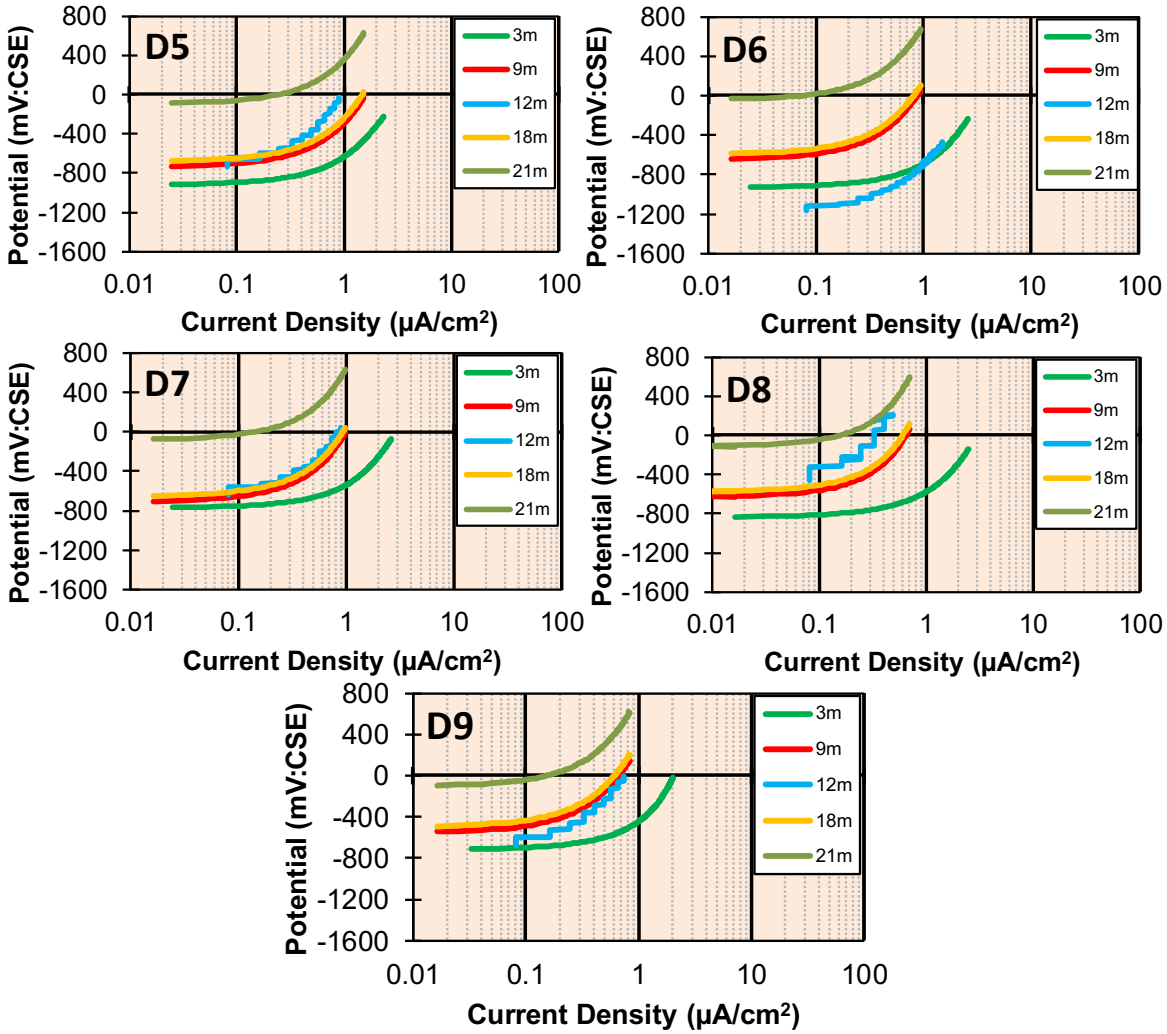

Figure 4.38 Anodic polarization curve of anodes in patch repair of RC-1

Sacrificial anodes in patch repair show lower maximum current density than in non-patch repair. It means that the sacrificial anodes in patch repair have lower generated current flow than sacrificial anodes in non-patch repair. It may be caused by the sacrificial anodes in non-patch repair have larger size and different anode material components.

The identical anodic polarization curve of sacrificial anodes trend also can be seen in the RC-2 specimen, as shown in **Figure 4.40** and **Figure 4.41**. Generally, the trend of anodic polarization curve of anodes move to left sides. It indicates that reduction of maximum current density occurs time dependently. It confirms that the protective current density generated by each sacrificial anodes. The lower current density produced by anodes the longer its service life. It may be caused the current density of anodes change the environmental conditions of surrounding steel bars so the required current flow by anodes decrease over time.

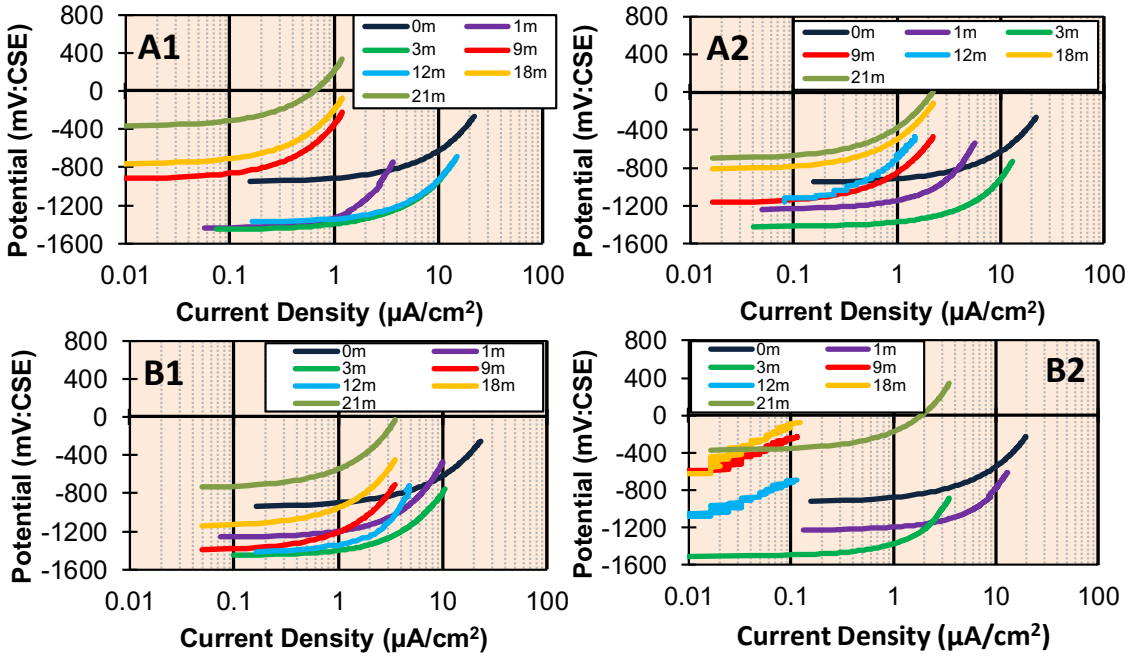

Figure 4.39 Anodic polarization curve of anodes in non-patch repair of RC-1

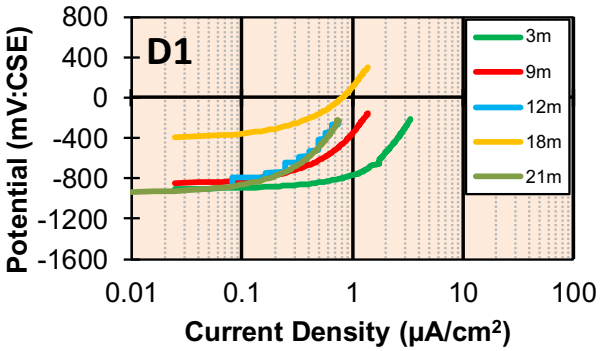

Figure 4.40 Anodic polarization curve of anodes in patch repair of RC-2

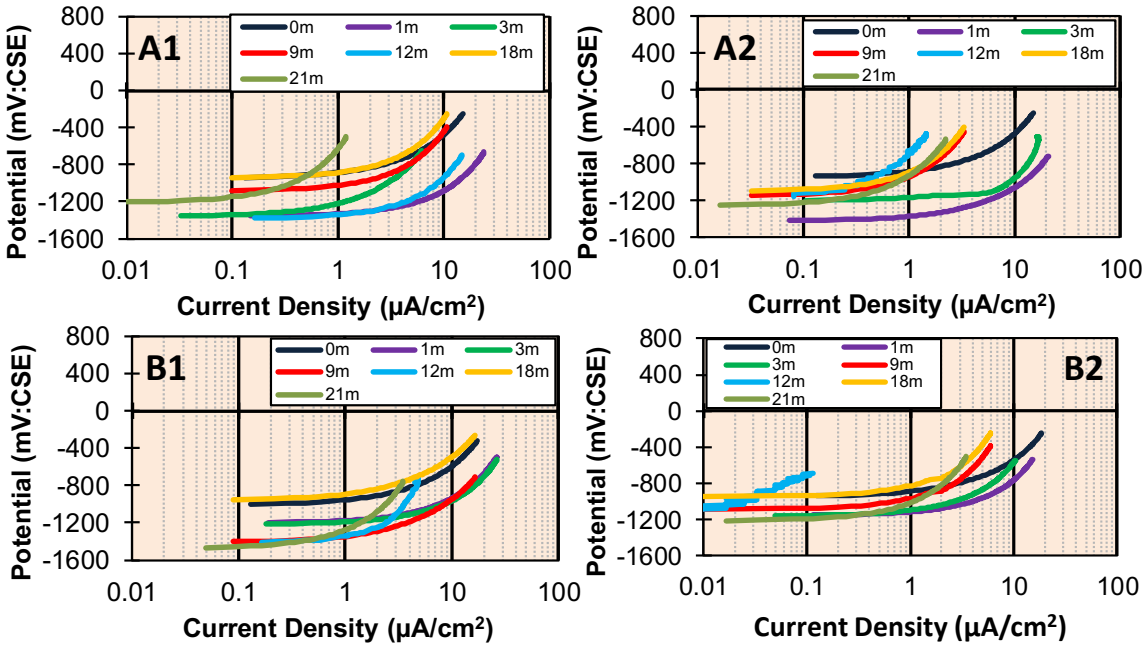

Figure 4.41 Anodic polarization curve of anodes in non-patch repair of RC-2

4.7.4 Potential development of steel bar

In the first stage of repair, the nine and one sacrificial anodes were inserted in the polymer mortar as new patch material in the middle tensile part of RC-1 and RC-2 beams, respectively. This repair method was previously discussed by Rafdinal (2016) and Astuti *et al.* (2019a). The potential development of steel bars until two-months of sacrificial anodes protection was presented in this paper. Instant-off and rest potential of tensile rebar in RC-1 and RC-2 (**Figure 4.42 and Figure 4.43**) by sacrificial anodes were performed in the patch repair area. Nine-sacrificial anodes in RC-1 polarize steel bar in patch repair until 100 mm of distance from the boundary, but one sacrificial anode in RC-2 shows 200 mm of polarization from anode setting position.

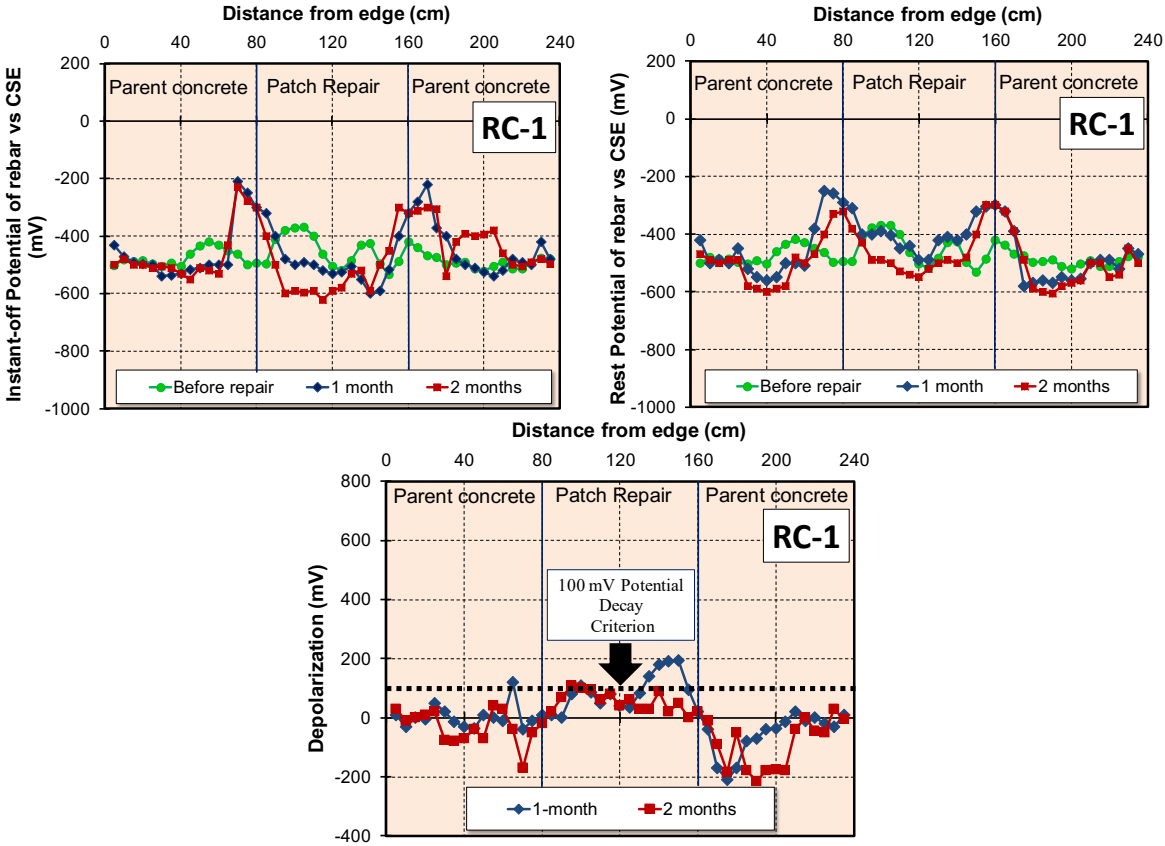

Figure 4.42 Potential development of tensile steel bar in RC-1 during Stage I of repair

From the depolarization test value, the polarization effect of anode only occurred in the patch repair section, and it cannot reach the existing concrete due to electrochemical incompatibility between two different concrete resistivity. In RC-1, all area in patch repair section is in protection condition, while only in the radius of 200 mm away from anode position is in protection condition for RC-2. It indicated that the number of anodes effect on the protection area and the optimum distance of each anode in patch repair is 400 mm.

After 200 days of connection, sacrificial anodes in patch repair were interrupted almost for one-year as the Stage II of repair. The RC beams were exposed to a dry condition in the laboratory.

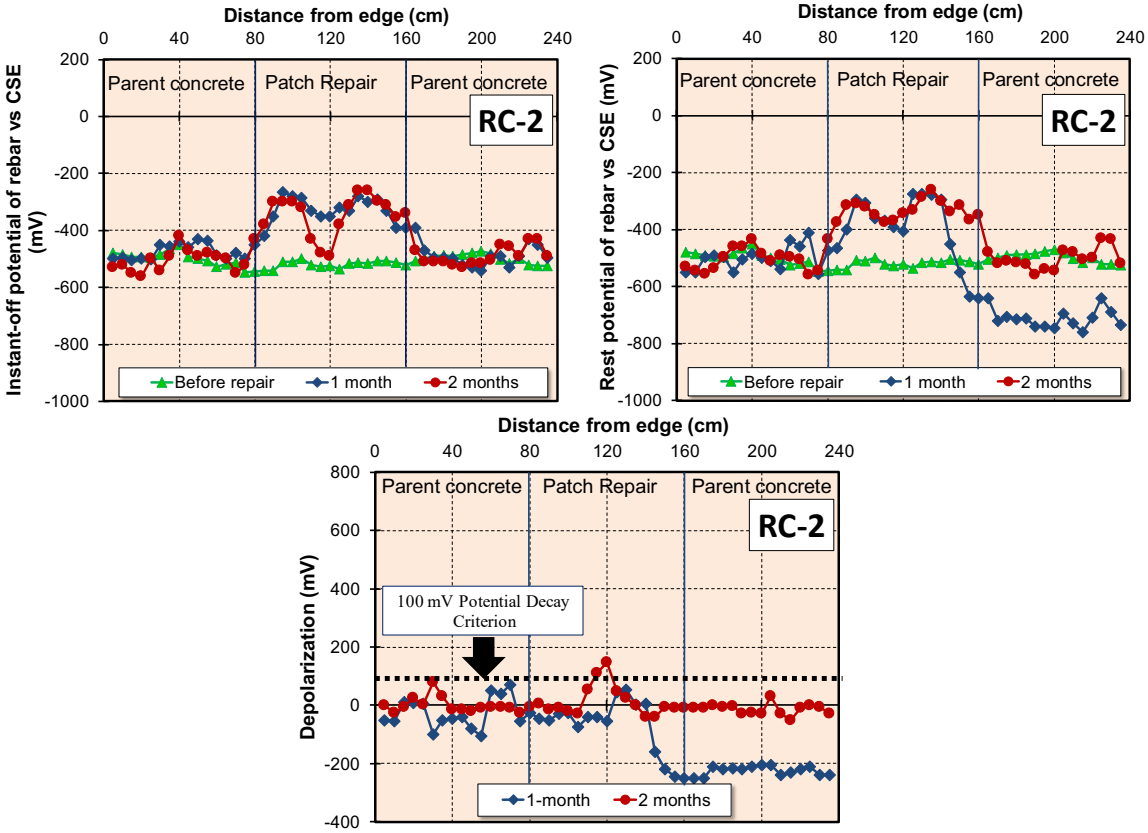

Figure 4.43 Potential development of tensile steel bar in RC-2 during Stage I of repair

The rest potential of tensile rebar before and after one-year of current interruption is presented in **Figure 4.44**. It presents the rest potential shift of the tensile steel bar in patch repair is greater than in the non-patch repair area. Both in RC-1 and RC-2, the rest potential value of steel bar in the patch repair section is in 90% no corrosion probability. It may because of the effectiveness of polymer modified mortar as a new replacement material and the absence of chloride contamination.

As the last stage of repair, four additional sacrificial anodes were installed at both sides of existing concrete to protect its area. After two months of additional anodes connection, the re-connection of sacrificial anodes in patch repair was conducted.

The polarization development of tensile steel bars in RC-1 and RC-2 including instant-off potential, rest potential, and depolarization test value of tensile rebar in until one-year observation was shown in **Figure 4.45** and **Figure 4.46**. The instant-off potential of rebar

was check immediately after the current interruption of sacrificial anodes and rebar. The half-cell potential of rebar after 24-hour off-condition is described as rest potential.

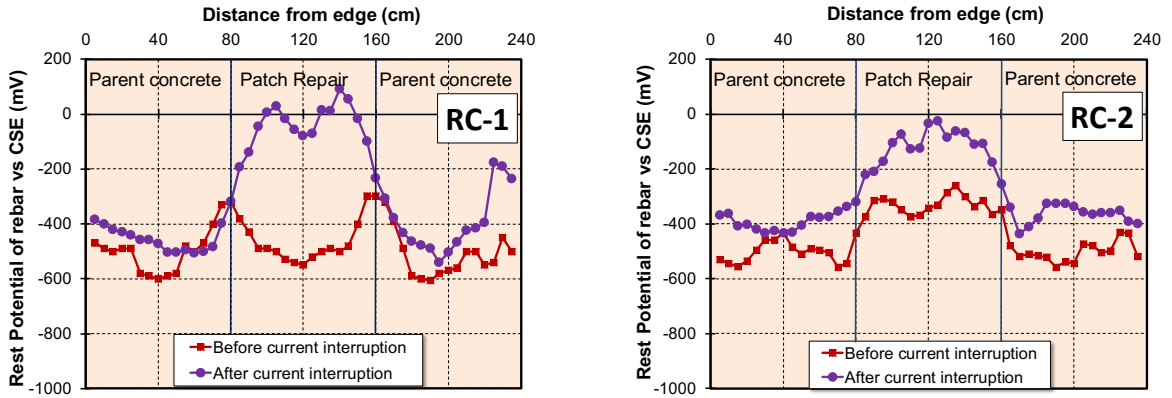

Figure 4.44 Rest potential of tensile steel bar of RC-1 and RC-2 during Stage II of repair

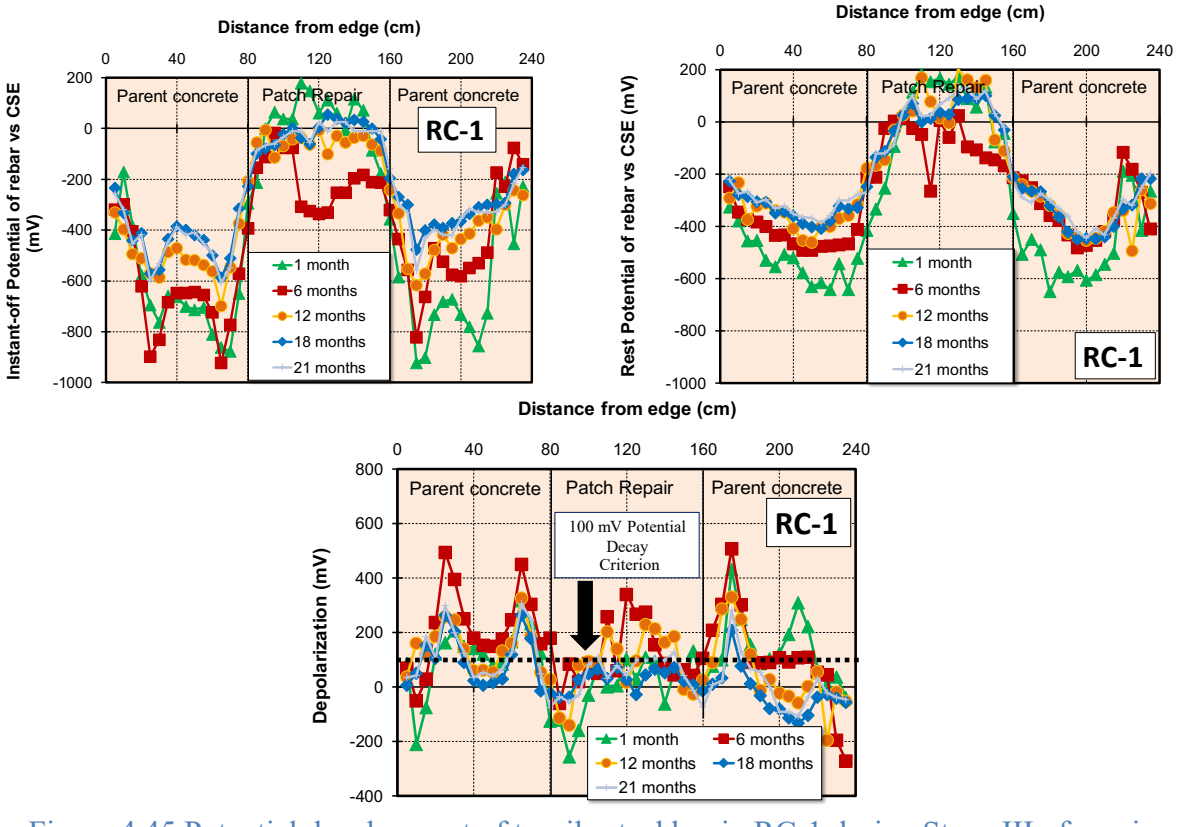

Figure 4.45 Potential development of tensile steel bar in RC-1 during Stage III of repair

The different potential value between instant-off potential and rest potential is defined as depolarization test value, a parameter to categorize the effectiveness of cathodic protection. 100 mV potential decay, the common criterion is used to evaluate the performance of sacrificial anode cathodic protection. A fall in potential was observed for all specimens following the application of additional sacrificial anodes in non-patch repair. It indicates the additional anodes polarising the rebar to more negative potential than 750 mV vs. CSE. In this case, the potential shift is almost limited to the distance of approximately

200 mm away from the position of anodes. It indicates that the optimum distance of sacrificial anodes in non-patch repair is 400 mm.

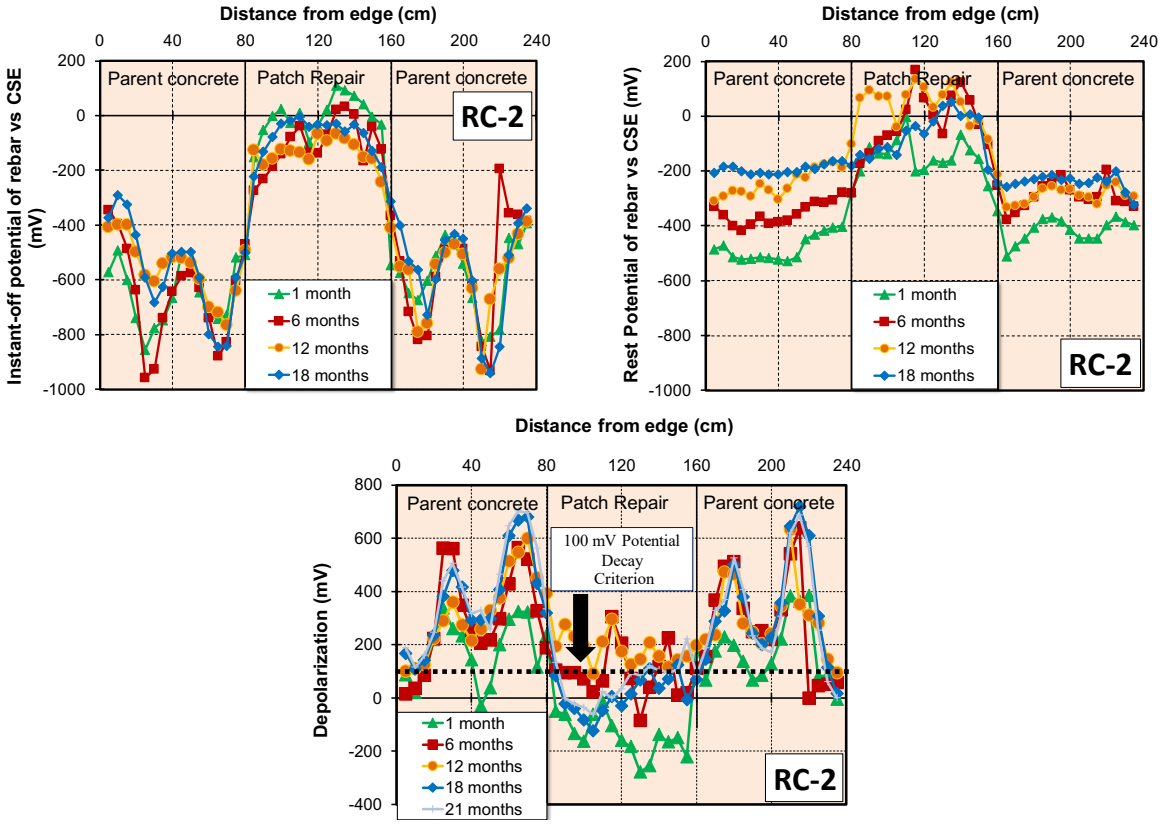

Figure 4.46 Potential development of tensile steel bar in RC-2 during Stage III of repair

The 24-h decay or depolarization test value from instant-off potential was monitored monthly after sacrificial anodes switch off. Both of specimens showed similar behavior and satisfied the 100 mV decay since 3-months of connection. It indicates that the protection is achieved within 3-months. It is consistent with the age and condition of rebars, with no long term corrosion existing, unlike in real marine RC structures, where a longer passivation period would be expected. At the conclusion of the trial, instant-off potentials were recorded. As would be expected, both specimens demonstrated a drop less negative potentials, with all achieving a potential decay at least 100 mV, satisfying the potential decay criterion. **Figure 4.47** and **Figure 4.48** presented the development of rest potential and protection area during observation.

1 - month	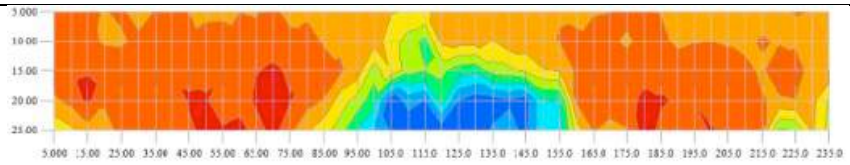
3 - months	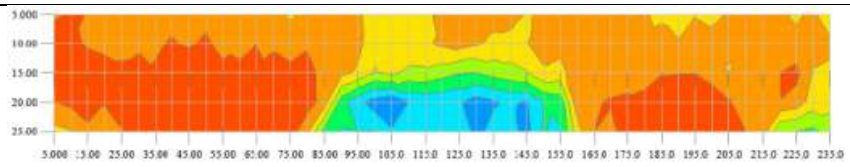
6 - months	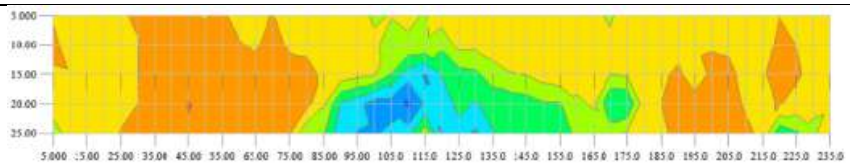
9 - months	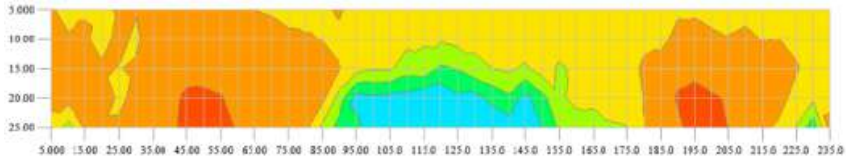
12 - months	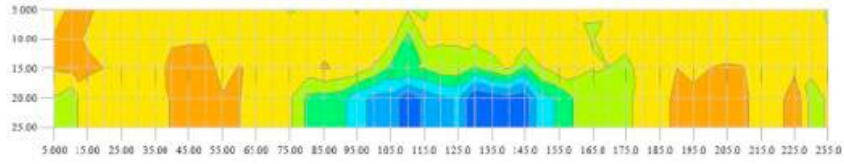
15 - months	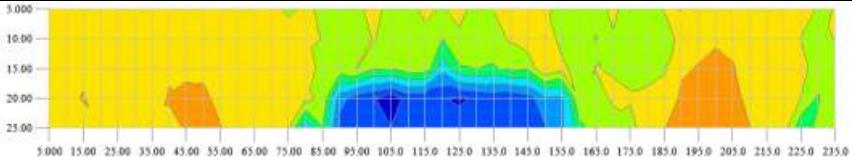
18 - months	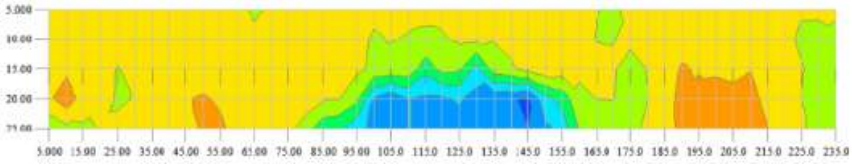
21 - months	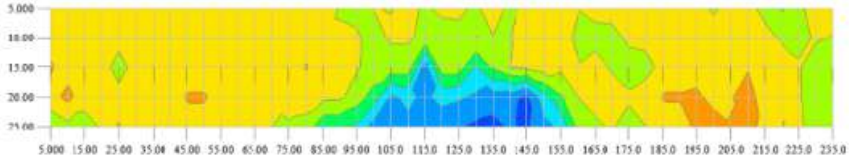

Remark:

(a) Rest potential of RC-1

1 - month	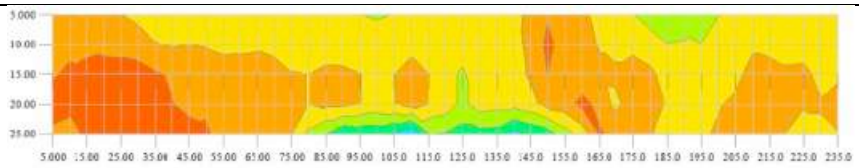
3 - months	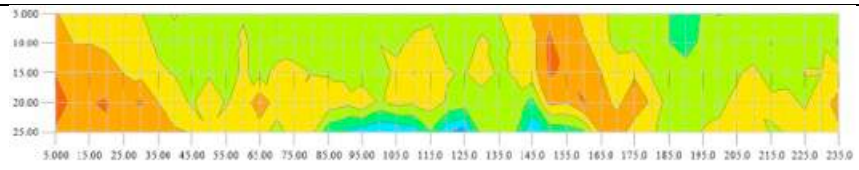
6 - months	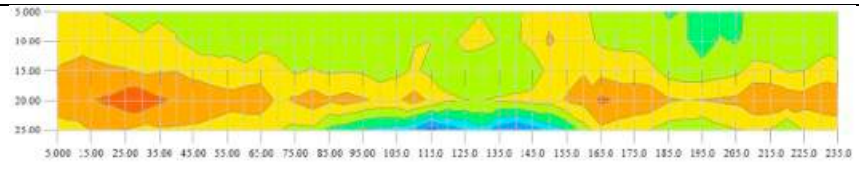
9 - months	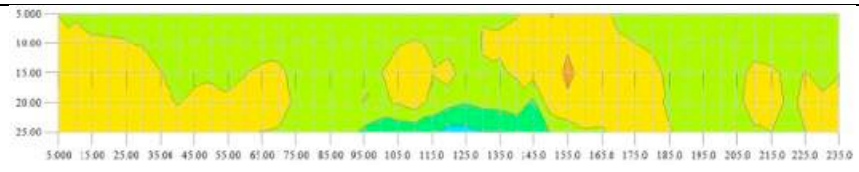
12 - months	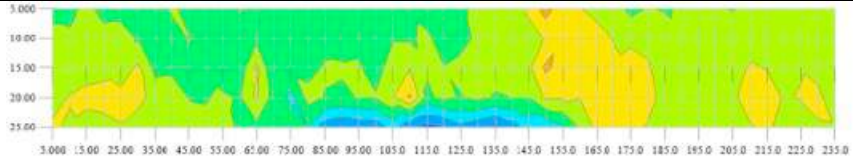
15 - months	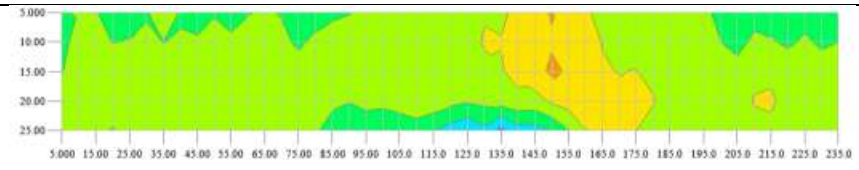
18 - months	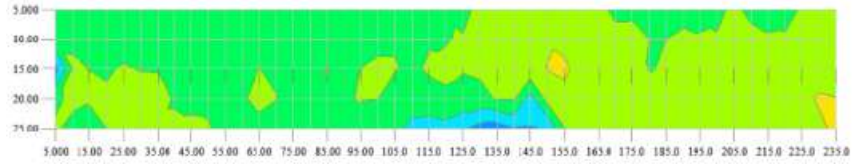
21 - months	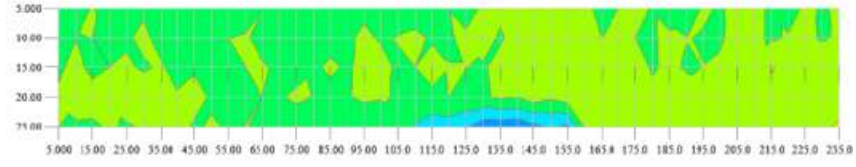

Remark:

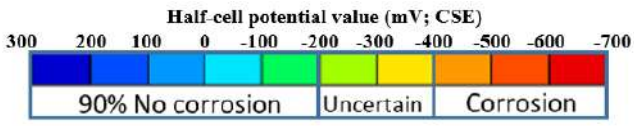

(b) Rest potential of RC-2

Figure 4.47 Rest potential development of RC-1 and RC-2

The rest potential of rebar in all cross-sectional beams was slightly more positive compared to before the repair period. It can be attributed to the generation of hydroxyl ions at the steel bar/ cement interface and repulsion of chloride ion from the vicinity of the rebar due to the application of sacrificial anodes. These secondary effects of cathodic protection cause the re-passivation effects of the rebar and move the rest potential to a more positive value (Glass and Chadwick 1994). It showed that there was no significant change of rest potentials in the patch repair section at the end of the test. Moreover, the protection improvement was shown in existing concrete due to the protective current flow of sacrificial anodes installation. The rest potential of rebar in existing concrete in RC-1 was more negative (-300 ~ -400 mV vs CSE) than RC-2 (-200 ~ -300 mV). It may be due to the lower reinforcing density of RC-1 than RC-2.

The depolarization test values show a different trend between RC-1 and RC-2. In RC-1, the protected area is decreased over time since 3-months of exposure. It because of the decreased anode performance in B2 position indicated by significantly decreasing current flow. The depolarization test value of steel bar in RC-2 presents better protection conditions due to its increasing value since initial of exposure until 21-months.

1 - month	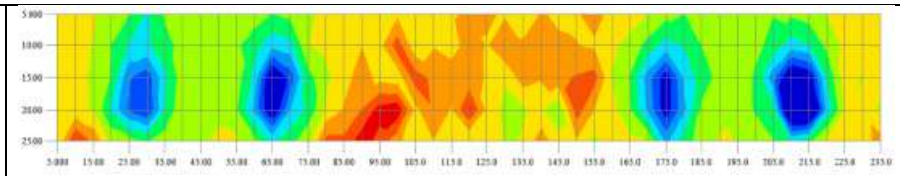
3- months	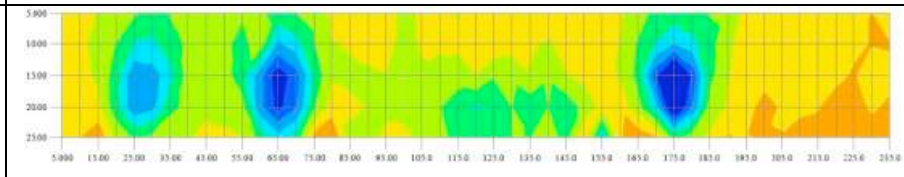
6 - months	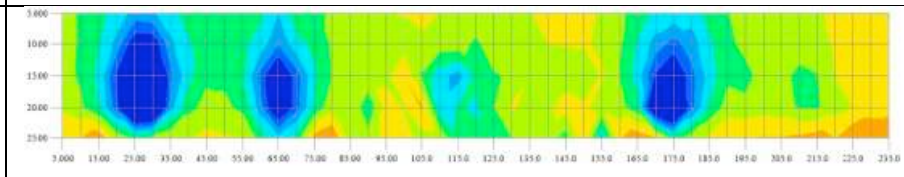
9 - months	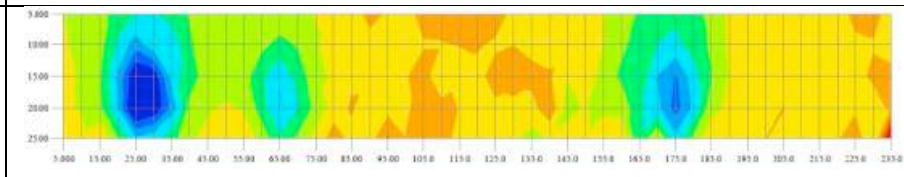
12 - months	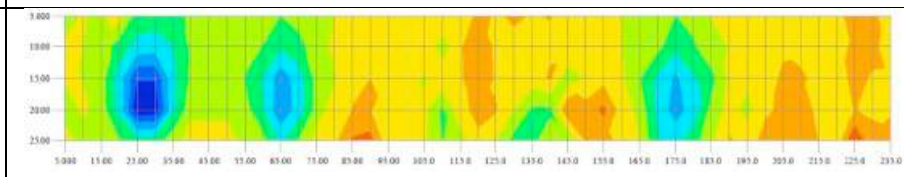
15 - months	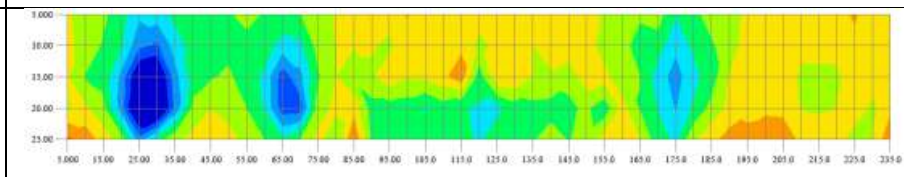
18 - months	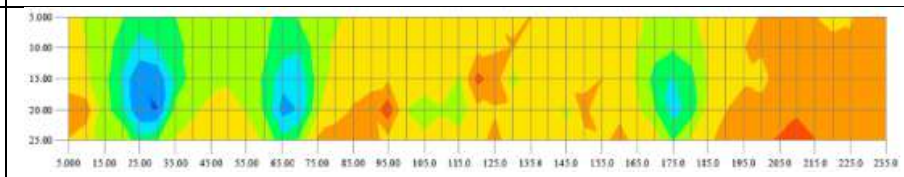
21 - months	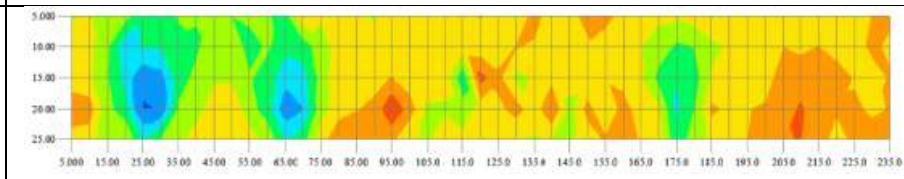

Remark:

Depolarization test value (mV)

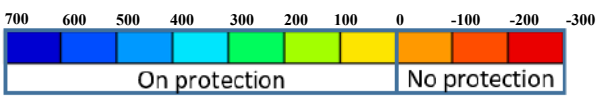

(a) Depolarization test of RC-1

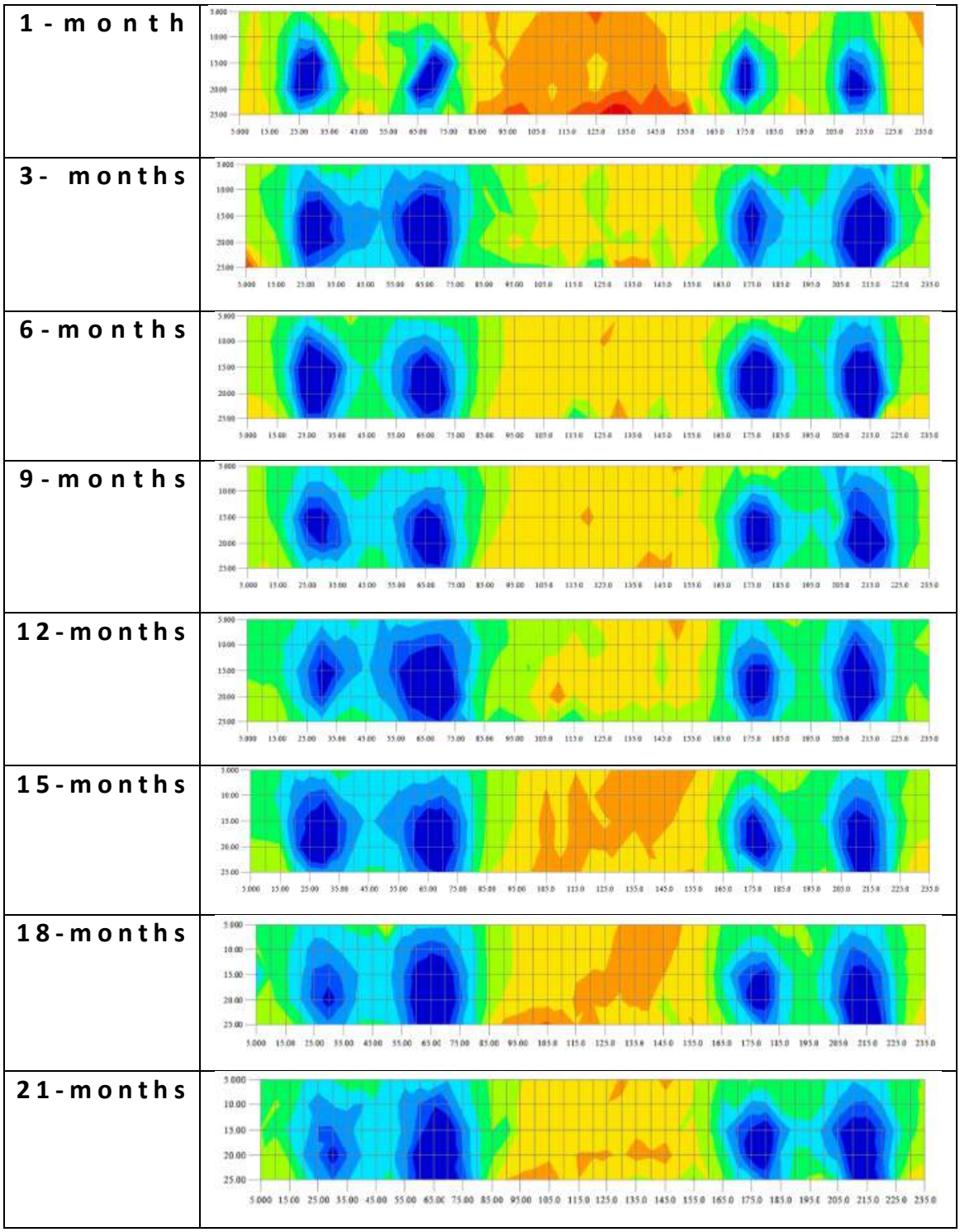

(b) RC-2

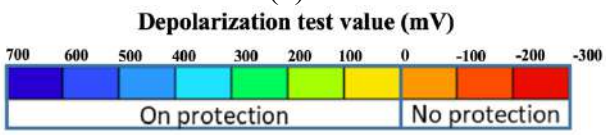

Figure 4.48 Depolarization development of RC-1 and RC-2

4.7.5 Anodic and cathodic polarization behavior of steel bar

The anodic and cathodic polarization curve of tensile and compressive steel bars of RC-1 in 15 cm, 40 cm, 80 cm, and 120 cm from the edge were presented in **Figure 4.49** and **Figure 4.50** during Stage III of repair. **Figure 4.51** and **Figure 4.52** present the anodic and cathodic polarization curve of tensile and compressive steel bars of RC-2 in 15 cm, 40 cm, 80 cm, and 120 cm from the edge. The measurement point is measured from the left edge.

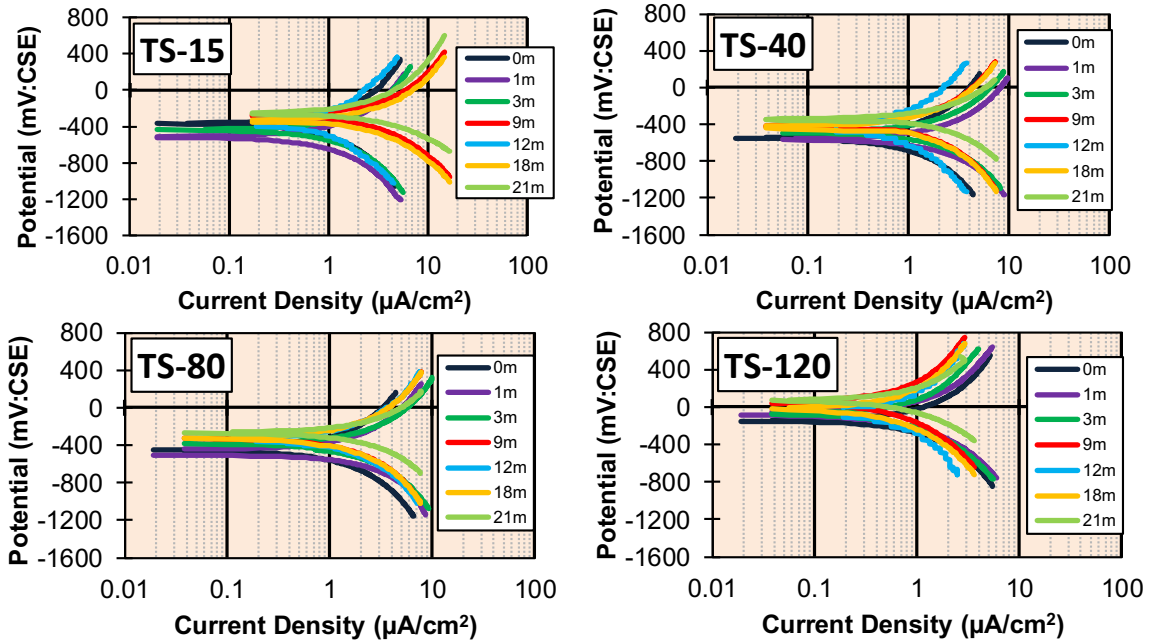

Figure 4.49 Anodic-cathodic polarization of tensile steel bar in RC-1 during Stage III of repair process

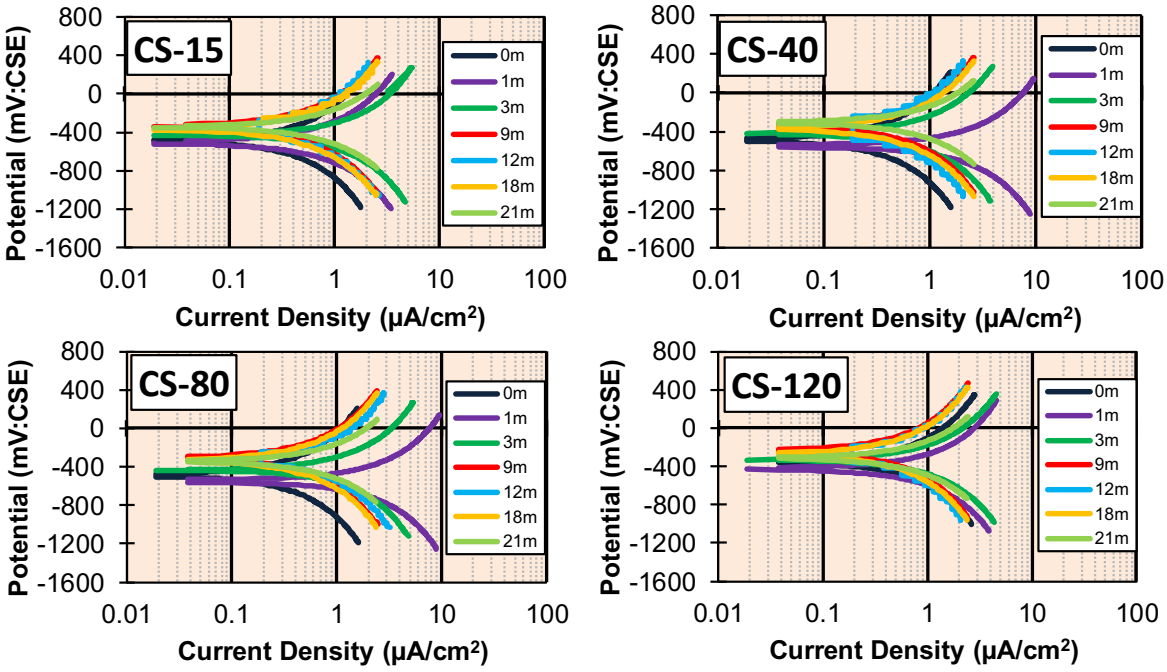

Figure 4.50 Anodic-cathodic polarization of compressive steel bar in RC-1 during Stage III of repair process

The maximum current density of steel bar measured by anodic polarization curves in tensile and compressive steel bars shows generally decrease. In the early age of exposure condition, the steel bar conditions were in Grade 3 (when 1 μA/cm^2 ≤ current density (I) < 10 μA/cm^2 between +200 mV and +600 mV (vs. SCE)) and it gradually shifts to Grade 4 (when current density (I) ≥ 1 μA/cm^2 in at least one point between +200 mV and +600 mV (vs. SCE)) until one-year of SACP application based on Otsuki *et al.* (1992).

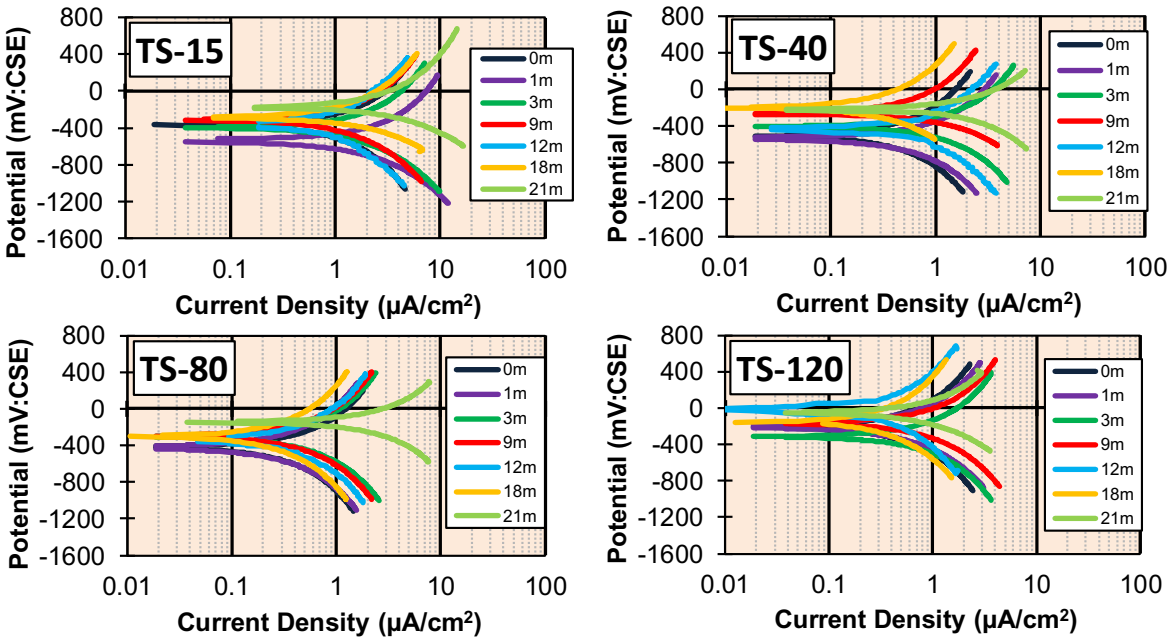

Figure 4.51 Anodic-cathodic polarization of tensile steel bar in RC-2 during Stage III of repair process

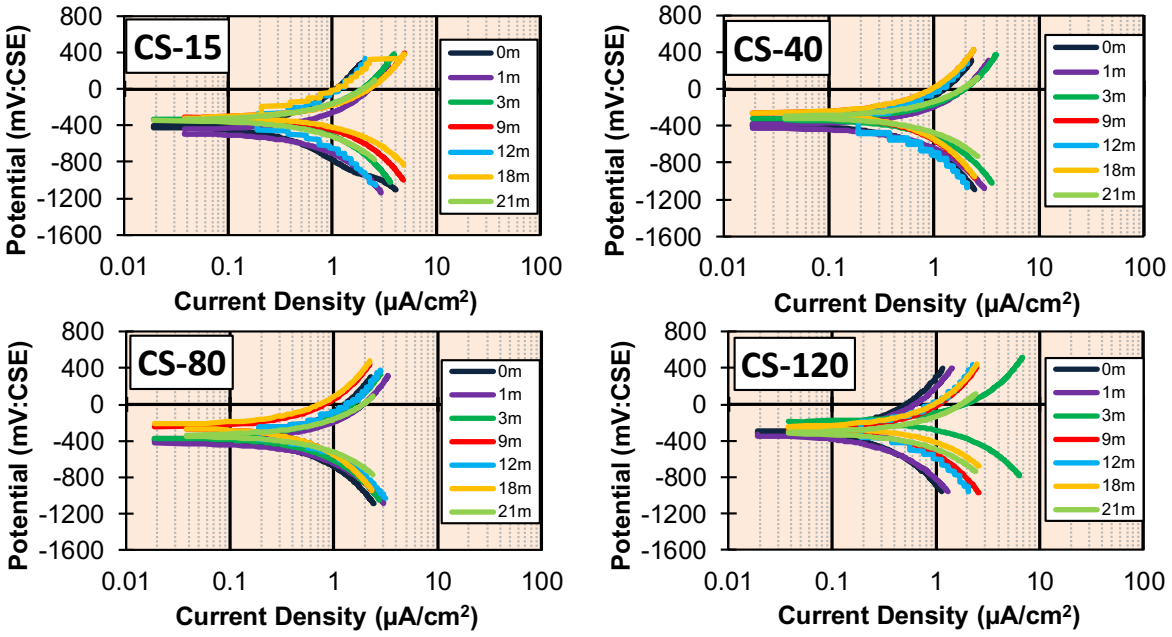

Figure 4.52 Anodic-cathodic polarization of compressive steel bar in RC-2 during Stage III of repair process

The cathodic polarization curves of these steel bars move to the right side. It indicates that the availability of oxygen O_2 is reduced during the application of current supply by sacrificial anodes. Grade 3 means some degree of passivity which is better than passivity Grade 2 meanwhile some degree of passivity which is better than passivity Grade 3 is defined as Grade 4. From the results of the anodic polarization curve in this experiment indicates that the passivity condition of steel bars increases over time. The improvement of passivity condition occurs not only in the tensile steel bars but also in the compressive steel bars. It may be caused by the stirrups connection between tensile and compressive steel bars.

4.7.6 Polarization resistance

The polarization resistance of the tensile steel bar in RC-1 and RC-2 specimens were expressed in **Figure 4.53**. In these specimens, three observation points were decided at 400 mm from the edge (non-patch repair part), 800 mm from the edge (the boundary between patch and non-patch repair for tensile steel bar only), and 1200 mm from the edge (patch repair part). The passivity limit of steel bars is 130 kΩ.cm^2 (CEB, 1998). Based on the results, the polarization resistance of the tensile steel bar at the patch and non-patch repair in both specimens can reach 130 kΩ.cm^2 after the repair process.

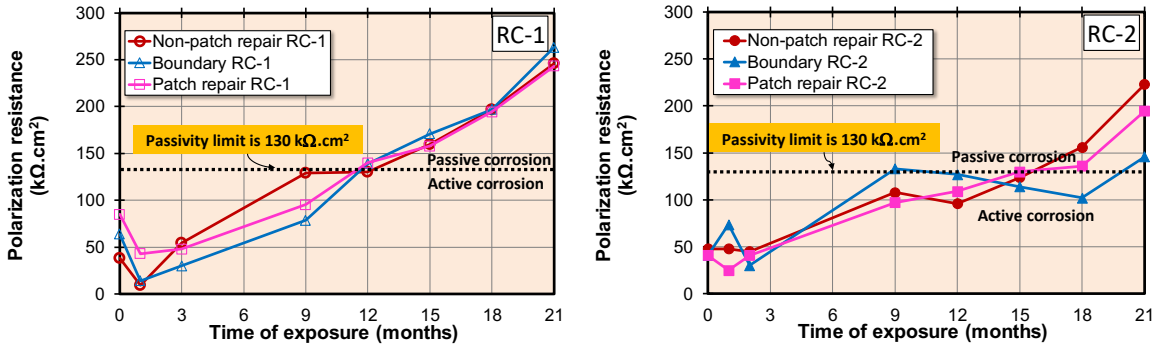

Figure 4.53 Polarization resistance of tensile steel bar in RC-1 and RC-2

4.7.7 Corrosion current density

The monitoring of corrosion current density of tensile steel bars in non-patch repair, patch repair, and boundary of a repair part is shown in **Figure 4.54** for RC-1 and RC-2. The passivity limit is generally defined as a corrosion current density of 0.1 μA/cm^2 (Andrea and Alonso, 2000).

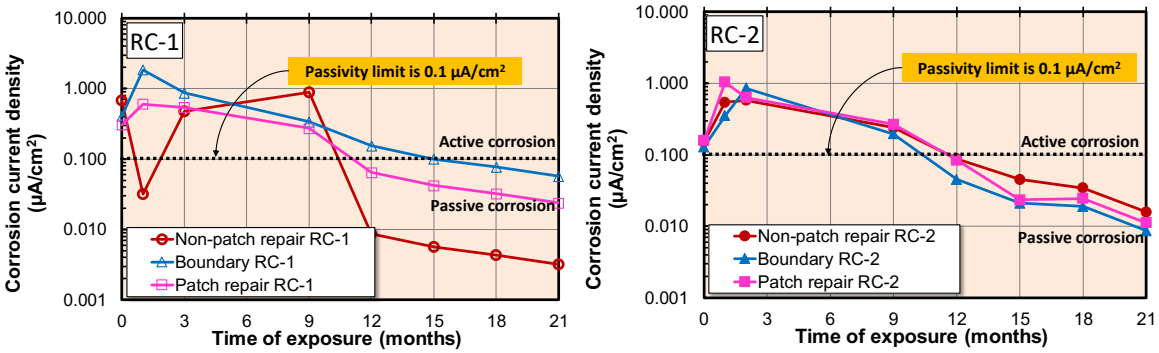

Figure 4.54 Corrosion current density of tensile steel bar in RC-1 and RC-2

The initial condition of a tensile and compressive steel bar of both specimens is active corrosion indicated by corrosion current density that exceeded the passivity limit of 0.1 µA/cm^2. After the repair methods were applied, the corrosion rate was significantly decreased. At the end of the test at 21-month, it was the passive condition. It indicates that the repair strategy of sacrificial anodes application in the patch and non-patch repair is sufficient to suppress corrosion.

4.7.8 Service life prediction of anodes in existing concrete

In order to assess the service life of sacrificial anodes, it was necessary to calculate the total mass loss of zinc material during the operational lives. In this research, theoretical predictions using Faraday's law by weighing the anodes and recording the variation of weight time dependency. **Figure 4.55** presents the cumulative charge flow from two types of specimens. It computed by converting the cumulative current flow and integrating this graph to find the area under the current flow–time graph to determine the charge passed.

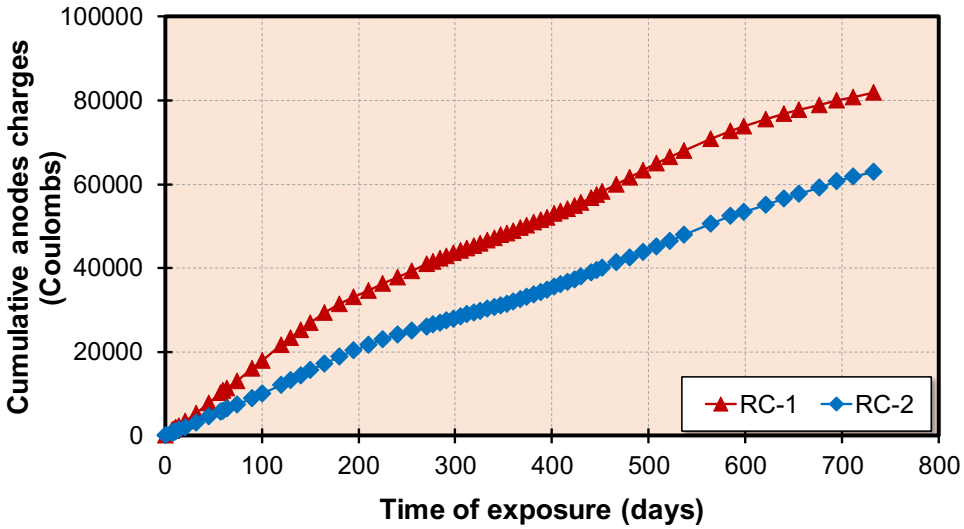

Figure 4.55 Cumulative anodes charges of RC-1 and RC-2

Based on Faraday's law, the mass loss of zinc is defined as **Equation 4.2**.

$$Mass\ Loss\ (g) = \frac{Charge\ passed\ (C)}{Faraday's\ constant\ \left(\frac{C}{mol}\right)} \times \frac{Molecular\ Mass\ of\ Zinc\ \left(\frac{g}{mol}\right)}{Valency\ of\ Zinc} \quad \textbf{(4.2)}$$

where,
Faraday's constant = 96500 Coulomb/mol
Molecular mass of zinc = 65.382 g/mol
Valency of zinc = 2

As the cumulative charges of sacrificial anodes until 732 days of operation in RC-1 and RC-2 are 81830 Coulomb and 62986 Coulomb, the substituting values in the **Equation 4.2** give a theoretical mass loss of 110.89 grams and 109.84 grams for four sacrificial anodes in each of specimen. The average initial weight of four additional sacrificial anodes installed in non-patch repair is 1667 grams. The remaining service life of anode can be predicted by **Equation 4.3**. **Table 4.5** presents the predicted service life based on the experimental rate of four anodes consumption by assuming a constant rate of consumption of anodes for the entire service life. The results show a service life prediction of 17 years and 29 years for RC-1 and RC-2 specimens after 21-months of the repair operation.

$$Service\ life\ (year) = \frac{Initial\ weight\ of\ anodes\ (g)}{Rate\ of\ consumption\ \left(\frac{g}{day}\right) \times 365} \quad \textbf{(4.3)}$$

Table 4.5 Experimental rate of four anodes consumption per day in RC-1 and RC-2

Specimens	Initial weight of four anodes (gram)	Mass loss until 732 days (gram)	Rate of consumption (gram/day)	Predicted remaining service life (year)
RC-1	1667.6	110.89	0.038	17.47
RC-2	1666.4	109.84	0.038	29.09

Dasar *et al.* (2017) reported the correlation of deterioration progress and performance degradation of the typical RC beams with initial pre-crack and without initial pre-crack until 40 years of exposure time based on recorded data on 10-years (Hamada *et al.* 1988), 20-years (Yokota *et al.* 1999a, Yokota *et al.* 1999b, Watanabe *et al.* 2001), and 40-years. The deterioration stages of structures due to corrosion involves initiation, propagation, acceleration, and deterioration period. In each stage, it performs different implications on the RC beams structures. The judgment criteria of deterioration assessment based on Yokota *et al.* 1999a are shown in **Table 4.6**.

Table 4.6 Assessment criteria of deterioration stage (Yokota *et al.* 1999a)

Evaluation Items	Deterioration Degree					
	0	1	2	3	4	5
Corrosion of reinforcing steel (X_1)	None	Rust spots found on concrete surface	Partial rust stains found on concrete surface	Significant rust staining	Significant floating rust	Dramatically increased amount of floating rust
Cracking (X_2)	None	Partial cracks found on concrete surface	Some cracks	Many cracks, including some of several millimeters or more in width	Many cracks of several millimeters in width	-
Spalling covering concrete (X_3)	None	None	Partial floating concrete found	Partial spalling found	Significant spalling	Drastic spalling

Total deterioration progress value = $X_1 + X_2 + X_3$

In this research, two RC beams without initial pre-crack were used to demonstrate the effectiveness of both of repair methods. The specimens of RC-1 and RC-2 are almost in the same deterioration degree in 41-years with no pre-crack specimens tested by Dasar *et al.* 2017. **Figure 4.56** presents the repair methods are effective to stop deterioration progress and performance degradation until 62 years and 74 years for RC-1 and RC-2, respectively. Regular monitoring of potential and current flow generated by sacrificial anodes is required until the expected of service life in these repair methods.

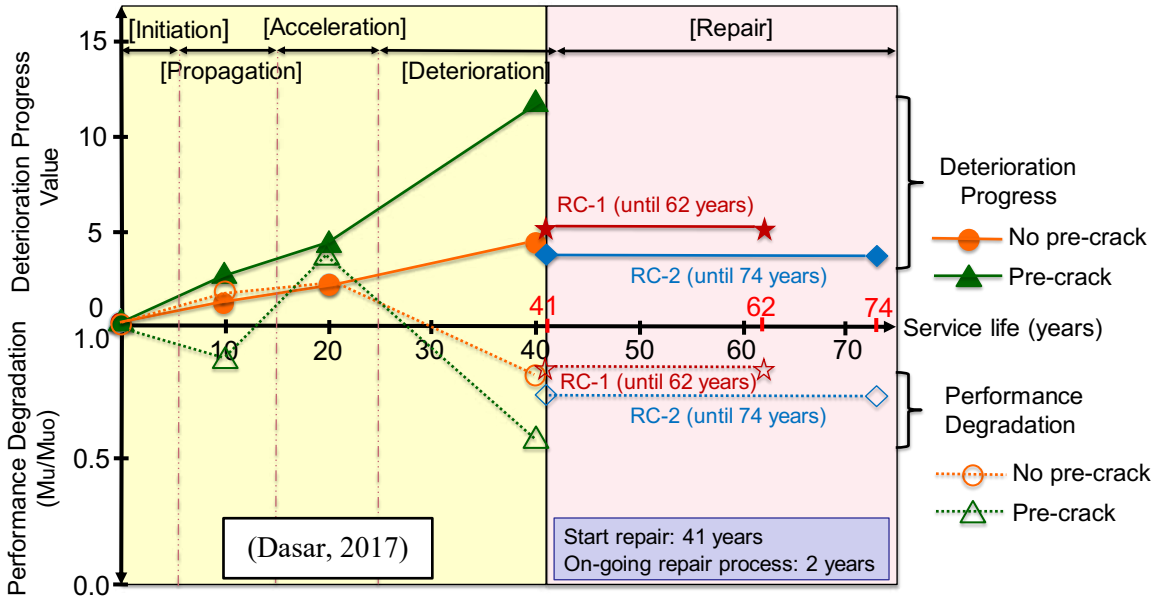

Figure 4.56 Effect of repair to the deterioration progress and performance degradation

4.7.9 Actual specimen condition after two-years of repair

The surface appearance after two years of repair by using current flow as a corrosion prevention method was conducted. Several new cracks formation were generated in the surrounding of patch repair area. The crack formation of RC-1 and RC-2 after two years of

repair are presented in **Figure 4.57** and **Figure 4.59**. It is drawn that new cracks concentrate on the new patch material. The new cracks are connected to the existing cracks in old concrete materials. It may because the macro-cell corrosion exists on the steel bars although the sacrificial anodes were installed in the patch repair for two-years before application of new anodes in non-patch repair.

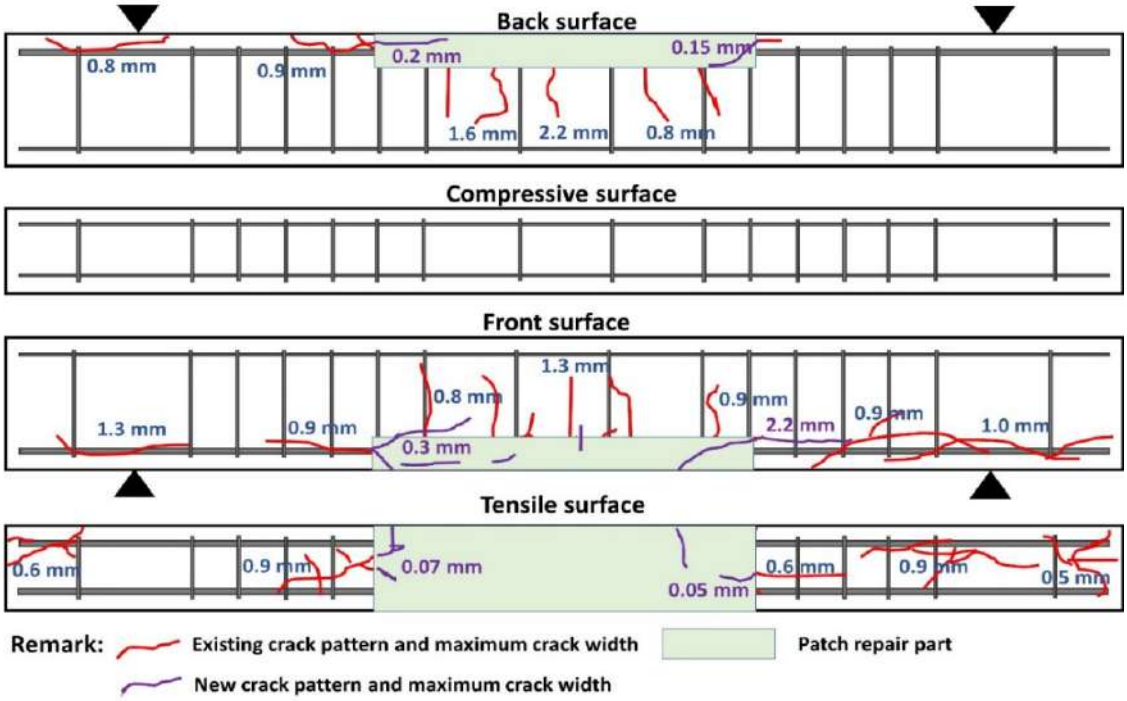

Figure 4.57 Crack formation of RC-1 after two-years of repair

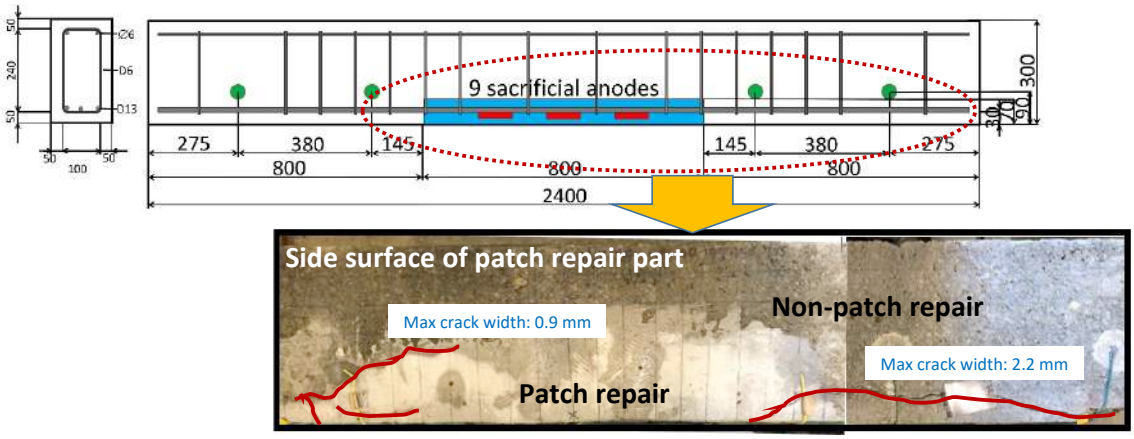

Figure 4.58 New crack formation in patch repair area of RC-1

Figure 4.58 and **Figure 4.59** show the actual picture of new crack formations in the patch repair area of RC-1 and RC-2, respectively. RC-1 presents more severe new cracks formation with 0.3 mm of maximum crack width than RC-2 with 0.2 mm of maximum crack width. This phenomenon is may due to the initial deterioration condition of the beam of RC-

1 is more severe than RC-2 indicated by larger crack width and number of cracks. Several cracks in RC-1 also form and follow the boundary pattern between patch repair and old concrete due to the imperfect new patch repair fabrication of this specimen.

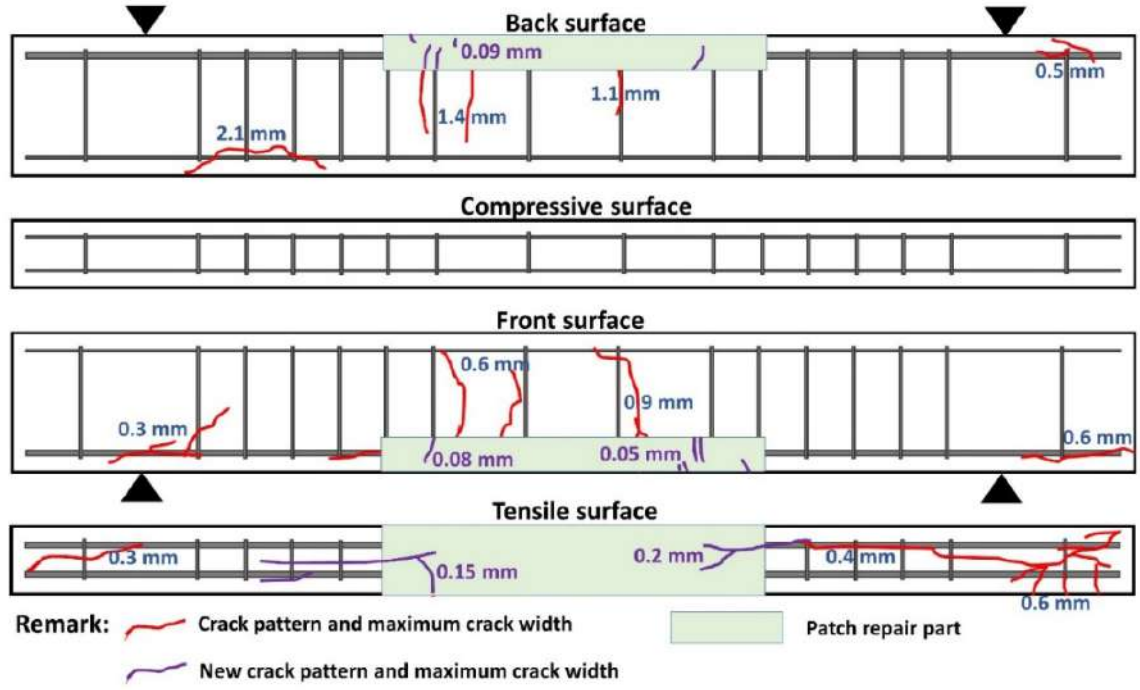

Figure 4.59 Crack formation o RC-2 after two-years of repair

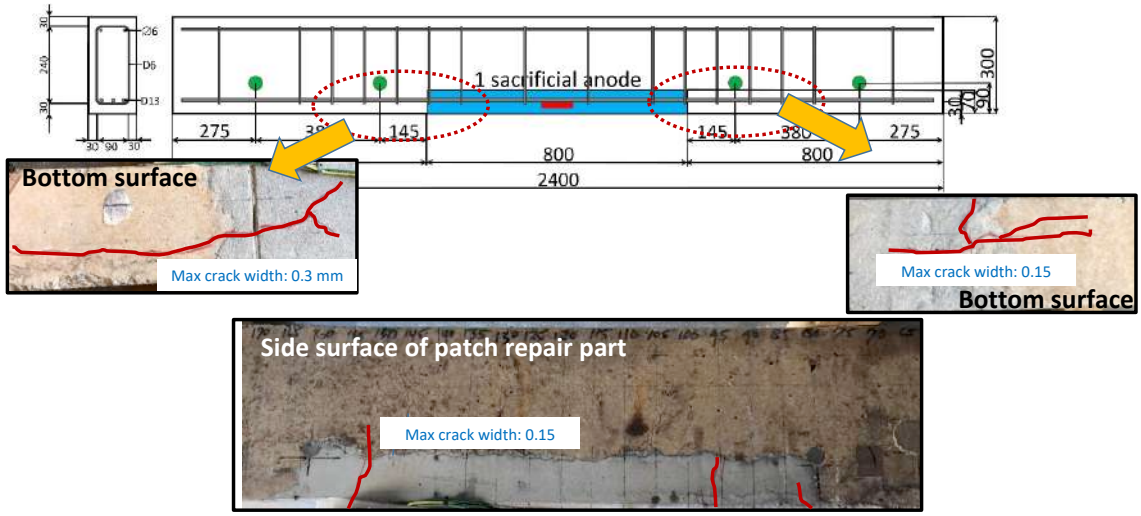

Figure 4.60 New crack formation in patch repair area of RC-2

Based on the current flow data of sacrificial anodes in the patch repair area, it demonstrated small current flow after the new additional sacrificial anodes installed in the old concrete. On the other hand, the higher current flow generated and protected the area in existing concrete. It may be caused by the new macro-cell corrosion formation in the patch area.

4.7.10 Conclusion

From this research, several conclusions are derived as follows,

1. Application of sacrificial anodes in the patch repair concrete has effectively controlled the corrosion of the rebar indicated by the rest potential shift to the noble value even though its protection cannot reach the existing concrete due to electrochemical incompatibility.
2. After a year in current interruption, the steel bar embedded in the polymer-modified mortar with chloride-free contamination has remained passive with no corrosion sign. It indicated that polymer-modified mortar has a persistent protective effect in the absence of protective current from cathodic protection.
3. Sacrificial anodes both in non-patch and patch repair concrete are sufficient to control the corrosion of rebar with an optimum distance of 400 mm.
4. After two-years of repair by additional sacrificial anodes in existing concrete, new cracks formation were observed in the patch repair area. It may be caused by the macro-cell corrosion owing to the imperfect of new patch material and the different current flow of anodes in the patch and non-patch area.
5. The service life prediction of anodes in existing concrete methods by using Fadaray's law and current flow measurement was 17 to 29 years. Therefore, it is estimated that by the repair method of this study, the lifetime of RC beams could be extended until about 70 years.

4.8 **Application of sacrificial anodes in non-patch repair and corrosion inhibitor**

Patch repair of deteriorating concrete is a common intervention to rehabilitate defecting reinforced concrete (RC) structure. Some standards suggest that the section that shows chloride concentration greater than 0.3 percent by weight of cement and half-cell potential value less than -350 mV should be removed (Christodoulou, 2008). Concrete replacement, in this case, can be costly (NACE, 2005). Sacrificial anodes have been used to limit the extent of concrete replacement and extend the service life of patch repair to RC members. They respond to the changes in the environmental conditions they are exposed to (John & Cottis, 2003; NACE, 2005; Christodoulou *et al.,* 2009). Such an effect will be more dominant in parent concrete that has a residual level of chloride contamination as opposed to non-contaminated repair concrete or mortar (Holmes *et al.,* 2011). Another practical method for control of steel corrosion in concrete is the use of corrosion inhibitors. The

curative and preventive treatments can be distinguished depending on the mode of the inhibitor application. The curative treatment consists of the application of corrosion inhibitors directly on the surface of exploited and corroding reinforced concrete structures. The preventive treatment consists in the introduction of corrosion inhibitors within mixing water to the fresh concrete. The curative corrosion inhibitor was chosen in this study as easy to use approach for application in the steel bar surface of the patch repair part (Elsener, 2001).

This sub-chapter analyzed the performance of sacrificial anodes installed within the parent concrete as opposed to the previous approach of placing sacrificial anodes within the patch repair section itself and the effect of the application of rust inhibitor in patch repair section after one-year exposure are presented. The anodes were monitored to assess their performance, and the results provide a better understanding of the corrosion mechanism in the patch and non-patch repair section and the suitable improved repair method. The detail of the specimens was presented in **Figure 4.20**. After the concrete removal process in the patch repair part, the rebar condition in the middle tensile area (patch repair section) was observed before the casting process of polymer modified mortar as shown in **Figure 4.61**.

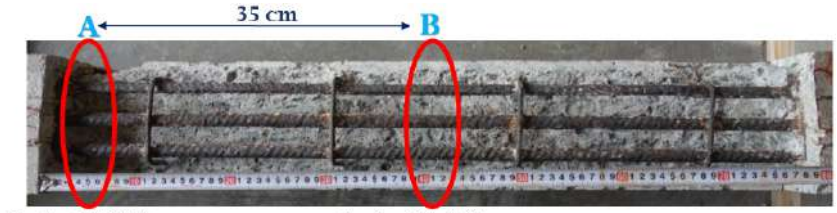

(a) RC-3

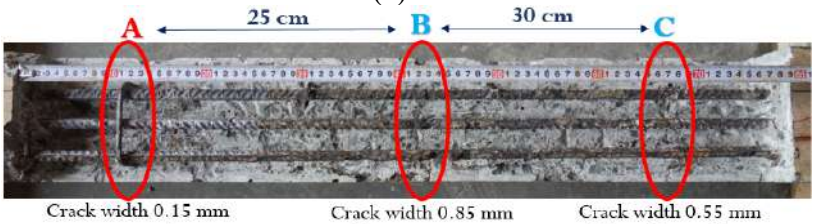

(b) RC-4

Figure 4.61 Rebar condition in the middle tensile area of (a) RC-3 and (b) RC-4

Table 4.7 Summary of crack condition on RC-4

Crack Location	Potential (mV; CSE)	Crack Width (mm)	Total Cross Section Area (mm^2)	Visual Condition
A	-262	0.15	352.8	Good
B	-377	0.85	248.1	Pitting
C	-356	0.55	339.3	Pitting

In RC-3, uniform corrosion occurred in all of the rebar surfaces and there are two points where serious corrosion was recognized at the location of the two concrete cracks at the locations (A) and (B) with 0.70 mm and 0.85 mm crack width, respectively. On the other hand, the different corrosion condition was found in RC-4. Pitting corrosion was recognized at the location of (B) and (C). However, the surface condition of the steel bar at the location of (A) is good. In this case, it is estimated that the rebar in section A is the passivated (cathode). Therefore, the galvanic corrosion might occur between two visibly separated areas. This kind of galvanic corrosion is known as macro-cell corrosion which is due to a non-homogeneity in oxygen supply, crack in the concrete, or localized chloride ion content (Qian *et al.*, 2006; Astuti *et al.,* 2018). The macro-cell is accelerated by initial pre-cracked by $0.25M_u$ applied to the RC-4 specimen before it exposed to the marine environment.

4.8.1 Protective current density

After 28 days of patch repair fabrication and anodes installation, the sacrificial anodes were connected to the steel bar. The time dependency of current flow and protective current density generated by sacrificial anodes and air temperature during the one-year observation was provided in **Figure 4.47** and **Figure 4.48** whereas one-month observation data was presented in the previous study (Astuti *et al.,* 2018; Astuti *et al.,* 2019b). It shows that both RC-3 and RC-4 have protective current density exceed the minimum design limit of cathodic protection more than 10 mA/m^2 as specified in EN 12696 (2012).

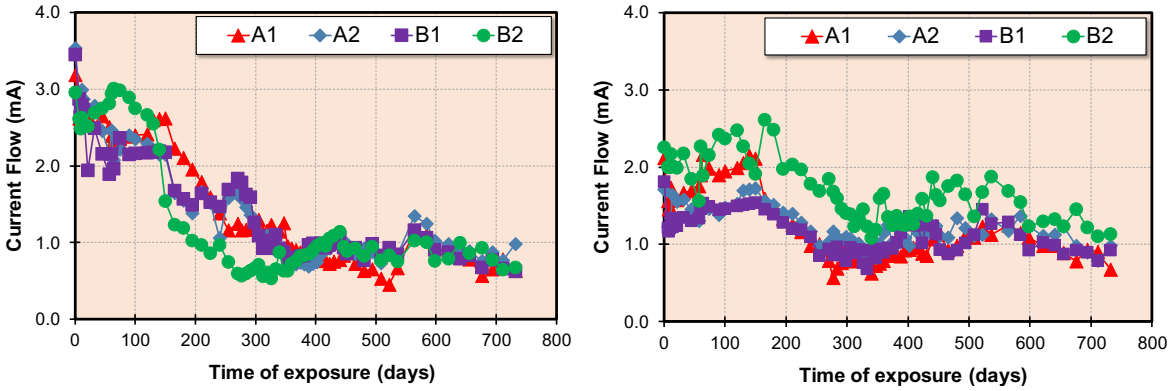

(a) RC-3 (b) RC-4

Figure 4.62 Current flow of sacrificial anodes in RC-3 and RC-4

In the first 150 days, RC-3 shows a higher protective current density than RC-4. It may be due to the difference of initial corrosion and cracking conditions indicated by higher total chloride ion concentration in RC-3 (6.05 kg/m^3) than in RC-4 (3.08 kg/m^3). Besides, the number of the crack of RC-3 is more than RC-4. This condition reveals that the current flow of sacrificial anodes changes the environmental condition around the steel bar into stable

until 150 days, and after that, the current density of both beams becomes almost the same and slightly decreases time dependency.

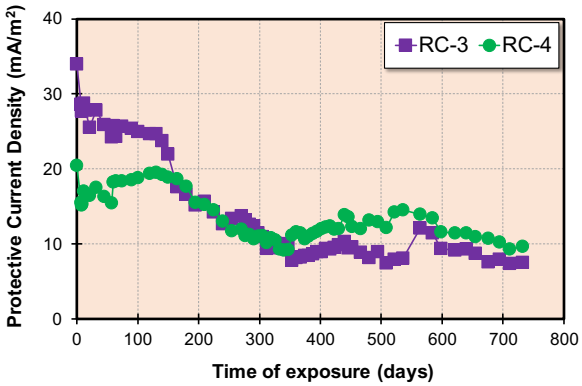

Figure 4.63 Protective current density of sacrificial anodes in RC 3 and 4

4.8.2 Potential development of sacrificial anodes

The instant-off potential of sacrificial anodes in RC-3 and RC-4 was presented in **Figure 4.64**. In RC-3, the instant-off potential of sacrificial anodes in early connection is around -850 mV ~ -500 mV then, it gradually decreases into around -1200 mV. After 100-days of exposure, it increases to -700 mV ~ -500 mV and it becomes stable until 18-months. The sacrificial anodes in RC-4 is continuously shift to noble value from -1500 mV ~ -900 mV at initial condition until -900 mV ~ -600 mV at 18-months of exposure.

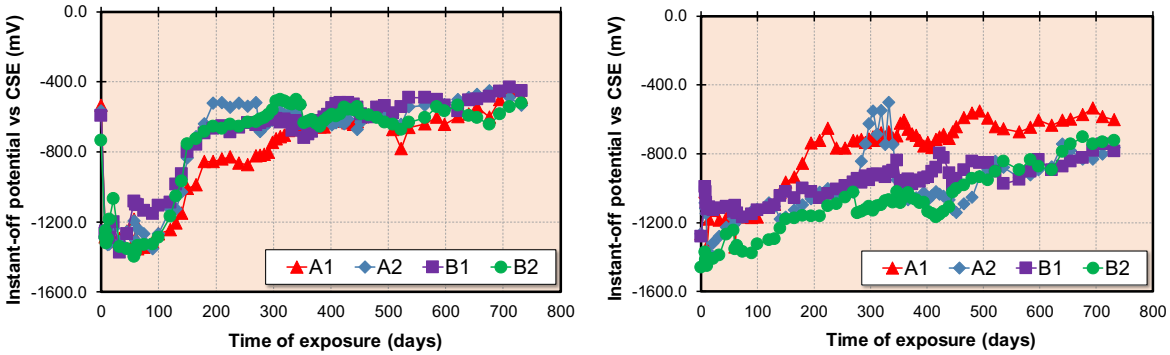

(a) RC-3 (b) RC-4

Figure 4.64 Instant-off potential of sacrificial anodes in RC-3 and RC-4

4.8.3 Anodic polarization behavior of anodes

The anodic polarization curve of sacrificial anodes in RC-3 and RC-4 was presented in **Figure 4.65** and **Figure 4.66**, respectively.

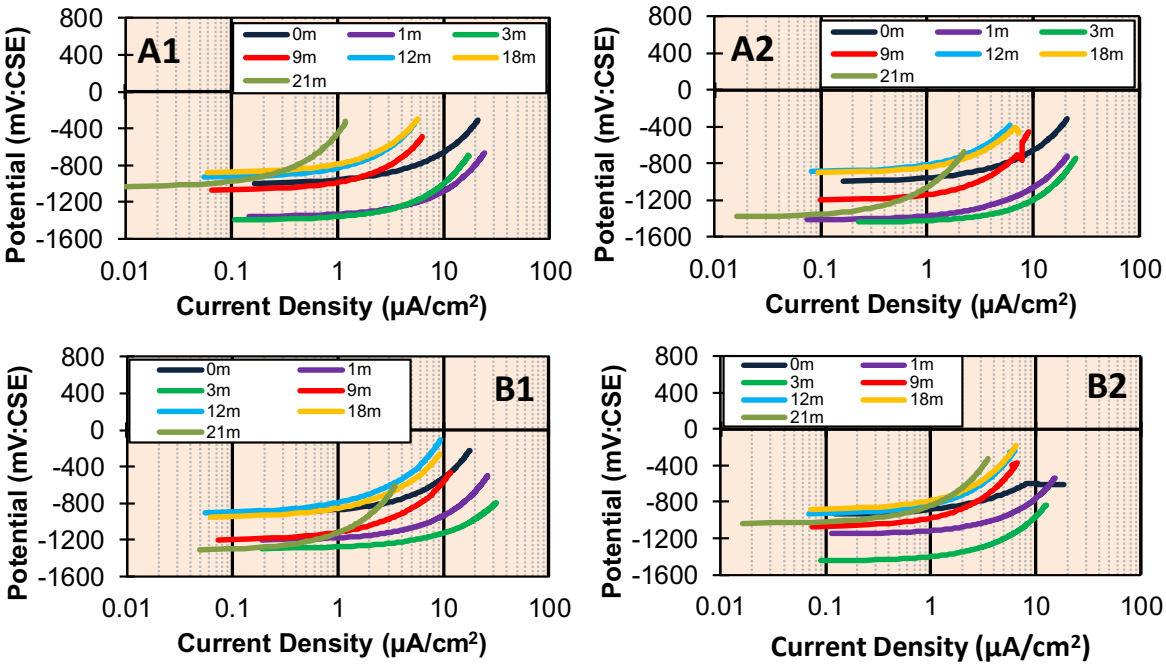

Figure 4.65 Anodic polarization curve of sacrificial anodes in RC-3

Generally, it can be seen that the trend of anodic polarization curve of anodes moves to the left sides. It indicates that the reduction of maximum current density occurs time-dependently. It confirms that the protective current density generated by each sacrificial anodes decreased. The lower current density produced by anodes the longer its service life. It may be caused by the current density of anodes change the environmental conditions of surrounding steel bars so the required current flow by anodes decreases over time.

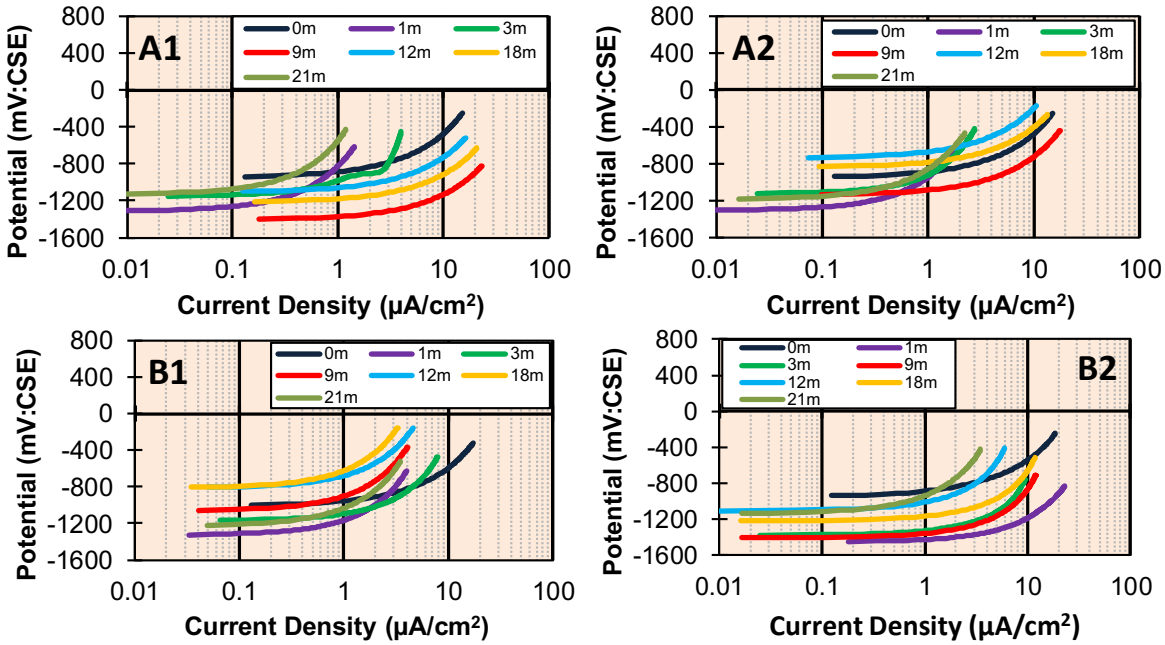

Figure 4.66 Anodic polarization curve of sacrificial anodes in RC-4

4.8.4 Potential development of steel bar

In order to access the performance of sacrificial anode cathodic protection, the potential of rebar and sacrificial anodes during connection (on potential), immediately after disconnection (instant-off potential), and half-cell potential after 24-hours of disconnection (rest potential) were recorded. The obtained on and instant-off potential values of all sacrificial anodes in RC-3 and RC-4 are -1400 mV~-1000 mV during 0 days until 120 days and it shifted to noble value around -1000 mV~-600 mV after 18-months whereas the rest potential of anodes is around -1400 mV ~ -1000 mV. On and instant-off potential of rebar shows that the sacrificial anodes affected the potentials to a distance of approximately 200 mm from the anode position until 21-months of observation.

The time-dependent trends of the polarization effects of tensile rebar afforded by the distance of the sacrificial anode away from the edge of the beams were monitored in **Figure 4.67** and **Figure 4.68**. The rest potential showed that the time dependency of rest potential of rebar shifted to noble value in RC-4. However, it was not significantly changed in RC-3. The depolarization test of rebar was checked 24 hours after the disconnection of sacrificial anodes. The difference value calculated between instant-off and rest potential. Normally, the potential decay criterion of 100 mV is adopted for assessing the performance of cathodic protection. The depolarization test values after 1, 3, 9, 12, 18, and 21 months of exposure were illustrated. It shows that the depolarization test value of rebar in parent concrete of both specimens can exceed 100 mV. It indicated that sacrificial anodes are effective to stop corrosion in chloride contaminated concrete. However, the depolarization is limited in patch repair due to the difference in material properties between the patch and non-patch repair. The application of corrosion inhibitor in RC-4 demonstrated higher depolarization than in RC-3. There was no significant effect of corrosion inhibitor in the early age of repair but it gradually increased time-dependently. After 18 months of rehabilitation, the depolarization test value of rebar in patch repair with corrosion inhibitor can reach 100 mV.

This study investigated the performance of sacrificial anodes installed in parent concrete on two identical RC beams damaged by corrosion and corrosion inhibitor applied for rebar surface in patch repair section in one of the specimens. Monitoring was performed by close interval relative potential mapping in the concrete surface to verify that sacrificial anodes were still active, and at staged distances away from the position of the anode to assess the polarization effect afforded by the sacrificial anodes to the steel in the parent concrete and patch repair.

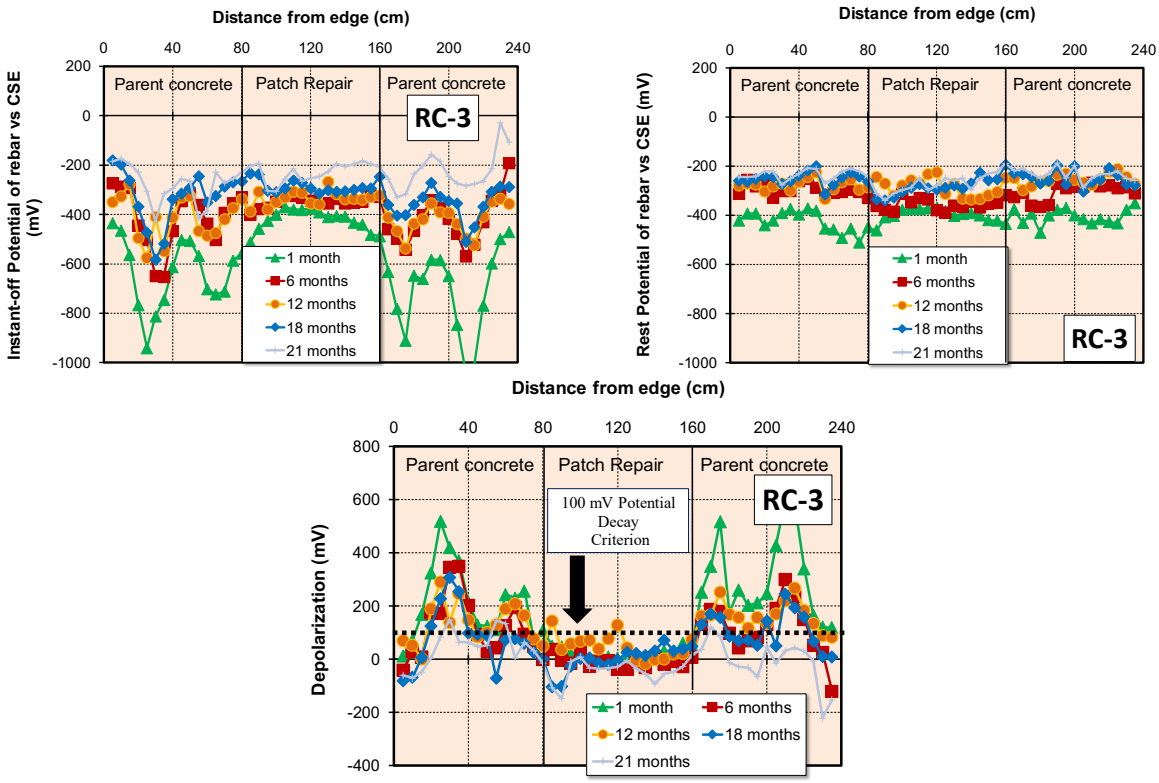

Figure 4.67 Potential development of tensile steel bar in RC-3

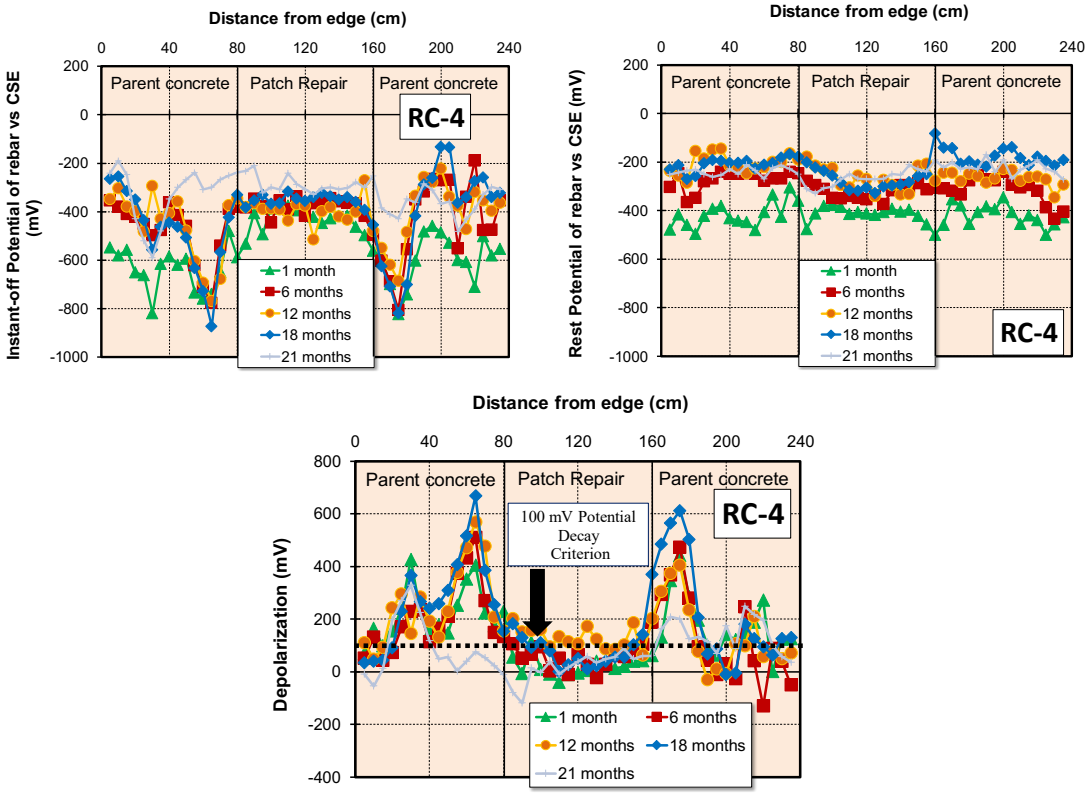

Figure 4.68 Potential development of tensile steel bar in RC-4

The performance monitoring data indicates that the sacrificial anodes affected rebar potentials concentrically in parent concrete at a distance away from the position of the

anodes. The corrosion and protection mapping of the RC-3 and RC-4 specimens were presented in **Figure 4.69** and **Figure 4.70**.

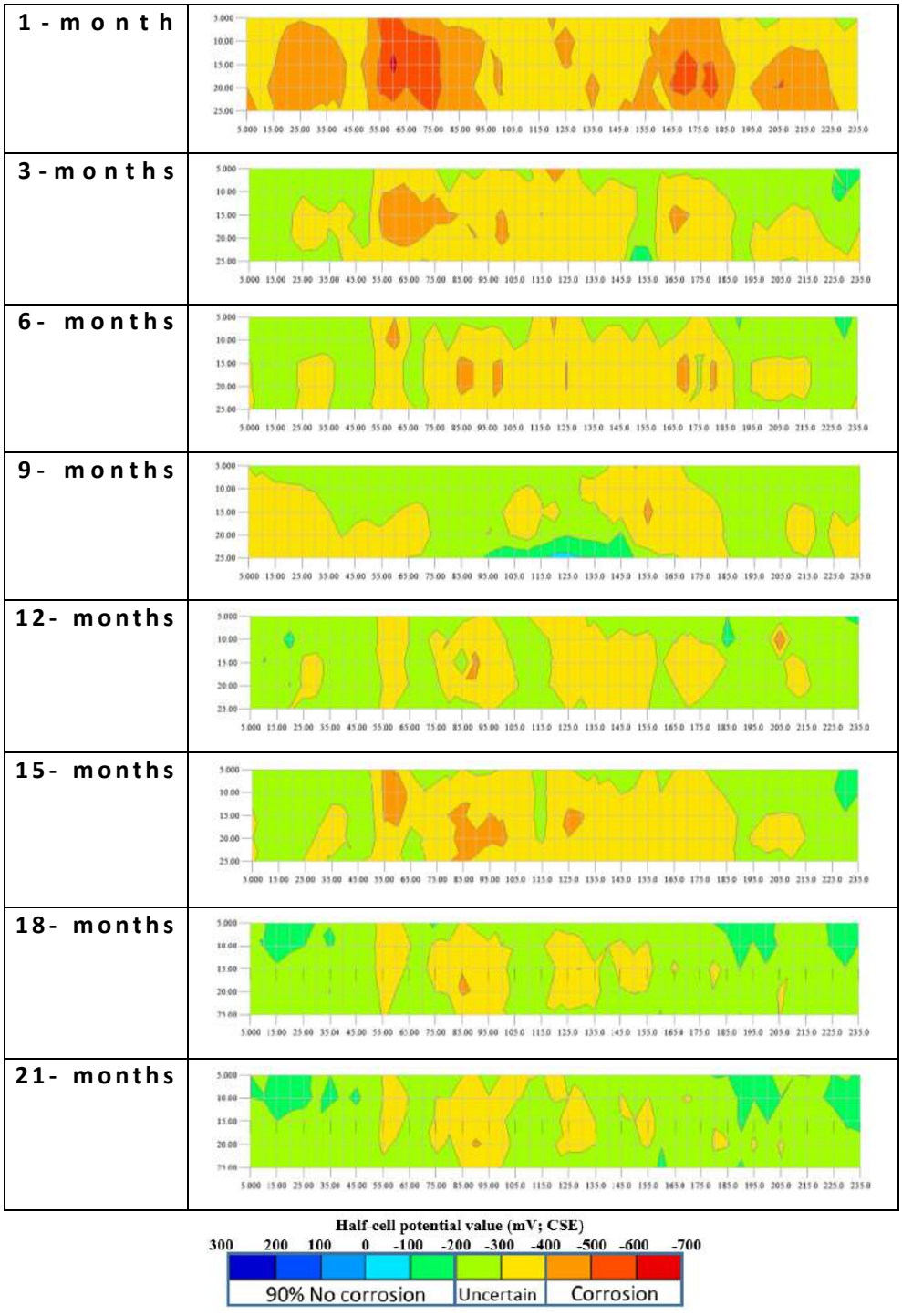

Figure 4.69 Corrosion map development of RC-3 during repair process

The rest potential as corrosion mapping shows that RC-4 performs better potential recovery since 1-month of repair. Protection mapping specified by the depolarization test value also reveals the same trend. For RC-3, with patch repair only, the polarization effect was to a distance of approximately 15 cm away from the position of the anodes. For RC-4,

with corrosion inhibitor in patch repair, the polarization effect afforded was increased to approximately 30 cm from anodes position. It indicates that sacrificial anodes have limitations, and the existence of a corrosion inhibitor extends the polarization of rebar. The corrosion inhibitor membrane reduced the required electric current for attaining the potential change in patch repair.

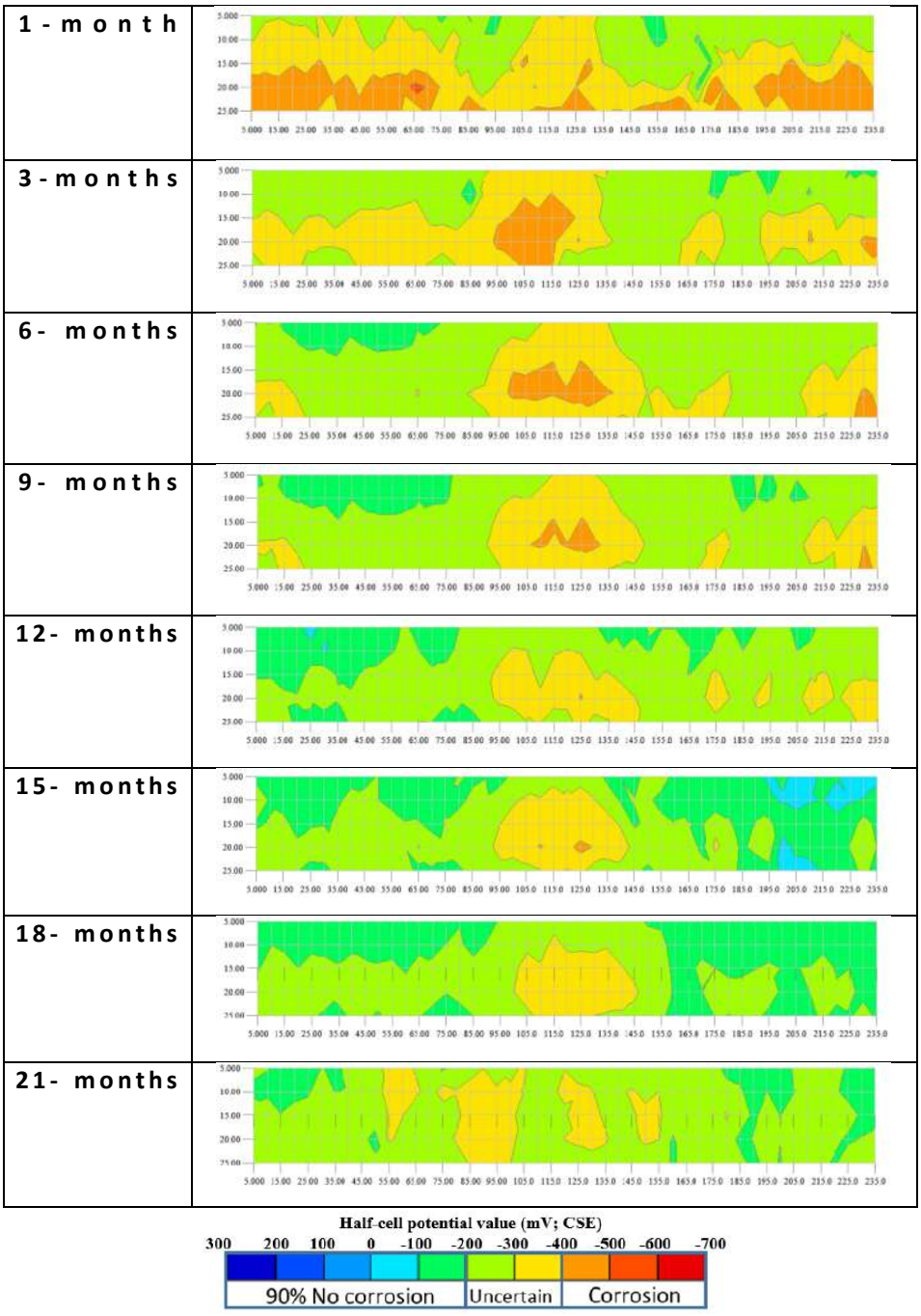

Figure 4.70 Corrosion map development of RC-4 during repair process

The depolarization map development of RC-3 and RC-4 were presented in **Figure 4.71** and **Figure 4.72**. An alternative performance criterion, to that of 100 mV potential decay,

may be adopted for assessing the performance of sacrificial anodes system utilizing potential mapping to obtain the spatial variations. Sacrificial anodes in parent concrete should demonstrate that it affords a dominant influence on the rebar potentials away from the position of the anode that is at least equal to half the spacing between anodes position. This alternative criterion is also in line with the work of previous researchers' works (Holmes *et al.,* 2011; Cristodoulou *et al.,* 2014).

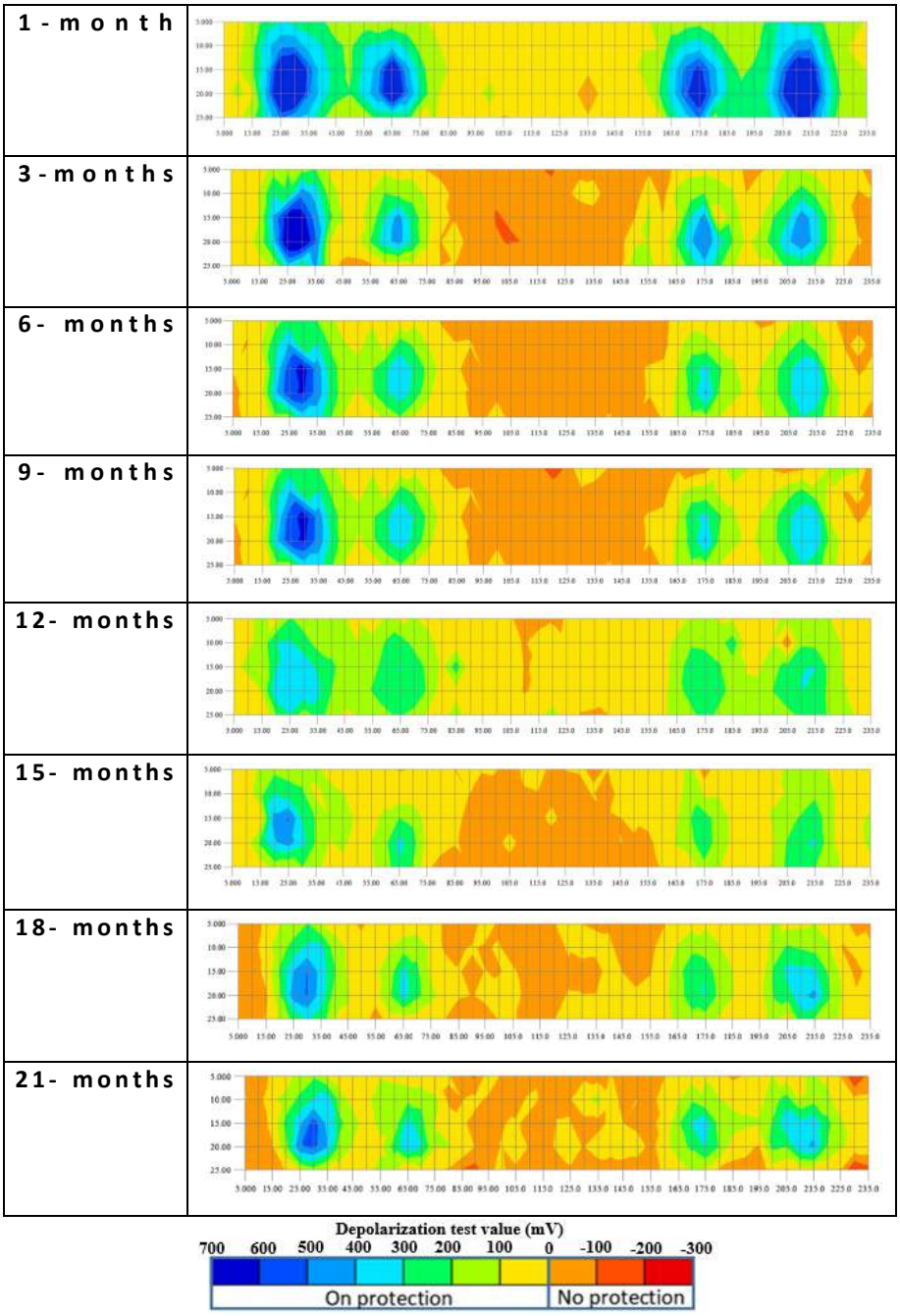

Figure 4.71 Depolarization map development of RC-3 during repair process

Standard for structural repairs as BS EN 1504 (2015) confirms that patch repair materials such as polymer modified mortar did not affect the performance of sacrificial anodes

installed in parent concrete around of repair, although it is not generally considered suitable for together usage with sacrificial anodes due to its high resistivity (BS EN ISO 12696,2012). In the contrary, such materials will improve the quality and longevity of the repair itself, and due to its higher resistivity will preferentially direct current from sacrificial anodes to rebar in parent concrete, which is considered to be at higher risk (Cristodoulou *et al.*, 2014).

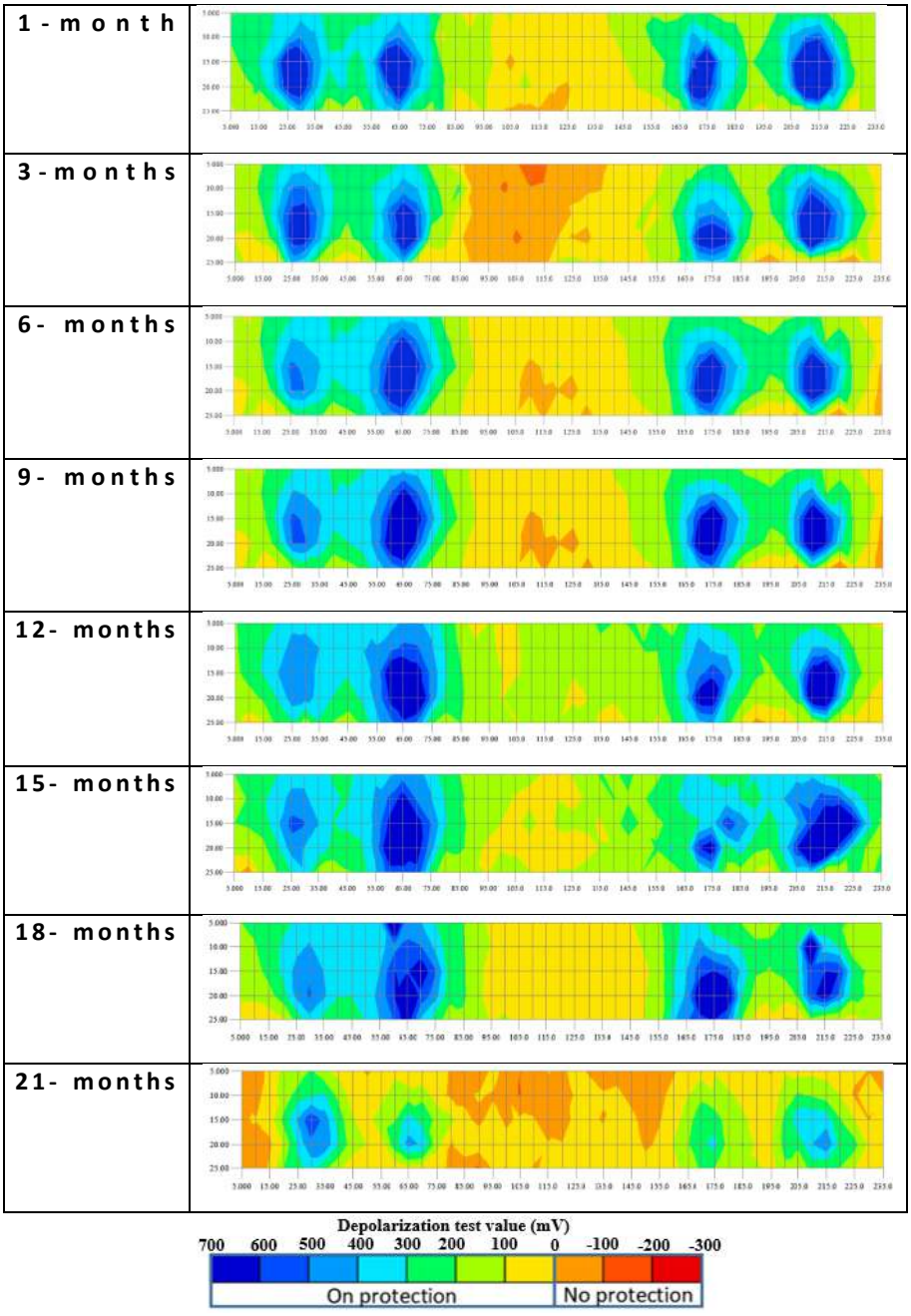

Figure 4.72 Depolarization map development of RC-4 during repair process

4.8.5 Anodic and cathodic polarization behavior of steel bar

The passivity degree of rebar is one indicator to understand the performance of the repair method. A systematic way to evaluate the passivity degree of rebar provided by rebar can be

presented by using the grading criteria for passivity (Otsuki *et al.,* 1992). The criteria were based on the behavior of the anodic polarization curves of rebar. The degree of passivity was presented as different grades depending on how the current densities behaved between +200 mV and +600 mV (vs. SCE) potential on the anodic polarization curve. When the anodic curve towards a lower current density region, the passivity degree of rebar tends to a better condition. Another corrosion performance parameter is the concentration of oxygen in the corrosion process, especially illustrating the reduction in oxygen content shifts the cathodic curve to lower current densities over a wide range of potentials. The Anodic and cathodic polarization curve time dependency of tensile and compressive rebars in parent concrete, patch repair, and the boundary between parent concrete and patch repair at 150 mm, 400 mm, 800 mm, and 1200 mm from the edge were depicted in **Figure 4.73** and **Figure 4.74**.

Generally, the maximum current density of rebars was decreased in both of two repaired specimens. At the end of the test, the passivity condition was categorized as grade 3 (current density are between 1 and 10 μA/m^2), which indicates a certain degree of passivity exist. During 18-months of exposure, RC-4 (specimen with a corrosion inhibitor in patch repair) demonstrated better performance indicated by greater shift of anodic polarization curve than RC-3 (specimen without corrosion inhibitor). It shows that the application of corrosion inhibitor in patch repair part of RC-4 delivers the polarization effect of sacrificial anodes from parent concrete to patch repair section.

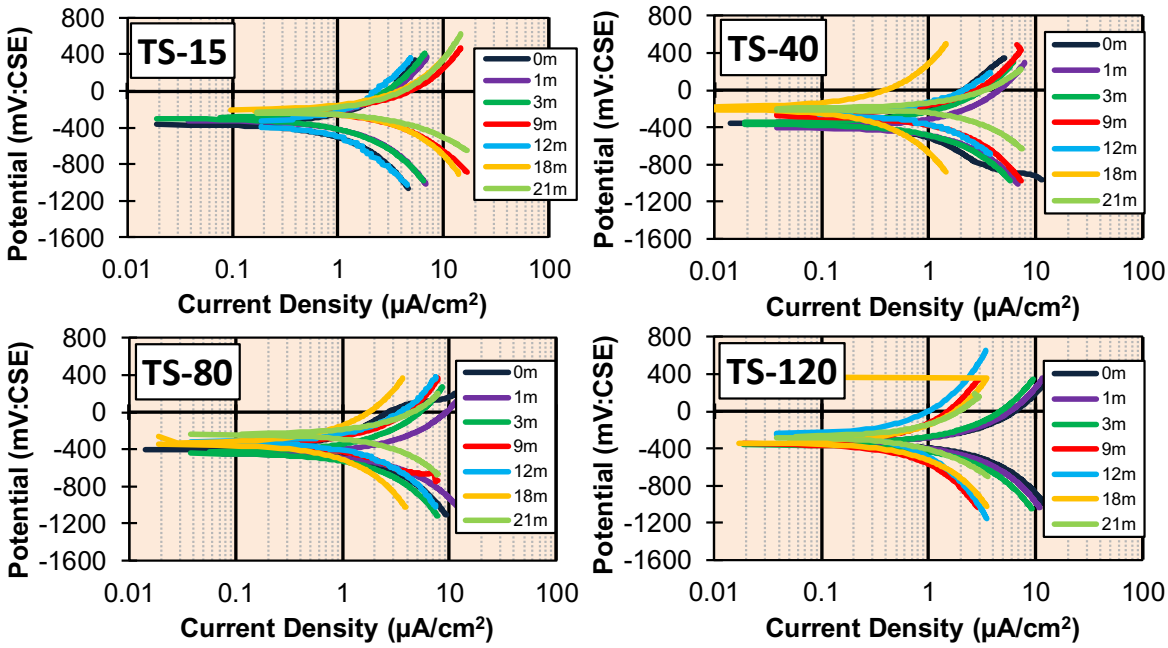

Figure 4.73 Anodic-cathodic polarization of tensile steel bar in RC-3

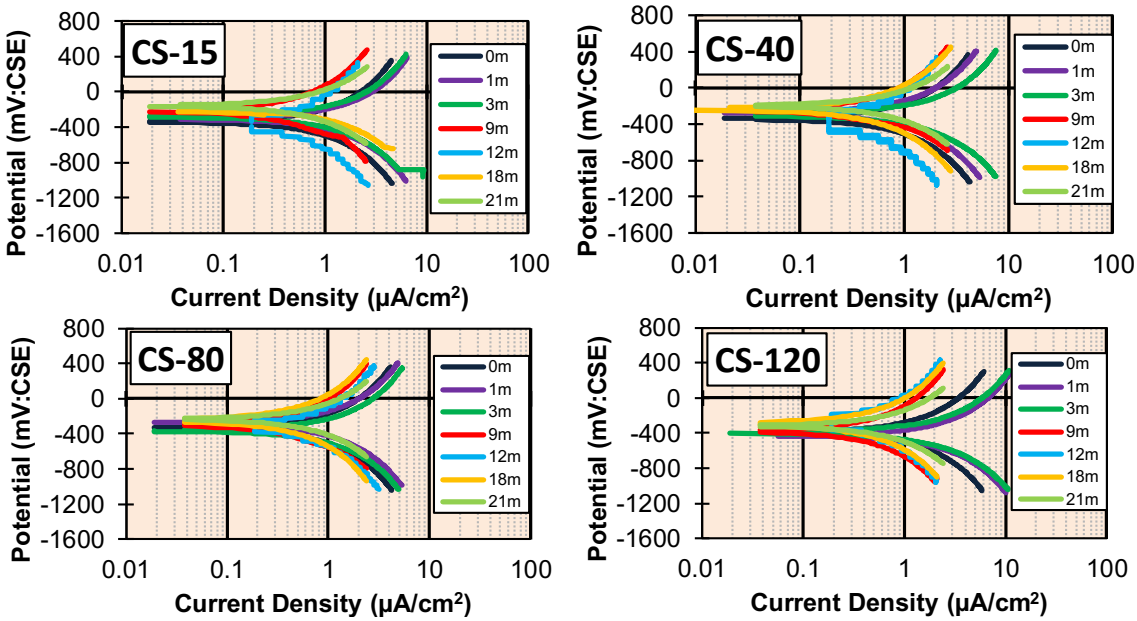

Figure 4.74 Anodic-cathodic polarization of compressive steel bar in RC-3

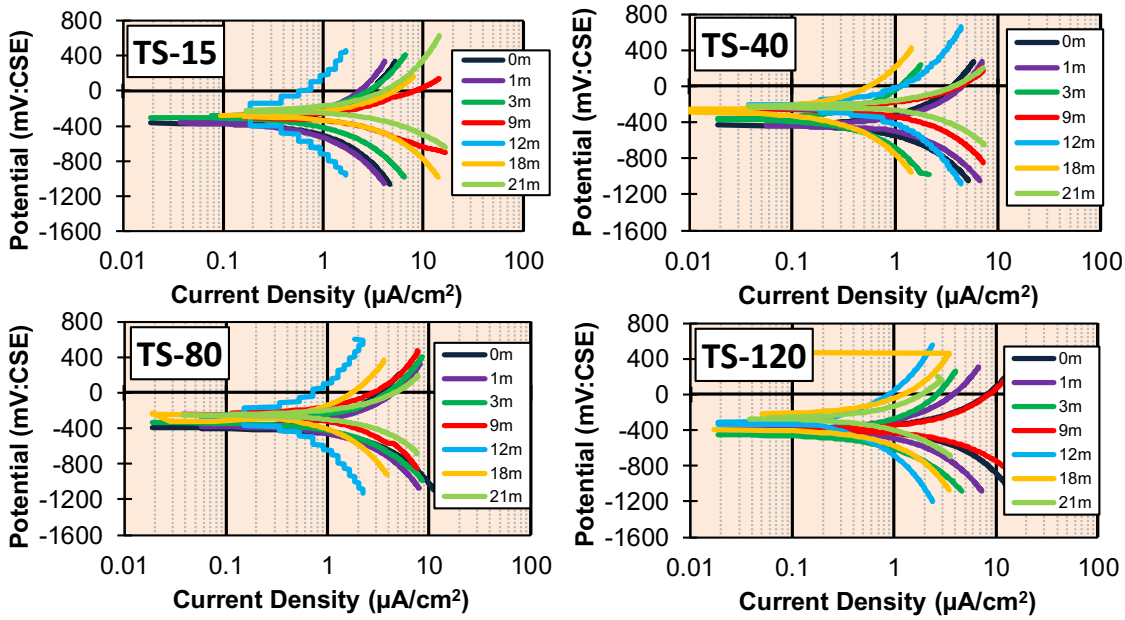

Figure 4.75 Anodic-cathodic polarization of tensile steel bar in RC-4

4.8.6 Polarization resistance

The polarization resistance of the tensile steel bar in RC-3 and RC-4 was depicted in **Figure 4.77**. Generally, the results show that the polarization resistance of tensile steel bars increases both RC-3 and RC-4. But, the existence of corrosion inhibitor applied for steel bar surface in patch repair at RC-4 performs better polarization resistance. The passivity limit of polarization resistance is 130 kΩ.cm^2 based on CED (1992).

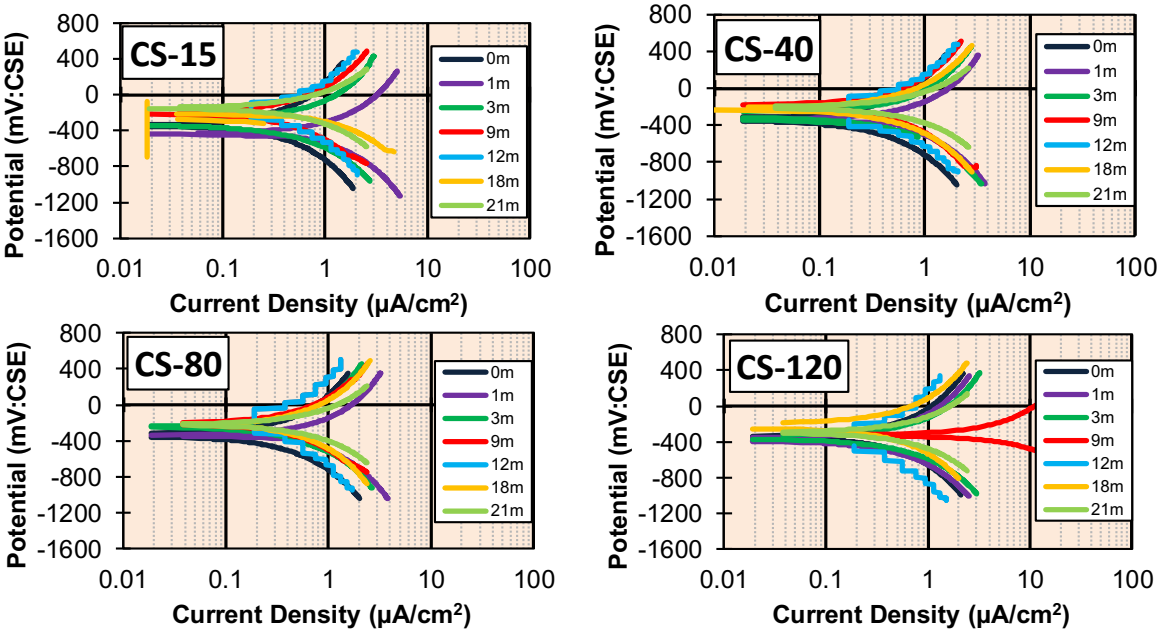

Figure 4.76 Anodic-cathodic polarization of compressive steel bar in RC-4

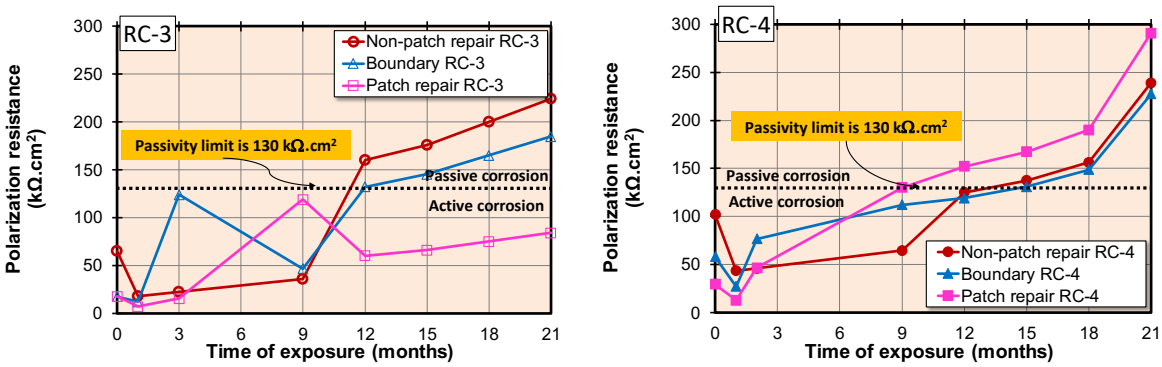

Figure 4.77 Polarization resistance of tensile steel bar in RC-3 and RC-4

4.8.7 Corrosion current density

The monitoring of corrosion current density of rebar in non-patch repair, patch repair, and boundary of a repair part of RC-3 and RC-4 is shown in **Figure 4.78**. The passivity limit is generally defined as a corrosion current density of 0.1 μA/cm^2 (CEB, 1998).

The initial condition of the rebar of both specimens is active corrosion indicated by corrosion current density that exceeded the passivity limit of 0.1 μA/cm^2. After the repair methods were applied, the corrosion rate was significantly decreased. After 21-month of exposure, it was the passive condition. It indicates that the repair strategy of patch repair and corrosion inhibitor is sufficient to suppress corrosion.

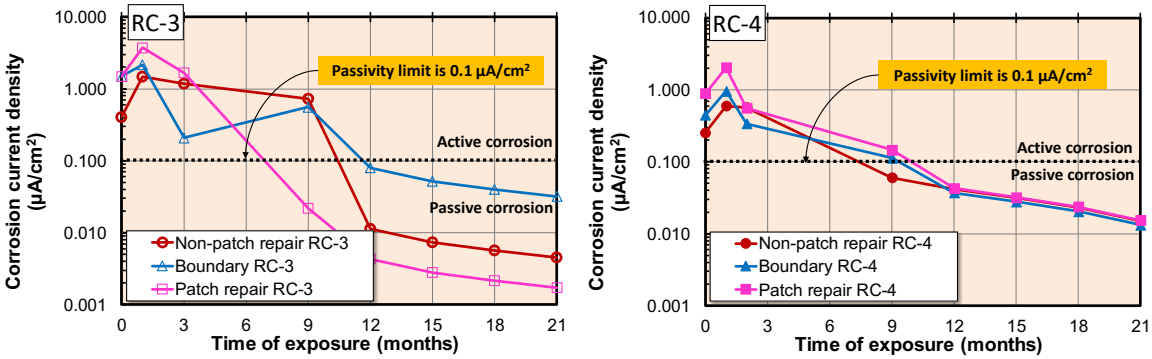

Figure 4.78 Corrosion current density of tensile steel bar in RC-3 and RC-4

4.8.8 Service life prediction of anodes in existing concrete

In order to assess the service life of sacrificial anodes, it was necessary to calculate the total mass loss of zinc material during the operational lives. In this research, theoretical predictions using Faraday's law by weighing the anodes and recording the variation of weight time dependency. **Figure 4.55** presents the cumulative charges flow from two types of specimens. It computed by converting the cumulative current flow and integrating this graph to find the area under the current flow–time graph to determine the charge passed. Based on Faraday's law, the mass loss of zinc is defined as **Equation 4.2**.

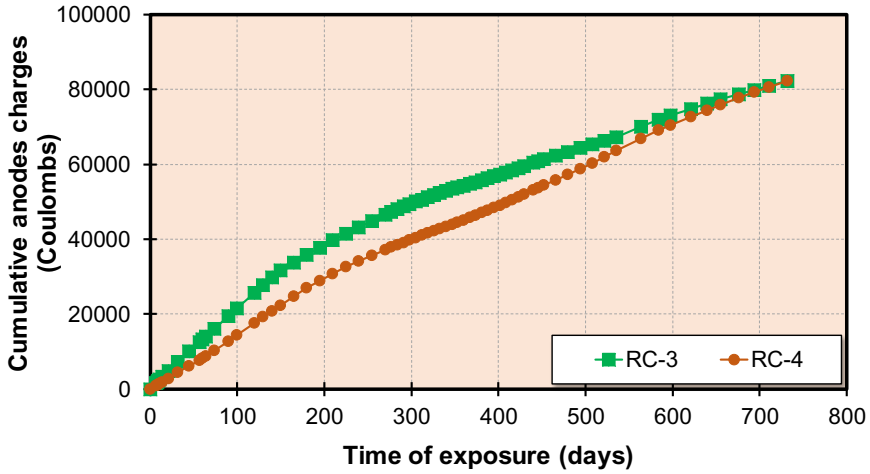

Figure 4.79 Cumulative anodes charges of RC3 and RC-4

As the cumulative charge for sacrificial anodes until 732 days of operation in RC-3 and RC-4 are 82216 Coulomb and 82261 Coulomb, the substituting values in the **Equation 4.2** give a theoretical mass loss of 111.41 grams and 111.47 grams for four sacrificial anodes in each of specimen. The average initial weight of four additional sacrificial anodes installed in non-patch repair is 1667 grams. The remaining service life of anode can be predicted by **Equation 4.3**. Error! Reference source not found. presents the predicted service life based o

n the experimental rate of four anodes consumption by assuming a constant rate of consumption of anodes for the entire service life. This shows a service life prediction of 28.09 years and 28.78 years for RC-3 and RC-4 specimens after 21-months of the repair operation.

Dasar *et al.* (2017) reported the correlation of deterioration progress and performance degradation of the typical RC beams with initial pre-crack and without initial pre-crack until 40 years of exposure time based on recorded data on 10-years (Hamada *et al.* 1988), 20-years (Yokota *et al.* 1999a, Yokota *et al.* 1999b, Watanabe *et al.* 2001), and 40-years. The deterioration stages of structures due to corrosion involves initiation, propagation, acceleration, and deterioration period. In each stage, it performs different implications on the RC beams structures. The judgment criteria of deterioration assessment based on Yokota *et al.* 1999a are shown in *Dasar et al.* (2017) reported the correlation of deterioration progress and performance degradation of the typical RC beams with initial pre-crack and without initial pre-crack until 40 years of exposure time based on recorded data on 10-years (Hamada *et al.* 1988), 20-years (Yokota *et al.* 1999a, Yokota *et al.* 1999b, Watanabe *et al.* 2001), and 40-years. The deterioration stages of structures due to corrosion involves initiation, propagation, acceleration, and deterioration period. In each stage, it performs different implications on the RC beams structures. The judgment criteria of deterioration assessment based on Yokota *et al.* 1999a are shown in **Table 4.6.**

Table 4.6 Experimental rate of four anodes consumption per day in RC-3 and RC-4

Specimens	Initial weight of four anodes (gram)	Mass loss until 732 days (gram)	Rate of consumption (gram/day)	Predicted remaining service life (year)
RC-3	1667.6	111.41	0.038	28.09
RC-4	1666.4	111.47	0.038	28.78

In this research, two RC beams with and without initial pre-crack were used to demonstrate the effectiveness of both of repair methods. The specimens of RC-3 and RC-4 are almost in the same deterioration degree in 44-years with no pre-crack specimens tested by Dasar *et al.* 2017. **Figure 4.80** presents the repair methods are effective to stop deterioration progress and performance degradation until 73 years for RC-3 and RC-4. Regular monitoring of potential and current flow generated by sacrificial anodes is required until the expected of service life in these repair methods.

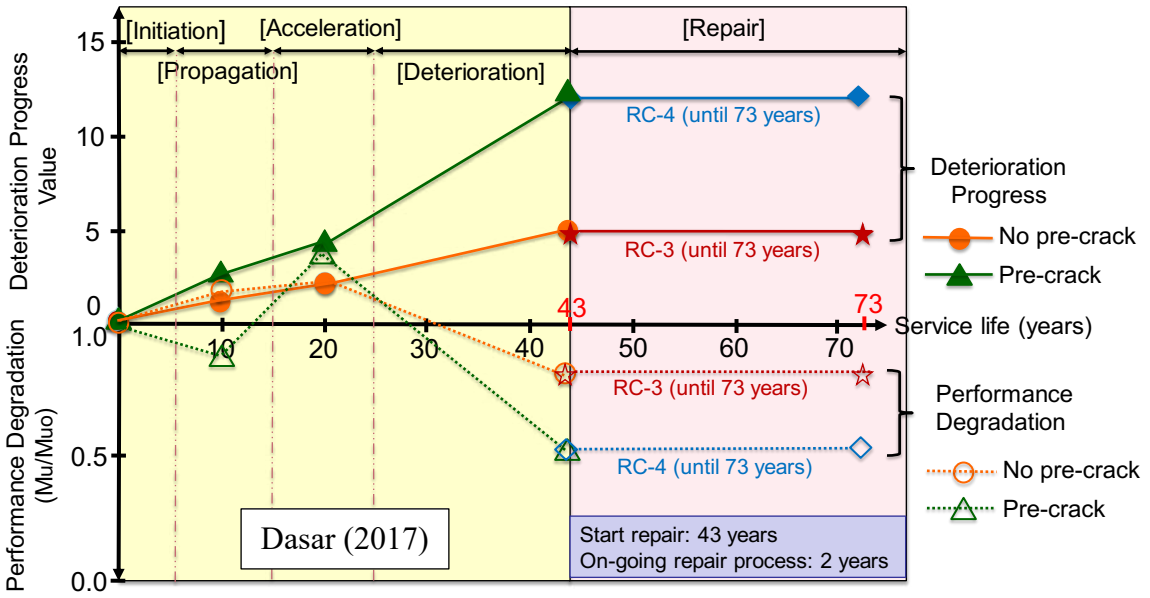

Figure 4.80 Effect of repair to the deterioration progress and performance degradation in RC-3 and RC-4

4.8.9 Actual specimen condition after two-years of repair

The actual condition of specimens after two-years of repair was observed. **Figure 4.81** and **Figure 4.83** present the crack mapping of RC-3 and RC-4, respectively. It was observed that only small crack (0.15 mm and 0.09 mm of maximum crack width in RC-3 and RC-4, respectively) that not related to the old cracks was found. The actual picture of the patch repair area of specimens in RC-3 and RC-4 were depicted in **Figure 4.82** and **Figure 4.84**.

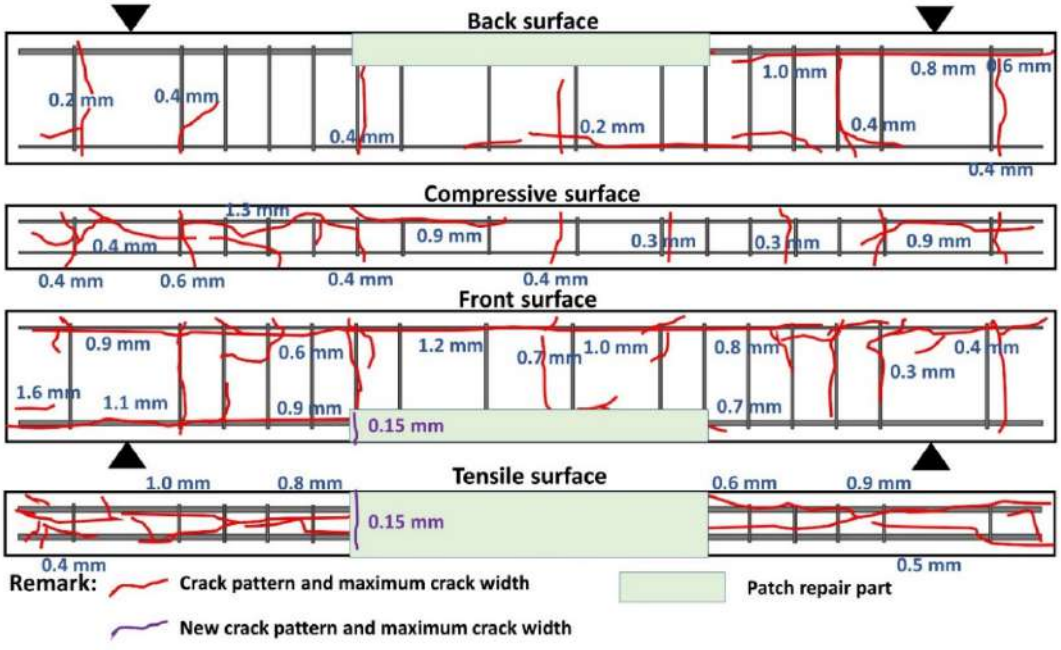

Figure 4.81 Crack formation of RC-3 after two years of repair

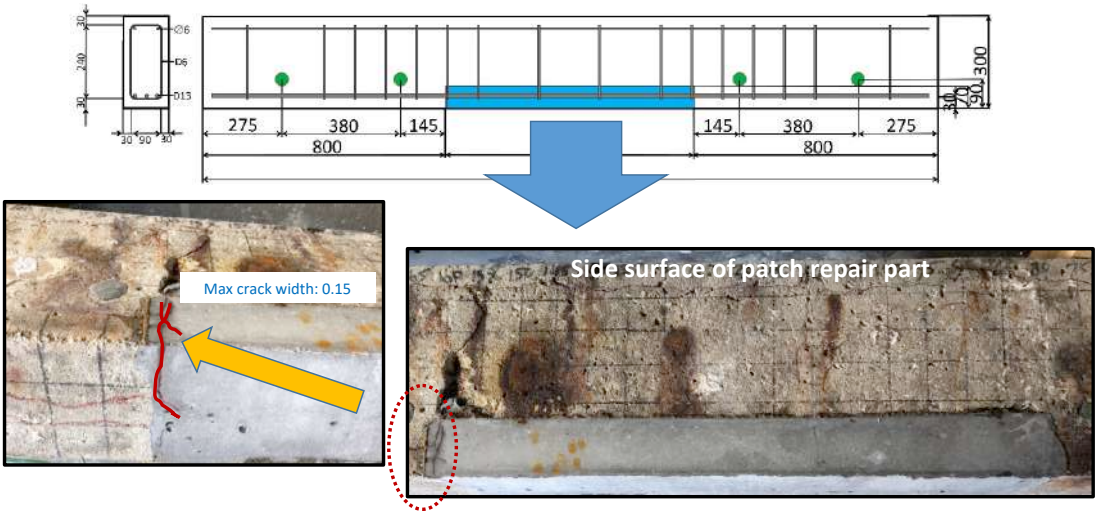

Figure 4.82 New crack formation in patch repair area of RC-3

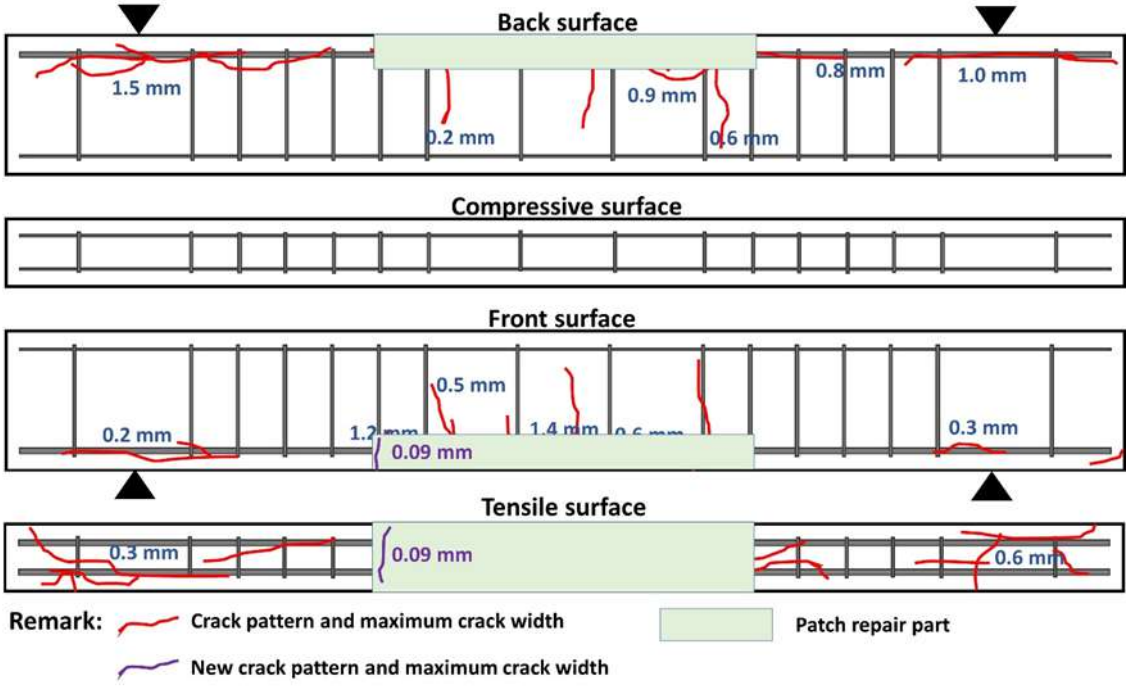

Figure 4.83 Crack formation of RC-4 after two years of repair

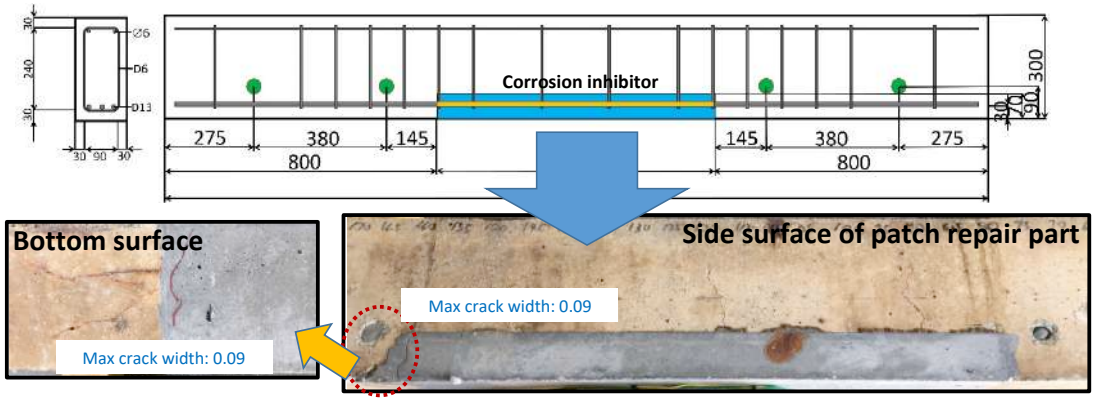

Figure 4.84 New crack formation in patch repair area of RC-4

The new cracks formation of specimens in RC-3 and RC-4 presents different conditions. It may be caused by the different type of polymer modified mortar used (RIS321 for RC-1 and RC-2, RIS Finish Ace for RC-3 and RC-4), material age (four years of RC-1 and RC-2, two-years of RC-3 and RC-4), and the existence of current flow in the patch repair area (exist for RC-1 and RC-2, not exist for RC-3 and RC-4).

4.8.10 Conclusion

From the experimental programs, several findings are explained as follows.

1. The sacrificial zinc anode tested in this research affects polarizing the potential of rebar in the RC member damaged by corrosion. However, the high polarization is limited to the surrounding of anodes in parent concrete, not in the patch repair section, due to the inherent differences in the properties of patch repair material and parent concrete.
2. The application of corrosion inhibitor in the rebar surface of the patch repair part extends the polarization distance significantly until two times during 18-months of exposure due to its membrane reduced the required electric current for attaining the potential change in patch repair. There is no new corrosion crack formation at the patch repair part until two-years of observation.
3. An alternative performance criterion, to that of 100 mV potential decay, maybe adopt for assessing the performance of sacrificial anodes, the sacrificial anodes in parent concrete should demonstrate that it affords a dominant influence on the rebar potentials away from the position of the anode that is at least equal to half the spacing between anodes.

4.9 Application of different kinds of sacrificial anodes in patch and non-patch repair

Steel bar corrosion leads to deterioration, damage, and destruction of reinforced concrete (RC) structures, and it is a major issue in infrastructure maintenance (Raupach, 2014). Excessive corrosion can be dangerous and costly (Chiu & Lin, 2014; Higuchi & Macke, 2008; Val & Stewart, 2005). The annual cost of corrosion worldwide is estimated to be 3–4% of the gross domestic product (GDP) of industrialized countries (Schmitt, 2009), with US$17 billion annual maintenance investment reportedly needed to improve bridge conditions in the USA (ASCE, 2009).

There are several circumstantial and interconnected influences in designating which repair method to use, including weight restrictions, budget, the need for a monitoring system, maintenance requirements, traffic management during repairs, the extent and severity of the damaged, aesthetics, and technical limitation (Pearson & Patel, 2002). Patch repair is the most widely used but is limited to low-impact localized damage (Qian *et al.,* 2006; Raupach, 2006; NACE, 2005). The most negative impact of this method is the risk of incipient anodes causing corrosion of the surrounding areas of the steel bar (Pearson & Patel, 2002). Sacrificial anode cathodic protection has been used to limit the extent of concrete replacement and extend the service life of patch repair to RC members. They respond to the changes in the environmental conditions they are exposed to (John & Cottis, 2003; Christodoulou *et al.,* 2009; Holmes *et al.,* 2011). Cathodic protection applies a small current into the steel bar, forcing it to act as the cathode as opposed to the dissolving anode in an electrochemical cell (Holmes *et al.,* 2011). It controlled corrosion in the whole area treated, thus reducing the extent of concrete repair (UK Highway Agency, 2002). Such an effect will be more dominant in parent concrete that has a residual level of chloride contamination as opposed to non-contaminated repair concrete or mortar (UK Highway Agency, 2002).

In this subchapter, an experimental study on the repairing system by using a different kind of sacrificial anodes in patch repair and parent concrete was demonstrated on severely damaged reinforced concrete (RC) beam aged more than 40-years exposed to the natural marine environment. The sacrificial anodes setting position is presented in **Figure 4.85**. Three sacrificial anodes connection pattern, as explained in **Figure 4.86**, were demonstrated in this study.

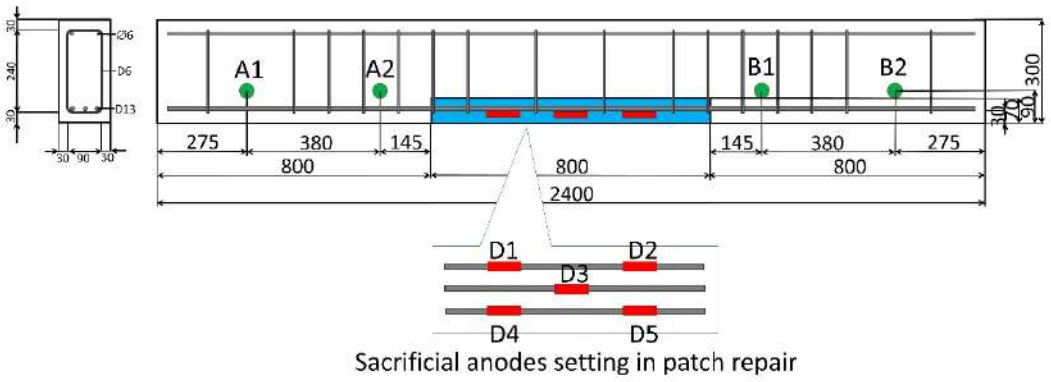

Figure 4.85 Sacrificial anodes setting position

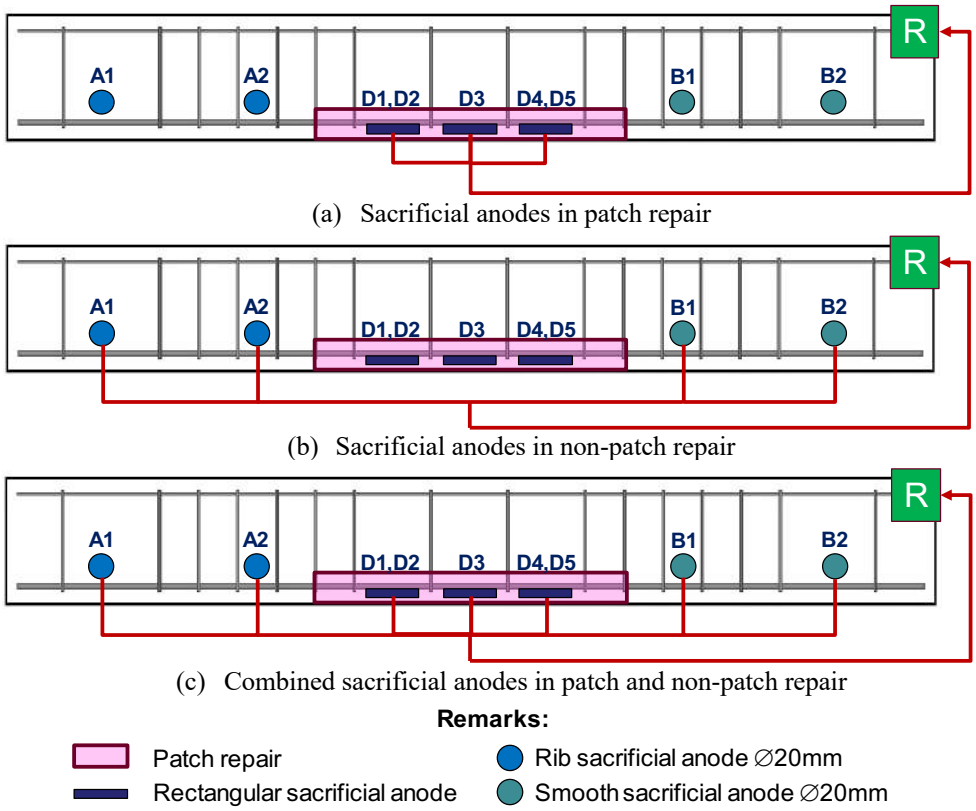

Figure 4.86 Connection pattern of sacrificial anodes and steel bar

Half-cell potential test of rebar according to ASTM C876-15 was conducted by the calomel-saturated electrode (CSE) and high impedance multimeter (voltmeter setting) on every 50 mm square grid at the compressive and tensile rebar position after one hour of pre-wetting to evaluate the potential of the steel bar. On-potential (E_{on}) of rebar and the anode are measured under sacrificial anode cathodic protection. Instant-off potential (E_{iof}) is checked immediately after disconnection, and the rest potential (E_{corr}) is measured at 24 hours after interruption of the steel bar and the anode.

Sacrificial anodes in patch repair only were connected to the steel bar as the first pattern. The second pattern describes sacrificial anodes in non-patch repair connected to the

steel bar. The last pattern, all sacrificial anodes both in the patch and in patch repair were connected to steel bar. Each pattern was observed during one month of exposure. A similar pattern by a different type of sacrificial anodes and backfill material were done in the previous study (Rafdinal, 2016; Astuti *et al.*, 2019a).

4.9.1 Current flow of sacrificial anodes

The current flow of each sacrificial anode in the three connection pattern was presented in **Figure 4.87**. It shows that the current flow of sacrificial anode both in the patch and non-patch repair is 0.7~0.8 mA. However, the current flows increase become 1.3~1.4 mA and 0.8~0.9 mA for the sacrificial anode in the patch and non-patch repair, respectively. So, the combined of anodes stimulate incremental of current flow. The total protective current density of all anodes in the combined method is 44.02 mA/cm^2.

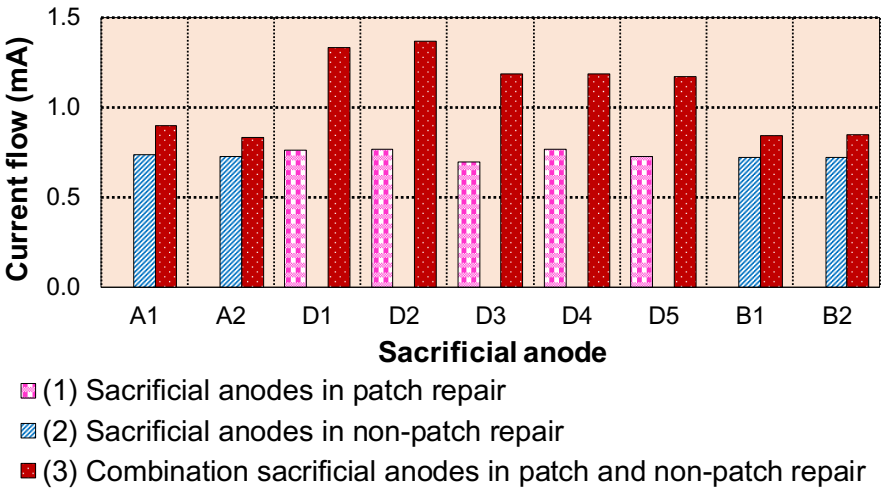

Figure 4.87 Current flow of sacrificial anodes

4.9.2 Polarization of anodes

After one-month of connection, the potential development of steel bar including instant-off potential, rest potential, and depolarization test value is presented in **Figure 4.88**. The potential of rebar and sacrificial anodes during connection (on potential), immediately after disconnection (instant-off potential), and rest potential after 24-hours of disconnection (half-cell potential) were recorded in this experiment. The polarization of the sacrificial anode effect can be presented by using instant-off potential data. The rest potential is used to understand the corrosion probability based on ASTM C 876. The effectiveness of cathodic protection is categorized based on the 100 mV potential decay criterion.

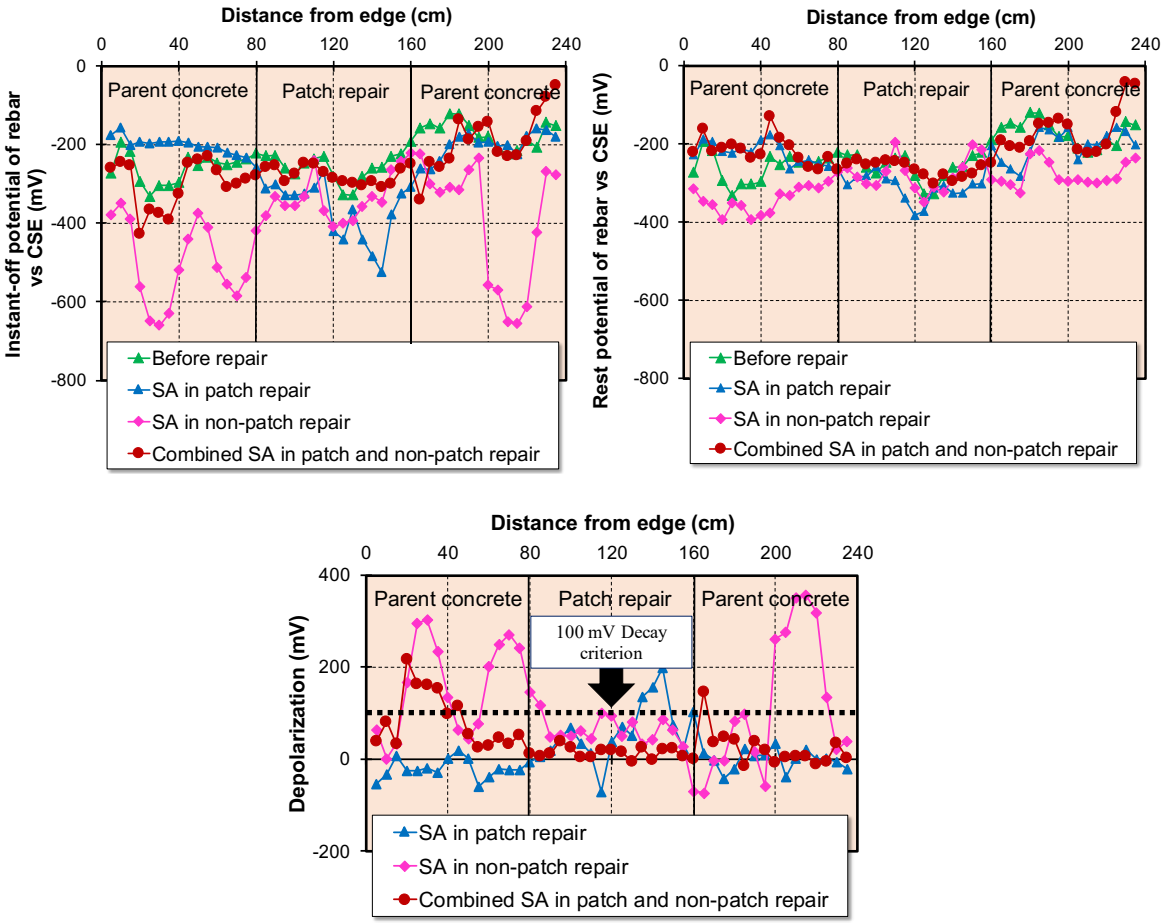

Figure 4.88 Potential development of tensile steel bar, (a) instant-off potential, (b) rest potential and (c) depolarization test value

From the first pattern, when sacrificial anodes in patch repair are connected to a steel bar, the polarization only occur in the patch repair area. It is confirmed by depolarization value that it can reach 100 mV potential decay only in the patch repair area. The second connection pattern also shows that the steel bars in non-patch repair are polarized by the application of sacrificial anodes in non-patch repair. The depolarization value shows that the protection is concentrated in the surrounding of a sacrificial anode setting position until 300 mV~It may due to electrochemical incompatibility between polymer modified mortar as patch material and existing concrete (Astuti *et al.*, 2018; Astuti *et al.*, 2019a). The first and second connection patterns perform well to protect the steel bar in its area. The third pattern reveals the less polarization effect of steel bar due to combined different kinds of sacrificial anodes in the patch and non-patch repair. The polarization only occurs around A1 and none in other sacrificial anodes.

The protection condition of each connection pattern is illustrated as a depolarization map of the steel bar and it was presented in **Figure 4.89**. Although the current flow of

sacrificial anodes is generated from combined sacrificial anodes, it is not clear the current circulation from anodes to steel bar. So, the protection trend is unfavorable. The depolarization map presents that the application of SACP in patch repair has less effect on the polarization of the steel bar observed from the side of the beam. On the other hand, the application of four SACP in non-patch repair shows great depolarization value at the anode position. Unfortunately, the application of combined SACP both in patch and in patch repair demonstrated low depolarization of less than 50 mV.

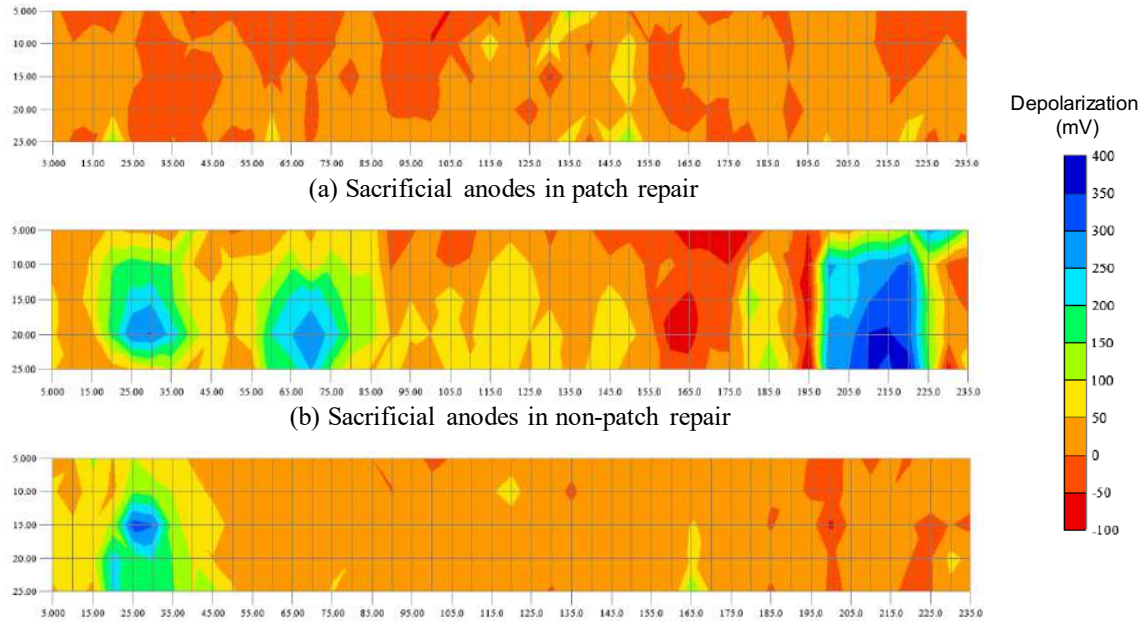

(a) Sacrificial anodes in patch repair

(b) Sacrificial anodes in non-patch repair

(c) Sacrificial anodes in patch and non-patch repair

Figure 4.89 Depolarization map

4.9.3 Conclusion

The repair method by combining a different kind of sacrificial anodes in the patch and non-patch repair presented no significant polarization of rebar nor current flow. Therefore, the combined sacrificial anodes in the patch and non-patch repair method at the same time with closed distance could not be suitable repairing system.

4.10 **Discussion**

The tensile steel bar condition during the repair process in non-patch repair (400 mm from edges) and patch repair (1200 mm) is presented in **Figure 4.90**. The improvement of steel bar condition is identified by the increase of passivity grade, polarization resistance ($k\Omega.cm^2$), and rest potential (mV vs CSE) and also the decrease of corrosion rate(I_{corr}) (mA/m^2). The observation points of both non-patch repair and patch repair are at 400 mm (from left and right edges) and 1200 mm (middle span), respectively. The results show the steel bar condition in both points is improved during 18-months of repair process. It means that the application of sacrificial anodes in four repair methods is effective to improve the steel bar condition.

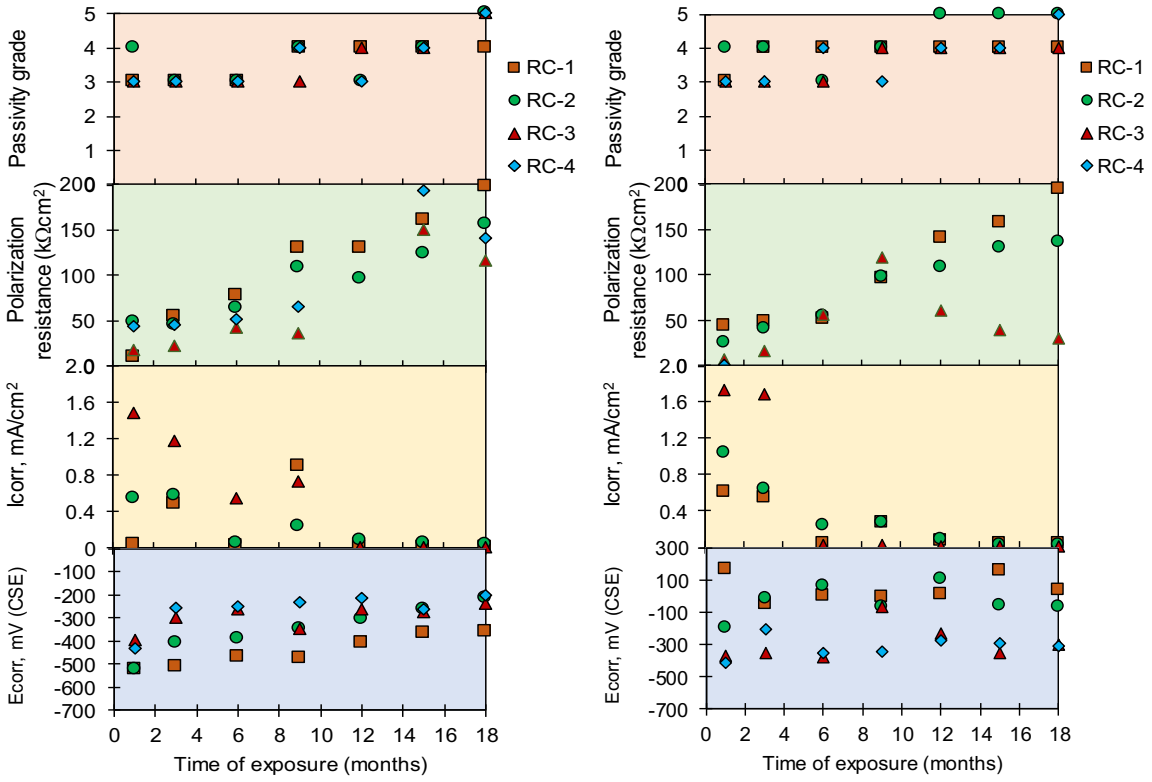

(a) Non-patch repair (b) Patch repair

Figure 4.90 Steel bar condition change time-dependently

In cathodic protection system, depolarization value is the important parameter to categorize the effectiveness of the system. **Figure 4.91** and **Figure 4.92** present the correlation between depolarization and parameter of steel bars condition on 0-3 months, 6-12 months, and 15-18 months of repair process. The data inform that low correlation between the depolarization value more than 100 mV to the improvement of steel bar condition indicated by the correlation coefficient that less than 0.70.

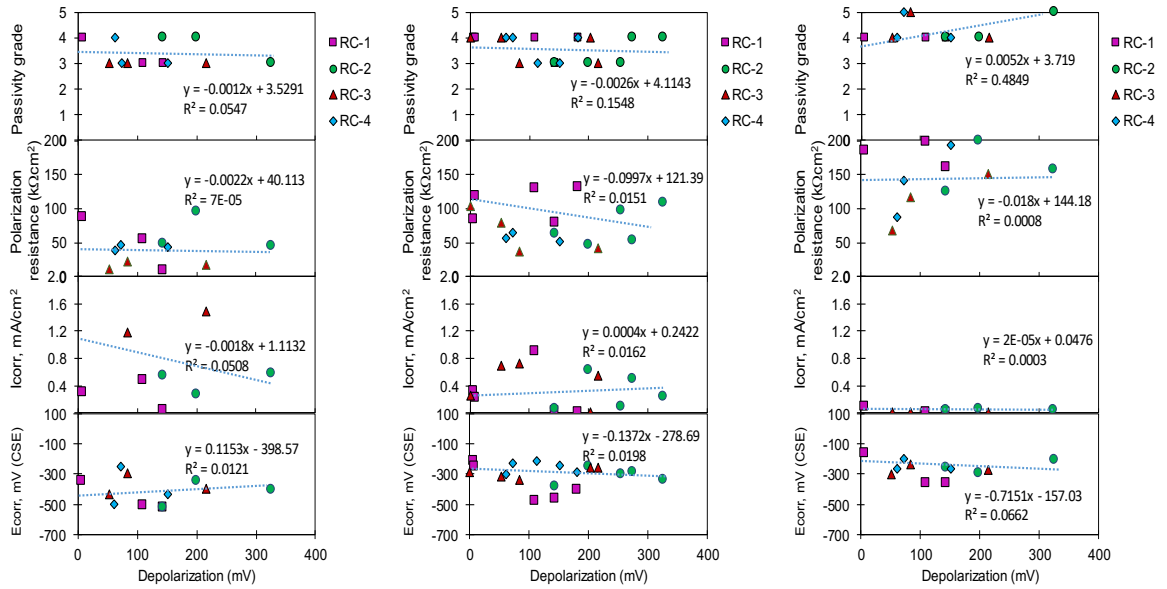

(a) 0-3 months (b) 6-12 months (c) 15-18 months

Figure 4.91 Correlation of depolarization to steel bar condition in non-patch repair at 400 mm from edges

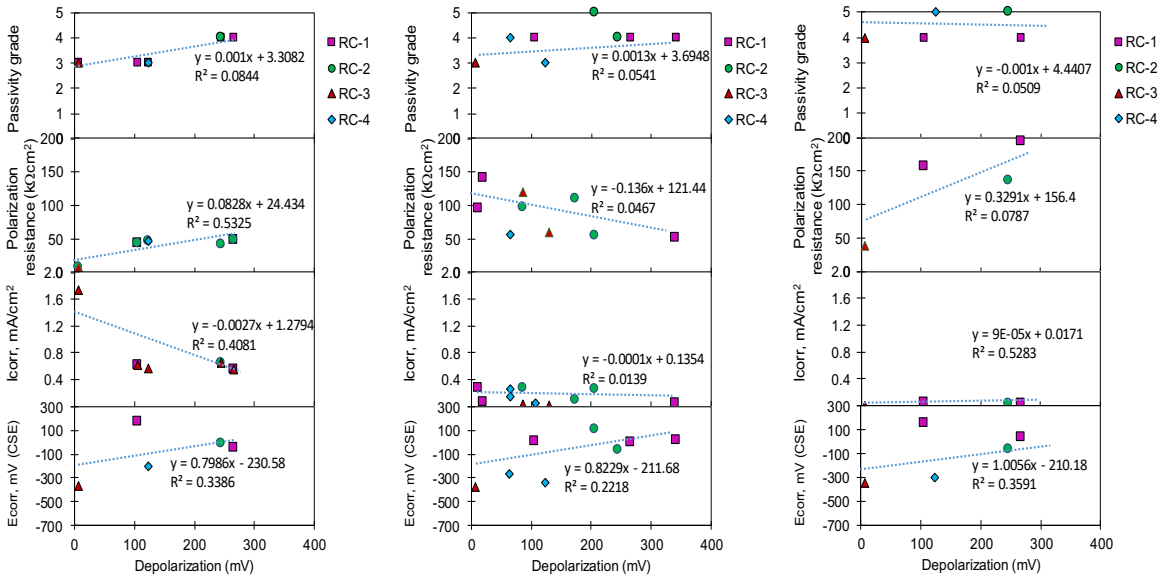

(a) 0-3 months (b) 6-12 months (c) 15-18 months

Figure 4.92 Correlation of depolarization to steel bar condition in patch repair at 1200 mm from edges (middle span)

4.11 **Conclusion of application of sacrificial anodes in severely damaged RC beams**

From the experimental programs of repairing method by sacrificial anodes, it can be concluded that small current flow generated by sacrificial anodes affects not only on polarization but also modifies the steel bar condition. Several findings of each repairing techniques are explained as follows.

a. Application of sacrificial anodes in the patch and non-patch repair

- Application of sacrificial anodes in the patch repair concrete has effectively controlled the corrosion of the rebar indicated by the rest potential shift to the noble value even though its protection cannot reach the existing concrete due to electrochemical incompatibility.
- After a year in current interruption, the steel bar embedded in the polymer-modified mortar with chloride-free contamination has remained passive with no corrosion sign. It indicated that polymer-modified mortar has a persistent protective effect in the absence of protective current from cathodic protection.
- Sacrificial anodes both in non-patch and patch repair concrete are sufficient to control the corrosion of rebar with an optimum distance of 400 mm.
- After two-years of repair by additional sacrificial anodes in existing concrete, new cracks formation were observed in the patch repair area. It may be caused by the macro-cell corrosion owing to the imperfect of new patch material and the different current flow of anodes in the patch and non-patch area.
- The service life prediction of anodes in existing concrete methods by using Fadaray's law and current flow measurement was 15 to 28 years. Therefore, it is estimated that by repair method of this study, the lifetime of RC beams could be extended until about 70 years.

b. Application of sacrificial anodes in non-patch repair and corrosion inhibitor

- The sacrificial zinc anode tested in this research affects polarizing the potential of rebar in the RC member damaged by corrosion. However, the high polarization is limited to the surrounding of anodes in parent concrete, not in the patch repair section, due to the inherent differences in the properties of patch repair material and parent concrete.
- The application of corrosion inhibitor in the rebar surface of the patch repair part extends the polarization distance significantly until two times during 18-months of exposure due to its membrane reduced the required electric current for attaining the potential change in patch repair. There is no new corrosion crack formation at the patch repair part until two-years of observation.
- An alternative performance criterion, to that of 100 mV potential decay, maybe adopt for assessing the performance of sacrificial anodes, the sacrificial anodes in parent concrete should demonstrate that it affords a dominant influence on the rebar potentials away from the position of the anode that is at least equal to half the spacing between anodes.

c. Application of different kinds of sacrificial anodes in patch and non-patch repair

The repair method by combining a different kind of sacrificial anodes in the patch and non-patch repair presented no significant polarization of rebar nor current flow. Therefore, the combined sacrificial anodes in the patch and non-patch repair method at the same time with closed distance could not be suitable repairing system.

4.12 **References**

Andrade, C., and González, J. A., 1978. "Quantitative measurements of corrosion rate of reinforcing steels embedded in concrete using polarization resistance measurements", *Materials and Corrosion*, Vol. 29, No. 8, pp. 515-519.

ASCE (American Society of Civil Engineers), 2009. "*Report card for America's infrastructures – Facts about transportation – Bridges*", American Society of Civil Engineers, Reston, VA, USA.

ASTM C 597, 2002. "Standard Test Method for Pulse Velocity Through Concrete". American Society for Testing and Materials.

ASTM C87, 2015. "Standards test method for half-cell potentials of reinforcing steel in concrete". American Society for Testing and Materials.

Astuti, P., Rafdinal, R.S., Mahasiripan, A, Hamada, H., Sagawa, Y., and Yamamoto, D., 2018. "Potential Development of Sacrificial Anode Cathodic Protection Applied for Severely Damaged RC Beams Aged 44-years." *Journal of Thailand Concrete Association*, 6 (2), 24-31.

Astuti, P., Rafdinal, R.S., Hamada, H., Sagawa, Y., and Yamamoto, D., 2019a. "Application of sacrificial anode cathodic protection for partially repaired RC beams damaged by corrosion." *4th International Symposium on Concrete and Structures (CSN2019)*, Kanazawa, Japan 17-19 June 2019. Kanazawa: Kanazawa Institute of Technology, 284-291.

Astuti, P., Rafdinal, R.S., Kamarulzaman, K., Hamada, H., Sagawa, Y., and Yamamoto, D., 2019b. "Repair method of deteriorated RC beams by sacrificial anode cathodic protection and corrosion inhibitor." *3rd ACF Symposium 2019 Assessment and Intervention of Existing Structures*, Kanazawa, Japan 10-11 2019. Sapporo: Hokkaido University.

British Standard, BS EN 1504, "Product and systems for the protection and repairs of concrete structures", 2005.

British Standards Institution, BS EN ISO 12696:2012, "Cathodic protection of steel in concrete, 2012, London, UK.

CEB, 1998. "Strategies for Testing and Assessment of Concrete Structure", *Bulletin* No.243, pp.183.

Cheaitani, A., 2000. "Cathodic Protection criteria and Practical Completion Issues for CC of Reinforced Concrete Structures", *Corrosion2000*, NACE (National Association of Corrosion Engineer), No. 00805.

Christodoulou, C., 2008. "Electrochemical treatments of corroded reinforcement in concrete." in M. Alexanders et al. Eds. *Concrete repairs, rehabilitation, and retrofitting II – Proceeding of 2nd International Conference on Concrete Repair, Rehabilitation and Retrofitting (ICCRRR-2)*, Cape Town 24-26 November 2008. United Kingdom, Taylor & Francis Group, pp. 297-298.

Christodoulou, C., Glass, G., and Webb, J., 2009. "Corrosion management of concrete

structures", *The Structural Engineer*, Volume 87, 23/24, December 2009.
Christodoulou, C., Goodier, C. I., Austin, S. A., Glass, G. K., Webb, J., 2014. "A new arrangement of galvanic anodes for the repair of reinforced concrete", *Construction and building materials,* Vol. 50, pp. 300-307.
Chiu, C. K. & Lin, Y. F., 2014. "Multi-objective decision-making supporting system of maintenance strategies for deteriorating reinforced concrete buildings." *Automation in Construction,* Vol. 39, pp. 15-31.
Dasar, A., Hamada, H., Sagawa, Y., and Yamamoto, D., 2017. "Deterioration Progress and Performance Reduction of 40-year-old reinforced concrete beams in natural corrosion environment." *Construction and Building Materials*, Vol. 147, pp. 690-704.
Elsener, B., 2001. "Corrosion Inhibitors for Steel in Concrete – State of the Art Report", *European Federation of Corrosion Publication,* No. 35, Maney Publishing, London.
Glass, G. and Buenfeld, N., 1997. "The presentation of the chloride threshold level for corrosion of steel in concrete", *Corrosion Science*, Vol. 39, pp. 1001-1013.
Glass, G. and Chadwick, J. R., 1994. "An investigation into the mechanism of protection afforded by a cathodic current and the implications for advances in the field of cathodic protection." *Corrosion Science*, Vol. 36, pp. 2193-2209.
Glass, G. and Christodoulou, C., 2012. "Towards rendering steel reinforced concrete immune to corrosion." *Australiasian Corrosion Association 2012 Annual Meeting*, Melbourne, 11-14 November 2012. New York: Red Hook, NY Curran Associates, Inc., No. 159, pp. 1-11.
Hamada, H., Otsuki, N., and Haramo, M., 1988. "Durability of concrete beams under marine environments exposed in port of Sakata and Kagoshima (after 10 year's exposure)." *Technical Note of the Port and Airport Research Institute*, 614, 3-43.
Higuchi, S. & Macke, M., 2008. "Cost-benefit analysis for the optimal rehabilitation of deteriorating structures." *Structural Safety,* Vol. 30, No. 4, pp. 291-306.
Highway Agency (HA), 2002. "*Design manual for roads and bridges, cathodic protection for use in reinforced concrete highway structures*". Vol. 3, Highway Agency, London, UK.
Holmes S.P., Wilcox G.D., Robins P.J., Glass G.K., and Roberts A.C., 2011. "Responsive behaviour of galvanic anodes in concrete and the basis for its utilization", *Corrosion Science*, Vol. 53, pp. 3450 – 3454.
Japan Society of Civil Engineer (JSCE), 2007. "JSCE standard specification for concrete structures, Part: Maintenance", Japan.
John G., and Cottis B., 2003. "Laboratory Testing and Computer Modelling of the Performance of Sacrificial Anodes for use in Reinforced Concrete Structures", Paper number 03302, *Corrosion 2003*, NACE International, Houston, USA.
NACE International Publication 01105, 2005. "Sacrificial Cathodic Protection of Reinforced Concrete Element", *A state of the art report*, USA, March 2005.
Otsuki, N., 1985. "A study of effectiveness of Chloride on Corrosion of Steel Bar in Concrete", *Report of Port and Harbor Research Institute*, pp. 127-134.
Otsuki, N., Nagataki, S., and Nakashita, K. 1992. "Evaluation of AgNO3 solution spray method for measurement of chloride penetration into hardened cementitious matrix materials," *ACI Materials Journal,* Vol. 89. No. 6.
Pearson, S. and Patel, R. G., 2002. "*Repair of concrete in highway bridges – A practical guide.*" Transport Research Laboratory, Wokingham, UK, AG43.
Pech-Canul, M. A., and Castro, P., 2002. "Corrosion measurements of steel reinforcement in concrete exposed to a tropical marine atmosphere", *Cement and Concrete Research*, Vol. 32, No. 3, pp. 491-498.

Rafdinal, R. S., 2016. "*Life Extension of RC Structure by Cathodic Protection using Zinc Sacrificial Anode Embedded in Concrete.*" Thesis (PhD), Department of Civil and Structural Engineering, Kyushu University, Fukuoka, Japan.

Raupach, M., 2006. "Patch repairs on reinforced concrete structures – model investigations on the required size and practical," *Cement and Concrete Composites,* Vol. 28, No. 8, pp. 679-684.

Raupach, M., 2014. "*History of Efc-Wp11 'Corrosion in concrete'*." Institute for Building Material Research of Aachen University, Aachen, Germany.

Rincon, O. T., Lopez, Y. H., Moreno, A. V., Acosta, A. T., Barrios, F., Montero, P., Salinas, P. O., and Montero, J. R., 2008. Environmental Influence on Point Anode Performance in Reinforced Concrete." *Construction and Building Materials*, 22, 494-503.

Schmitt, G., 2009. "*Global needs for knowledge dissemination, research, development in materials deterioration and corrosion control*." World Corrosion Organization, New York, NY, USA.

Song, H.W., Kim, H. J., Saraswathy, V., and Kim, T. H., 2007, "A Micro-mechanics based Corrosion Model for Prediction of Service Life in Reinforced Concrete Structures", *International Journal of Electrochemical Science*, Vol. 2, pp. 341-354.

Stern, M., and Geary, A. L., 1957. "Electrochemical polarization I. A theoretical analysis of shape of polarization curves", *Journal of the Electrochemical Society*, Vol. 104, No. 1, pp. 56-63.

Val, D. V. and Stewart, M. G., 2005. "Decision Analysis for deteriorating structures", *Reliability Engineering & System Safety,* Vol. 87, No. 3, pp. 377-385.

Qian, S, Zhang, J., and Qu, D., 2006. "Theoretical and experimental study of microcell and macrocell corrosion in patch repairs of concrete structures", *Cement and Concrete Composites,* Vol. 28, No. 8, pp. 685-695.

Watanabe, H., Hamada, H., Yokota, H., and Yamaji, T., 2001. Long-term Performance of Concrete and Reinforced Concrete under Marine Environment, in: N. Banthia, K. Sakai, O.E. Gjørv (Eds.), *Proceedings 3rd International Conference on Concrete Under Severe Conditions*, Vancouver, Canada: The University of British Columbia.

Yokota, H., Akiyama, T., Hamada, H., Mikami, A., and Fukute, T., 1999a. "Effect of degradation of concrete on mechanical properties of reinforced concrete beams exposed to marine environment (for 20 years in Sakata)." *Report of the Port and Airport Research Institute*, Vol. 38, No. 2.

Yokota, H., Fukute, T., Hamada, H., and Akiyama, T., 1999b. "Structural Assessment of Deteriorated RC and PC Beams Exposed to Marine Environment for more than 20 years." *Wakachiku Kensetsu Doboku Gijutsu Nenpo 8*, pp. 78-84.

CHAPTER V

Utilization of new embeddable corrosion monitoring sensor in repaired RC members

5.1 Introduction

Half-cell (or reversible electrode) to exist, a dynamic reversible equilibrium must be established between different material phases at least one of which is a metal and another must be an electrolyte solution (Mularidharan *et al*., 2005). Gaseous (e.g., hydrogen) or solid non-metallic phases (e.g., silver chloride) may also be involved (Itoh *et al.,* 1996; Nolan *et al.,* 1997; Suzuki *et al.,* 1998; Eden and Quirk, 2001; Krebs, 2003; Mularidharan *et al*., 2005). The potential of the half-cell is dependent upon the chemical potentials of the reaction involved. There is no known method for determining the absolute potentials of a single electrode with an electrode of known potential and measuring the electrochemical potential of the resulting cell (Mularidharan *et al*., 2005).

Corrosion monitoring of steel reinforcing bar in concrete requires reliable stable potentials. Such measurements are important when designing and maintaining cathodic protection systems for RC structures. In particular, accurate measurements are mandatory for RC structures where over-protection can be as deleterious as under-protection. The increasing usage performance over an extended period (Ansuini & Dimond; 2001). The embeddable reference electrodes are useful in corrosion monitoring of rebar in concrete for long-term exposure and controlled by cathodic protection. An adequate embeddable reference electrode must require some conditions such as it must be stable, invariant to chemical and thermal changes in concrete, tolerant to the climatic condition and have the ability to pass small currents with a small polarization and hysteresis effects, display long-term performance, be cost-effective and result from safe environmental manufacturing (Mularidharan *et al*., 2005).

The utilization of the reference electrode was reported by several previous researchers (Arup and Sorenson, 1992; Bennet and Mitchell, 1992; NACE, 2000). Saturated calomel electrode (SCE) is conventionally used for laboratory measurements in alkaline environments due to its compatibility and easy to use. Silver/silver chloride (Ag/AgCl)

reference electrode is commonly used in RC structures to measure the potential of steel bars. Their electrodes have developed a reputation for being reliable and stable in a variety of underground, aqueous, medical, and laboratory applications. Yet, there are occasional reports of their stability when used in RC, particularly during cold periods (Schell & Manning, 1985; Ansuini & Rimond, 2003), or in long-term applications (Bennet & Mitchell, 2992; Ansuini & Rimond, 2003). Ag/AgCl reference electrodes are true reference electrodes in the thermodynamic sense; the reference potential established at the element/electrolyte interface is only dependent upon the chloride ion activity and the temperature (Ansuini & Rimond, 1994; Ansuini & Rimond, 2003). It would seem likely, therefore, that any erratic behavior of these electrodes must be related to some other cause. The second type of reference electrode which is being used extensively in RC structures is graphite. Some short term testing has shown graphite cells to have performed satisfactorily (Schell & Manning, 1985; Ansuini & Rimond, 2003), however, they are not thermodynamically true reference electrodes (NAE, 2000; Ansuini & Rimond, 2003). This means that no reversible reaction has been identified for graphite in this environment. The third type of reference electrode based on manganese oxide (MnO_2) was developed for concrete use (Arup & Sorenson, 1992; Ansuini & Rimond, 2003). Initial reports on its behavior show it to be a stable reference.

The present investigation deals with the experimental studies on the potential reading observation of the embeddable reference electrode consist of titanium probe activated by iridium-enriched mixed metal oxide in cylindrical polymer mortar and in actual 44-years corroded RC beams repaired by sacrificial anode cathodic protection and polymer-modified mortar in several patterns. The repaired RC beams are the same as the specimens used in Chapter 4 and based on the previous research (Rafdinal, 2016; Astuti *et al.,* 2018; Astuti *et al.,* 2019).

5.2 Embeddable corrosion monitoring sensor

The wire sensor consists of a titanium probe activated with iridium-enriched mixed metal oxide and 3 mm in diameter was used as sensor electrodes in this study. The schematic of the embeddable titanium wire sensor (TWS) for concrete structures is shown in **Figure 5.1**. The electrical contact of the sensor is through the body length of titanium wire. The sealant was designed to extend the durability of lead wire and titanium wire connection.

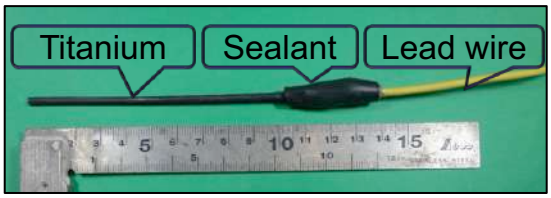

Figure 5.1 Schematic of embeddable titanium wire sensor (TWS)

Fifteen TWS with 100 mm of length exposed to some temperature conditions, i. e. 0°C, 31°C, 48°C, and 66°C, were observed during the feasibility study reported by Rafdinal *et al.,* (2018). The experiment scheme of the feasibility study is presented in **Figure 5.2**. Voltmeter and potentiostat were used to test all the electrochemical aspects of this study. The temperature coefficient of these sensors was converted to the standard reference electrodes such as Ag/AgCl, $Cu/CuSO_4$, Pb, Mn/MnO_2. The linear polarization condition corresponded to a potential sweep rate of 1 mV/s and potential ranges of +200 mV to -1500 mV from the open circuit potential (natural potential) and the results are converted to Ag/AgCl electrode.

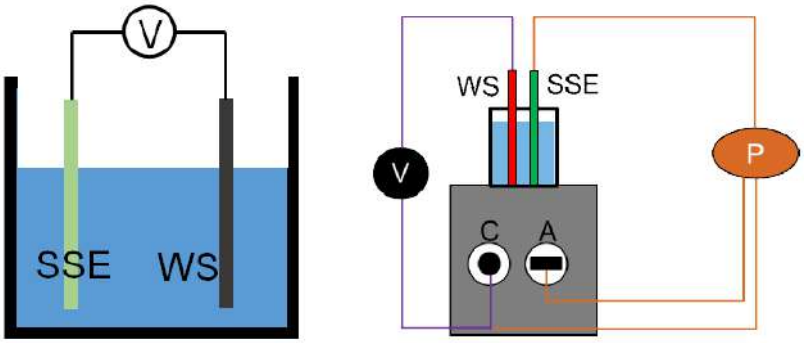

(a) Method 1 (b) Method 2

Figure 5.2 Potential measurement of titanium wire sensor (Rafdinal *et al.,* 2018)

Temperature is one of the external factors which affect the potential of a reference electrode (RE). Potential of RE changes with temperature for the reason that both electrochemical reactions and chemical solubility. In electrical resistance, a temperature coefficient describes the relative change of a physical property associated with a given change in temperature. It is necessary to know the temperature coefficient (TC) to minimize errors in potential reading and to know the electrical resistance of RE. **Equation 5.1** estimates the TC as following:

$$E = E_{025} + (t - 25)\, dE/dt \qquad \textbf{(5.1)}$$

E is the potential of RE at t (mV), E_{025} is potential of RE at t = 25 ºC (mV), t is the temperature (ºC) and dE/dt is temperature coefficient (mV/°C). **Figure 5.3** illustrates the

effect of temperatures (i.e., 10 ºC, 31 ºC, 48 ºC, and 66 ºC) on the potential of WS against the SSE electrode. From this test, it was observed that the potential of WS steadily decreased with the raised temperature.

Furthermore, **Figure 5.3** also presents the temperature coefficient for several reference electrodes, namely Titanium Wire Sensor (WS), Copper Sulfate Electrode (CSE), Plumbum Electrode (Pb) and Manganese Dioxide Electrode (Mn/MnO_2). Accordingly to this figure, the TC of CSE and Pb have a positive temperature coefficient which means the higher coefficient, the greater the increase in electrical resistance for a given increasing temperature. Meanwhile, WS, SSE, and Mn/MnO_2 have the negative temperature coefficient which means the lower the coefficient, the greater the decrease in electrical resistance for a given increasing temperature. It means even though the WS reference electrode shows stability at ambient temperature, but it had a decrease in electrical resistance when the temperature raised.

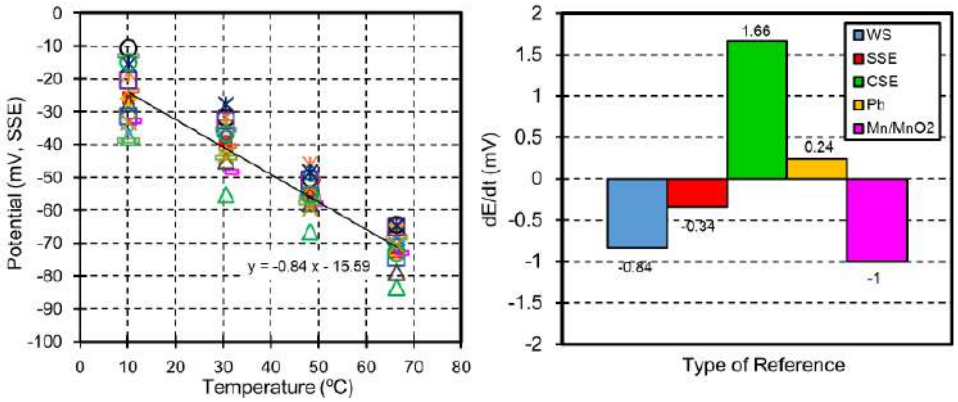

(a) Potential of TWS (b) Temperature coefficient

Figure 5.3 Potential of titanium wire sensor and temperature coefficient (Rafdinal *et al,.* 2018)

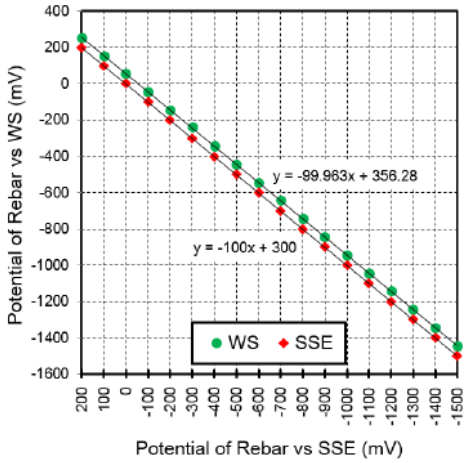

Figure 5.4 Potential of steel bar vs. Titanium wire sensor and SSE (Rafdinal *et al.,* 2018)

Figure 5.4 shows the potential of rebar during linear polarization measurement measured by WS and SSE. The potential of the rebar was varied from + 200 mV to -1500 mV (vs. SSE). The data measured by the WS electrode exhibits the same trend as the SSE electrode, even with 57 mV indifference. It indicates that WS is reliable to monitor the change of rebar potential in concrete as same as the SSE electrode.

5.3 Application of sensor in existing concrete during repair process by sacrificial anodes in patch ad non-patch repair concrete

5.3.1 Specimen design

This sub-chapter presents the demonstration of an embeddable corrosion monitoring sensor made from titanium wire (titanium wire sensor) in existing concrete during the application of sacrificial anode cathodic protection. The specimens in this part are the same as the RC beams used in **Chapter 4.7**.

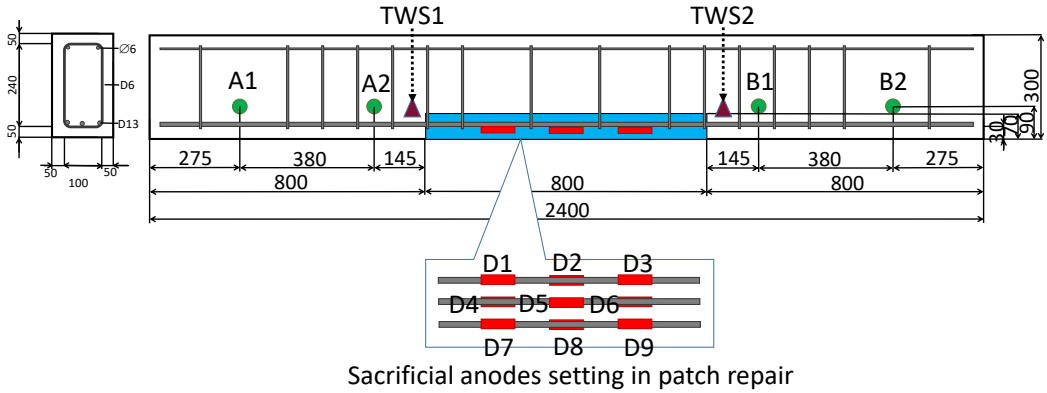

(a) RC-1

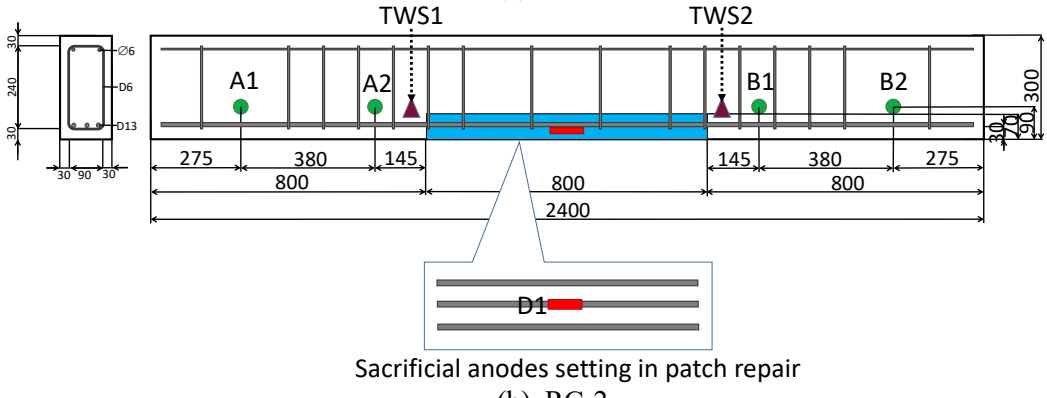

(b) RC-2

Figure 5.5 Titanium wire sensor (TWS) setting position in RC-1 and RC-2

The titanium wire sensors were installed by pre-cavities 20 mm in diameter at 50 mm from the boundary of the patch repair area in the existing concrete. Those sensors are denoted as TWS 1 and TWS2 for the left and right positions, respectively, as presented in **Figure**

5.5. **Figure 5.6** shows the cross-sectional illustration of the TWS setting position. TWSs were installed and operated since stage III of the repair was started.

The specimens were exposed to two-days of wet followed by five-days of the dry condition by water spraying and a wet towel covering until one-year and it continued by dry laboratory condition.

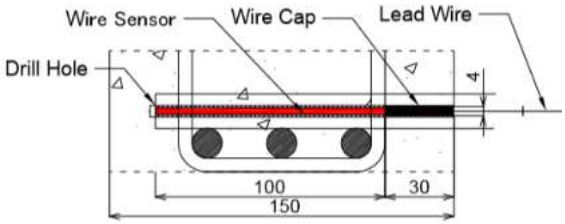

Figure 5.6 Titanium wire sensor position in the cross-sectional area of non-patch repair

5.3.2 Measurement methods

The comparative potential result between titanium wire sensor (TWS) and saturated calomel electrode (SCE) was presented in this paper. Two types of potential measurement methods of saturated calomel electrode (SCE) were depicted in **Figure 5.7**. In method A, the position of SCE measurement was in one point beside the TWS position, and the average potential value between two rebars in the bottom surface is recorded as Method B.

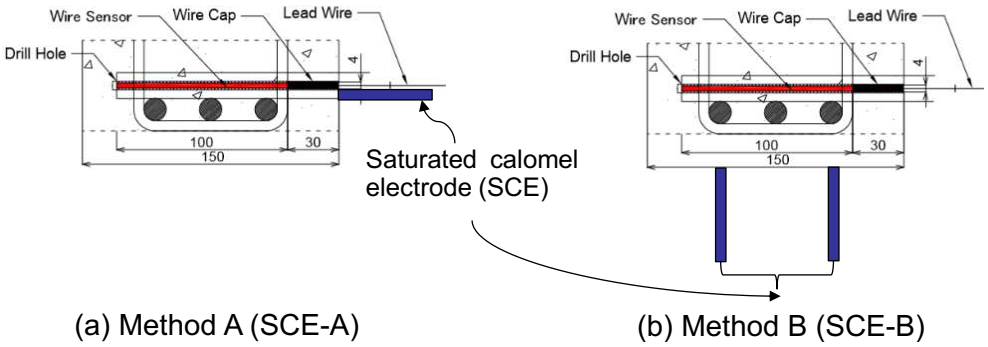

Figure 5.7 Measurement position of SCE in RC-1 and RC-2

In order to evaluate the performance of titanium wire sensor (TWS) in repair concrete with sacrificial anode cathodic protection, on, instant-off, and rest potential of rebar were conducted by two types of reference electrode; saturated calomel electrode (SCE) as movable reference electrode and titanium wire sensor (TWS) as the embeddable reference electrode. On-potential (E_{on}) of rebar and the anode are measured under sacrificial anode cathodic protection. Instant-off potential (E_{iof}) is checked immediately after disconnection, and the rest potential (E_{corr}) is measured at 24 hours after interruption of the steel bar and the anode.

5.3.3 Potential development of embeddable corrosion monitoring sensor

The observation of potential was conducted during protection of sacricial anodes operation and 24-hour after switching of sacrificial anodes operation. The potential development of titanium wire sensors (TWS) measured by saturated calomel electrode (SCE) and converted to copper/copper sulfate electrode (CSE) in 25°C for RC-1 and RC-2 during on and off protection of sacrificial anodes was depicted in **Figure 5.8**. It shows that the potential development of titanium wire sensors in existing concrete is in stable value at -300 mV ~ -100 mV from initial installation until 732-days of exposure. TWS1 in RC-2 shows the decrease potential value at 64-days, but it gradually recovered in stable value. It means that the performance of titanium wire sensors in chloride contaminated concrete or old concrete performs well from the viewpoint of potential development stability during both on and off sacrificial anodes operation. From this data, it indicates that the current flow of sacrificial anodes cannot interrupt the potential value of sensors.

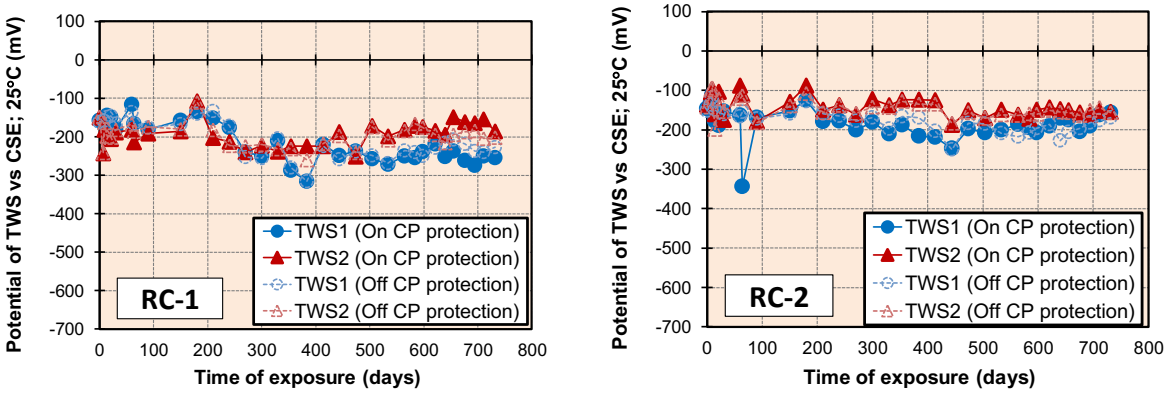

Figure 5.8 Potential development of titanium wire sensor (TWS) vs. CSE, 25°C in RC-1 and RC-2

5.3.4 Potential development of steel bars measured by the new embeddable sensor and standard reference electrode

The potential reading (on potential, instant-off potential, rest potential, and depolarization test value) of steel bars protected by sacrificial anodes in the titanium wire sensor (TWS) position at RC-1 measured by TWS, SCE method A, and SCE method B until 655 days of exposure were presented in **Figure 5.9**, **Figure 5.10**, **Figure 5.11**, and **Figure 5.12**.

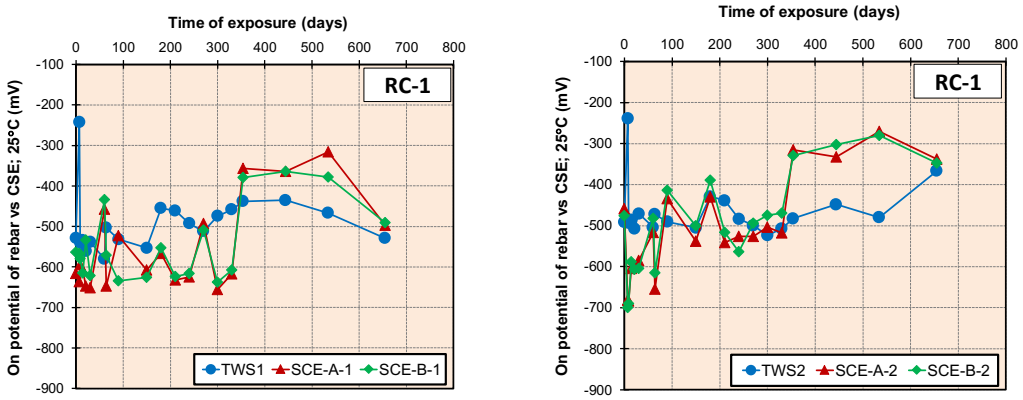

Figure 5.9 On potential of steel bar coincides TWS position vs. TWS and SCE in RC-1

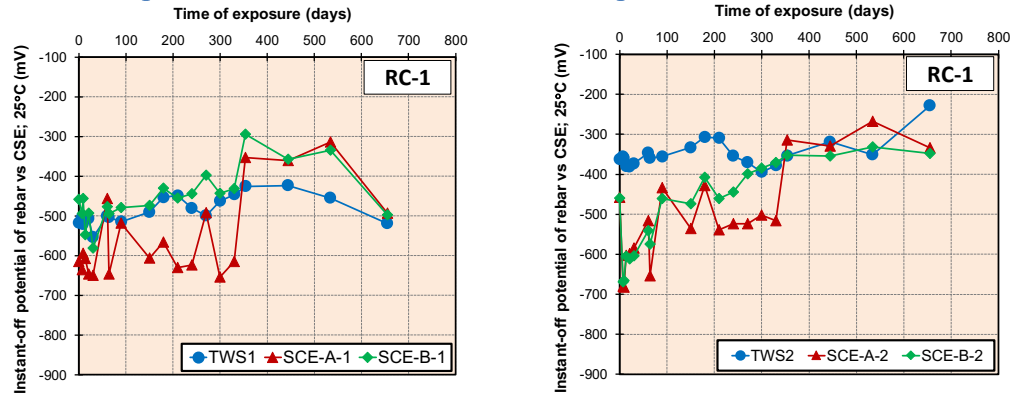

Figure 5.10 Instant-off potential of steel bar coincides TWS position vs. TWS and SCE in RC-1

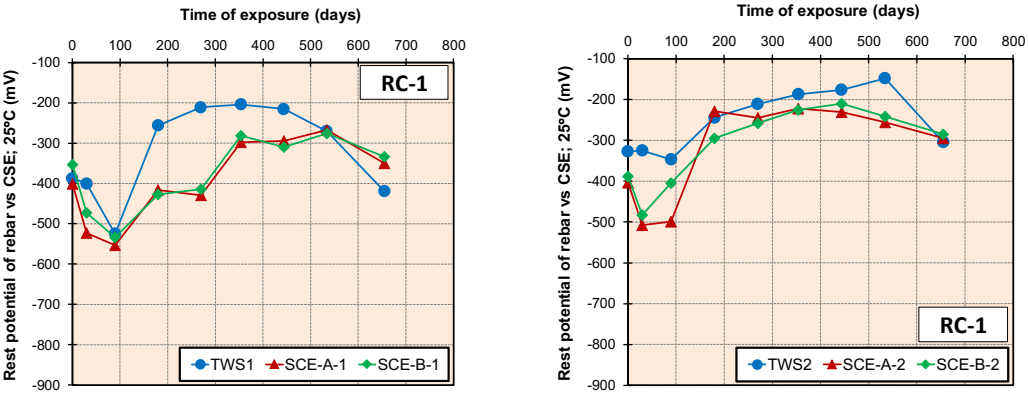

Figure 5.11 Rest potential of steel bar coincides TWS position vs. TWS and SCE in RC-1

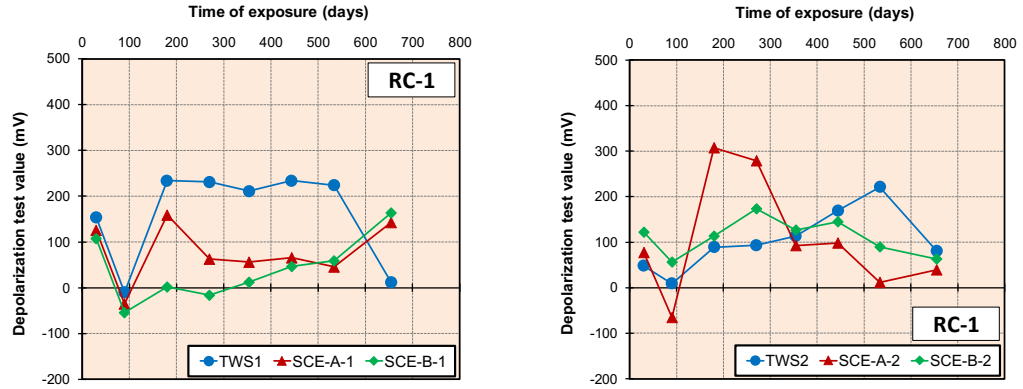

Figure 5.12 Depolarization test value of steel bar coincides TWS position vs. TWS and SCE in RC-1

The potential development of steel bar protected by sacrificial anodes were depicted in **Figure 5.13**, **Figure 5.14**, **Figure 5.15**, and **Figure 5.16**. The results of potential reading in RC-1 and RC-2 illustrate that the titanium wire sensor (TWS) reading is in good agreement with both SCE-A and SCE-B. The TWSs can be used as reference electrodes to measure the potential development of steel bars during the repair process using cathodic protection in existing concrete with a 50 mm distance from the patch repair boundary.

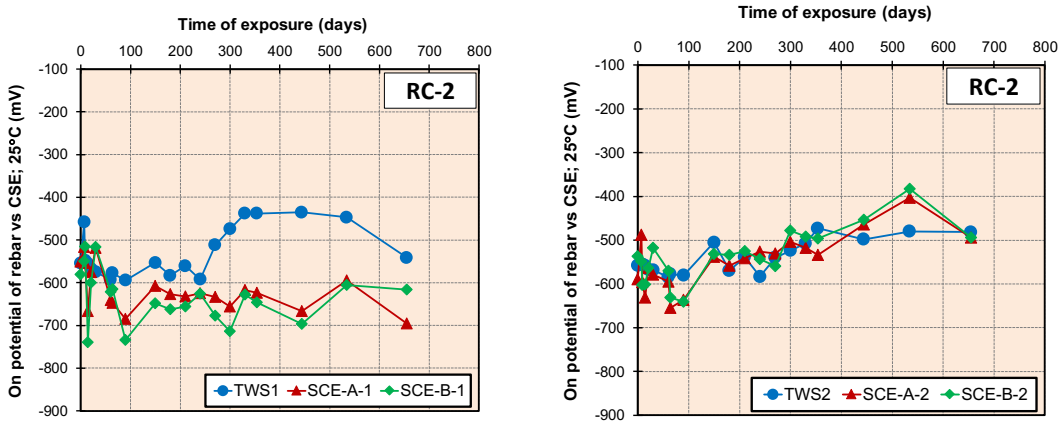

Figure 5.13 On potential of steel bar coincides TWS position vs. TWS and SCE in RC-2

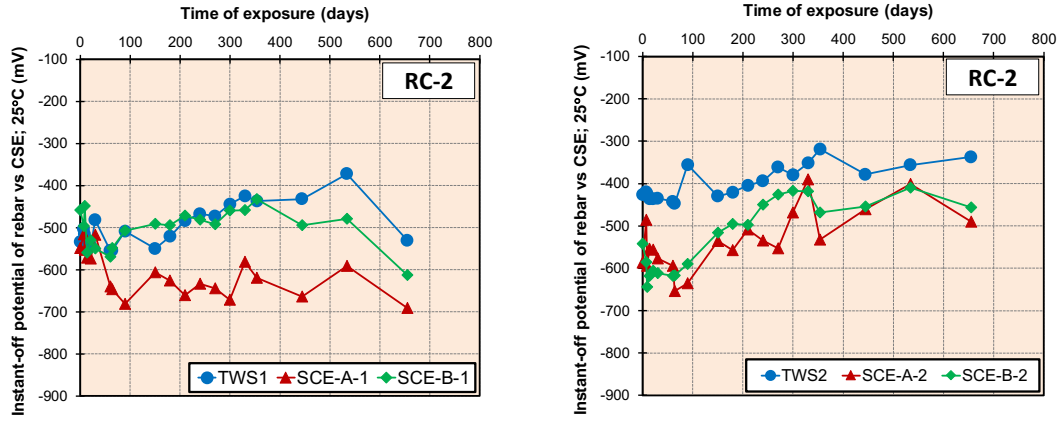

Figure 5.14 Instant-off potential of steel bar coincides TWS position vs. TWS and SCE in RC-2

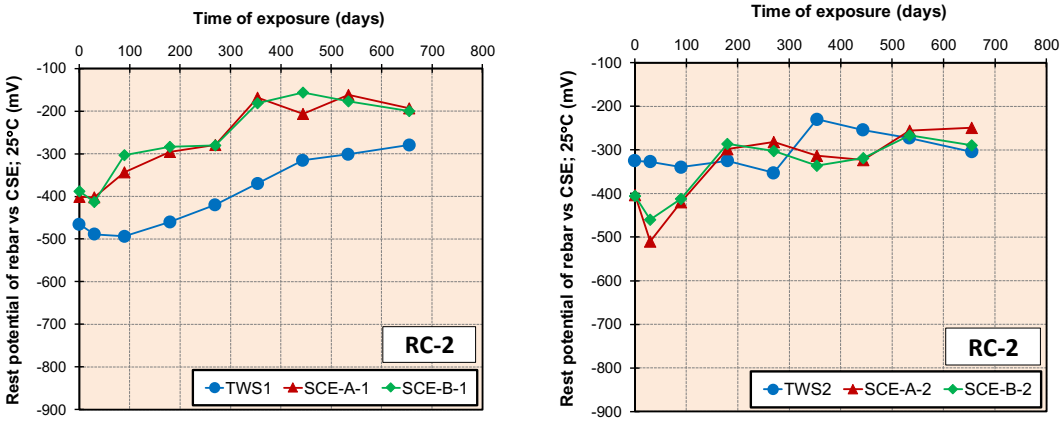

Figure 5.15 Rest potential of steel bar coincides TWS position vs. TWS and SCE in RC-2

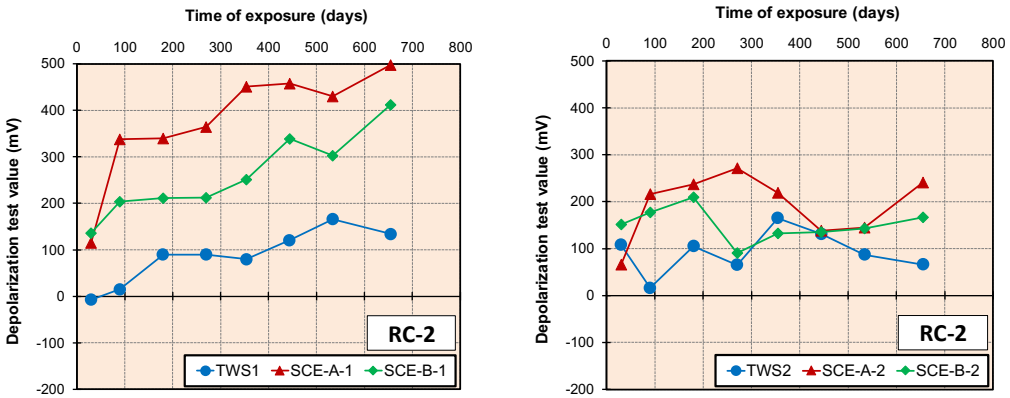

Figure 5.16 Depolarization test value of steel bar coincides TWS position vs. TWS and SCE in RC-2

The result of TWS in these specimens can be used as the indicator or sensor to detect the potential of steel bar in the surrounding of TWS position in existing concrete. The results of potential reading in RC-1 and RC-2 illustrate that the titanium wire sensor (TWS) in position TWS2 reading is in good agreement with both SCE-A and SCE-B with some deviation value due to inhomogeneous environmental condition at the measured point. TWS1 in RC-2 presents large deviation value among three type of measurement methods. But, in other points, the TWSs can be used as reference electrodes to measure the potential development of steel bars during the repair process using cathodic protection in existing concrete with a 50 mm distance from the patch repair boundary. The result of TWS in these specimens can be used as the indicator or sensor to detect the potential of steel bar in the surrounding of TWS position in existing concrete.

5.4 Application of embeddable corrosion monitoring sensor in patch and non-patch repair concrete during sacrificial anodes cathodic protection

5.4.1 Specimen design

In this subchapter, 44-years RC beams damaged by natural corrosion having a length of 2400 mm and a cross-sectional area of 150 mm was examined for new embeddable corrosion sensors application during the repair process by sacrificial anode cathodic protection, as shown in **Figure 5.17**.

Ordinary Portland Cement (OPC) was used as a binder of the concrete with the average of compressive strength and elastic modulus after 40 years were 30.0 MPa and 29.0 GPa, respectively (Dasar *et al*., 2017; Astuti *et al*., 2018). The deformed steel bar with a diameter of 13 mm and a yield strength of 363 MPa (Dasar *et al*., 2017) was used as tensile rebar, and

non-deformed steel of 6 mm in diameter was used as compressive rebar. Stirrups with a space of 100 mm were embedded in the beam.

The polymer-modified mortar (**Figure 5.19(a)**) was applied in the middle of tension area with the dimension of 70 x 150 x 800 mm after replacing the chloride-contaminated existing concrete by crushing process and rust removal using an EVA (Vinyl Acetate / Ethylene) copolymer emulsion as an adhesive material coating agent (**Figure 5.19(b)**) between parent concrete and patch repair mortar. Cylindrical ribbed sacrificial zinc anode A1, A2, B1 and B2 (**Figure 5.19(c)**) with a diameter of 30 mm, a length of 139 mm and an approximate weight of 417 grams were installed in pre-drilled holes of 40 mm diameter in parent concrete and cementitious coating material with LiOH (**Figure 5.19(d)**) was used to cover the anodes after settling position in the hole.

The embeddable reference electrode consists of titanium probe activated by iridium-enriched mixed metal oxide, 3 mm in diameter and 150 mm in length, defined as titanium wire sensor (TWS) and saturated calomel electrode (SCE) were utilized as corrosion monitoring sensor in this study as presented in **Figure 5.20**.

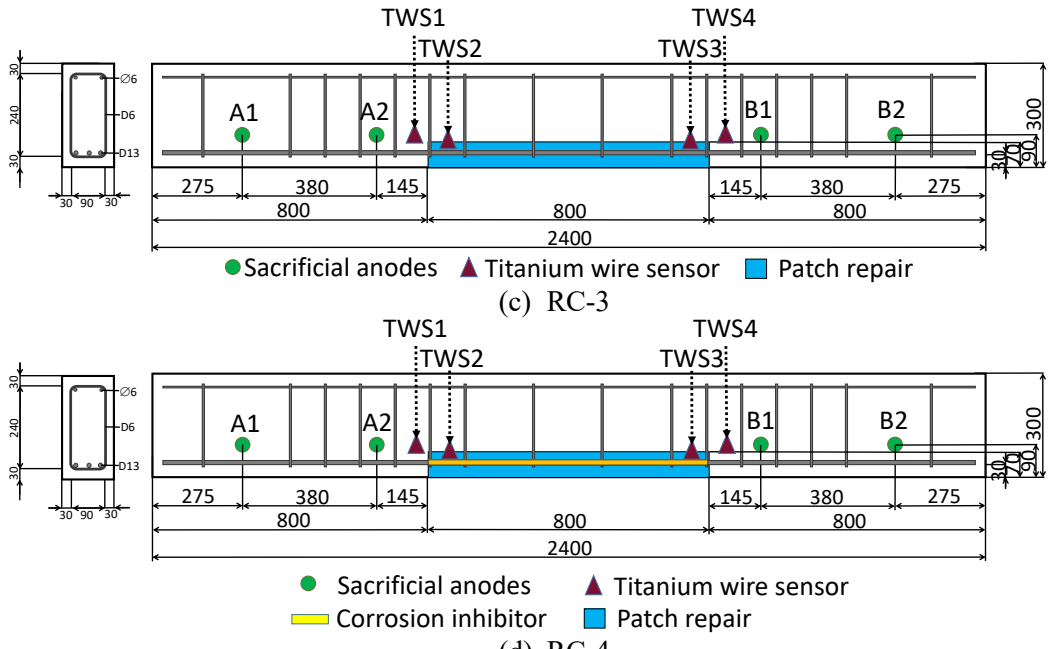

(c) RC-3

(d) RC-4

Figure 5.17 Titanium wire sensor (TWS) setting position in RC-3 and RC-4

The titanium wire sensors were embedded in both existing and patch repair concrete as shown in **Figure 5.21**. In existing concrete, the sensors were installed in the pre-drilled hole with a diameter of 20 mm and it was covered by polymer-modified mortar.

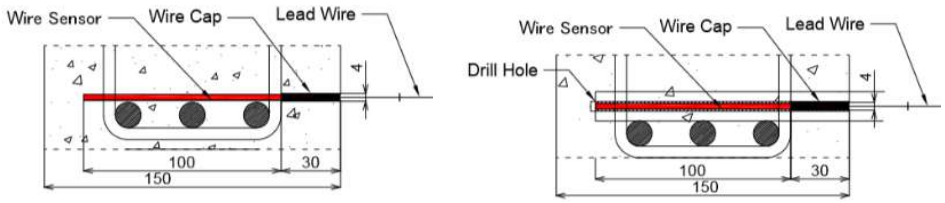

(a) In patch repair (b) In non-patch repair

Figure 5.18 Titanium wire sensor position in the cross-sectional area of patch and non-patch repair

(a) (b) (c) (d)

Figure 5.19 Materials for repair: (a) polymer modified mortar, (b) coating agent, (c) cylindrical ribbed sacrificial zinc anode and (d) Cementitious anode coating material mixed with LiOH

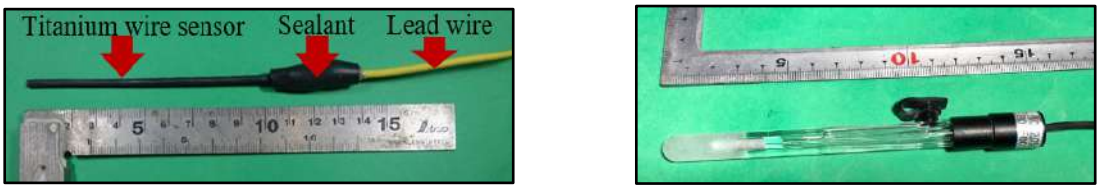

(b) (b)

Figure 5.20 Reference electrode: (a) titanium wire sensor (TWS) and (b) saturated calomel electrode (SCE)

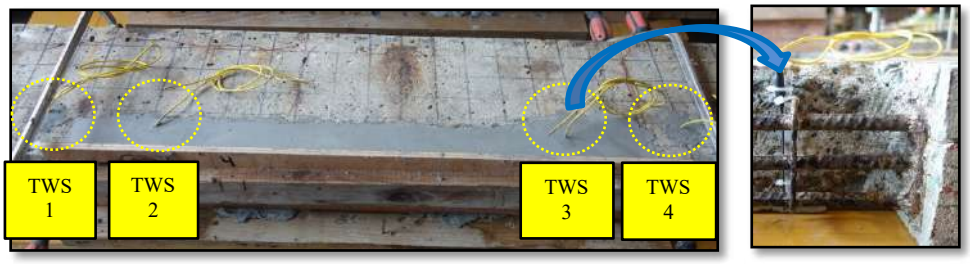

Figure 5.21 The installation process of titanium wire sensor in concrete

5.4.2 Measurement methods

In order to evaluate the performance of titanium wire sensor (TWS) in repair concrete with sacrificial anode cathodic protection, on, instant-off, and rest potential of rebar were conducted by two types of reference electrode; saturated calomel electrode (SCE) as movable reference electrode and titanium wire sensor (TWS) as the embeddable reference electrode. On-potential (E_{on}) of rebar and the anode are measured under sacrificial anode cathodic protection. Instant-off potential (E_{iof}) is checked immediately after disconnection,

and the rest potential (E_{corr}) is measured at 24 hours after interruption of the steel bar and the anode.

The comparative potential result between titanium wire sensor (TWS) and saturated calomel electrode (SCE) was presented in this paper. Two types of potential measurement methods of saturated calomel electrode (SCE) were depicted in **Figure 5.22**. In method A, the position of SCE measurement was in one point beside the TWS position, and the average potential value between two rebars in the bottom surface is recorded as Method B.

The TWS and SCE potential readings were converted to copper/copper sulfate electrode in 25°C (CSE; 25°C) using the following equation, $E_{CSE} = E_{TWS} - 120.1 - 2.84(T-25)$ and $E_{CSE} = E_{SCE} - 74.5 - 1.66(T-25)$, where, E_{CSE} is potential in 25°C CSE standard, E_{TWS} is potential reading of TWS and E_{SCE} is potential reading of SCE.

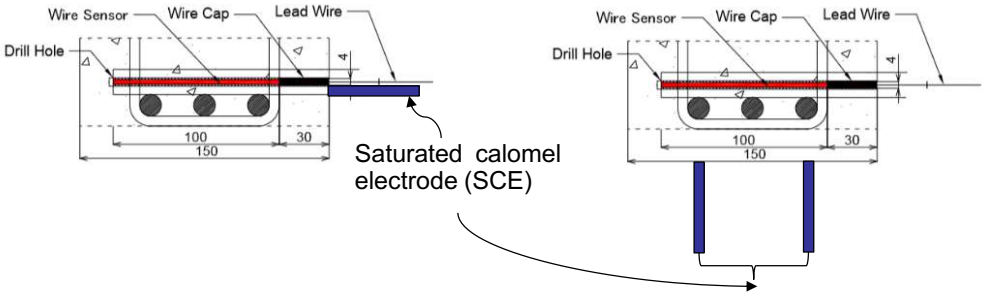

Figure 5.22 Measurement position of SCE in RC-3 and RC-4

The potential measurement method is commonly used worldwide as one of the non-destructive tests to predict the corrosion probability of reinforcing steel in concrete by measure the rest potential of rebar. Also, the potential monitoring of rebar during the repair process of RC structures damaged by corrosion is an important issue to achieve effective repair techniques. The potential development of titanium wire sensor (TWS) was measured by the SCE electrode to understand the potential stability of TWS.

The comparative result of potential monitoring between titanium wire sensor (TWS) and standard sensor (saturated calomel electrode (SCE)) also were presented during one-year of repair process observation on a corroded RC beam. The environmental condition of the specimen was in laboratory air condition with two days of wet, followed by five days of dry condition. Two methods of SCE observation from beside TWS position (Method A) and from the bottom part of RC member (Method B) also were demonstrated. On potential of rebar is checked to evaluate the potential condition during the connection between sacrificial and rebar. The potential value within one second after the current interruption is defined as

instant-off potential. Therefore, the potential of rebar after switch off for 24-hour is categorized as rest potential or natural potential. Depolarization value is calculated by the potential difference value between instant-off potential and rest potential, and 100 mV potential decay is used to evaluate the protection condition of rebar.

5.4.3 Potential development of embeddable corrosion monitoring sensor

The potential development of titanium wire sensors (TWS) measured by saturated calomel electrode (SCE) and converted to copper/copper sulfate electrode (CSE) in 25°C was depicted in **Figure 5.23**. The observation of potential was conducted during protection of sacrificial anodes operation and 24-hour after switching of sacrificial anodes operation.

In the first of six months of TWs in RC-3, the potential of TWS was stable at around -300 mV in patch repair and around -300 mV in existing concrete. It gradually increases and becomes steady in around -100 mV of potential until one-year of exposure both in chloride contaminated concrete and polymer-modified mortar. The potential development of TWS in RC-4 shows a stable value from initial until 732-days of exposure. The TWS1 in the non-patch repair presents the highest potential value around 0 mV. TWS2, TWS 3, and TWS4 show a potential value of around -200 mV ~ -100 mV. There is no significant deviation value during on and off current flow of sacrificial anodes.

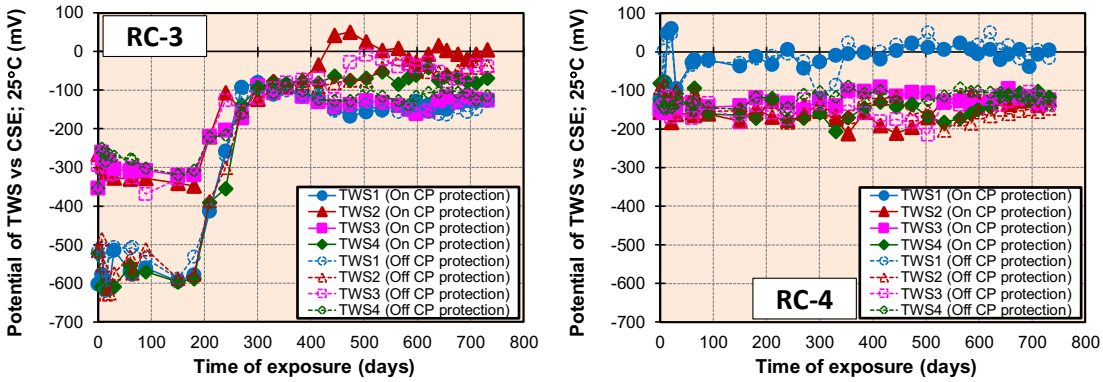

Figure 5.23 Potential development of titanium wire sensor (TWS) vs. CSE, 25°C in RC-3 and RC-4

5.4.4 Potential development of steel bars measured by new embeddable sensor and standard reference electrode

The potential development of steel bars in RC-3 consists of on potential, instant-off potential, rest potential and depolarization test value are illustrated in **Figure 5.24**, **Figure 5.25**, **Figure 5.26**, and **Figure 5.27**, respectively. **Figure 5.28**, **Figure 5.29**, **Figure 5.30**, and **Figure 5.31** show the potential development of steel bars in RC-4.

The results of potential reading until 655-days of exposure in RC-3 and RC-4 illustrate that the titanium wire sensor (TWS) reading is in good agreement with both SCE-A and SCE-B. The TWSs can be used as reference electrodes to measure the potential development of steel bars during the repair process using cathodic protection in existing and new patch repair concrete with a 50 mm distance from the patch repair boundary.

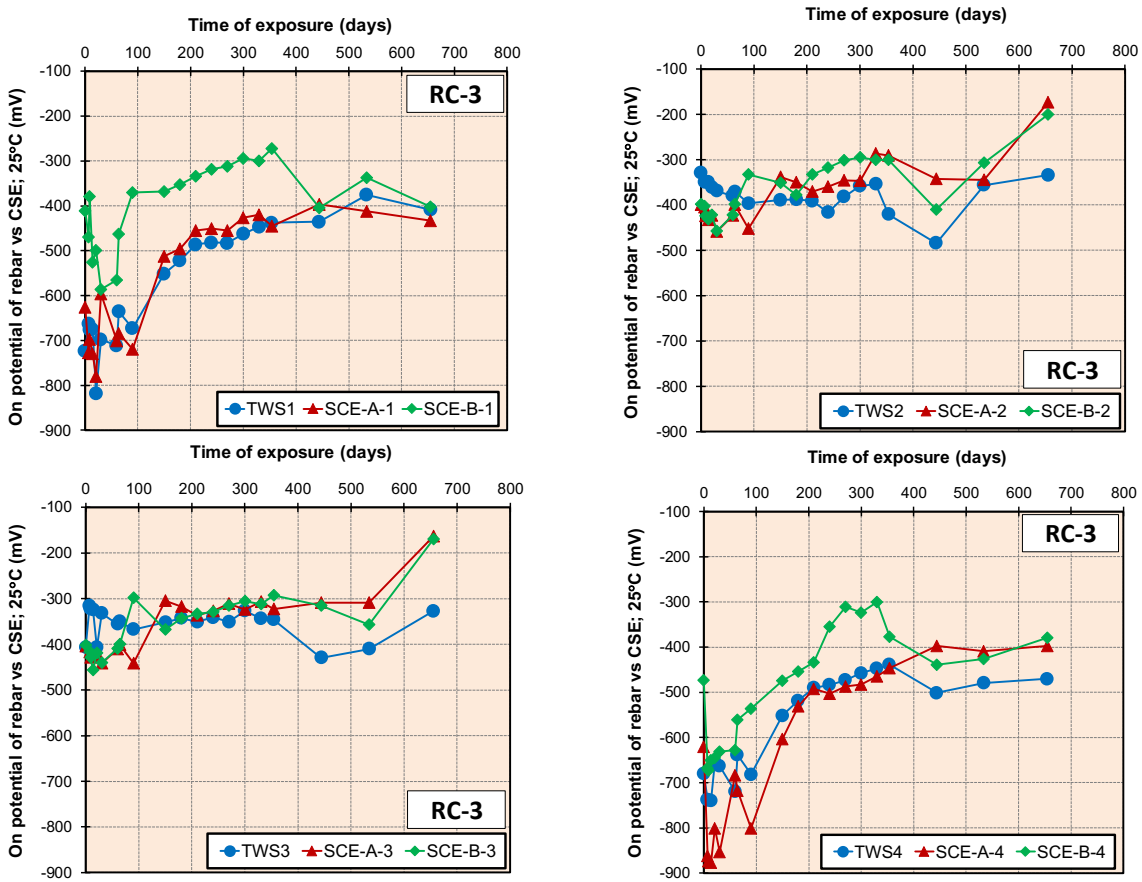

Figure 5.24 On potential of steel bar coincides TWS position vs. TWS and SCE in RC-3

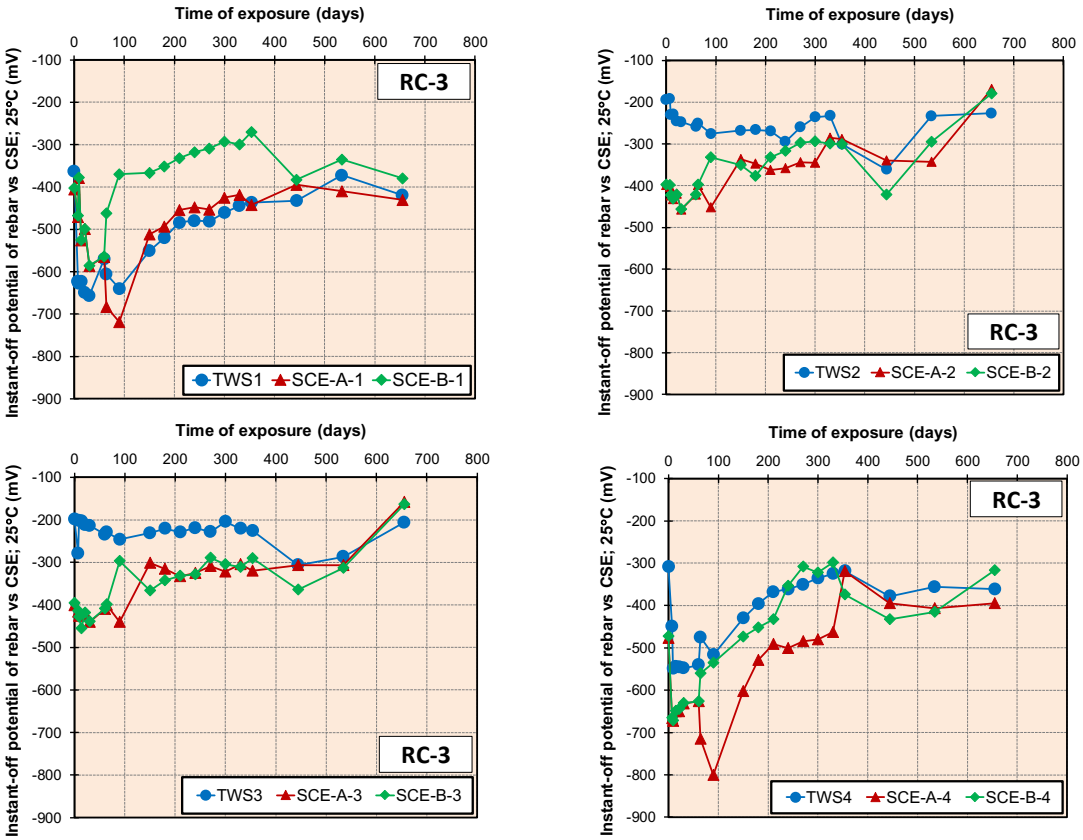

Figure 5.25 Instant-off potential of steel bar coincides TWS position vs. TWS and SCE in RC-3

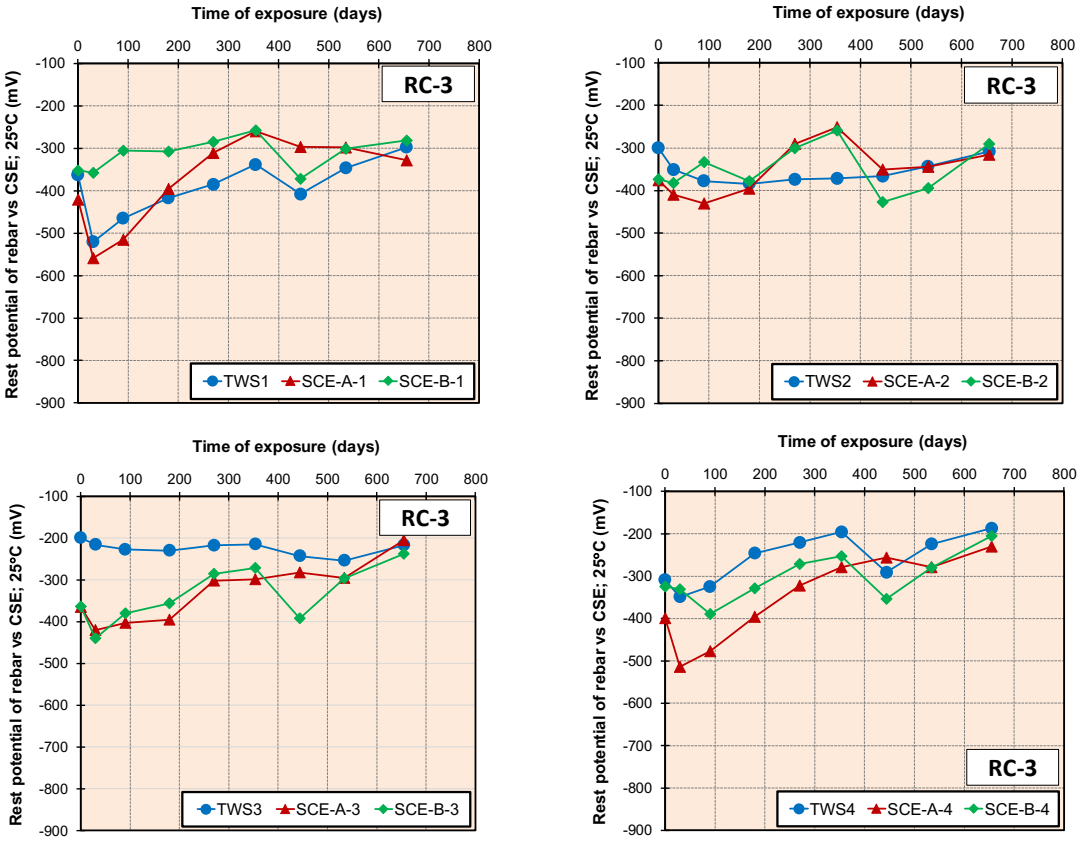

Figure 5.26 Rest potential of steel bar coincides TWS position vs. TWS and SCE in RC-3

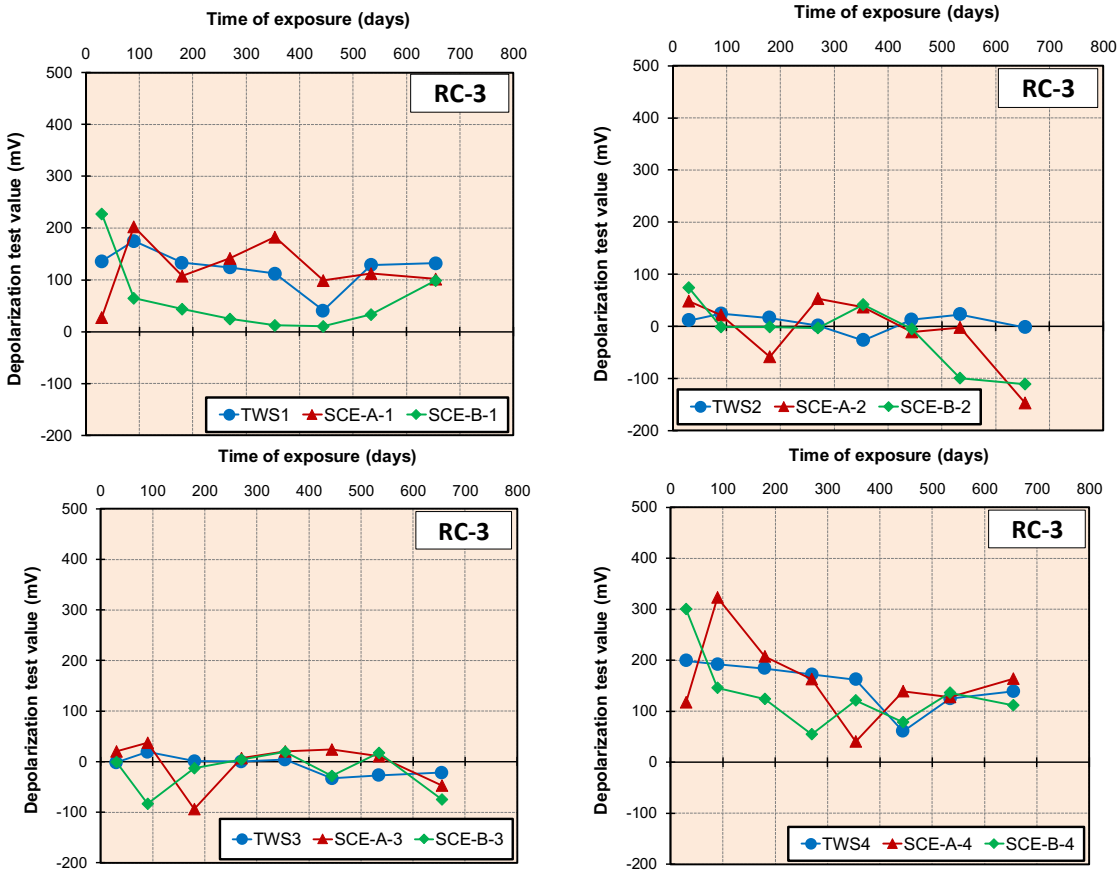

Figure 5.27 Depolarization of steel bar coincides TWS position vs. TWS and SCE in RC-3

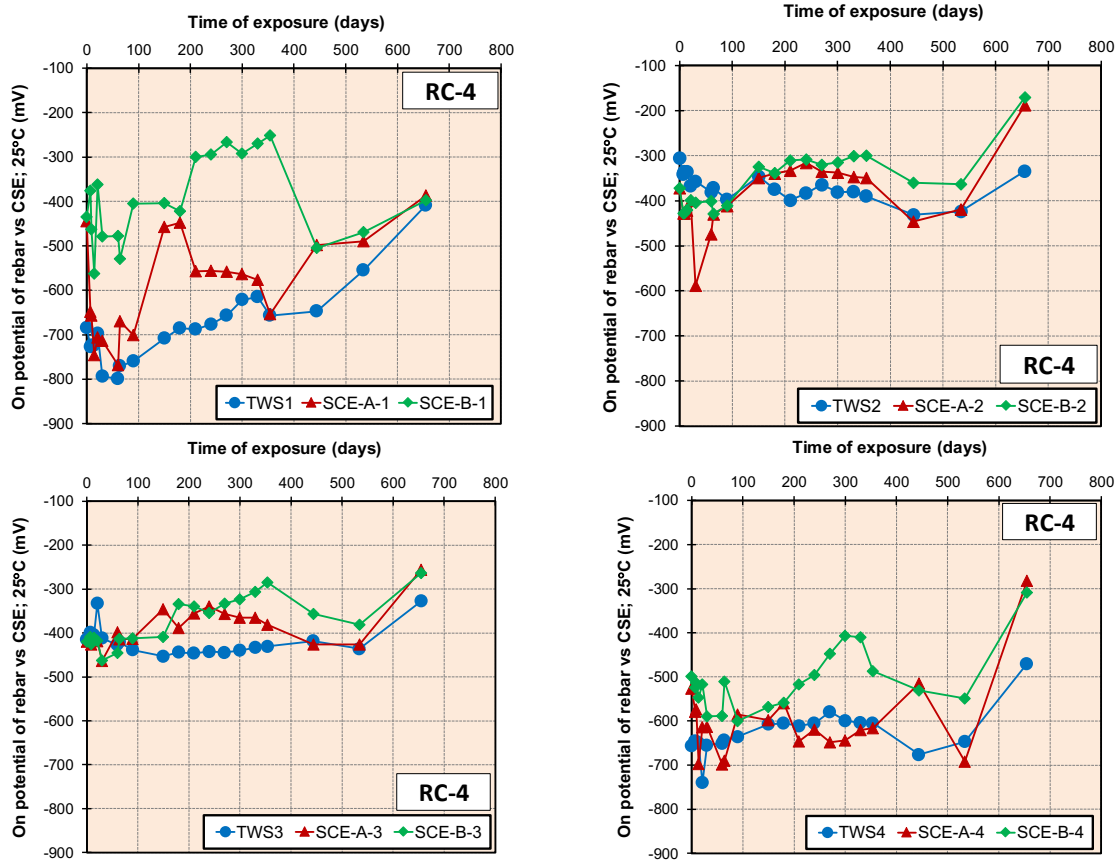

Figure 5.28 On potential of steel bar coincides TWS position vs. TWS and SCE in RC-4

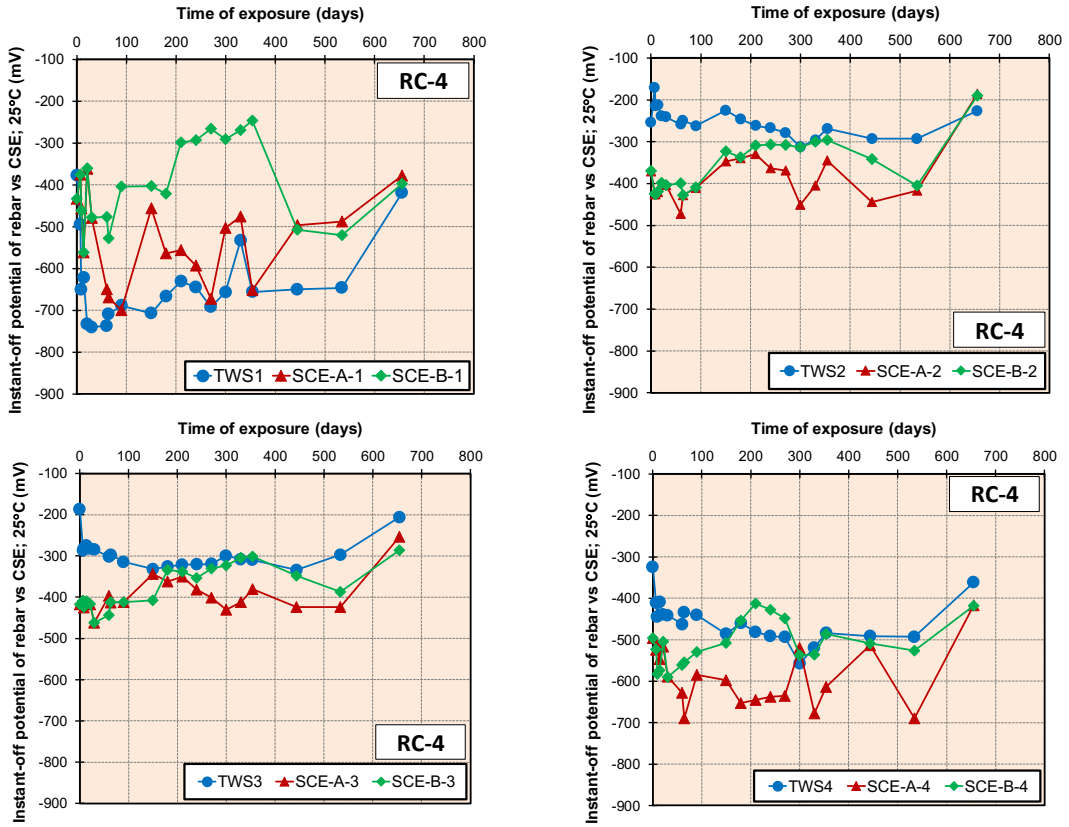

Figure 5.29 Instant-off potential of steel bar coincides TWS position vs. TWS and SCE in RC-4

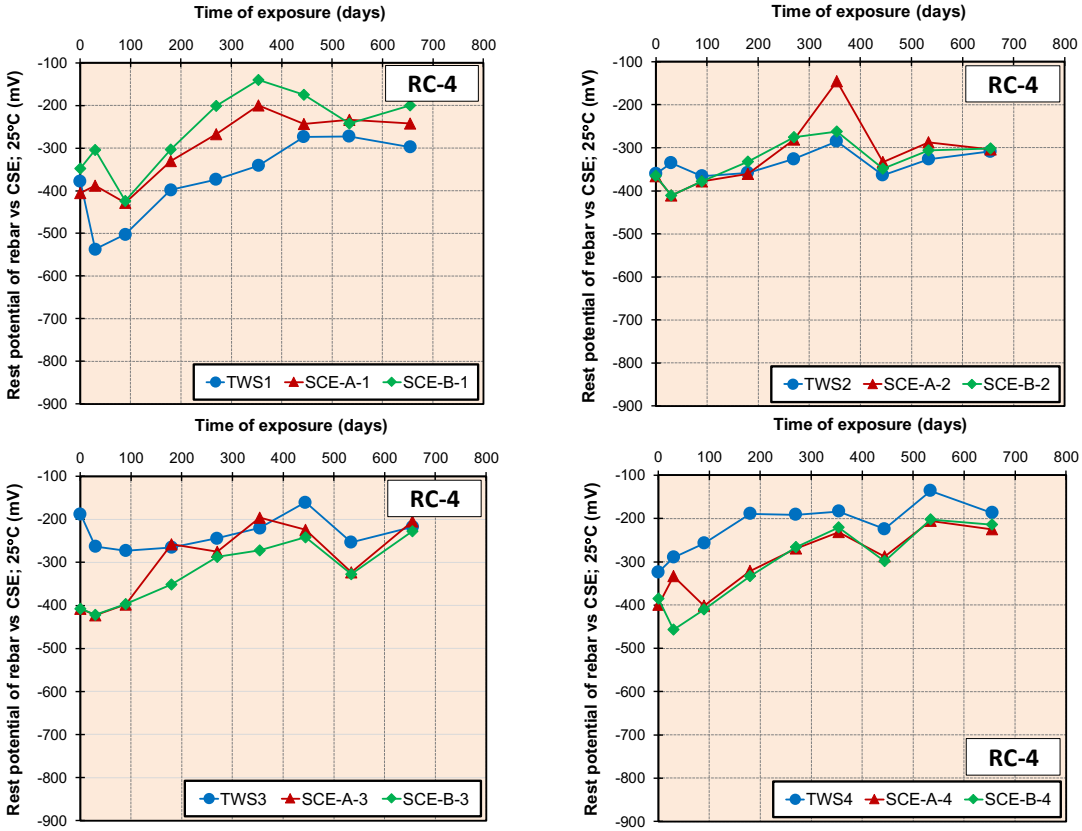

Figure 5.30 Rest potential of steel bar coincides TWS position vs. TWS and SCE in RC-4

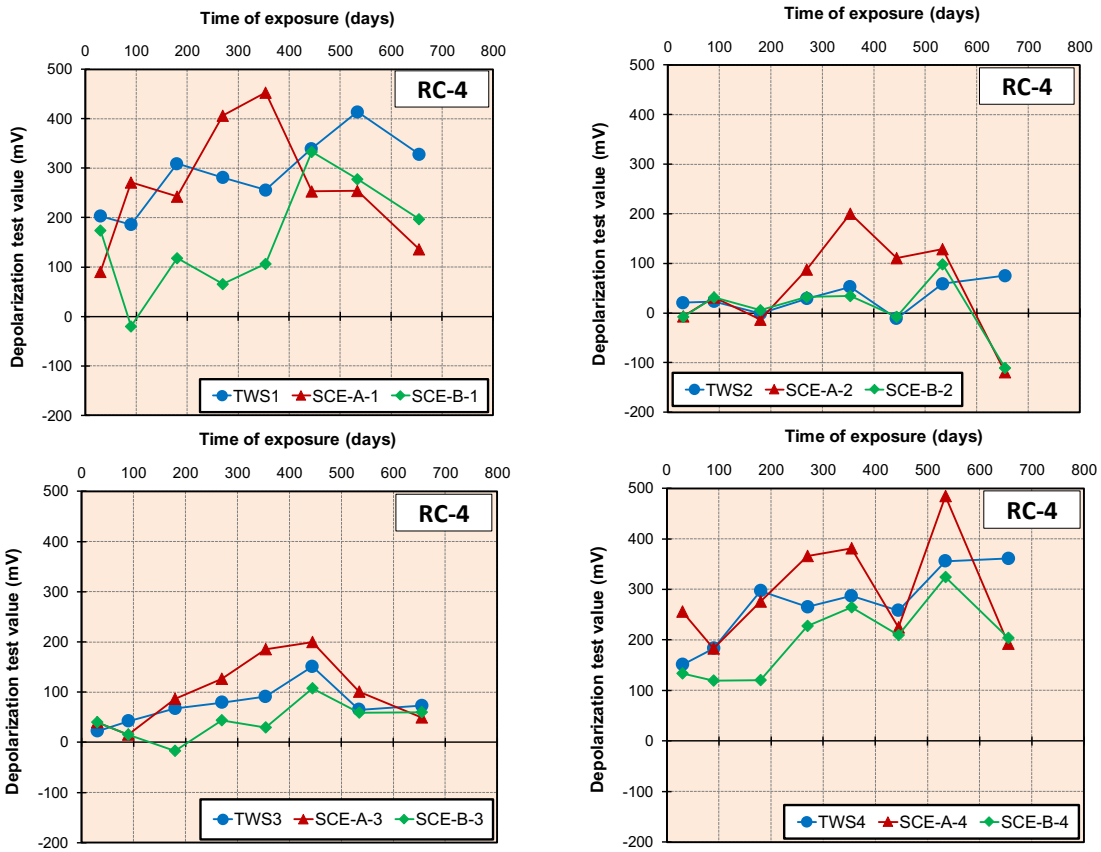

Figure 5.31 Depolarization test value of steel bar coincides TWS position vs. TWS and SCE in RC-4

The results also inform that the titanium wire sensor (TWS) performs better sensitivity in the polymer-modified mortar than in chloride contaminated existing concrete. It may be caused by the uniformity of electrochemical properties of polymer modified mortar. Even though the polymer-modified mortar was used as backfill material in the pre-holes of TWS embedded in existing concrete with 20 mm in diameter, the imperfect fabrication may occur. The result of TWS in these specimens can be used as the indicator or sensor to detect the potential of steel bar in the surrounding of TWS position in existing and new patch concrete.

5.5 **Stability of embeddable corrosion monitoring sensor**

As the corrosion monitoring sensor embedded in the repaired RC member, it should perform potential stability. The current flow generated by sacrificial anode should not polarize the sensor. The potential of titanium wire sensor vs. current density of anodes are presented in **Figure 5.32**, **Figure 5.33**, **Figure 5.34**, and **Figure 5.35** for RC-1, RC-2, RC-3, and RC-4, respectively.

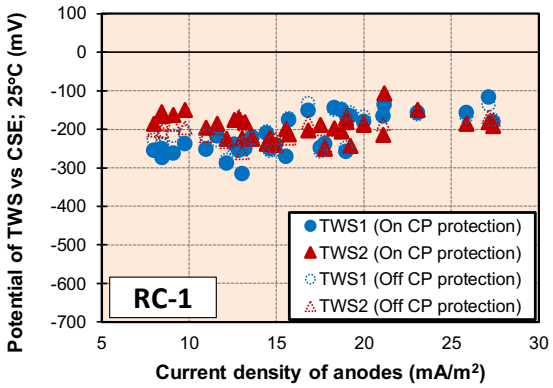

Figure 5.32 Potential of TWS vs. current density of sacrificial anodes in RC-1

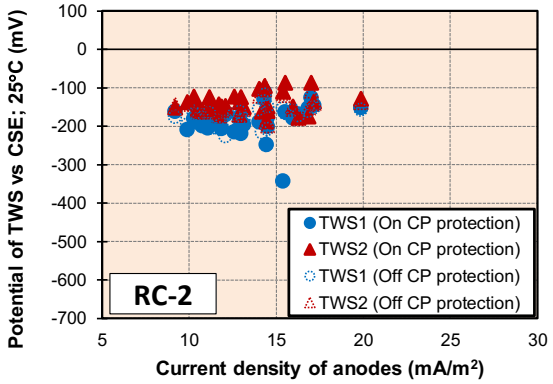

Figure 5.33 Potential of TWS vs. current density of sacrificial anodes in RC-2

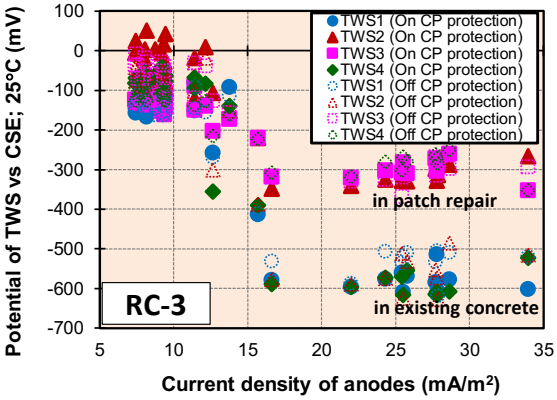

Figure 5.34 Potential of TWS vs. current density of sacrificial anodes in RC-3

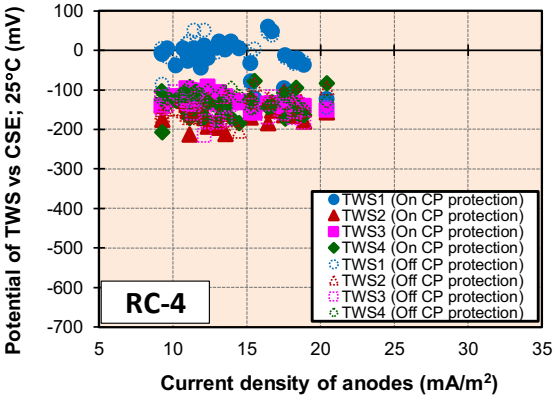

Figure 5.35 Potential of TWS vs. current density of sacrificial anodes in RC-4

The potential development of sensors in RC-1, RC-2, and RC-4 is normally stable from initial exposure until 21-months in the range -300 mV ~ -100 mV vs. CSE in 25°C. One sensor, TWS 1 in RC-4, shows a stable potential value in around 0 mV vs. CSE in 25°C. It may due to the different characteristics of the sensor. The results also present that the potential of sensors is stable and the current density generated by sacrificial anodes cannot polarize the potential of sensors in RC-1, RC-2, and RC-4.

The sensors in RC-3 demonstrate a different potential trend. The polarization curve of titanium wire sensor in RC-3, as depicted in **Figure 5.36**, shows that the potential of sensor polarize to the cathodic direction around -300 mV vs. CSE at patch repair and -600 mV at non-patch repair when the current that flowing to it is more than 10 mA/m^2. It may due to the sensors are affected by the stray current flow of anodes. It confirmed by the correlation between the potential of sensor and current density of anodes. The potential value is in the range of -200 mV ~ -100 mV when the current density is less than 12 mA/m^2. Then, the potential value of sensors in the patch and non-patch repair are in -300 mV and -600 mV when the current density of anodes is more than 20 mA/m^2 and 40 mA/m^2, for non-patch and patch repair, respectively.

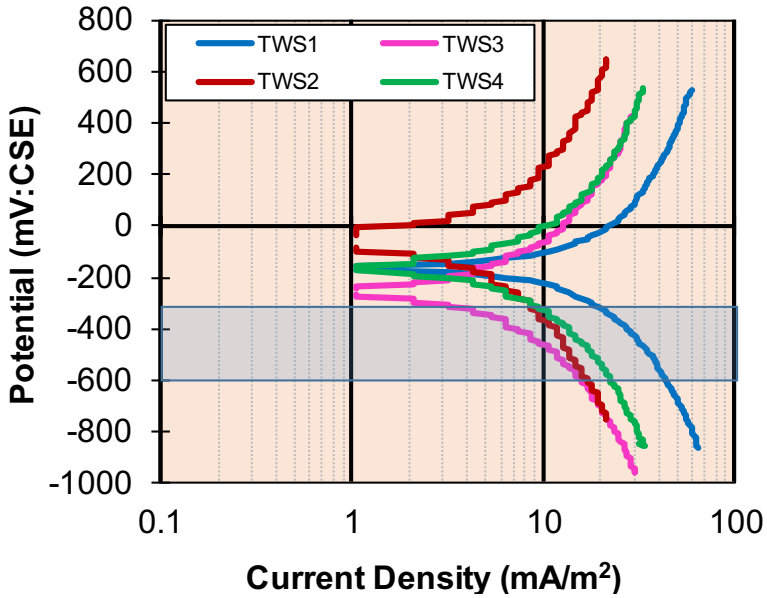

Figure 5.36 Polarization curve of titanium wire sensor (TWS) in RC-3

The potential condition of the sensors is recovered at 250-days and it becomes a normal potential value. It may due to the stray current is stopped. In order to prevent the possibility of stray current flowing in the sensor, it is necessary to monitor the natural potential of sensors and it should be around -100 mV vs. CSE.

5.6 **Conclusion**

From the experimental results, the following conclusions are derived.

1. Titanium wires sensor (TWS) is working as a corrosion monitoring sensor in concrete with stable potential reading in around the areas wherein it is embedded until 18 months of exposure.
2. The polarization effect of sacrificial anodes cathodic protection, including on-potential, instant-off potential, and rest potential of rebar can be detected by using a titanium wire sensor (TWS).
3. The comparative potential reading shows that the titanium wire sensor (TWS) performs better sensitivity in the polymer-modified mortar than in deteriorated existing concrete due to the uniformity of material properties of new patch material.
4. The stable performance of titanium wire sensor in the repaired RC member protected by sacrificial anode cathodic protection in this study is indicated by the stable potential development of sensors vs. time and current density.
5. There is a possibility of stray current generated in titanium wire sensor so the initial and periodic monitoring of potential is required.

5.7 **References**

Ansuini, F. J., and Dimond, J. R., 1994. "Factors affecting the accuracy of reference electrodes," *CORROSION/94*, No. 323, Houston, TX.

Ansuini, F. J., and Dimond, J. R., 2001. "Long-term field tests of reference electrodes for concrete – ten year results," *CORROSION2001*, No. 1296, Houston, TX.

Arup, H. and Sorenson, B., 1992. "A new embeddable reference electrode for use in concrete", *NACE Corrosion/92*, Vol. 208**.** Houston, TX.

Astuti, P., Rafdinal, R.S., Mahasiripan, A, Hamada, H., Sagawa, Y., and Yamamoto, D., 2018. "Potential Development of Sacrificial Anode Cathodic Protection Applied for Severely Damaged RC Beams Aged 44-years." *Journal of Thailand Concrete Association*, 6 (2), 24-31.

Astuti, P., Rafdinal, R.S., Hamada, H., Sagawa, Y., and Yamamoto, D., 2019. "Application of sacrificial anode cathodic protection for partially repaired RC beams damaged by corrosion," *4th International Symposium on Concrete and Structures (CSN2019)*, Kanazawa, Japan 17-19 June 2019. Kanazawa: Kanazawa Institute of Technology, 284-291.

Bennett, J. E. and Mitchell, T. A., 1992. "Reference electrodes for use with reinforced concrete structures," *NACE Corrosion/92,* Vol. 191, Houston, TX.

Christodoulou, C., Goodier, C. I., Austin, S. A., Glass, G. K. and Webb, J., 2014. A new arrangement of galvanic anodes for the repair of reinforced concrete structures," *Construction and building materials,* Vol. 50, pp. 300-307.

Dasar, A., Hamada, H., Sagawa, Y., and Yamamoto, D., 2017. "Deterioration Progress and Performance Reduction of 40-year-old reinforced concrete beams in natural corrosion environment." *Construction and Building Materials*, Vol. 147, pp. 690-704.

Muralidharan, S., Ha, T., Bae, J., Ha, Y., Lee, H., Park, K., and Kim D., 2005. "Electrochemical studies on the solid embeddable reference sensors for corrosion monitoring in concrete structure," *J. Materials Letters,* Vol. 60, pp. 651-655.

NACE, 2000. "Use of reference electrodes for atmospherically exposed reinforced concrete structures," *NACE Technical Committee Report 11100.*

Rafdinal, R. S., Aoyama, T. and Fukagawa, N., 2018. "Development of titanium wire sensor for corrosion monitoring in the concrete structures," *P.S. Mitsubishi Construction Co. Ltd. Technical Report,* No. 16.

Schell, H. C., and Manning, D. G., 1985. "Evaluating the performance of cathodic protection systems on reinforced concrete bridge substructures," *CORROSION/85*, No. 263, Houston, TX.

CHAPTER VI

Design of appropriate repairing method by using sacrificial anodes cathodic protection in RC structures

6.1 Introduction

Corrosion of steel bars in concrete is well known as one of the major factors that cause deterioration of reinforced concrete structures. This study introduces the application of sacrificial anode cathodic protection (SACP) to mitigate the corrosion problem. The cathodic protection system is achieved by supplying an external current source from active metals and it causes a potential shift of the steel bar. The -850 mV vs. CSE is most widely used in practical CP design on reinforced concrete structures that were adopted on the protection of underground structures. However, in structures where much of the steel bar is naturally cathodic (in a passive state) and the dissolved oxygen available, the application of such criteria has been found to result in very high unneeded current requirements (Bennet & Bromfield; 1997). It may lead to premature deterioration of anode, hydrogen evolution and bond reduction between steel bar and concrete (Caronge; 2015).

Another underground CP criterion is 100 mV decay potential in which commonly use today for evaluating the effectiveness of cathodic protection of reinforced concrete structures. These are the principal criteria currently used to energize the CP system for reinforced concrete structures. However, this 100 mV decay potential is not confirmed to be sufficient to ensure the CP of steel in concrete. Some of the researchers have suggested that decay potential criterion should be increased to 150 – 200 mV, while others have suggested that it should be reduced depends on the amount of chloride concentration in concrete (Caronge; 2015), deterioration degree of structures, environmental condition, and expected lifetime of repairs.

Corrosion monitoring of steel reinforcing bar in concrete requires reliable stable potentials. Such measurements are important when designing and maintaining cathodic protection systems for RC structures. In particular, accurate measurements are mandatory for RC structures where over-protection can be as deleterious as under-protection. The increasing usage performance over an extended period (Ansuini & Dimond; 2003). The application of a new embeddable corrosion monitoring sensor was performed in Chapter 5.

Based on the research output conducted in **Chapters 3, 4, and 5**, the recommendation of the appropriate repairing method by using SACP for reinforced concrete structures were attempted.

6.2 Review of SACP design for RC structures exposed to marine environment

In the marine environment, corrosion region of the RC structures was categorized regarding the seawater level as submerged zone (always in below sea water level), splash zone and tidal zone (a region in the intermittently wet and dry condition), and atmospheric zone (above the mean high tide level) as illustrated in **Figure 6.1** (Daily, 1999).

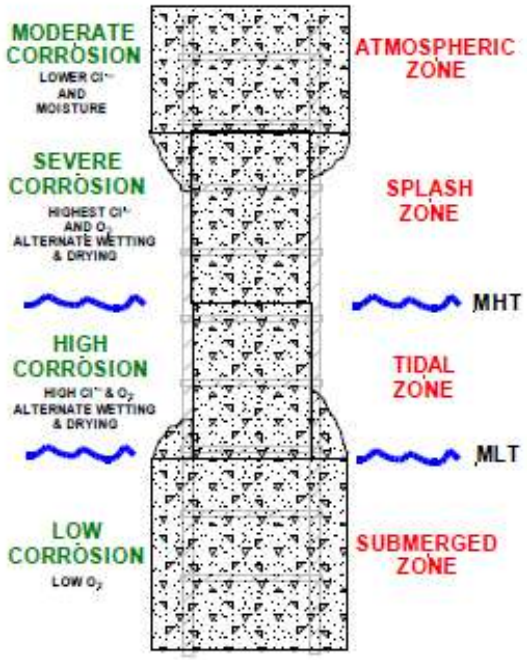

Figure 6.1 Corrosion regions of concrete structure in marine environments (Daily, 1999)

Each of the zones has very different corrosion characteristics. For instance, the corrosion rate below the water level is limited by low oxygen availability, and conversely lower chloride and moisture content limit the corrosion rate above high tide. Corrosion is found more severe within the splash and tidal zones where alternate wetting and drying result in high chloride and oxygen content. Consequently, the protection criteria applicable to CP, in this case, maybe relatively complex.

Glass et al. (2000) classified the CP criteria for reinforced concrete in marine exposure zones. In the submerged zone, immunity to corrosion is readily achieved by shifting the potential of the steel bar to a sufficiently negative value due to the restricted access of oxygen. In the atmospheric zone, CP induces steel passivity that is indicated by the achievement of 100 mV of a negative potential shift by a relatively small applied current

density. A major protective effect of CP in this zone is the improvement in the local environment at the steel-concrete interface resulting from the removal of aggressive ions and the production of inhibitors. In the splash zone, the type of the CP system may be similar to that installed in the atmospheric zone. The installation of a CP system in the tidal zone is complicated by the intermittent presence of seawater. The protection criteria applicable to this zone might be a combination of those applied in the atmospheric and submerged zone.

The 100 mV decay potential (depolarization value) has been used to determine the effectiveness of CP for steel in concrete. The choice of 100 mV is based on the theory that the polarization of corroding steel bars in the cathodic direction will inhibit anodic (corrosion) reactions (Bennett & Turk, 1994). Most disagreement about this criterion is focused on the amount of polarization needed to protect the steel bar against corrosion. For cases of severe corrosion (i.e. very high chloride concentration), the polarization requirement should be higher than 100 mV (Ansuini & Dimond, 2001; Funahasi & Young, 1992; Takewaka, 1993). **Table 6.1** summarized the depolarization level requirements based on the chloride concentration in concrete from previous researchers.

Table 6.1 Summary of the depolarization level requires under various chloride concentration (Caronge, 2015)

Source	**Exposure condition**	**Chloride concentration (% wt. of concrete)**	**Depolarization needed (mV)**
Funahashi &Young (1992)	Moisture condition (T: 7ºC, 25ºC & 25ºC)	0.16 – 1	>100
Takewaka (1993)	Dry/wet cycles (T: 40%, RH: 95%)	0.5	150 – 200
Bennett & Turk (1993)	unknown	<0.2 0.2 – 0.3 0.3 – 0.8 0.8 – 1.6 >1.6	0 60 80 100 150
Caronge (2015)	Dry condition (T: 20±2ºC, RH: 60%)	0.58 1.45 2.86	25 – 50 50 – 100 >100

The use of 100 mV depolarization value criterion is reasonable if the chloride concentrations in concrete are not known. Although it should be increased to 150 – 200 mV if conditions are known to be very corrosive. The depolarization needed not only depend on the chloride content in concrete, but also environmental condition. The presence of moisture and oxygen in concrete could increase the corrosion rate of the steel bar. As a consequence,

the higher protection level is required. An adjustment of depolarization value based on the chloride concentration in concrete, as presented in **Table 6.1,** would have the advantage of reducing the deleterious effects and extending the service life of the cathodic protection system.

The protection level was increased with increasing polarization time due to the cathodic protection current (higher than 100 mV depolarization value). It can lead in over protection, especially for structures that have been polarized for a long period and in which more passive condition has been achieved as a result of cathodic protection current flow (Ansuini & Dimond; 2003).

6.3 Review of SACP monitoring and maintenance in RC structures

Maintenance of sacrificial anode cathodic protection (SACP) is one of the most important activities necessary to ensure the long-term performance of the system. Cathodic protection maintenance mainly consists of two activities, namely cathodic protection potential monitoring and cathodic protection system inspection. Cathodic protection potential monitoring is conducted to evaluate the adequacy of cathodic protection level in the RC structures. Guyer (2014) categorized two types of maintenance as scheduled preventive maintenance and unscheduled maintenance requirements.

Scheduled preventive maintenance is defined as the minimum requirement for all installed cathodic protection systems to comply with the environmental regulations, public law, and industrial standards. In the SACP application, the close-interval corrosion survey by a non-interrupted potential survey is needed. The purpose of this survey is to ensure that adequate cathodic protection is maintained over the entire protected structure. A close-interval survey must be conducted thirty days after the cathodic protection system installation and five years from the last close-interval corrosion survey.

The unscheduled maintenance requirement is the required action if adequate cathodic protection does not exist on the protected structure, then troubleshooting must be accomplished to determine the cause of this lack of protective current. There are two major components to the operational of the sacrificial anode system: the anode and the structure lead.

The sacrificial anode cathodic protection is inherently maintenance-free. The current is merely a result of the potential difference between the two metals. Recurring maintenance checks are performed to ensure continued satisfactory performance. Normally, sacrificial anode consumes themselves at a constant rate and failure can be predicted by current

measurement versus time. The most common problem in sacrificial anode systems is shorts wound or failure of dielectrics on isolated protected structures. Due to the very limited voltage, sacrificial anodes usually cannot supply sufficient current to protect the structures if isolation is lost.

Failure of the anode lead wires is uncommon since copper exposed by nicks or insulation defects is cathodically protected by the anodes. However, their wire can be cut by extraneous excavations. Exercising control over digging permits in the areas of the anode ground beds may ensure that if the wires are cut, they can be repaired on-site, before backfilling occurs. Troubleshooting to locate the break at a later date is usually not successful, and the replacement of a prematurely failed anode is more economical in almost all cases. A sudden zero anode current output reading indicated probably failed lead wires.

When the sacrificial anode system reaches the end of their useful life, potential and current measurements begin to change. When performing recurring maintenance, a significant drop in anode current indicated the imminent failure of the anode. Potential measurements over the protected structure will begin to show dips or drops in the areas of failed anodes. A significant drop in anode potential indicated a failed anode. Anode current may reverse after failure, due to the copper center tap of the anode being cathodic to the protected structure. When drops in the potential of the protected structure begin to occur, a closer inspection should be made to determine the extent of the damage to the anodes (Guyer, 2014).

6.4 Discussion and recommendation of effective repair method by SACP for deteriorated RC structures

Cathodic protection systems are particularly suited to large structures requiring massive patch repair caused by chloride-induced corrosion. In such situations, the only other option is, to demolish and rebuild, structurally strengthen or completely encase the RC structure from ingress of deleterious substances (Rashidi *et al.*, 2018).

Sacrificial anode, one of the cathodic protection types that have some advantages and less maintenance, was chosen as a repair method for chloride-induced RC structures in this study. Cathodic protection will immediately half or reduce corrosion but cannot rehabilitate the steel nor return it to its original condition. They require a supplemental anode to be bonded to the surface of the concrete. These anode materials must be capable of sustaining oxidation reactions without suffering physical damage. When the sacrificial anode cathodic protection system is applied, by connecting the anode to the steel bars, the electrons are

forced into the steel bars. The voltages made by anode forces the steel bars to become more electronegative (Woodson, 2009). Electrons are produced by the anodes and consumed at the steel bars, which is cathodically protected. Reduction reaction and hydroxyl ions production occur at the steel bar surface. The production of hydroxyl ions reverts the pore water to an alkaline substance, which regenerated the passivating state of the steel bars. An additional benefit to the cathodic protection method is that the negatively charged chloride ions are forced away from the more electro-negative steel bars towards the anodes, which further assists in the establishment of the passivating layer on the steel bars (Rashidi *et al.*, 2018).

Based on the case study on RC-1, RC-2, RC-3, RC-4, and RC-5 from **Chapter IV**, several designs of sacrificial anodes application were proposed and explained in this sub-chapter. Even the small current flow generated by sacrificial anodes, the polarization of steel bar occurs and the steel bars condition was improved. It means that the repair methods demonstrated in **Chapter IV** are effective.

From the experiments, the proper of sacrificial anode cathodic protection application in the deteriorated RC beams are summarized as follows.

1. The application of sacrificial anodes in patch repair deliver limited protection in patch repair only.
2. The application of sacrificial anodes in existing concrete can cover protection not only in existing concrete but also in some part of patch repair.
3. In the application of sacrificial anodes both in the patch and in non-patch repair, it can protect a bigger area, but the time-lapse application of it is important.
4. The embeddable corrosion monitoring sensor is recommended due to its stability. The data recording is required every three months to check the anodes and the polarization condition.

From all experimental programs conducted in this thesis, the summarized the protective current density and depolarization value as the parameter of application of sacrificial anodes cathodic protection in repair RC members are presented in **Table 6.2**. The required protective current density of anodes and depolarization set values are presented each parameter including environmental condition, structural deterioration degree, and repairing technology.

Table 6.2 Summary of design parameters for SACP in repaired RC members

No	Aspect	Threshold	Current Density (mA/m^2)	Depolarization (mV)
A. Parameter of environmental condition				
1	Temperature (**Chapter 3.4**)	Low (-17°C)	$1x10^{-4}$–$1.0x10^{1}$	0–300
		High (40°C)	$1x10^{-4}$–$3.0x10^{1}$	0–380
2	Exposure condition **(Chapter 3.3)**	Dry (atmospheric zone)	$1x10^{-4}$–$2.0x10^{1}$	0–200
		Wet (submerged zone)	$1x10^{-4}$–$0.4x10^{1}$	0–120
		Dry-wet (splash/tidal zone)	$1x10^{-4}$–$0.5x10^{1}$	0–250
B. Parameter of structural deterioration				
1	Corrosion degree (**Chapter 3.3**)	Low (non-rusted steel bar)	$1x10^{-4}$–$0.5x10^{1}$	0–220
		High (rusted steel bar)	$1x10^{-4}$–$0.6x10^{1}$	0–80
2	Chloride concentration (**Chapter 3.2**)	4 kg/m^3	$1x10^{-4}$–$1.8x10^{1}$	0–320
		10 kg/m^3	$1x10^{-4}$–$1.0x10^{1}$	0–420
3	Size of defect **(Chapter 3.2)**	Small (110 mm x 150 mm)	$1x10^{-4}$–$1.8x10^{1}$	0–320
		Large (195 mm x 150 mm)	$1x10^{-4}$–$1.3x10^{1}$	0–420
C. Parameter of repairing technology				
1	Anode Type A **(Chapter 4.7)** 	SACP in patch repair	$1x10^{-4}$–$2.5x10^{1}$	0–200
2	Anode Type B **(Chapter 4.8)** 	SACP in non-patch repair	$1x10^{-4}$–$3.5x10^{1}$	0–600
3	Combine (A&B) with timelapse **(Chapter 4.7)**	SACP in patch and non-patch repair with timelapse	$1x10^{-4}$–$4.0x10^{1}$	0–720
4	Combine (A&B) without timelapse **(Chapter 4.9)**	SACP in patch and non-patch repair without timelapse	$1x10^{-4}$–$4.5x10^{1}$	0–380
5	Hybrid CP system **(Chapter 3.5)**	ICCP was applied for 30-days before SACP connection	$1x10^{-4}$–$3.0x10^{1}$	0–300

From the environmental aspect, sacrificial anodes in the high temperature around 40°C and exposed to the dry-wet condition required higher current density and depolarization value than in the low temperature. The corrosion degree, chloride concentration, and the size of the defect are required parameters that could be considered based on the structural deterioration level. Also, each repairing methods perform different current density and polarization value as presented at part C.

6.5 Conclusion

From this chapter, several conclusions are summarized as follows.

1. The application of sacrificial anodes in patch repair deliver limited protection in patch repair only.
2. The application of sacrificial anodes in existing concrete can cover protection not only in existing concrete but also in some part of patch repair.
3. In the application of sacrificial anodes both in the patch and in non-patch repair, it can protect a bigger area, but the time-lapse application of it is important.

4. The embeddable corrosion monitoring sensor is required to monitor the polarization effect of anodes.
5. The design parameter of SACP application including environmental conditions, structural deterioration degree, and repairing technology was proposed by using the different protective current density and depolarization set values.

6.6 References

Ansuini, F. J., and Dimond, J. R., 2001. "Long-term field tests of reference electrodes for concrete – ten year results," *CORROSION2001*, No. 1296, Houston, TX.

Bennett, J. and Broomfield, J. P., 1997. "An Analysis of Studies Conducted on Criteria for the Cathodic Protection of Steel in Concrete", *NACE CORROSION/97*, Paper No. 251.

Bennett, J. and Turk, T., "Criteria for the Cathodic Protection of Reinforced Concrete Bridges Elements," SHRP-S-359, National Research Council, Washington DC, 1994.

Caronge, M. A., 2015. "A study on the effectiveness of cathodic protection for steel bars in concrete structures", *Doctoral Thesis,* Kyushu University, Fukuoka, Japan.

Daily, S. F., 1999. "Using Cathodic Protection to Control Corrosion of Reinforced Concrete Structures in Marine Environments," Corrpro Companies, Inc.

Glass, G. K., 2000. "CP Criteria for Reinforced Concrete in Marine Exposure Zones," *Journal of Materials in Civil Engineering*, Vol. 12 (2), pp. 164-171.

Guyer, J. P., 2014. "An introduction to cathodic protection systems maintenance," Continuing Education and Development, Inc., No. E03-021.

Rashidi, M., Anrich, E., Ghodrat, M., and Buckley, P., 2018. "Review of the most common repair techniques for reinforced concrete structures in coastal areas," *IABSE Conference – Engineering the Developing World*, April 25-27, Kuala Lumpur, Malaysia, pp. 370-377.

Woodson, R. D., 2009. "Concrete structures protection, repair, and rehabilitation," *Elsevier.*

CHAPTER VII

Conclusion and recommendation

7.1 **Summary**

Chloride induced corrosion is one of the major deterioration of structures in marine environment condition that lead to performance degradation and premature failure before the expected service life. In the last decades, several electrochemical repair techniques were developed for offering chloride-induced corrosion. From the literature, cathodic protection (CP) is one of the reliable repairing methods that proven to control corrosion. The CP is usually used in repaired concrete which contains the high chloride contamination and from the standard that the section shows the chloride ion contamination greater than 0.3% by weight of cement and half-cell potential value higher than −350 mV should be removed.

On the contrary, the concrete replacement work on chloride contaminated structures can be very onerous and expensive. Therefore, sacrificial anodes, which is one of CP type with less instrument and maintenance requirement, have been used to limit the extent of concrete replacement and extend the service life of patch repairs to corrosion damaged RC structures. However, the specification of the repair method by sacrificial anodes in repair RC members is still unclear.

Therefore, the objective of this study is to find a suitable repair strategy on naturally damaged RC beam structures by sacrificial anodes cathodic protection. Several considerations of utilization sacrificial anodes in repair structures were demonstrated in laboratory cases such as temperature effects, steel surface condition, the ability of sacrificial anodes to mitigate macro-cell corrosion, and an attempt to decrease the high consumption of sacrificial anodes in the early stage of repair. Further, the application of several repair methods on 44-years naturally damaged RC beams structures using sacrificial anodes, patch repair, and corrosion inhibitor were presented as a field case. Also, a new corrosion monitoring device made of titanium probe iridium-enriched mixed with metal oxide was used as a new sensor in repair strategy. The repair and maintenance procedures based on laboratory and field applications were proposed.

7.2 Overview of contributions and conclusions

Chapter 1 explains the background of the study, research objectives and limitations, research contribution and standing point, and dissertation arrangement. The objectives of this study are to investigate the repair method by sacrificial anode cathodic protection in laboratory and field application cases and the utilization of new embeddable corrosion monitoring sensor in RC member. Further, the application of sacrificial anodes, in 3-4 years of exposure and observation were presented in the laboratory cases and more than 40-years of deteriorated RC beams by natural marine environment were demonstrated in the field application cases. The expected result of this study is to propose the suitable repairing method by sacrificial anodes and the utilization of a new embeddable corrosion sensor in repaired RC members.

Chapter 2 describes the literature review from the previous study related to the durability issues in the RC structures due to chloride-induced corrosion (e.g., corrosion mechanism, chloride-induced corrosion, and electrochemical aspect on corrosion); corrosion inspection, assessment, and monitoring method; and repair method of chloride-induced corrosion in RC structures. The results from the previous study are important information as references to design the reliable repair strategy in Chapter 4.

Chapter 3 presents the fundamental research on the utilization of sacrificial anodes in laboratory cases. From the viewpoint of arresting macro-cell corrosion due to different chloride contamination (4 kg/m^2 and 10 kg/m^2) after five years of observation, the point sacrificial anodes in the repair part is still generating protection to the segmented steel bars indicated by the depolarization test value. The longer the span of repair part the higher depolarization value. In the preparation of sacrificial anodes application, rust removal process on steel surface in repair concrete is necessary due to the non-rusted is the most desirable initial condition of steel bars when the sacrificial anode is applied on it based on the observation until four years of exposure. Regarding the temperature in the exposure condition, it can be reported that the application of sacrificial anodes in low temperature around -17°C performs a good result until three years but four years of utilization sacrificial anodes in high temperature (40°C) presents not effective protection due to crack formed around the steel bar protected by anodes. The experiment to reduce the high anode consumption in the early connection was succeeded in the last part of this chapter by the implementation of half of the initial sacrificial anodes current flow by using the impressed-

current method. The current source was switched when the potential of steel bar is similar to stable steel bar potential affected by sacrificial anodes only.

Chapter 4 demonstrates repair methods by sacrificial anodes cathodic protection in more than 40-years severely damaged RC beams. RC-1 and RC-2 present the application of sacrificial anodes in patch repair to protect patch area only due to the electrochemical incompatibility of polymer mortar and existing concrete and after one year, the additional sacrificial anodes were applied in the non-patch repair. Both RC-1 and RC-2 show good protection identified by depolarization and improved steel bar conditions in all cross-sectional of the beams. RC-3 and RC-4 present the application of sacrificial anodes in non-patch repair only while the corrosion inhibitor was painted in the steel bar surface in the patch repair area. RC-4 show better protection than RC-3 due to the corrosion inhibitor membrane reduces the required electric current for attaining the steel bar potential change in the patch repair. So, the application of corrosion inhibitor is recommended in RC structures repaired by sacrificial anodes. From RC-1~RC-4, it can be seen that small current flow generated by sacrificial anodes affects not only on polarization but also modifies the steel bar condition. Depolarization values of more than 100 mV can not have a significant effect on the improvement of steel bar conditions. The application of sacrificial anodes in the patch and non-patch repair is also presented in RC-5. The obtained result indicates that the repair method by combining a different kind of sacrificial anodes in the patch and non-patch repair presented no significant polarization of rebar nor current flow. Therefore, the combined sacrificial anodes in the patch and non-patch repair method at the same time with closed distance could not be suitable repairing system.

Chapter 5 illustrates the utilization of titanium wire sensors as a new embeddable corrosion monitoring sensor in four RC members repaired by sacrificial anodes cathodic protection. Titanium wires sensor (TWS) is working as a corrosion monitoring sensor in concrete with stable potential reading in around the areas wherein it is embedded until 18 months of exposure. The comparative potential reading shows that the titanium wire sensor (TWS) performs better sensitivity in the polymer-modified mortar than in deteriorated existing concrete due to the uniformity of material properties of new patch material. The stable performance of titanium wire sensor in the repaired RC member protected by sacrificial anode cathodic protection in this study is indicated by the stable potential development of sensors vs. time and current density.

Chapter 6 formulates the proper sacrificial anode cathodic protection application method in the deteriorated RC beams. The installation of sacrificial anodes in patch repair deliver limited protection in patch repair only. If the sacrificial anodes were installed in existing concrete, it can cover protection not only in existing concrete but also in some part of patch repair. The application of sacrificial anodes both in the patch and in non-patch repair can protect a bigger area, but the time-lapse application of it is important. The design parameter of SACP application based on experimental results including environmental conditions, structural deterioration degree, and repairing technology was performed by the different protective current density and depolarization set values.

7.3 **Recommendation for future research**

In this research, the current of sacrificial anodes cannot flow in the polymer-modified mortar as patch repair due to its high resistivity. For future research, the patch repair material should be low resistivity in order to allow the current of sacrificial anodes to deliver to the patch repair area.